R-11-04

Low-pH concrete plug for sealing the KBS-3V deposition tunnels

Richard Malm, Vattenfall Power Consultant AB

Januari 2012

Svensk Kärnbränslehantering AB
Swedish Nuclear Fuel
and Waste Management Co

Box 250, SE-101 24 Stockholm
Phone +46 8 459 84 00

ISSN 1402-3091
SKB R-11-04

Low-pH concrete plug for sealing the KBS-3V deposition tunnels

Richard Malm, Vattenfall Power Consultant AB

Januari 2012

This report concerns a study which was conducted for SKB. The conclusions and viewpoints presented in the report are those of the author. SKB may draw modified conclusions, based on additional literature sources and/or expert opinions.

A pdf version of this document can be downloaded from www.skb.se.

Summary

In SKB's main alternative for final repository of radioactive material, KBS-3V, the backfilled deposition tunnels will be separated from the remaining tunnel system with concrete plugs. These concrete plugs will be designed for a life span of 100 years and their function shall maintain until the transport tunnels outside the plug are backfilled and the natural geohydrological conditions have been restored.

The purpose of this report is to document the results and the evaluation from this project and motivate the choice of the most appropriate design for closing the deposition tunnels in the spent fuel repository. The purpose has also been to investigate and present the loads acting on the plug system and determine the load capacity of the concrete plug. This report is the result of a project conducted between 2009-01-01 – 2010-12-31 and the project group has made its assessment based on the conditions and requirements that are present today.

The entire design of the plug system is part of this project, where the plug system consists of a filter, a bentonite seal and a cast-in-place concrete plug. Two different conceptual design alternatives for the concrete plug have been studied in this report, one long tapered plug and one dome shaped plug. The results in this report focus on the choice of the conceptual design for the concrete plug and its possibility to assist the entire plug system to satisfy its requirements.

It is a complicated task to dispose the radioactive waste and it sets high technical requirements on the design and the production of the backfill and the closing of the deposition tunnels. The aim of this project is to design and develop a plug system suitable for production. This is done by the means of numerical calculations and analyses. The primary function of the concrete plug is to act as a resistance to the external loads originated from the axial expansion of the backfill and the water pressure. However, the entire plug system has a requirement on being watertight, which also affects the design of the concrete plug. In the spent fuel repository, low-pH concrete should be used instead of conventional concrete. The reason for this is to the largest extent to reduce the negative effect that basic materials could have on the function of the bentonite clay. For this purpose, a new low-pH concrete recipe has been developed and this changes the conditions for using reinforcement, cooling and grouting compared to the use of conventional concrete.

The report shows the possibilities to use an unreinforced plug made of low-pH concrete as a resistance in the deposition tunnels. Today, some parameters are unknown and some data may be classified as uncertain, primarily regarding the long-term properties of the low-pH concrete material and the bentonite clay. It will take several years until all questions can be answered and a full-scale test is vital to validate the assumptions and the performed numerical simulations. The report should therefore be considered based on that data and conclusions will be studied further and be experimentally verified under realistic and controlled conditions.

The project group consists of: Patrik Gatter (VPC), Richard Malm (VPC), Lennart Börgesson (Clay Technology AB), Lars-Olof Dahlström (NCC-Teknik), Jonas Magnusson (NCC-Teknik), Christina Claeson-Jonsson (NCC-Teknik), Morgan Johansson (Reinertsen), Rikard Karlzén (SKB), Pär Grahm (SKB), Sten Palmer (Sten Palmer Engineering AB) and Hans Wimelius (NCC AB).

Sammanfattning

I SKB:s huvudalternativ KBS-3V, för slutförvar av radioaktivt avfall kommer de återfyllda deponeringstunnlarna att åtskiljas från det övriga tunnelsystemet med betongpluggar. Dessa betongpluggar skall dimensioneras för en livslängd på ca 100 år, och deras funktion skall vara fullgod fram till dess att transporttunneln utanför pluggen har återfyllts och naturliga geohydrologiska förhållanden har återställts.

Syftet med denna rapport är att dokumentera underlag och projektets utredning samt motivering för val av lämpligaste design för förslutning av deponeringstunnlar i kärnbränsleförvaret. Syftet har också varit att utreda och sammanställa de laster som verkar på pluggsystemet och utreda betongpluggens bärförmåga. Projektet som ligger till grund för denna rapport har bedrivits mellan 2009-01-01 – 2010-12-31, och projektgruppen har gjort sin bedömning utifrån de förutsättningar och krav som är kända idag.

Projektet behandlar hela designen, vilken bygger på ett system som innefattar filter, bentonittätning och ytterst en platsgjuten betongkonstruktion som huvudsakligen fungerar som mothåll. I föreliggande rapport studeras olika alternativa utformningar av betongkonstruktioner, en kupolformad plugg respektive en lång kilformad friktionsplugg. Resultatet i denna rapport fokuserar på valet av betongpluggen och dess möjligheter att se till att hela designen kan uppfylla de krav som ställs.

Det är en komplex uppgift att omhänderta det använda kärnbränslet och det ställer mycket höga tekniska krav på design och produktion av systemet för återfyllnad och förslutning av deponeringstunnlarna. Projektets målsättning är att designa och konstruera ett produktionsanpassat pluggsystem, med stöd av beräkningar och analyser, som kan möta rådande krav och förutsättningar. Betongpluggens funktion är i första hand att fungera som ett mothåll, men hela designen har höga krav på täthet, vilket också påverkar utformningen av betongpluggen. I kärnbränsleförvaret skall låg-pH betong användas i stället för konventionell betong. Orsaken till detta är för att i största möjliga mån undvika de negativa effekter som basiska material kan ha på bentonitlerans egenskaper. För detta ändamål har ett nytt betongrecept tagits fram i syfte att uppfylla de krav som ställs på designen. Förutsättningarna för armering, kylning och injektering är i och med detta skilda mot användandet av standardbetong.

Rapporten redovisar potentialen i att använda en oarmerad konstruktion tillsammans med en låg-PH betong som mothåll till svällande lera i deponeringstunneln. För närvarande är en del parametrar okända och en del data kan klassas som osäkra, främst avseende långtidsegenskaper hos betongmaterialet och bentonitleran. Det kommer att ta flera år innan samtliga frågor kan redas ut och ett fullskaletest bedöms vara nödvändigt för att slutligen verifiera antaganden och genomförda numeriska simuleringar. Rapportens resultat ska således betraktas mot horisonten att data och slutsatser kommer att studeras vidare och verifieras experimentellt under realistiska och kontrollerade former.

Projektgruppen består av; Patrik Gatter (VPC), Richard Malm (VPC), Lennart Börgesson (Clay Technology AB), Lars-Olof Dahlström (NCC-Teknik), Jonas Magnusson (NCC-Teknik), Christina Claeson-Jonsson (NCC-Teknik), Morgan Johansson (Reinertsen), Rikard Karlzén (SKB), Pär Grahm (SKB), Sten Palmer (Sten Palmer Engineering AB) samt Hans Wimelius (NCC AB).

Contents

1 Introduction

1.1 Background

SKB has decided to build the final repository for spent nuclear fuel in Forsmark. In the main alternative, KBS-3V, for the deposit of nuclear waste, the canisters with the spent fuel will be placed in a system of horizontal tunnels, at a depth of about 470 meters with vertical deposition in the crystalline basement rock. It is estimated that the tunnels will be about 300 meters long, and that they will be positioned about 40 meters apart. In the floor of the tunnels there will be deposition holes about six meters apart. A copper canister will be placed in the deposition holes and embedded in a bentonite clay buffer. When all the spent nuclear fuel has been deposited in the crystalline basement rock, the tunnels and shafts will be filled in with swelling clay.

The backfilled deposition tunnels will be separated and sealed from the transport tunnels with a plug, consisting of different material layers and at the end, a cast-in-place concrete plug. These plugs shall be designed for a lifespan of approximately 100 years and their function shall be maintained until the transport tunnels are backfilled and the natural geohydrological conditions have been retained. A principle illustration of the layout of the KBS-3V system is shown in Figure 1-1.

The impermeable copper canister fully contains the spent fuel, as seen in Figure 1-2. The bentonite buffer protects the canister against corrosion and movements of the rock. If a fracture occurs in a canister, the bentonite clay buffer will prevent water from penetrating into the canister. The buffer will also prevent the leakage of radioactive substances from the canister. The rock provides a natural environment in which the function of the technical barriers is maintained over a very long period. The rock, coupled with the great depth of the repository, effectively isolates the spent fuel from human beings and the environment.

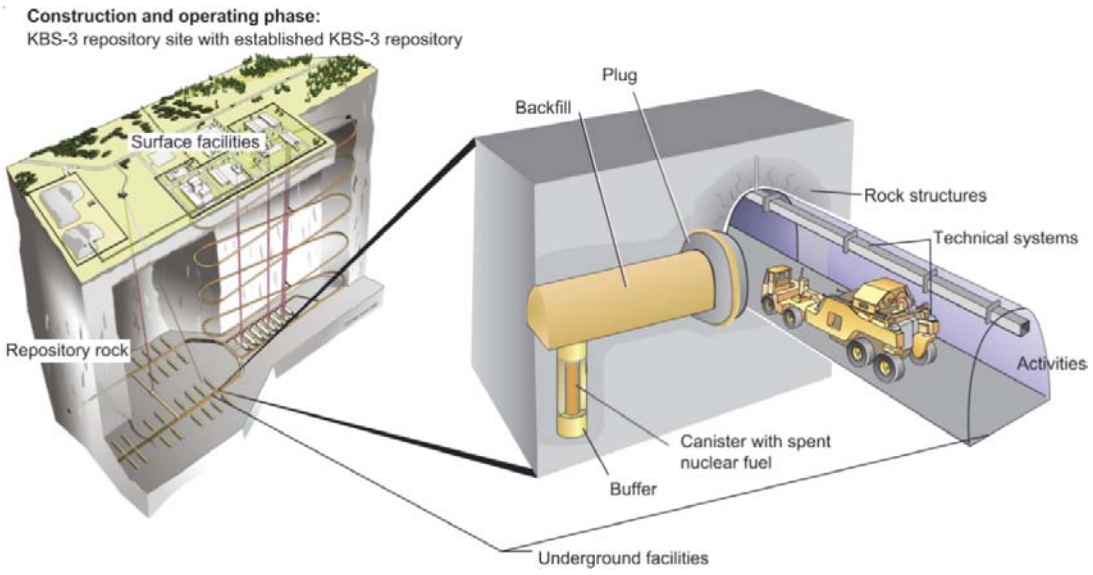

Figure 1-1. *Principle layout of the KBS-3V system, from SKB (2009).*

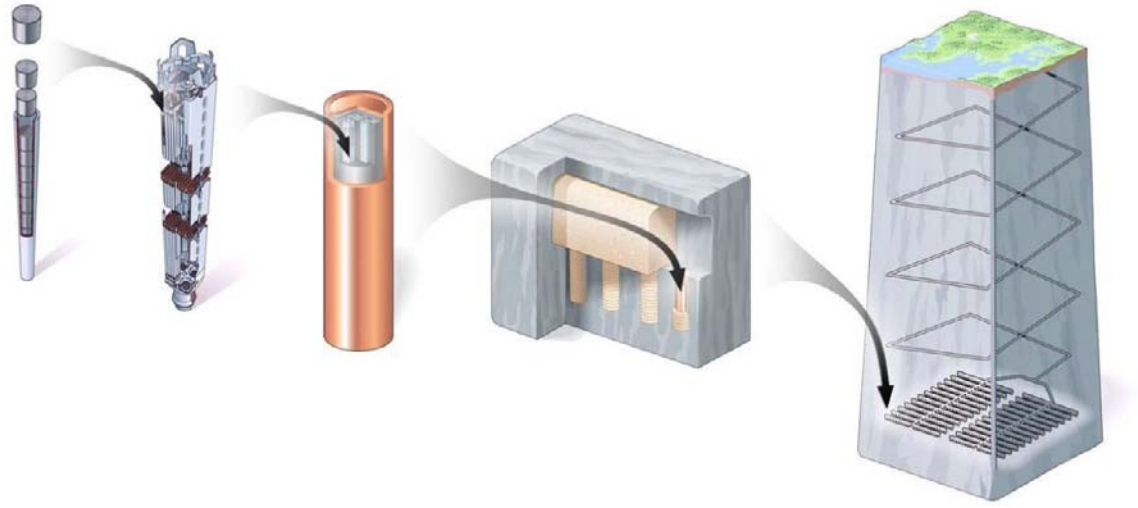

Figure 1-2. *The figure illustrates the process where the spent nuclear fuel is first placed in cast iron and then in the copper canister. The canister is placed in vertical holes in the floor of the deposition tunnel. The deposition holes and the deposition tunnel are filled with bentonite clay.*

1.1.1 Motivation for choice of basic design

In this report, an evaluation of the reference plug design intended for closing the backfilled deposition tunnel is presented. The outer barrier at the end of the deposition tunnels is designed as a concrete plug. The function of a prototype plug has earlier been constructed and tested in the Prototype Repository at Äspö HRL, see Dahlström (2009). However, the reference design has continuously been developed and assumptions changed during the process. This requires an updating of the design and at the same time, more detailed calculations that consider the variation in conditions from the time of casting to the end of the plug systems life span. The suggestions for the reference design made in this report are not part of the SKB reference design, instead it should be considered as recommendations for modification. The focus in this report is the evaluation of the concrete plug, which is the outer part of the plug system.

Different conceptual designs for the concrete plug have previously been evaluated. The two main alternatives that have been studied for the design of the concrete plug and that are presented in this report are shown in Figure 1-3. The alternative to the left is somewhat cone-shaped, called the tapered plug, and based on cohesion and friction to transfer the loads from the concrete plug to the surrounding rock.

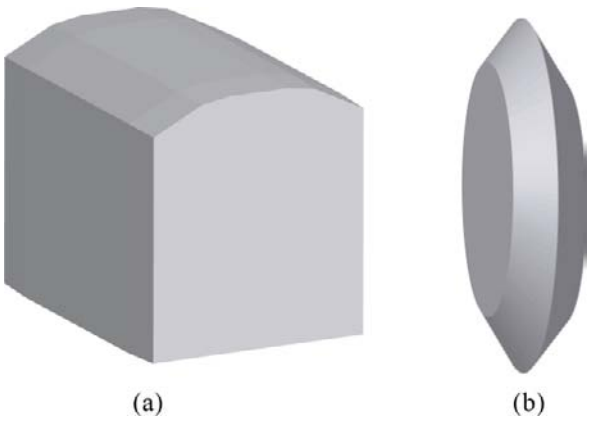

Figure 1-3. *Principle 3D sketches for the studied alternatives of concrete plug, a) tapered plug and b) dome shaped plug.*

The alternative to the right is dome shaped and the compressive forces in the concrete plug are transferred to the surrounding rock via its abutment. In the early investigations of this project, both of these two alternatives were studied. After progress in the project it was concluded that the dome shaped plug had a better possibility of satisfying the requirements of the concrete plug, especially regarding preventing leakage. For the remaining part of the project, the focus therefore shifted to primarily study the dome shaped plug. The long tapered plug was however not rejected as a possible design alternative, but it has some disadvantages that need to be compensated to become a competitive solution. More information behind the decision between the two alternatives is presented in Chapter 5 of this report.

One important factor when designing the concrete plug was to study the possibility of designing a concrete plug without reinforcement. In the initial studies of the concrete plug, it was found that only the minimum amount of reinforcement according to design codes was required to satisfy the design criteria's for the dome shaped plug. The reason for this is that due to the shape of this conceptual design, mainly compressive stresses occur within the structure (Dahlström 2009). After this, it was decided by SKB that low-pH concrete should be used for the concrete plug. Low-pH concrete is defined to have a pH-value below 11, while normal concrete have a pH-value above typically 12.5. The reason for this requirement is to minimize the effect that basic materials may have on the function of the bentonite clay. The developed recipe (Vogt et al. 2009) showed a large amount of autogenous shrinkage. It was feared that this would cause cracking due to the restraint forces in the reinforcement. With reinforcement, several small cracks would occur due to the shrinkage restraint and these cracks could potentially be leakage paths. In a concrete plug without reinforcement, the idea is that the concrete plug releases from the surrounding rock and thereby is subjected to free shrinkage. The slot between the concrete plug and the rock should thereafter be grouted. Studies were performed to determine whether it was possible to design an unreinforced concrete plug (Fälth and Gatter 2009, Dahlström et al. 2009) for the tapered and dome shaped plug respectively.

Another reason why it would be beneficial to design an unreinforced concrete plug is that recent studies at the Cement and Concrete Institute (CBI) show that low-pH concrete may have a lower resistance to prevent reinforcement corrosion. The high salt percentage in the groundwater leads to a high risk of corrosion of the reinforcement bars, which would cause corrosion spalling and thereby creating cracks and potentially a structure that could not prevent leakage of water and erosion of bentonite clay out from the deposition tunnel. The corrosion of the steel reinforcement would occur after a short time-period and thereby making it unsafe to rely on their strength in a design stage. The risk of corrosion could of course be prevented if stainless steel is used for the reinforcement. This would however, not prevent the risk of cracking due to the autogenous shrinkage and could therefore cause potential leakage out from the deposition tunnel.

One benefit of not using reinforcement is the amount of time saved, compared to reinforcing the concrete plug. In Section 1.1.3, the amount of reinforcement used in a previous full-scale concrete plug is shown. Designing an unreinforced concrete plug has benefits regarding both saving time and saving costs. This is not a critical issue, but it is an additional advantage with an unreinforced design.

In summary, the following factors indicate the reasons why it is beneficial to design an unreinforced concrete plug

- A dome shaped concrete plug is mainly subjected to compressive stresses and previous studies have shown that only minimum reinforcement is required to satisfy the design criteria.
- The low-pH concrete has a high amount of autogenous shrinkage and if the concrete plug is reinforced, there is a risk of restraint-induced cracks.
- Low-pH concrete has likely a lower corrosion protection for the reinforcement than compared to ordinary concrete.
- It saves time and costs to construct the concrete plug without reinforcement.

In the design phase of the concrete plug, the dome shaped plug was chosen after comparisons regarding pros and cons, risks, possibilities, etc., with the tapered concrete plug, see the results in Chapter 5.2. After which, the optimization phase of the geometry of the dome shaped plug started. Parallel to this, continuous development and experimental tests are being performed to optimize the concrete recipe.

1.1.2 Terminology

In this report, different terms are used and it is important to clarify what these terms are referring to and therefore they are summarized below. Below, a short description of the purpose and requirements of each part in the plug system is briefly explained.

Plug design or plug system – Referring to the complete design studied in this report as shown in Figure 1-4, including the layers (from inside the deposition tunnel and out):

1. Delimiter (wall of concrete beams).
2. Filter.
3. Delimiter (wall of concrete beams).
4. Bentonite seal.
5. Delimiter (wall of concrete beams).
6. Concrete plug.

Delimiters or wall of concrete beams – Referring to the pre-cast (prefabricated) concrete beams used as a delimiter to separate the different layers in the plug design. The prefabricated concrete beams are reinforced unlike the concrete plug. The concrete beams are assembled at site to form a wall. The concrete beams are made with the same low-pH concrete as the concrete plug.

Filter – Consisting of sand (or gravel) material and intended to be used to drain the tunnel while the concrete plug is being cast and matures. The filter is also used for artificially controlled wetting of the bentonite seal.

Bentonite seal – The watertight seal in the plug system. Consists of bentonite clay but has most likely a different density compared to the bentonite used in the buffer and the backfill.

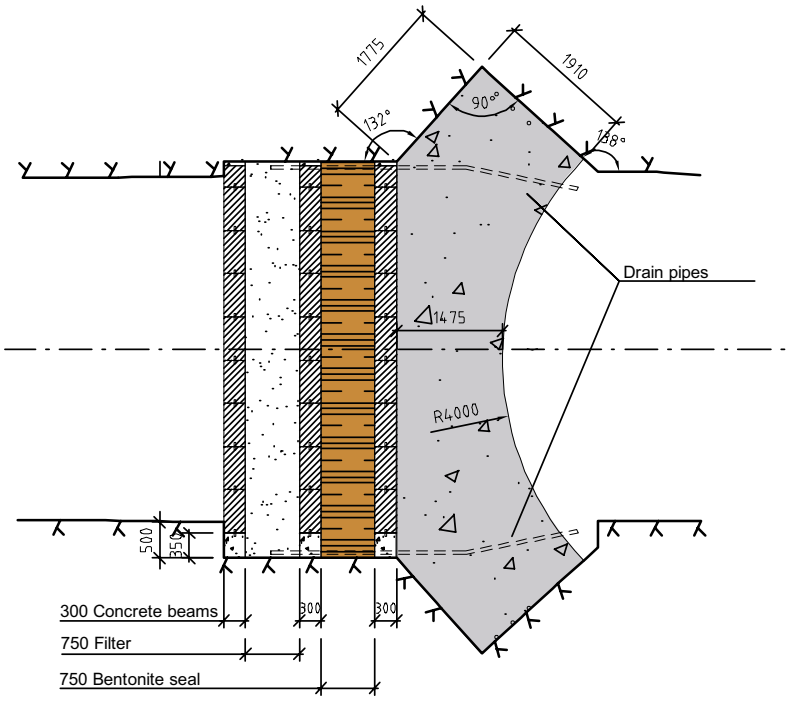

Figure 1-4. Sketch of the suggested plug design.

Concrete plug – Cast-in-place, unreinforced concrete plug made of low-pH concrete. The concrete plug has a dome shaped design, but other design alternatives have been studied. The dome shaped design has been referred to as the arch shaped plug in previous reports.

Lately, a geotextile has been considered to be placed between the last delimiter and the concrete plug to minimize the cohesion between the newly cast concrete plug and the wall of concrete beams. Besides this, it is planned that a plastic sheet is used to cover the downstream surface of the concrete plug for accumulation of the leakage water passing through and around the plug system.

Other important terms used in this report are:

Backfill end zone – The backfill closest to the plug system. It will most likely be designed differently from the rest of the backfill to reduce the swelling pressure on the concrete plug.

Slot – A v-shaped slot has to be excavated in a circular pattern around the deposition tunnel at the location for the dome shaped concrete plug. The slot acts as a geometric controlled abutment for the dome shaped concrete plug.

Deposition tunnels – The tunnels used for deposition of the canisters with spent nuclear fuel. The canisters are placed in vertical holes, placed 6 meters apart, in the floor of the deposition tunnel see Figure 1-2.

Transport tunnels – The tunnels used for transport. The deposition tunnels are excavated perpendicularly to the transport tunnels; see Figure 1-1 or Figure 1-2.

Upstream side – The upstream side of the concrete plug refers to the surface of the concrete plug that is facing the deposition tunnel, i.e. the side subjected to the pressure from the swelling bentonite clay and the hydrostatic water pressure.

Downstream side – The downstream side of the concrete plug refers to the side of the plug that is facing the transport tunnel, i.e. the side of the concrete plug that is subjected to atmospheric pressure.

1.1.3 Full-scale tests

SKB has earlier installed three concrete plugs in full-scale at the Äspö HRL (Hard Rock Laboratory), but all of these have been reinforced and made of ordinary concrete (Dahlström 2009). It has been determined that low-pH concrete should be used for the final repository of the spent nuclear waste, as mentioned in Section 1.1.1. The use of a low-pH concrete results in changes in the material properties regarding strength, curing, shrinkage, etc compared to conventional concrete. The conditions for using reinforcement, cooling and grouting are due to this different compared to the use of conventional concrete, which results in consequences regarding the design of the concrete plug.

One concrete plug with low-pH concrete has been experimentally studied at the Äspö laboratory (SKB 2006, García-Siñeriz et al. 2008) as part of the ESDRED-project. However, the concrete plug was made of shotcrete, i.e. sprayed concrete. This plug was made for the KBS-3H deposit and therefore tested for a much smaller tunnel diameter. In addition, the shotcrete plug was tested at a lower depth than the planned repository, approximately 220 m below ground level.

In Canada, a full-scale test has been conducted on a high-performance concrete plug. The concrete plug studied was a combination of the two plug designs shown in Figure 1-3 and was subjected to a pressure of 4 Mpa (Martino et al. 2007).

Backfill and Plug Test

The Backfill and Plug Test was intended to test different backfill materials, emplacement methods and a full-scale plug design. This test was performed to study the integrated function of the backfill material and the near-field rock in a deposition tunnel excavated by blasting. The test was also intended to study the hydraulic and mechanical functions of a plug system. This test was made as a preparation for the Prototype Repository, described in the next section. (SKB 2008a)

The main objectives of the Backfill and Plug Test were to

- Develop and test different materials and compaction techniques for backfilling of tunnels excavated by blasting.
- Test the function of the backfill and its interaction with the surrounding rock in a full-scale tunnel excavated by blasting.
- Develop technique for the construction of tunnel plugs and to test their function.

The inner part of the tunnel was filled with a mixture of bentonite and crushed rock in six test sections, each separated by a permeable mat, with a bentonite content of 30%. The composition is based on results from laboratory tests and field compaction tests. The outer part was made as a filter, which was filled with crushed rock, i.e. without any bentonite additive. A slot of a few decimeters was left between the backfill and the ceiling and it was filled with a row of highly compacted blocks, with 100% bentonite content to ensure a good contact between the backfill and the rock. The remaining irregularities between these blocks and the ceiling were filled with bentonite pellets. (SKB 2008a)

After the filter, a wall of prefabricated concrete beams was installed for temporary support of the backfill and filter until the concrete plug was cast. The concrete plug was made with ordinary concrete and had reinforcement. It was made as a dome shaped plug, and a 1.5 m deep v-shaped slot was excavated and installed with an “O-ring” of highly compacted bentonite blocks at the inner rock contact. The layout of the Backfill and Plug test is illustrated in Figure 1-5. In Figure 1-6 the design of the concrete plug is illustrated.

The installation was completed and the wetting of the backfill from the permeable mats started at the end of 1999. The water pressure in the mats was increased to 500 kPa in steps of 100 kPa between October 2001 and January 2002 and kept at 500 kPa until the backfill was judged to be water saturated in the beginning of 2003. During 2003, the equipment was rebuilt for flow testing and the flow testing started at the end of that year. The year 2004 and most of 2005 were used for flow testing of the six test sections of the 30/70 bentonite/crushed rock mixture in the inner part of the tunnel. (SKB 2008a)

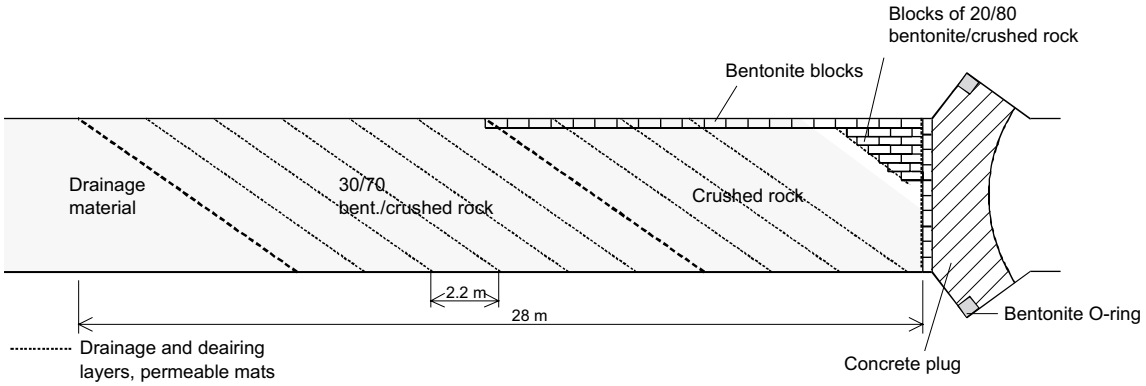

Figure 1-5. *Principle layout of the backfill and plug test.*

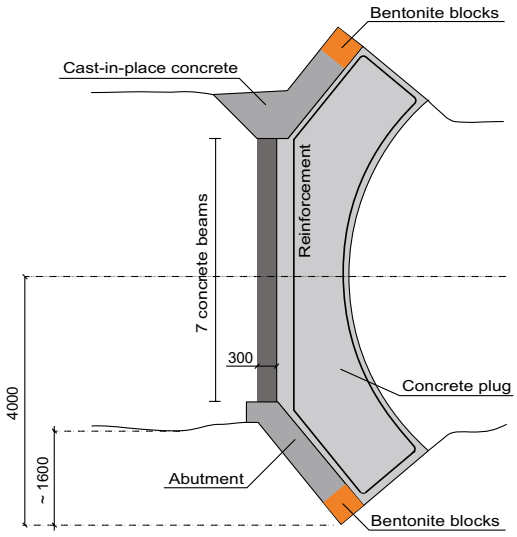

Figure 1-6. *Design of the concrete plug in the backfill and plug test.*

Prototype Repository

The location of the tunnel used for the prototype repository at Äspö HRL is shown in Figure 1-7. At Äspö HRL several different experiments have been performed or are ongoing. Some of the experiments are focused on research while others are focused to applications of different technologies. More information regarding the different experiments at Äspö HRL can be found on SKB's website (http://www.skb.se/Templates/Standard____29541.aspx).

The prototype repository is located at a depth of 450 m, as seen in Figure 1-7. The length of the tunnel used in the experiment was about 65 m. All material and scale were corresponding to the SKB-3V concept at the time. The spent nuclear fuel, generating heat, was however replaced with electric heaters.

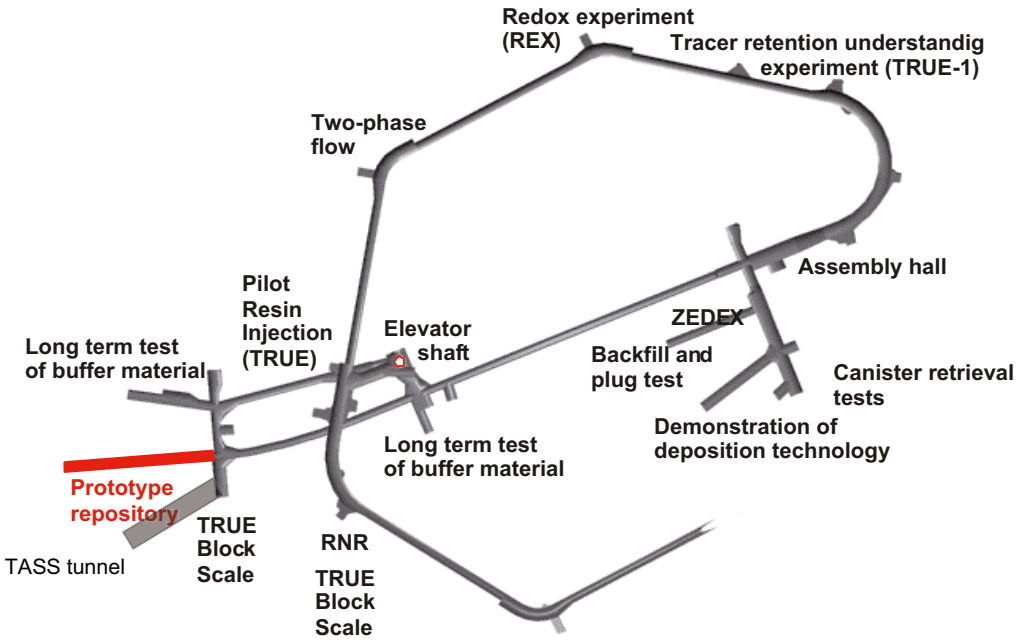

Figure 1-7. *Location of the prototype repository at Äspö HRL.*

The Prototype experiment consists of two sections for deposition of canisters, see Figure 1-8. Concrete plugs were constructed to separate the two sections, to achieve mechanical support to the backfill material, facilitate to enhance the water pressure around the experiment and separate the experiment from the surrounding tunnel system that is operated at atmospheric pressures. The inner section was planned to be retrieved after 20 years and the outer section was planned to be retrieved after 5 years. (Dahlström 2009)

The first prototype repository full-scale test, Section I in Figure 1-8, was made during summer and autumn 2001 and consisted of four full-scale deposition holes, copper canisters equipped with electric heaters, bentonite buffer consisting of blocks and pellets and a deposition tunnel backfilled with a mixture of bentonite and crushed rock ending with a concrete plug.

The second prototype full-scale test, Section II in Figure 1-8, was made during spring and summer 2003 and consisted of two full-scale deposition holes with a backfilled tunnel section ending with a concrete plug. Plug II, was comprehensively instrumented to investigate its mechanical response to the pressure load.

The main objectives for the prototype repository project were the following

- Test and demonstrate the integrated function of the repository components under realistic conditions at full-scale and to compare the results with model predictions and assumptions.
- Develop, test and demonstrate appropriate engineering standards and quality assurance methods.
- Simulate appropriate parts of the repository design and construction processes.

In the Prototype Repository the demand of leakage control is very high and the maximum length of the plugs is constrained due to available clearance space, experimental set-up and configuration. Therefore, a typical long tapered plug, see Figure 1-3 a), normally used to block waterways in connection with hydropower plants, was not suitable. Instead, a plug constructed as a dome shaped plug with a v-shaped abutment was considered, see Figure 1-3 b) and Figure 1-9. (Dahlström 2009)

To minimize the Excavation Damaged Zone (EDZ), seam drilling with coring technique was used to excavate the abutment, in which the plug was cast.

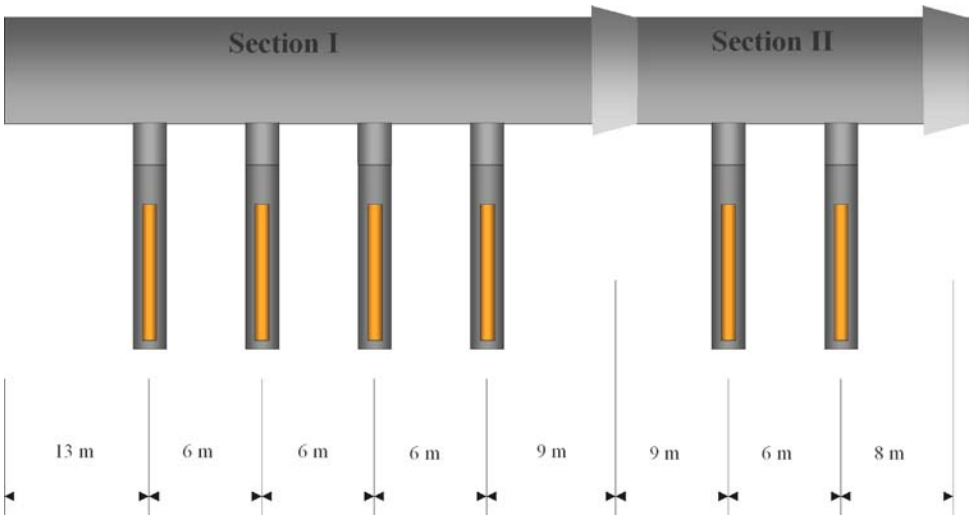

Figure 1-8. *A longitudinal layout of the prototype repository illustrating six deposition holes with canisters embedded in buffer clay and two concrete plugs.*

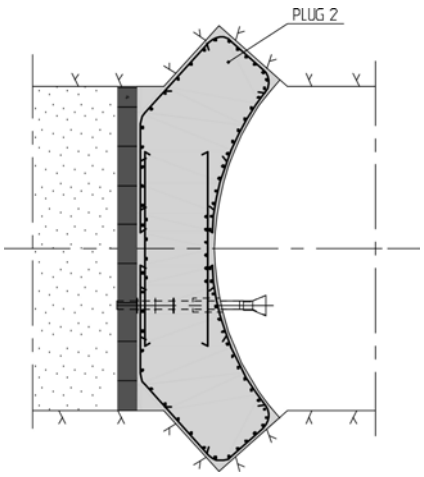

Figure 1-9. *A 2D sketch of Plug II in the Prototype Repository.*

The steel formwork was pre-assembled at the ground surface before taken down to the tunnel. The steel beams were bolted and welded together and crossbars and plywood were mounted on top. Before taken down to the tunnel, the formwork was separated into smaller pieces that were easier to transport down the tunnel but easy to assemble at the Prototype Repository experiment. Before assembling the formwork, a retaining wall was installed to resist the earth and compaction pressure developed from the backfill material. The retaining wall consists of pre-fabricated concrete beams that were installed in parallel with the installation of the backfill.

Reinforcement was cut and bent at the factory and ready for installation upon arrival at the site. Parallel to the installation of the reinforcement bars, the cooling system was installed together with measurement gauges and cables. A photo of the reinforcement of Plug II is shown in Figure 1-10.

Figure 1-10. *A photo of the reinforcement in Plug II in the Prototype Repository.*

Unlike the previous plug in the Backfill and Plug Test, both concrete plugs in the Prototype Repository were cast with Self Compacting Concrete (SCC). The SCC was mixed at the factory and continuously delivered on site. Mixing and casting SCC are more complex procedures than for standard concrete and require experienced personnel and a well-developed control program. It is important to use correct procedures and well-known ingredients when mixing SCC. After a controlled curing, the plug was cooled down to a temperature about 10 degrees below the ambient temperature to facilitate better penetration and filling of grout during contact grouting process. Contact grouting was performed through pre-installed grouting tubes. Mechanical measurements have been performed to monitor and verify the function and the behavior of the plug. Stresses and deformations are not perfectly correlated between the calculated and the measured. However, the measurements show that the plug behaves as expected and that the entire plug is compressed, which was the purpose of its design. (Dahlström 2009)

More than 1,100 transducers were installed in the rock, buffer and the backfill, according to Johannesson et al. (2007). The transducers measure the temperature, the pore pressure and the total pressure in different parts of the test area. The water saturation process was recorded by measuring the relative humidity in the pore system of the backfill and the buffer. Furthermore, transducers were installed for measuring the displacement of the canisters.

Transducers for measuring the stresses and the strains in the rock around the deposition holes in Section II were also installed. The purpose with these sensors was to monitor the stress and strain caused by the heating of the rock from the canisters. (SKB 2008a)

The heating of the canisters, was simulated with heating elements, each giving an initial power output of 1,800 W. Gradually the power of the heating elements was reduced to describe the radioactive decay.

At the beginning of November 2004 the drainage of the inner part of Section I and the drainage through the outer plug were closed. This led of course to a drastic change in the pressure (both total and pore pressure) in the backfill and the buffer, as seen in Figure 1-11. As the pressure increased one of the heaters failed and due to this, the drainage of the tunnel was opened again. The damage of the heating equipment in the canister was too severe to be used again. An additional problem with the heating of one of the other canisters has also occurred, which resulted in the heating power having to be reduced. The heating in the rest of the canisters is still working as intended. The drainage of the tunnel has been open since the heating failure of the first canister was detected. This has led to low water pressure been built up in the tunnel and resulting in slow saturation of both the backfill and the buffer. The pressure in the buffer is slowly but continuously increasing. However, the excavation of the nearby TASS-tunnel, which started in April 2007, is influencing the measured pressure in the Prototype Repository, as seen in Figure 1-11. (SKB 2008a)

In general, the installation of the buffer, canisters and backfill went well and so far almost all instruments have worked and yielded valuable results according to Johannesson et al. (2007). More information regarding the Prototype Repository full-scale test is found in SKB (2008a) and Johannesson et al. (2007).

Low-pH Shotcrete Plug Test

The Shotcrete Plug Test was part of an ESDRED project to develop and demonstrate low-pH concrete formulations suitable for the construction of underground repositories for the disposal of nuclear wastes. Two shotcrete plugs have been built, the first one at the Äspö Hard Rock Laboratory and a second one at Grimsel Test Site in Switzerland. The first plug was tested up to failure with a hydraulic pressure provided by a pump and thereafter dismantled and analyzed.

The plug tested at Äspö was 1 m long, without keys in the rock, i.e. and the tunnel was located at a depth of 220 m. The tunnel had a diameter of 1.85 m and was excavated with a boring technique. An insulation membrane covering the rock walls and the rear face of the plug was used to hydraulically seal the water chamber. The spraying of the shotcrete was performed manually, using a stand-alone concrete pump, see Figure 1-12.

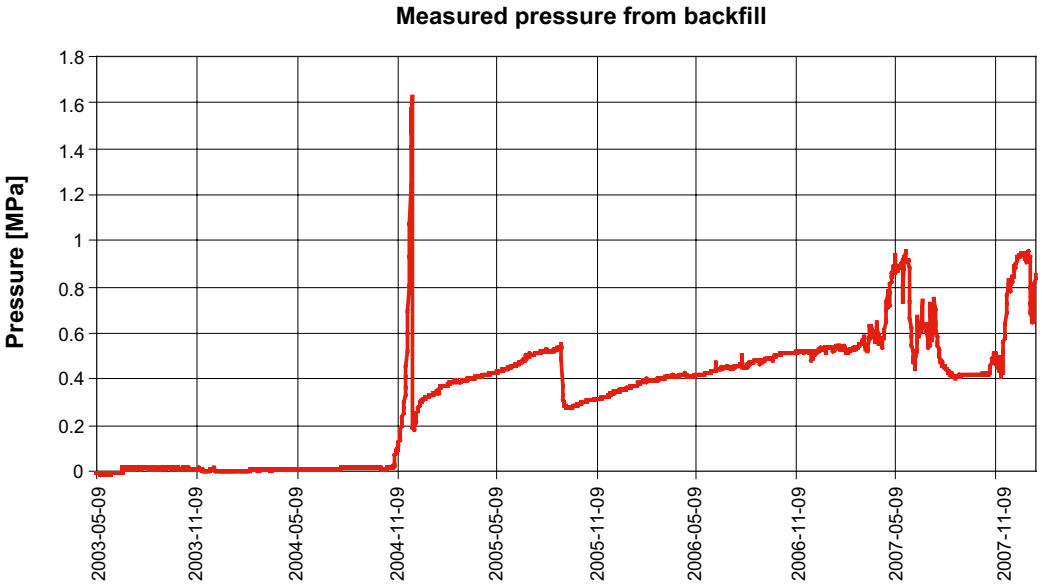

Figure 1-11. *Measured pressure in the backfill, from Dahlström (2009).*

Figure 1-12. *Photo of the Shotcrete Plug.*

Pressure cells, extensometers and acoustic sensors were installed within the plug and the surrounding rock. In the test, the pressure in the water chamber was increased step-by-step. The plug overcame elastic deformations during the pressure increase, with recovery when the pressure decreased. Despite the significant water leakage that was detected in the bottom of the plug, it was possible to increase the pressure up to 27 bar, i.e. 2.7 MPa, when it was judged that the plug had "failed", given the sudden increase in the rate of the displacement. After releasing the pressure, two additional load tests were performed and the plug started to move non-linearly when reaching a pressure of 25 bar, i.e. 2.5 MPa. According to the measurements the total displacement of the plug was 16 mm. (García-Siñeriz et al. 2008)

During the evaluation of this project, there were however concerns regarding if the shotcrete plug had moved and become wedged in the tunnel. This could have led to a case where the load capacity is over-estimated and thereby questioning the validity of the experimental results.

Unreinforced high performance concrete plug

In the tunnel sealing experiment (TSX) in Canada, a full-scale test of an unreinforced high-performance concrete plug has been studied. The design of the concrete plug is a combination of the two alternatives shown in Figure 1-3. The test set-up included both a concrete plug and a clay seal (consisting of keyed highly compacted clay block bulkhead) that were tested simultaneously. The tunnel section had an elliptical shape and was 4.4 m wide and 3.5 m high. The ambient temperature in the tunnel was 15°C. The test set-up and the dimensions of the concrete plug are shown in Figure 1-13. The operation of the TSX began on 1998 September 21 with the initial flooding of the chamber between the bulkheads. In the experiment, the tunnel was filled with water resulting in a pressure of 4 MPa on the concrete plug. (Martino et al. 2006)

During the initial pressure build up, large seepage in the contact between concrete and rock was observed. At a pressure of 0.3 MPa the seepage passing the concrete plug was measured to 1.6 l/min. It was judged that it would not be possible to operate under the full pressure of 4 MPa with an extrapolated seepage of 20 l/min. Due to this, the pressure was reduced and grouting was conducted using pre-installed tubes and geomembranes at the interface. According to Martino et al. (2007), the grouting reduced the measured seepage by three orders of magnitude. When the final pressure of 4 MPa was reached, the temperature on the upstream side of the concrete plug and the clay seal was increased to 50°C and then to approximately to 65°C in a second heating step. After this, a cooling period of three months was conducted prior to draining the tunnel.

At an ambient temperature and 4 MPa hydraulic pressure the seepage past the concrete plug and the clay seal were approximately 10 and 1 ml/min respectively after 1,400 days of operation, as seen in Figure 1-14. When the temperature was increased there was essentially no change in the seepage past the clay seal but because of the expansion of the concrete with heating the seepage past the concrete plug decreased to approximately 1 ml/min. During cooling, the seepage past the concrete plug increased again to approximately 2 ml/min.

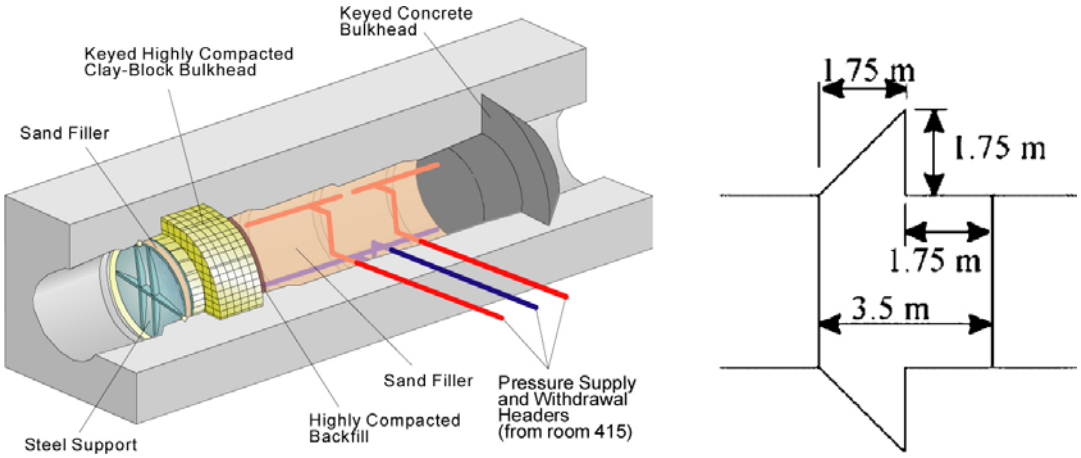

Figure 1-13. *Full-scale test of the TSX plug. The left figure shows the test set-up and the figure to the right shows the dimensions of the concrete plug.*

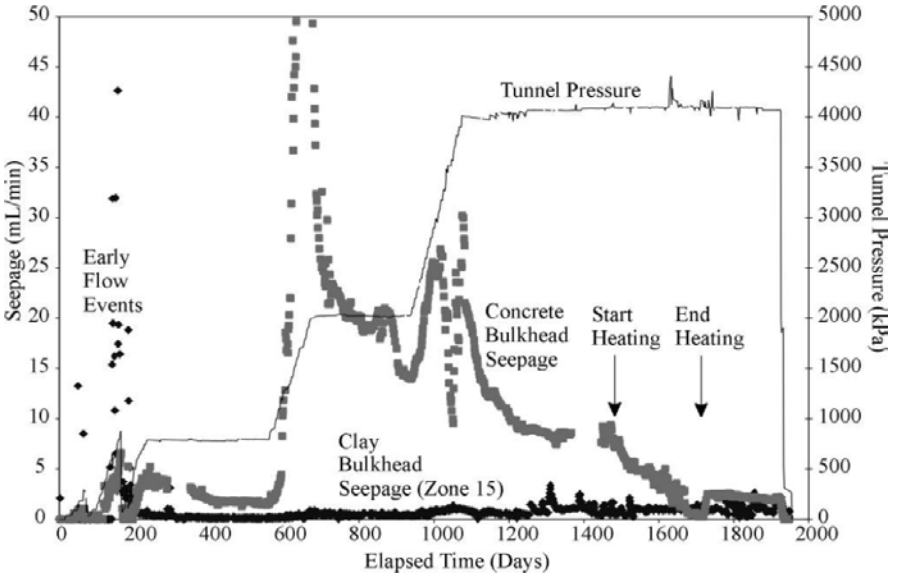

Figure 1-14. *Measured seepage past the concrete plug and the clay seal in the TSX plug, from Martino et al. (2006).*

Summary of full-scale experiments

None of the previous full-scale concrete plugs for the KBS-3V repository has been subjected to the expected pressure of hydraulic water pressure and the swelling pressure of the bentonite clay. In addition to this, the measurements of leakage have been performed in a manner, making it impossible to separate the three different types of leakage; through the concrete plug, in the contact between the concrete plug and the rock or only passing through the rock. The requirements of the plug system have changed over time and this has resulted in that the previous full-scale tests were not performed with materials of the same properties that are considered for the current reference design. For instance, the concrete plug in the suggested design is made of low-pH concrete and unreinforced. In addition, the bentonite seal, filter and drainage in the previous full-scale experiments have not been part of the plug design.

The requirement of water-tightness in combination with a concrete plug subjected to high pressure is a challenge. The experiences from the TSX plug in Canada (Martino et al. 2007) and the previous full-scale tests at Äspö HRL are valuable for the design of future full-scale tests.

1.1.4 Applications for tunnel plugging and sealing

Plugging or sealing of underground excavations is used for different applications and a variety of reasons. The different plugging approaches and applications have been defined in five categories for the purpose of discussion.

1. Civil construction industry – hydro electric, civil applications.
2. Construction of natural gas storage caverns.
3. Mining industry.
4. Nuclear waste isolation.
5. Military fortification.

Each of these applications has different goals and functional requirements that need to be met, and may thereby not meet the requirements set for a repository. In this section a brief summary of applications other than for the repository of nuclear waste are presented.

In many applications, the plugs need to restrain entirely water filled excavations where unrestrained flow could have catastrophic consequences. This situation is less likely to exist in a repository where the excavations have been backfilled with low permeability clay (Dixon et al. 2009). The purpose of the plug design for the final repository presented in this report is therefore somewhat different than in the other applications. In the plug design for the final repository, the purpose is mainly to control the seepage and preventing buffer erosion into still open areas, this is further described in Section 1.2.

Hydro electric and civil engineering applications

Construction and operation of high-head hydroelectric facilities need to be able to turn on and off and to control the rate of supply of the intake water to the penstocks and the turbines. These plugs typically consist of concrete that fill most of the tunnel and has a centrally located perforation that can be mechanically opened and closed to control water supply. In Norway, high-head hydroelectric facilities are common, where some have hydraulic heads as high as 900 m according to Dixon et al. (2009). These concrete plugs are made as tapered plugs, see Figure 1-3, and their length is about 17–23 m for cases with a distance of 500 m to the ground water level. The contact grouting is repeated several times until the flow is reduced to a level deemed acceptable. However, Bergh-Christensen (1988) reported that 90% of the leakage past these types of plugs is at the rock-concrete interface.

Natural gas storage

These facilities, located deep underground, often use abandoned mines that are capable of withstanding the high pressures that natural gas is stored at, which is approximately 12.5 MPa according to Pacovský (1999). The plugs for natural gas storage are quite similar to the plug required for repository, both have a potential to be subjected to high pressures on the upstream side and both have to prevent transfer of material (gas or water).

Results from a full-scale test conducted with a fiber reinforced shotcrete plug for natural gas storage is presented in Pacovský (1999). The natural gas storage facility was in a plutonic (granitic) rock mass, 950 m below the ground surface. The plug was 4.5 m long and was keyed 1.7 m into the walls of a tunnel having a nominal diameter of 3 m.

Mining industry

In many mining environments, a situation may develop where old excavations have to be plugged to continue excavating elsewhere. The purpose of the plugging is to reduce water inflow into operational sections of the mine to a level that can be managed by the mine dewatering pumps. The leakage through such plugs is however much higher than what will be allowed for the repository.

At the end of the service life of the mines, there is a need to install plugs and seals at critical locations. These plugs are often there to prevent intrusion into the old mine and to hydraulically isolate the mine from the surface environment.

Plugs may also be used in the mining industry for environmental control and remediation. One of the more serious issues facing the metals mining industry in recent years is that of acid mine drainage and associated heavy metals contamination of mine discharges. One way of dealing with this, once ore extraction has been completed and mine decommissioning is desired, is to seal the mine workings and limit future percolation of groundwater through and subsequently discharge into the surface environment. (Dixon et al. 2009)

Military fortification

The purpose of the protective barriers is to close a facility against enemy attacks and shall protect against conventional weapon effects, nuclear weapons and gas. The protective barriers are normally made as reinforced concrete plugs. The design is complicated due to their large thickness compared to its span and due to the fact that they primarily are designed to resist dynamic loads. According to construction recommendations presented by Sundquist and Örbom (1973), the concrete plug should be designed as a dome or arch to make better use of the concrete properties and to create a construction where its mode of action causes a more tightly connection against the rock abutments. The requirement of gas tightness is in Sundquist and Örbom (1973) only presented for pressures up to 0.1 MPa.

1.1.5 International nuclear waste management programs

Several countries are investigating the possibility to deposit spent nuclear fuel underground. In Table 1-1, the deposit environment, depth and the political strategy for a number of countries are summarized. Based on the international comparison it can be established that SKB is in the frontline in their developing work and that few experiences may be gathered from the other countries. The preconditions for the design are world unique and experiences from other types of constructions are difficult to apply on the plug design.

Table 1-1. Nuclear waste management programs in different countries, based on http://www.japannuclear.com/nuclearpower/program/waste.html [2010-12-20].

Country	Forms of Waste	Layers of Sites Proposed	Depth of Disposal Sites	Past Events	
USA	Spent Fuel Vitrified Waste	Tuff	Approx. 350 meters	1991: Started research of features of Yucca Mt. Site. 1998: Announced viability assessment of a repository. 2002: US Congress approved Yucca Mt. as a final disposal site. 2004: DOE applies to NRC for construction permit. 2005: DOE starts construction.	2010: Planned start operation of a final disposal site. In 2009 the Obama Administration stated that the site was no longer an option and proposed to eliminate all funding in the 2009 United States federal budget.
France	Spent Fuel Vitrified Waste	Granite Clay layer	400 ~ 1,000 meters	1995: 3 sites proposed for underground research facilities were selected. 1996: Application for construction permission and public hearing. 1999: Allowed to construct underground research facilities on a clay layer. 2000: Started site selection for underground research facility on granite, but selection was suspended due to opposition movement. 2006: National Evaluation Commission submits an overall evaluation report on waste studies.	~2015–2020 ANDRA: construction. ~2020–2025: Commercial operation.
Germany	Spent Fuel Vitrified Waste	Rock salt layer	660 ~ 900 meters	1977: Gorleben was selected as a site proposed. 1984: Safety study report on disposal (PSE). 1988: Characterization evaluation (CEC PAGIS). 1997: Finished digging shafts.	2030: Commencement of operation is planned.

Country	Forms of Waste	Layers of Sites Proposed	Depth of Disposal Sites	Past Events	
Belgium	Spent Fuel (Returned Waste)	Clay layer	220 meters	1974–89: Disposal safety research at Mol laboratories. 1989: Safety evaluation (SAFIR-I). 1994: Started making study programs of deep layer disposal.	2000–15: Verification tests on real waste. 2025: Receive permission of a disposal site by royal order. 2035: Start operation of a disposal site.
Finland	Spent Fuel	Granite	Approx. 500 meters	1983: Launched study activities. 1987: 5 sites to be surveyed were selected. 1995: Submitted an environmental assessment report. 2001: A disposal site proposed was decided (Parliament approved). 2003–04: Start constructing underground research facilities. 2006: Surveys at the depth of a disposal site.	2012: Construction license application. ~2018: Operation license application. ~2020: Start full operation.
Sweden	Spent Fuel	Granite	Approx. 500 meters	1983: Concept design, evaluation report (KBS-3). 1990: Started constructing underground research facilities. 1992: Safety evaluation (SKB91), announced SKB research development verification plans. 2000: Applied for site surveys at Oskarshamn, Östhammar, and Tierp. 2009: SKB decides to choose Forsmark (Östhammar) as site for disposal.	2012: Disposal for verification. ~2025: Start full operation.
Japan	Vitrified Waste	Granite Sedimentary rock	Deeper than 300 meters	1989: Important items and implementation of R&D (AEC). 1992: The first interim report (H3 report). 2000: Governmental evaluation on the second interim report. 2000: Law on final disposal of designated radioactive waste was promulgated.	2008–12: Selection of areas for detailed observation. 2023–37: Selection of a site for repository construction. ~2025: Design of the repository; start of construction. 2033–37: Start of operation.
Canada	Spent Fuel	Granite	Approx. 500 meters	2005: Canada's nuclear waste management organization (NWMO) recommended an "adaptive phased" approach to manage Canadian spent fuel.	2005–2035: Suitable site for deep geological repository selected. ~2060: Commercial operation.
Switzerland	HLW	Granite Clay		2 underground labs in granite (Grimsel) and clay (Mt Tersi) are in operation.	The Swiss law stipulates a geological disposal should open before 2040.

1.2 Objectives of the project

The project consists of the complete design of the plug system intended for sealing the deposition tunnels, as seen in Figure 1-4. The backfill, consisting of bentonite clay, closest to the plug system is going to be designed to reduce the swelling pressure from the clay. The plug system consists of a filter, bentonite seal and the cast-in-place concrete plug. These layers are separated from each other with delimiters, preventing the materials from mixing and to improve the production of the plug system. The delimiters are at this stage of the development, planned to be constructed of pre-cast concrete beams. Concrete beams have been used in the previous prototype plugs, as seen in Section 1.1.3, and are currently being planned to be used in the next full-scale test of the plug system. It is however possible that one or more of these concrete beam delimiters can be replaced with delimiters of an alternative material in the actual full-scale repository.

The purpose of the plug project is to develop a plug design that keeps the backfill in place and prevents an axial water flow and thereby preventing erosion of the buffer so that the buffer maintains its ability to prevent possible leakage of radioactive substances. The bentonite seal is intended to be the watertight seal in the plug system, but ultimately all individual parts should assist with the best of their capabilities to prevent leakage from the tunnel.

In order for the barrier system of the final repository to withstand conditions, events and processes that may impact their functions, the plug system shall:

- Withstand the hydrostatic pressure at repository depth and the swelling pressure of the backfill until the transport tunnel is filled.
- Limit water flow past the plug until the adjacent transport tunnel is filled and saturated.
- Be durable and maintain its functions in the environment expected at the repository facility and repository until the closure in the transport tunnel is saturated.

In order for the repository to maintain its multi-barrier principle, the plug design must (in the long-term perspective of the final repository):

- not significantly impair the barrier functions of the engineered barriers or the rock.

These functions and properties shall be secured and maintained during different periods of the lifetime of the plug.

The main requirement set on the plug design is to create a watertight barrier that prevents leakage from the deposition tunnel into the transport tunnel. This requirement results in other requirements on the different components in the plug design. The concrete plug has to carry the loads from within the deposition tunnel. These loads are external pressures, originating from water and swelling pressure of the bentonite clay, thermal increase from the spent nuclear fuel as well as load effects from the concrete plug itself such as shrinkage, etc. The backfill end zone is designed to limit the swelling pressure from the backfill to an acceptable level. The filter should contribute to limiting the swelling pressure from the backfill and be possible to be used to drain the deposition tunnel until the concrete plug has been grouted. The filter is also used for artificial controlled wetting of the bentonite seal. The bentonite seal has to prevent leakage from the deposition tunnel. It should be designed so that the swelling pressure on the concrete plug is within acceptable limits. Another design criterion is that the seal should be watertight as soon as possible after installation.

The objective of this project is to obtain a plug design that is deemed likely to fulfill all the requirements and that is suited for production.

The plug design project has resulted in design drawings and documents for a suitable full-scale test design. The next project, following this, has the focus on a full-scale test and to optimize the components in the suggested plug design.

1.3 Objectives of the report

The main purpose of this report is to summarize the evaluation process and the results of the suggested design for SKBs reference plug design.

The result in this report is focusing on the concrete plug and its possibilities of assuring that the complete plug design can satisfy all requirements. The design of the plug system behind the concrete plug, will for instance affect the loads on the concrete plug. The requirements on the complete plug system influence the design of the individual parts of the system and ultimately determine which concrete plug design is most suitable. During the project, it has therefore been important to study the requirements, functions, preconditions, risks and possibilities of all individual parts as well as the whole plug design.

The results in this report have a focus on the concrete plug in the reference design and the evaluation of its design and safety concept.

Within this project, a great deal of effort has been focused on defining the actions that influence the plug system. It has both been identifying the loads that may occur as well as estimating their effect and when the effect is likely to occur.

1.3.1 Limitations

The plug system presented in this report is not optimized and hence not the exact final design. This is the starting point for more extensive studies regarding optimization of all the internal components in the design. The present design is however suitable for production and is judged likely to fulfill all requirements. One issue that has been discussed extensively within the project group is the prefabricated concrete beams used as delimiters. Similar concrete beams have been used in the previous prototypes. There is a possibility that some of the concrete beams may be replaced with geo-textiles in the final design.

The other components of the reference design such as the filter and the bentonite seal are optimized in the next project. The backfill and the buffer are not treated in this report.

1.3.2 Program for quality assurance

The results from this project, presented in this report have been subjected to review on different levels. Most of the results presented in this report have either been published as internal SKB documents, each subjected to its individual reviewing process both internal and external. As the material has been assembled into this report additional reviewing has been performed both internally, within the project group, and then again by new external reviewers.

In this report, results from structural analyses are presented. The analyses have been performed with different numerical software's and by different individuals. These results are compared and evaluated in this report to verify that the results all indicate the same behavior and give similar results. During the progress of this project, the preconditions have been changed. Therefore, the preconditions in all analyses have not been the same. Hence, the results from all numerical analyses are not identical.

The preconditions have been interpreted differently in some cases and it is intended to show in this report that despite this, the results support each other and are not in contradiction. The principal strategy with the numerical analyses has been to perform them with a varying degree of conservatism. One example is the determination of the maximum swelling pressure from the bentonite clay. In the first analyses, a very conservative limit was used where the analyses were stopped when the stresses reached the design value. This could for instance be performed on either the actual structural design or on a reduced cross section where all concrete elements assumed cracked were removed from the analyses. In the following, more detailed analyses the non-linear behavior was introduced where the crack opening process and the reduction in concrete strength due to cracking was included. It is not possible to compare the design of the concrete plug with the design of normal structures according to Design Codes. The reason for this is that the loads that the plug design is subjected to are not covered by normal Design Codes. Therefore, the design of the concrete plug intends to show with

probability analysis that the structure is at least safer than what is specified according to the Swedish Design Code. The materials will be subjected to loads and environments that are unique and therefore several independent experiments are performed to determine the material behavior.

The numerical analyses should be verified in the next stage of the project by means of experimental studies. The whole suggested plug design, described in this project, is scheduled to be tested in a full-scale test at Äspö Hard Rock Laboratory in 2012. At the full-scale test, the production procedure can be tested and the leakage past the plug design can be measured.

1.3.3 Contents of the report

In Chapter 1 the background, project description and the objectives are presented.

In Chapter 2, the current reference design is described along with this projects recommendation for modification of its components and the construction procedure.

Chapter 3 presents the functional requirements of the plug design, together with a material description of its components and a summary of the loads acting on the plug design.

In Chapter 4, the numerical analyses performed to evaluate the structural behavior of the concrete plug are presented.

In Chapter 5, an evaluation of the reference design is presented together with risk assessment and the possibilities and limitations of the solution.

In Chapter 6 the conclusions from the project is presented.

In Chapter 7 the future work that needs to be performed are presented.

2 Design of plugs

In this section, the principle layout of the reference design and all its components, and their function, is presented. In addition, design drawings and sketches are included and the construction process is described for the suggested modification of the reference design.

2.1 Reference design of the KBS-3V concept

The canisters in the deposition holes will be surrounded with highly compacted bentonite rings, constituting the buffer. The deposition tunnels are backfilled with swelling bentonite clay in shape of blocks and pellets along the whole length of the tunnel up to the first delimiter (concrete beam) of the plug system. The primary function of the buffer is to be a watertight barrier around the canisters with spent nuclear fuel, which sets a requirement on the allowed density of the buffer material. A longer period of erosion of buffer material may jeopardize the possibility of the buffer to act as a barrier.

SKB plug reference design concept for closing of the deposition tunnels, when all canisters for spent nuclear fuel are deposited, is based on a bentonite sealing layer supported by a spherical concrete dome structure arching between recesses constructed in the rock walls.

In this report, the reference design is studied and suggestions are made regarding the dimensions and compositions of the layers and especially the shape of the concrete plug. These suggestions are not part of the SKBs reference design. Instead, these suggestions are the recommendations made by this project for modification of the SKB reference design.

The general requirements on the plug design are mainly related to the buffer and the risk of piping and erosion that could occur. The plug system has to be watertight to stop or reduce the axial flow from the buffer, and in addition to this also be able to keep the backfill in its place, i.e. it has to be able to resist the pressure from the hydrostatic water gradient and the swelling pressure from the clay. The requirements of the plug design are further described in Section 3.1.1.

The requirements on the backfill are related to the buffer around the canisters. The backfill of the deposition tunnels must be able to act as resistance for the axial expansion of the buffer, and it should also be able to heal leakage channels that could occur due to piping, and apply a pressure on the surrounding rock of at least 100 kPa.

2.1.1 General description

The first layer in the reference design, closest to the backfill, is a filter and consists typically of sand or gravel. Its purpose is to buffer water and to be used for controlled artificial wetting of the bentonite seal. The filter should also make it possible to drain water from the deposition tunnel until the concrete plug has reached adequate strength and, if required until, the contact grouting has been performed. The filter should thereby also control the water pressure inside the plug system until the concrete has cured. Drainpipes will be arranged from the filter to the downstream side of the plug, as seen in Figure 2-1, with the purpose to drain the filter until the concrete plug is grouted. The drainpipes can also be used to pump water into the filter again after the grouting, to control the time it takes to artificially saturate the bentonite seal and thereby ensuring a fast and homogenous wetting of the bentonite seal. The filter should also preserve a high water pressure in case the plug system is not sufficiently watertight. The controlled artificial wetting will ensure that the pressure build-up on the concrete plug is controlled regarding both its size and its time of arrival.

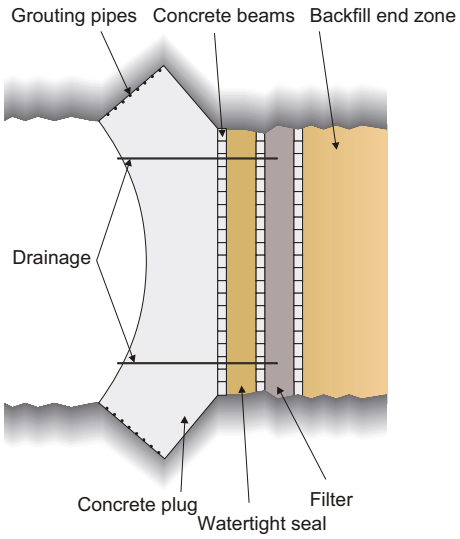

Figure 2-1. *Principle layout of the reference design of the plug system, from SKB (2010a).*

The layer closest to the concrete plug, the bentonite seal, consists of swelling clay of which the purpose is to prevent axial flow from the backfill and the buffer. The layer should intersect the EDZ, i.e. the excavated damaged zone. The purpose of the bentonite seal is to heal cracks that may initiate on the upstream side of the concrete plug, and thereby prevent leakage out from the deposition tunnel.

The final layer is the concrete plug, which should be cast with low-pH concrete and without reinforcement. The preferable geometry of the concrete plug is a dome shape.

Between each layer (filter, bentonite seal and the concrete plug) are delimiters assembled to separate the materials in the different layers from each other. In the present design the delimiters are arranged as prefabricated concrete beams, which was the solution used in the prototype test set-up. A principle sketch of the reference design is shown in Figure 2-1 and a drawing of the suggested plug system is shown in Figure 2-2.

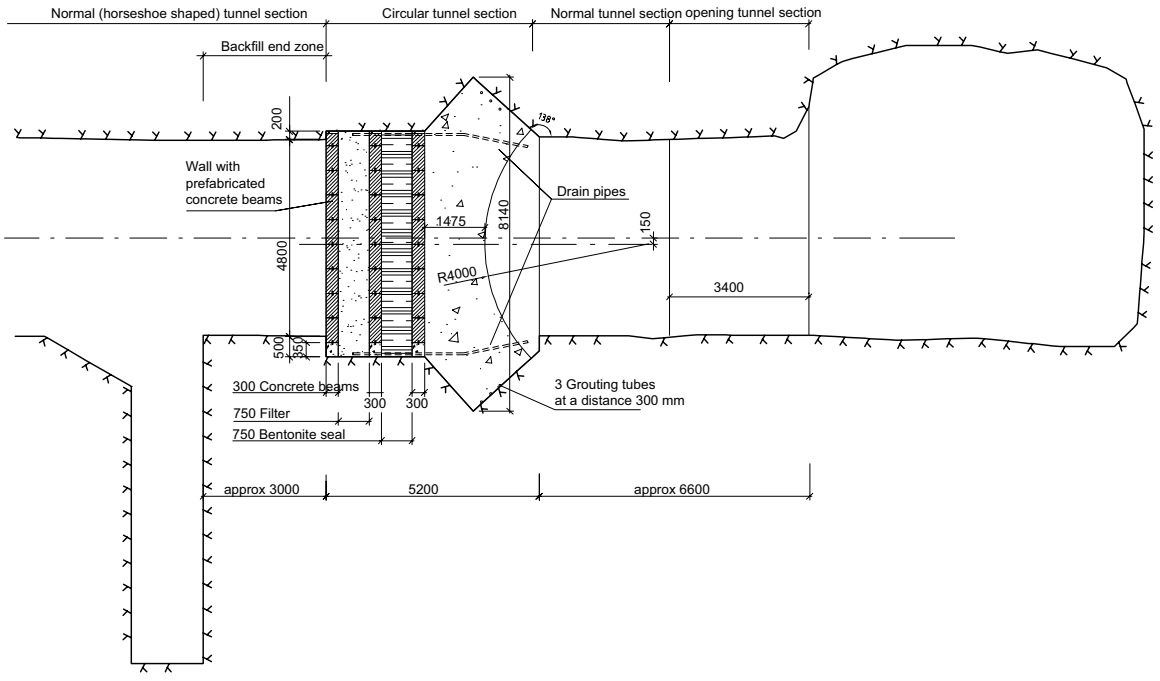

Figure 2-2. *Layout of the suggested design of the plug system.*

2.1.2 Backfill

Materials that may be used as backfill can be divided into three main categories: bentonite clays, smectite-rich mixed layer clays and mixtures of bentonite and ballast. In the reference design, the backfill material is low-grade bentonite clay, with the material composition specified in Table 2-1. Example of such materials are Milos (Greece), Wyoming (USA) and Kutch (India).

Table 2-1. Reference backfill raw material.

Design parameter	Nominal design (wt – %)	Accepted variation (wt – %)
Montmorillonite content	50–60	45–90

The design parameter of the raw material that determines the properties of the backfill is the montmorillonite content. The montmorillonite content in the backfill material shall be sufficient for the saturated backfill to yield and maintain the required hydraulic conductivity and swelling pressure. The montmorillonite content will also affect the compressibility of the material and the capacity of the backfill to restrict upwards swelling/expansion of the buffer. When determining the reference material the material specific relationships between density and hydraulic conductivity and swelling pressure as well as the loss of buffer density by upwards swelling were evaluated for alternative candidate materials (Johannesson and Nilsson 2006). Low-grade bentonites with a composition according to Table 2-1 were concluded to yield the required properties for technically achievable densities. (SKB 2010a)

Bentonite consists mainly of montmorillonite, which is the component responsible for the swelling ability of bentonite in contact with an aqueous solution. The montmorillonite mineral belongs to the smectite group, in which all the minerals have an articulated layer structure. The exceptional uptake of water and resulting swelling of the bentonite buffer is normally counteracted by the walls of the deposition hole in a KBS-3 repository, and a swelling pressure develops in the bentonite. (Birgersson et al. 2009)

The part of the backfill between the last deposit hole and the wall consisting of the concrete beams is referred to as the backfill end zone. The backfill end zone will differ from the rest of the backfill, since this zone has to be adjusted for the swelling pressure on the concrete plug to be evenly distributed and reach the desired value.

The backfill is not included in the reference design of the plug system, but the design of the backfill end zone will be studied in the next phase of this project.

The tunnel will be shaped like a horseshoe for the entire backfill section. The tunnel section will however be changed at the location of the plug design. At the plug section, the tunnel will be round or at least octagonal, depending on the excavation method used. The change in tunnel profile is made at the side of the backfill end zone facing the plug design, i.e. at the location of the first wall of concrete beams, see Figure 2-2.

2.1.3 Filter

The filter is approximately 750 mm thick and assembled between two walls of prefabricated concrete beams. The shape of the filter will be round or at least octagonal, depending on the excavation method. The material used for the filter should be sand or gravel (with small grain size).

The purpose of the filter is to buffer water and to be used for artificially controlled wetting of the bentonite seal. With the drainpipes it will be possible to drain water via the filter from the deposition tunnel until the concrete plug has reached adequate strength and, if required, the contact grouting has been performed. The filter should thereby also control the water pressure inside the plug system until the concrete has cured. The drainpipes can also be used to pump water into the filter again after the grouting, to control the time it takes to artificially saturate the bentonite seal and thereby ensuring a fast and homogenous wetting of the bentonite seal. The filter should also preserve a high water pressure in the case that the plug system is not watertight. The artificial wetting will ensure that the pressure build-up on the concrete plug is controlled regarding both its size and its time of arrival.

The backfill end zone is going to be designed for reducing the swelling pressure from the backfill, but additional compression of the filter is also beneficial. One additional feature of the filter is therefore that it should be compressible to reduce the swelling pressure from the backfill. This requires of course also that the concrete beams can move in the tunnel direction. The filter can in this way assist to create an evenly distributed pressure on the concrete plug.

2.1.4 Bentonite seal

The bentonite seal is approximately 750 mm thick with a round or at least an octagonal shape. The bentonite seal is assembled between two walls of concrete beams. The material suitable in the bentonite seal is currently being investigated. The dry density of the bentonite seal will be approximately 1,500 kg/m^3. The exact density of the bentonite seal will be determined in the next phase of this project. The bentonite seal will most likely be assembled by stacking compacted blocks of bentonite clay in combination with spraying bentonite pellets to cover irregularities against the rock surface.

The bentonite seal is now in its design phase, where experimental tests and numerical analyses are performed to decide the thickness of the bentonite seal, compacting pressure, water ratio, swelling pressure, hydraulic conductivity etc. The design phase of the bentonite seal is planned to be finished in the summer of 2011.

2.1.5 Concrete plug

The concrete plug will be dome shaped in a round or at least octagonal tunnel section. The concrete plug will be unreinforced and cast with low-pH concrete. In the concrete plug, the low-pH concrete recipe B200 developed by Vogt et al. (2009) is planned to be used. The main reason why it has to be unreinforced is the high amount of early shrinkage during the first 90 days, where reinforcement would cause cracking in the plug due to its restraint. Other important reasons why the concrete plug preferably has to be unreinforced are presented in Section 1.1.1.

In the repository, low-pH-concrete should be used instead of conventional concrete. The definition of a low-pH concrete is in this case a concrete with a leachate pH less than 11. For conventional concrete the leachate is usually having a pH equal or higher than 12.5. The low-pH of the concrete, has been achieved by replacing 40% of the cement weight with silica fume. According to current knowledge, low-pH concrete should not disturb the function of the bentonite. This is accomplished by avoiding the development of a high-pH leachate by replacing leachable calcium compounds with silica in the low-pH-concrete. (Vogt et al. 2009)

The main purpose of the concrete plug is to resist the loads acting on the structure, and thereby act as a support to the rest of the plug system and the backfill. The two main external loads acting on the concrete plug are the hydrostatic water pressure from inside of the deposition tunnel and the swelling pressure from the backfill and the bentonite seal. In addition to this, the concrete plug must also be watertight until the bentonite seal has saturated and reached homogenization. After which, the bentonite seal will on its own act as the watertight barrier preventing leakage from the deposition tunnel into the transport tunnel.

2.2 Construction procedures

The deposition tunnel is approximately 300 m long and shaped as a horseshoe, as shown in Figure 2-3 and excavated with a blasting technique. The nominal width of the tunnel is 4.2 m and the height is 4.8 m. The tunnel width and height will vary due to the blasting technique, where holes are drilled with an inclination into the rock. This will result in that, the tunnel is smaller in the beginning of a blasting round and larger at the end of a blasting round, see the left figure in Figure 2-3.

This technique will be used for the whole deposition tunnel and afterwards holes for the deposited nuclear fuel will be excavated in the tunnel floor. The distance between each hole for the deposited nuclear fuel is 6 m, or > 6 m when unfavorable rock conditions require adjustment of a deposition hole.

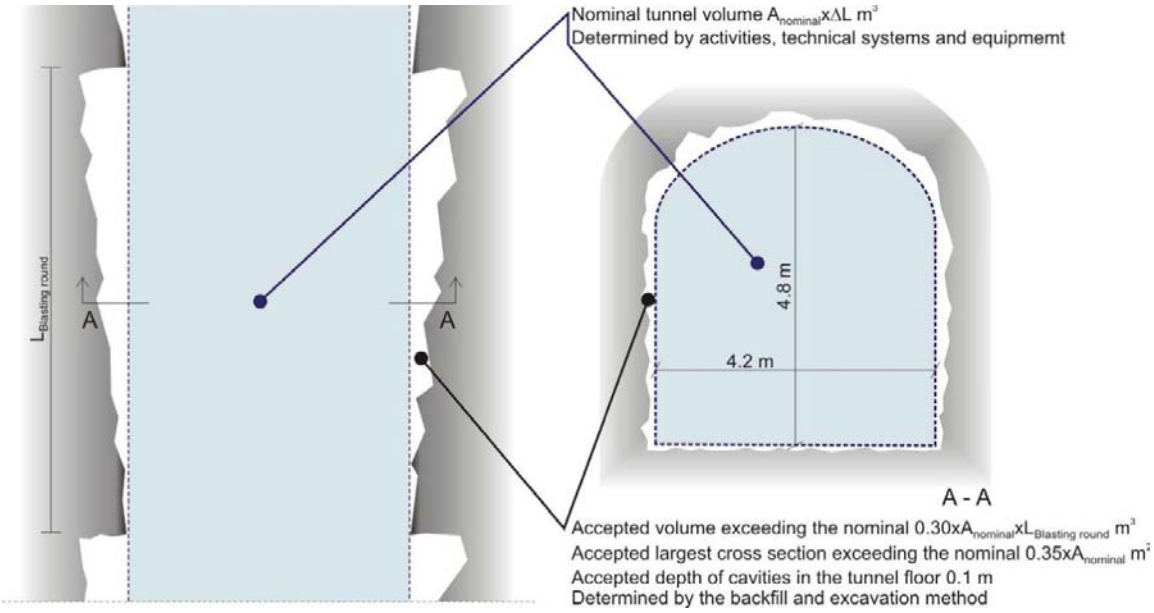

Figure 2-3. *Excavation of the deposition tunnels.*

Once the whole deposition tunnel is excavated, refined excavation has to be made from the outer deposition hole to the end of the section of the plug system. At the location of the first wall of concrete beams, the tunnel profile change to a round or at least octagonal section, see Figure 2-4. The reason for this is that the concrete plug requires a round shape to avoid being subjected to eccentric loads. In order to create this, also the bentonite seal and the filter have to have the same tunnel profile as the concrete plug.

The general requirement for the rock close at the location of the plug system is that it should have a low axial hydraulic conductivity. The different layers in the plug design have different criteria's as regards rock surface structure and friction properties, free from EDZ etc, and therefore it is likely that the different sections of the plug system will be excavated with different techniques or tolerances.

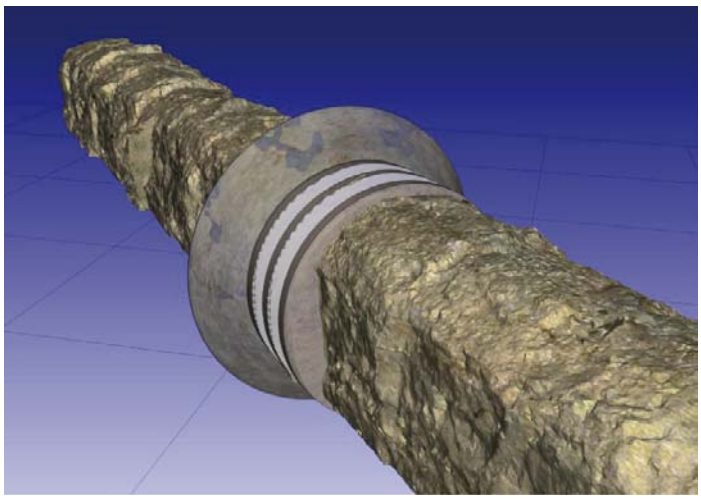

Figure 2-4. *Illustration of a round plug section in the horseshoe shaped excavated deposition tunnel.*

2.2.1 Tunnel work

As mentioned in the previous section, the tunnel profile at the location of the plug system requires additional excavation compared to the normal deposition tunnel excavation. Within this additional excavation, the transition from a horseshoe shaped tunnel into a round or octagonal shape of the tunnel profile (depending on the excavation method) and the slot that acts as the support for the dome shaped concrete plug has to be excavated.

A summary of the tunneling work is presented in the following:

1. The tunnel profile in the deposition tunnel is normally horseshoe shaped as seen in Figure 2-3 and excavated with a blasting technique. It is likely that the excavation of the deposition tunnel is performed to minimize the EDZ, for instance by using a more careful method to excavate the part closest to the theoretical tunnel profile. The actual location of the plug design is determined with respect to the requirements set on the surrounding rock by the plug system.
2. The v-shaped slot is needed as a geometrically controlled abutment for the dome shaped concrete plug. The whole tunnel section at the location of the plug intersects the excavated damaged zone (EDZ) from the excavation of the normal tunnel profile. The slot goes deeper in the rock and therefore further prevents axial leakage in the rock around the plug system.
3. The bentonite seal and the filter should both be excavated to a round or at least an octagonal profile, with an area larger than the normal tunnel profile, see Figure 2-2. Due to this, the EDZ from excavating the normal tunnel profile is removed and hence the axial flow through the rock out from the tunnel is reduced.
4. In some cases, grouting of the rock at the location of the plug may be necessary. The need for grouting the rock is determined at the investigation drilling, before the decision of the tunnel location is taken. Rock grouting should preferably be performed as pre-grouting from the transport tunnels, before the deposition tunnel is excavated.
5. The criteria for the individual parts of the plug system to work according to the design specifications is that they are separated with some sort of delimiters, for instance prefabricated concrete beams. Different requirements are defined for the different sections and the prefabricated concrete beams. In order for the drainage to work, a cast-in-place foundation is necessary for the wall with concrete beams closest to the concrete plug. The cast-in-place concrete foundation needs to be watertight, including the interaction between concrete and rock. It should also act as a bank for measuring the amount of water during the backfill of the tunnel. However, it is important that the upper surface of the foundation is outside the theoretical tunnel profile to make sure that the cross-section is larger than the theoretical profile to allow for transport and equipment access.

In Figure 2-5 the deposition tunnel at the location of the plug system is shown. It is likely that different requirements will be set on the rock surface for the different sections A-F in the figure. This could lead to that different sections may be excavated using different methods. There are also several methods to excavate the v-shaped slot, which constitute the abutment for the concrete plug. At present, different methods are evaluated regarding the excavation of the plug section. The possibility of each excavation method to create a smooth surface, and the amount of subsequent work needed to satisfy the requirements on the rock surface are studied.

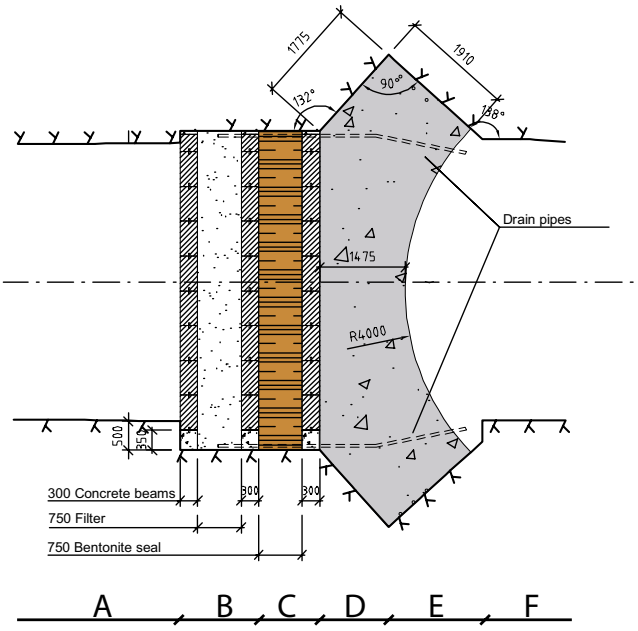

Figure 2-5. *Illustration of a round (or octagonal) plug fit into the horseshoe shaped excavated tunnel section. The notations A-F indicate the different sections where the tunnel profile and rock surface requirements may deviate from each other.*

2.2.2 Installation of the plug section

The construction of the backfill is performed with blocks and pellets of bentonite as shown in Figure 2-6. The blocks are assembled with a specially designed equipment and information and comparison regarding the different approaches for assembling the backfill can for instance be found in Wimelius and Pusch (2008).

The deposition tunnels are filled with bentonite blocks and pellets along their length. The backfill end zone, i.e. the last meters towards the first wall of concrete beams, is filled with different blocks and/or pellets than the rest of the backfill. The last part of the backfill end zone is filled parallel with the construction of the first wall of concrete beams, so that the wall acts as a support during assembly.

The concrete beams require supports in the rock to be mounted into a wall. The supports should be designed in a way that allows the concrete beams to move in the tunnels axial direction when subjected to pressure. The contact between the supports and the rock is proposed to be sprayed with shotcrete, to create a watertight barrier around the concrete wall. This is done, so that the main leakage through the concrete wall is directed to go between the different concrete beams. In this way, a more evenly distributed seepage is created. The assembly of the concrete beams is shown in Figure 2-7. The photo comes from the installation of the outer plug in the Prototype Repository. In the photo, it is possible to see the supports for the concrete beams, which allows them to move in the axial direction of the tunnel.

After the first wall with concrete beams has been assembled, the installation of the filter proceeds. The filter should consist of sand or gravel with a small grain size. Parallel with the installation of the filter, the second wall with concrete beams is assembled which acts as support for the filter during construction.

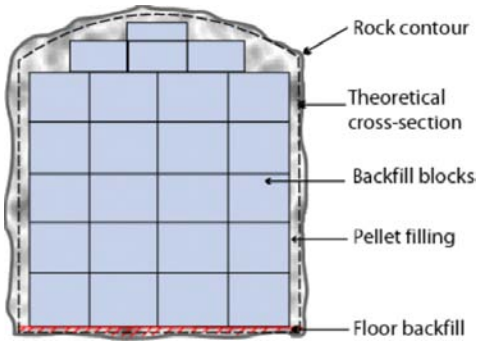

Figure 2-6. *Principle sketch of the backfilled tunnel.*

Figure 2-7. *Assembly of the wall with prefabricated concrete beams.*

After the second wall with concrete beams, the bentonite seal is installed. The last wall with concrete beams is installed parallel with the bentonite seal. The last wall with concrete beams is covered with shotcrete to prevent leakage out from the tunnel.

After the shotcrete, two plies of geotextile are installed and after that, the concrete plug is cast. The purpose of the geotextile is to remove the cohesion between the shotcrete on the wall with concrete beams and the cast-in-place concrete plug. The low-pH concrete has large early autogenous shrinkage and it is intended that the concrete plug releases from the rock in the top and on the sides of the tunnel section. This has to be done, to prevent extensive cracking during the early shrinkage. This is further discussed in Section 3.3.3.

During the period from the assembly of the filter to the time when the concrete plug is operational, i.e. after grouting the plug approximately 90 days after casting, the deposition tunnel should be drained via drain pipes from the filter to a water measuring bank outside the plug. This should be done to avoid water pressure on the concrete plug during construction.

2.2.3 Installation of the concrete plug

Before the concrete plug can be cast, installation of cooling pipes and grouting tubes have to be done. The purpose of the cooling pipes is to compensate for the temperature increase in the concrete due to the hydration. Due to the low amount of cement in the low-pH SCC, the heat development due to hydration is low but instead it lasts longer than in normal concrete. The cooling pipes will also be used to lower the temperature in the concrete plug before contact grouting, which is furthered described in Section 3.3.5. The layout of the cooling pipes is determined via thermal analyses to minimize the stresses in the concrete during the first days after casting.

Grouting tubes should be installed in circular patterns around the tunnel section, on both the upstream and the downstream side of the v-shaped slot, i.e. not just on the upstream side as shown in for instance Figure 2-1.

The concrete plug is cast against the geotextile (placed on the wall of the concrete beams), and the abutment (the v-shaped excavated slot). On the downstream side, steel girders covered with sheets of plywood comprise the formwork, and the concrete is pumped through valves attached in the formwork. The formwork has to be resistant to high form-pressure from the SSC. The formwork used in the Prototype Repository and the Backfill and Plug Test is shown in Figure 2-8.

Cooling should bee performed the first days after casting to compensate for the temperature increase in the concrete during the hydration. The actual time necessary for cooling will be determined by the layout of the cooling pipes. The concrete plug should cure approximately 90 days after casting. The low-pH concrete has large early autogenous shrinkage, which is described in Section 3.3.3. During this time, the concrete plug is intended to release from the rock in top and on the sides of the tunnel section. Thereby, some of the shrinkage will be unrestrained deformation. The early autogenous shrinkage can also be compensated by a long casting time. The concrete plug in the Prototype Repository had a casting time of 8 hours, according to Dahlström (2009). To compensate for the shrinkage in the low-pH concrete, longer casting time than this is required to minimize the risk of cracks. After 90 days, the concrete plug should have released from the sides and from the top of the tunnel, see Figure 3-10. At this point, cooling of the concrete plug begins again but this time the cooling is performed to force the concrete plug to reduce in volume. This increases the gap between the rock and the concrete surfaces, which simplifies the grouting of the concrete plug. One additional effect of the cooling before grouting is that this reduction in temperature results in a thermal prestress, after the grouting when the temperature is increased to normal again.

After successful grouting of the plug, the draining of the filter ends. Instead, the filter is filled with water for artificial wetting of the bentonite seal. This reduces the time needed for saturation of the bentonite seal and thereby decreases the time the concrete plug has to be watertight.

Figure 2-8. *Formwork for the downstream side of the dome shaped concrete plug, used in the Prototype Repository.*

3 Requirements of the reference design

3.1 Functional requirements

There are different functional requirements of the whole plug design and its individual components (layers) for different time-periods. In this section, the functional requirements are summarized and described.

3.1.1 Requirements of the plug system

The most important requirements on the plug system are that it should keep the backfill in place and that it should be a watertight barrier preventing axial water flow and erosion of bentonite from the deposition tunnel. The plug system is preventing erosion of the buffer so that the buffer maintains its ability to prevent possible leakage of radioactive substances from the deposited canister. The main requirement on the plug system is that it should be a watertight barrier preventing axial water flow and erosion of bentonite from the deposition tunnel and to resist the loads acting on the plug.

In the plug design, the bentonite seal is intended for preventing leakage and erosion, but ultimately all individual parts of the plug design should assist with the best of their capabilities to prevent leakage and erosion of material out from the tunnel. This means that for instance, an increased leakage resistance of the concrete plug improves the complete plug system.

When the bentonite seal has reached sufficient saturation it will prevent leakage into the transport tunnel. The time it takes for the bentonite seal to saturate depends on its geometry, initial water content and its composition, i.e. blocks or pellets etc but mainly on the amount and distribution of water. The time to full saturation will most likely be a few years. During the first years, the amount of water in the deposition tunnels is gradually increasing and the concrete plug is an important barrier to prevent leakage. After the bentonite seal has saturated, the leakage requirement on the concrete plug is redundant and the main purpose of the concrete plug is to act as a support and carry the loads from the water and swelling pressure from the deposition tunnel.

The bentonite buffer rings around the deposited canister is sensitive to erosion, and the Safety Analysis team has adopted maximum allowed accumulated leakage of $\leq$150 m^3 of water through a deposition hole during the expected plug lifetime of approximately 100 years (SKB 2010a, b). This requirement will consequently also render that only a small leakage through the concrete plug can be allowed. The Design Criteria for the acceptable leakage passing the plug is not yet determined. Future upcoming full-scale test (in year 2012, see Section 5.3 and Section 7.1.3) will be arranged for testing of maximum allowed leakage in the range of 0.0025 to 0.05 l/min, and obviously, the lower value will be the target value for the finally selected Design Criteria.

The transport tunnels, unlike the deposition tunnels, will be at atmospheric pressure until all canisters are deposited and the whole facility is sealed. Finally, when the transport tunnels are backfilled and saturated the function of the plugs is no longer required other than a volume mass to prevent the density loss of the bentonite backfill caused by possible erosion. However, the deposition will prolong for a long time and therefore the plug should be designed to function for at least 100 years.

3.1.2 Requirements of the components

The four general requirements set on the plug design are the following

1. The plug system and especially the bentonite seal should prevent water to leak out from the deposition tunnel until adjacent transport tunnel is backfilled and saturated.
2. The concrete plug should support the bentonite seal and transfer the loads from the hydrostatic pressure at repository depth and the swelling pressure of the backfill into the surrounding rock.
3. The plug must be functional until the transport tunnels at the outside are filled with bentonite clay. After this, nominal hydrostatic water pressure will be present on both sides of the concrete plug and the function of the plug system is no longer required.
4. Not significantly impair the barrier functions of the engineered barriers or rock.

The reason for these requirements is that bentonite clay cannot prevent leakage unless it is supported by the concrete plug so that the hydrostatic water pressure is carried by the concrete plug and transferred to the rock. The hydrostatic water pressure at large depths is too high for the swelling pressure of the bentonite clay to resist on its own. The result if the bentonite clay is subjected to high water pressures, is piping and thereafter erosion of material. The bentonite seal does not prevent leakage until the empty voids in the buffer and in the backfill are filled with water and the water gradient is carried by the plug system.

There is a risk that it could take several years until the bentonite clay has reached sufficient saturation and hence is able to prevent water leakage as intended. For this reason, the concrete plug has to prevent leakage out from the deposition tunnel until the bentonite seal is saturated and thereby prevents leakage. After this point, the requirement of the concrete plug to be watertight is no longer of importance. The requirement on the concrete plug after the bentonite seal has saturated, is that no cracks going through the entire thickness of the plug are allowed. If a crack is going through the concrete plug, it is likely that erosion of buffer and backfill material can occur. Even a small crack width of typically 0.05 mm (which is about the smallest crack width that can be detected by a naked eye) leads to high leakage due to the large hydrostatic water pressure, unless the cracks are sealed by bentonite clay.

The second requirement above is specified since it is important that the concrete plug can carry the hydrostatic water pressure so that any erosion damages that have occurred in the buffer or in the backfill should be able to heal. One important condition for the bentonite clay to seal is that a low water pressure does not occur in the erosion canals at the same time as high water pressures occur in the surrounding rock. Piping and erosion cannot occur if the inflow is so slow that the bentonite clay can absorb the water and swell at the same time as the water flows in. It is however not clear at what inflow this limit occurs, since it largely depends on the distribution of inflow.

The third requirement specifies that the life span of the concrete plug should last until the facility is closed and the water pressure on the outside of the concrete plug is the same as the hydrostatic pressure on its inside. When full hydrostatic water pressure on the outside of the concrete plug has occurred, leakage from the deposition tunnel is no longer possible.

The life span of the plug system lasts until the facility is closed and the hydrostatic water pressure has been stabilized in all tunnels, which is assumed to occur after approximately 100 years.

3.2 Material properties

3.2.1 Low-pH concrete

The low-pH concrete developed by Vogt et al. (2009), referred to as B200 should be used for the concrete plugs and the prefabricated beams used as delimiters between the layers in the plug design. It is possible that some alterations to this concrete recipe are introduced before the final deposition starts.

The values for compressive strength are based on tests performed at Luleå University of Technology. In Figure 3-1 the development in compressive cube strength with time is shown. The yellow symbol represents results using several test specimens (≥ 3 per symbol), while the green, pink and blue symbols are based on just one test specimen. There is only a small scatter in the results compared to the theoretical curve defined as "calculated" in the figure, see Vogt et al. (2009). The circles represent estimations of the strength at different ages of the concrete 28 days, 90 days, 1 year, 10 years, and 100 years. More information is found in Vogt et al. (2009).

A similar curve was obtained with the concrete mix B300, with the exception of an overall higher compressive strength. To use the compressive strength in future analyses it has to be recalculated as the cylinder strength, see Vogt et al. (2009).

A similar type of curve is shown for the development of the elastic modulus of the concrete mix B200, as seen in Figure 3-2.

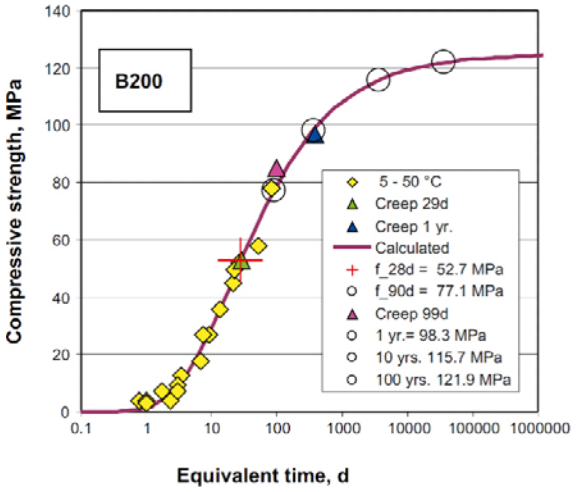

Time at loading	$f_{cm,cube}$, MPa
28 d	53
90 d	77
1 yr.	98
10 yrs.	116
100 yrs.	122

Figure 3-1. *Development of the compressive cube strength.*

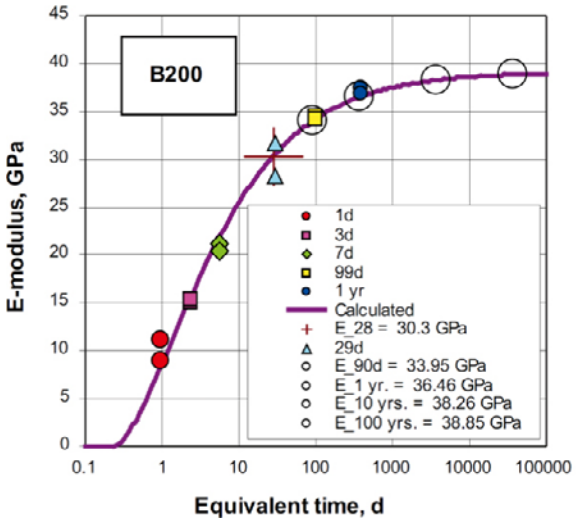

Time at loading	E_{cm}, GPa
28 d	30.3
90 d	33.9
1 yr.	36.5
10 yrs.	38.3
100 yrs.	38.8

Figure 3-2. *Development of the elastic modulus.*

All material parameters are based on the mean value strengths after 90 days of curing for the low-pH concrete in Vogt et al. (2009) and are presented below:

- Tensile strength 3.3 MPa (B200).
- Compressive strength 62 MPa (B200).
- Elastic modulus 33.9 GPa (B200).
- Poisons ratio 0.27.

Characteristic material data are intended for use in the structural analyses of the long-term behavior. All material parameters are based on the characteristic strengths of the low-pH concrete in Vogt et al. (2009) and are presented below:

- Tensile strength 2.9 MPa, (B200).
- Compressive strength 54 MPa (B200).
- Elastic modulus 33.9 GPa (B200).
- Poisons ratio 0.27.

The permeability was estimated from two measurements of water penetration as $3.9 \cdot 10^{-14}$ m/s for B200 and $1.4 \cdot 10^{-14}$ m/s for B300. However, the experimental results are too limited to be based on the values mentioned above. The recommendation made by Vogt et al. (2009) was that a conservatively chosen permeability of 10^{-11} should be used in analyses.

The concrete material properties, such as the creep and the shrinkage are presented in Section 3.3.3.

3.2.2 Rock

The rock in the plug position should have a low axial hydraulic conductivity. An evaluation of the properties of the rock type found at Forsmark is presented in SKB (2008b) and in Table 3-1. The plug section will be placed in an area with good and homogenous rock, which means that any larger variation in deformation properties around the abutment for the concrete plug is not to be expected. Table 3-1 below, only includes values for intact rock in fracture domains FFM01 and FFM06, which are the only areas where a concrete plug may be placed. The rock properties at Forsmark are more favorable than the Äspö properties, which have been used earlier in this project. The mean value of the permeability of rock type FFM01 is according to measurements $5.2 \cdot 10^{-10}$ m/s at a depth of 200–400 m and an even smaller value at a greater depth (SKB 2008b). The measurements performed for the rock type FFM06 show that it is at least as low as FFM01.

3.2.3 Bentonite

The numerical analyses of the bentonite material for buffer, backfill and the bentonite seal are based on material properties of Wyoming bentonite (MX-80). However, this material is not planned to be used as backfill. The material devoted for this (i.e. IBECO RWCBF), only has limited data at the moment, but exhibits many similarities to data for MX-80 according to Åkesson et al. (2010a).

The material properties of the bentonite clay used in the analyses is found in Åkesson et al. (2010a) and the numerical analyses of the backfill, buffer and bentonite seal are found in Åkesson et al. (2010b).

The bentonite seal can consist of bentonite pellets, pre-compacted blocks or a combination of them both. At present, different combinations are studied for the bentonite seal. It is likely that the bentonite seal will be made similarly to the backfill. The density of the bentonite seal will be determined after the design of this layer is complete. The bentonite seal will be designed to yield a maximum swelling pressure of 2 MPa on the concrete plug and a minimum swelling pressure that is high enough to fulfill the sealing requirements.

The last part of the backfill, closest to the plug section, may be designed to reduce the swelling pressure from the backfill on the plug, and therefore, a lower density of this section could be beneficial in this aspect.

Table 3-1. Laboratory strength and deformation properties for intact rock in fracture domains FFM01 and FFM06, from SKB (2008b).

Parameter	FFM01		FFM06	
	101057 Mean/stdev Min-Max Uncertainty	101061 Mean/stdev Min-Max Uncertainty	101057 Mean/stdev Min-Max Uncertainty	101058 Mean/stdev Min-Max Uncertainty
Number of tests	47	13	10	5
Youngs modulus (GPa)	76/3 69–83 ± 1%	74/4 69–80 ± 3%	80/1 78–82 ± 1%	83/3 80–86 ± 3%
Poisson's ratio	0.23/0.04 0.14–0.30 ± 4%	0.30/0.04 0.26–0.35 ± 5%	0.29/0.02 0.26–0.31 ± 4%	0.27/0.03 0.25–0.31 ± 8%
Uniaxial Compressive strength (MPa)	226/29 157–289 ± 4%	214/33 158–266 ± 8%	373/20 338–391 ± 3%	310/58 229–371 ± 16%
Crack initiation stress (MPa)	116/23 60–187 ± 7%	114/18 85–140 ± 15%	196/20 180–250 ± 6%	169/29 125–200 ± 15%
Cohesion M-C (MPa)	28	33	–	–
Friction angle M-C (MPa)	60	56	–	–
Constant m_i, H-B	28	18	–	–
Number of tests	82	12	10	–
Indirect tensile strength (MPa)	13/2 10–18 ± 2%	12/3 8–16 ± 9%	15/1 13–17 ± 5%	–

Note: The uncertainty of the mean is quantified of a 95% confidence interval. Minimum and maximum truncation values are based on the observed min and max for the tested population. The cohesion and friction angle are determined for a confinement stress between 0 and 15 MPa.

101057 – Granite to Granodiorite, metamorphic, medium grained (albitized in FFM06).

101058 – Granite, metamorphic, alplitic (albitized).

101061 – Pegmatite, pegmatitic granite.

3.3 Loads acting on the concrete plug

The purpose of this section is to summarize the expected structural loads acting on the plug, regarding their expected load values, distribution and at what time they appear. In addition to this, recommendations regarding design values etc are provided.

3.3.1 Water pressure

In the design of the concrete plug, the nominal value of the groundwater pressure should be based on the vertical distance from the groundwater level to the actual tunnel level, according to $p_w = \rho_w g h$. In this project, the nominal value for the water pressure has been taken as 5 MPa, which implies a depth of 500 m. The water pressure will have a small variation over the height of the concrete plug, where the difference in pressure is about 1% of the nominal value between the top and the bottom of the tunnel. The variation in pressure over the height of the concrete plug is small and should therefore be assumed as evenly distributed over the surface. The water pressure should be considered as a permanent load for the design of the concrete plug.

During excavation, the tunnels will be subjected to atmospheric pressure, which means that it will lower the pressure and a pressure gradient towards the tunnels will be the result. At the perimeter of the tunnel, the water pressure will be zero and the pressure increase in the rock mass with the distance from the tunnel in a radial direction up to the level of the natural water pressure. This means that deposition tunnels will affect each other and the water pressure on watertight constructions, such as the plugs, will vary with time.

It is probable that the maximum one-sided water pressure, based on the distance from the groundwater level, never will occur due to the adjacent tunnels and the disturbed groundwater situation. Due to the hydrogeologic inhomogeneous properties of the rock, frequency and transmissivity of fractures, the water pressure will vary on the concrete plugs. As a conservative limit, it is therefore reasonable to take the maximum hydrostatic water pressure as the design value for the water pressure.

The discussion above regarding the probable size of the hydrostatic water pressure, is verified by hydraulic analyses performed by Svensson (2006). In Figure 3-3, the calculated reduction in water pressure is shown based on a calculation with a repository depth of 415 m below groundwater level. In this figure, grouting has been accounted for by introducing a low conductivity where the maximum conductivity is set equal to 10^{-11} m/s. In the figure, the hydrostatic pressure is excluded (in this case ~4.15 MPa) and therefore the areas with maximum hydrostatic pressure are equal to zero and visualized as a red/orange color. The tunnels and adjacent areas have a reduced pressure, where the transport tunnels with blue color have a pressure equal to atmospheric pressure.

According to the hydraulic calculations for the Forsmark site shown in Figure 3-3 above, the water pressure inside the backfilled parts of the repository will be about 3 MPa at a maximum due to drainage of the rock caused by the excavations (Svensson 2006).

When the repository is closed, i.e. when all deposition tunnels are backfilled and have a plug system installed and the transport tunnels are filled with bentonite clay, nominal water pressure is obtained for the whole area. For the watertight plug construction, this means that the pressure is leveled out and a pressure is build up on both sides of the plug.

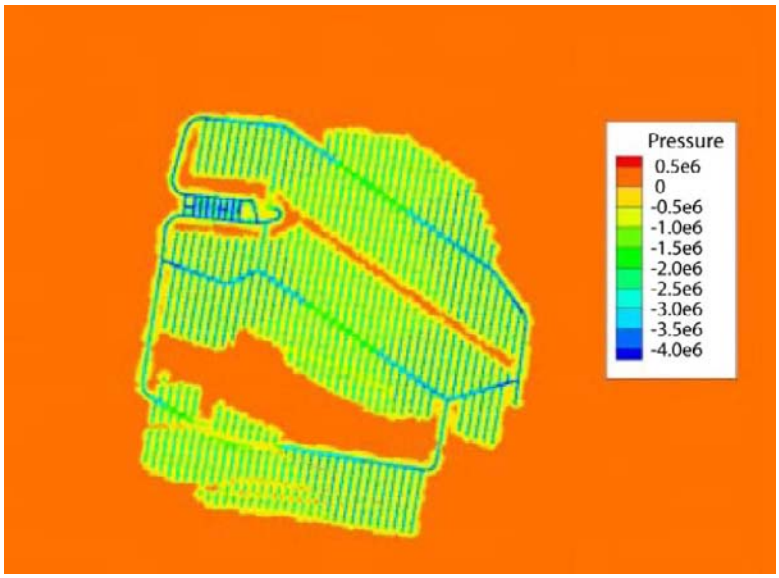

Figure 3-3. *Calculated reduction on hydrostatic water pressure due to the excavation of the tunnels. From Svensson (2006).*

3.3.2 Swelling pressure of bentonite

The concrete plug is being designed to withstand an expected swelling pressure equal to 2 MPa, with a design value of 4 MPa. Uncertainties regarding the reduction in the swelling pressure on the concrete plug because the filter, seal and backfill end zone are not currently designed yet, a safety factor equal to two has been decided for this load. A high density of the backfill and the bentonite seal will introduce higher swelling pressure. The expected maximum swelling pressure in the backfill is about 6 MPa – 10 MPa, depending on the density of the bentonite used. The swelling pressure in the backfill must therefore be reduced before it reaches the concrete plug. The filter in the plug design can be compacted to a certain extent, which thereby reduces the swelling pressure on the concrete plug. This may however not be enough to reduce the swelling pressure to about 2 MPa on the concrete plug. Due to this, the backfill closest to the plug system may have to be designed differently than the rest of the backfill. By reducing the density of the backfill closest to the plug a total reduction in swelling pressure can be achieved.

Analytical calculations and numerical finite element calculations have been performed to determine the design of the backfill closest to the plug, the bentonite seal and the filter. The analytical method was shown to be a useful tool for testing different designs of the plug. In Figure 3-4 the principle for reduction of the swelling pressure from the backfill is shown. In the figure, it is seen that due to the compaction of the filter a reduction in swelling pressure can be achieved. The displacements and the stresses after homogenization of the bentonite seal were calculated through consideration of the backfill, the filter and the seal. The swelling of the backfill and the seal was assumed to follow a defined swelling pressure curve and relies on the friction at the rock wall. The filter was assumed to exhibit an elastic behavior. The general solution for the stress distribution was derived based on the assumed force balance in Figure 3-4 to

$$\sigma(z) = \sigma(0) \cdot \exp\left(-\frac{2\tan(\phi) \cdot z}{r} \right)$$

For the swelling of the backfill, the origin was chosen at the point of unaffected swelling pressure and the stress at this point was thereby the swelling pressure of the initial void ratio. The length of the affected part of the backfill could thus be given by the stress at the interface towards the filter. A similar approach could be used for the bentonite seal, with the exception that the initial length is know instead of the stress at its boundaries. The filter is subjected to equal pressures on both sides (i.e. no shear transfer is assumed) and hence the compression of the filter could be determined. The equilibrium stresses could thereafter be determined by the condition that the sum of the displacements should be zero, i.e. the expansion of the affected part of the backfill and the expansion of the seal should be equal to the compression of the filter. More information regarding the analytical model and the results can be found in Åkesson et al. (2010b).

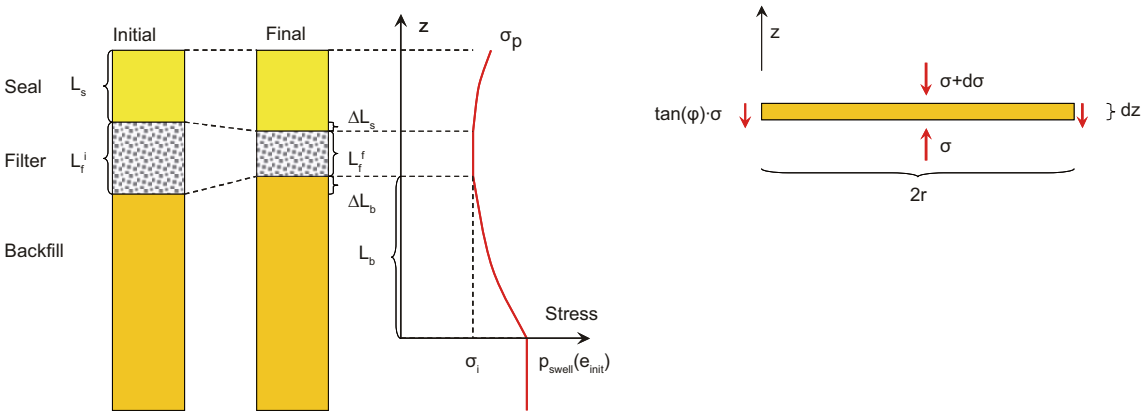

Figure 3-4. *Analytical model to calculate the reduction in swelling pressure on the concrete plug due to compaction of the filter and reduced swelling of the backfill end zone. (Åkesson et al. 2010b).*

The calculation of 12 different cases showed that the swelling pressure on the concrete plug could be between about 1.8 and 7 MPa for the configurations tested. Based on these calculations, it could be determined that the final pressure at the centre of the plug will be significantly higher than 2 MPa unless the seal and the outer part of the backfill are designed to reduce the stresses. (Åkesson et al. 2010b)

In Figure 3-5, the axisymmetric FE model is shown. The elements in blue color are defined with properties that represent pellets filling, the element in green are given properties that represent bentonite blocks and the magenta elements are defined with properties to represent the filter. Roller boundaries were applied to all mechanical boundaries, except the outer boundary (facing the tunnel surface) where the displacements in horizontal direction were restrained. In this study, water filling of the filter and the bentonite pellets were introduced in the model during a few days (0.01 years) and then the saturation of the bentonite and the evolution of the swelling pressure on the concrete plug were calculated. In Figure 3-6, the calculated swelling pressure on the concrete plug is shown for different time periods. The purpose of this study is to study the development of swelling pressure under a fast wetting of the filter and pellets. More information regarding the model and the results can be found in Åkesson et al. (2010b).

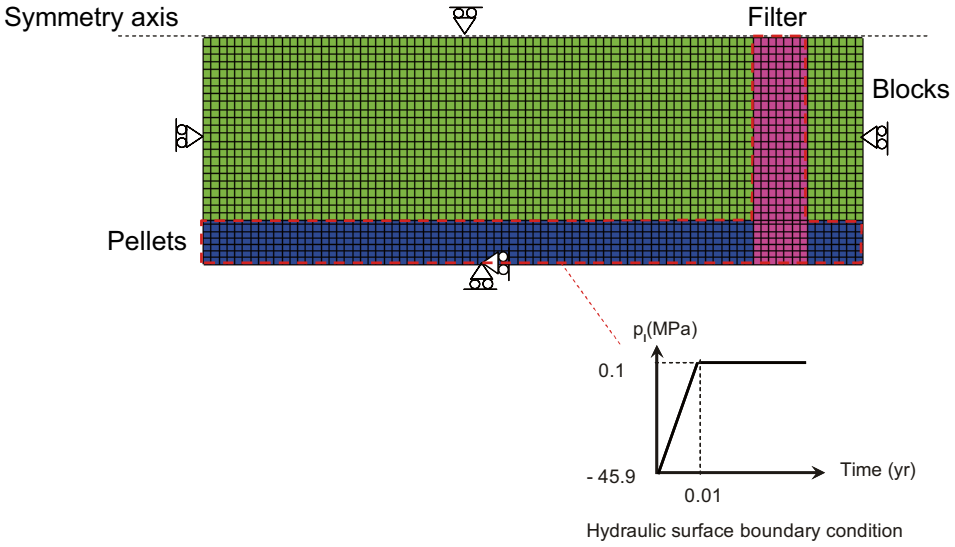

Figure 3-5. *FE model to calculate the swelling pressure on the concrete plug. (Åkesson et al. 2010b).*

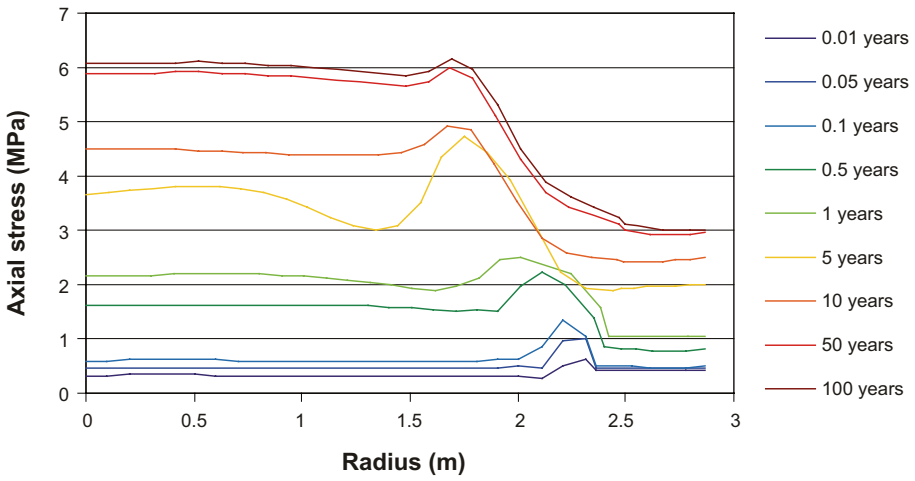

Figure 3-6. *Distribution of swelling pressure on the concrete plug for different time-periods. (Radius = 0 m is the centre of the plug). (Åkesson et al. 2010b)*

In the figure, it can be seen that for this configuration, with fast water filling of the pellets and the filter, a swelling pressure of 2 MPa is reached after about one year and the swelling pressure keeps increasing significantly for the following 50 years. There is only a small difference in swelling pressure between the 50 and 100 years.

Calculations were also performed to study the time it takes for saturation of the bentonite seal. The calculations showed that a fast hydration of approximately five years relies on piping through the pellets filled slot and the slots between the concrete beams. If, on the other hand, the pellets would seal very quickly, effectively turning the problem to a one-sided hydration, then the time of hydration would increase with a factor of four (Åkesson et al. 2010b). Considering the low probability for a double-sided hydration to work adequately during a longer period, the latter longer time for hydration should be given precedence.

3.3.3 Shrinkage and creep

Shrinkage

The concrete shrinkage was measured with three different methods in Vogt et al. (2009). In the first method, a volumetric measurement of the autogenous shrinkage was performed on samples in a tight flexible latex membrane submerged in a bath of water. The samples' change in volume was measured by the change in weight (reduced buoyancy, according to Archimedes' principle). The measurement started about 30 minutes after mixing. In the second method, a digital dilatometer was used to measure the early autogenous shrinkage. The method and equipment are described in Esping (2007). The measurement started about one hour after mixing. The concrete specimen was cast in a flexible plastic tube and placed in a measuring frame. In the third method, standard beams (SIS 2000) of 100 × 100 × 400 mm^3 were demoulded one day after casting. Half of the samples were sealed with special gas-tight butyl tape. The other half of the samples were stored with their free surface in 50% RH. Shrinkage and weight measurements started 24 hours after casting.

The most accurate result for the early autogenous shrinkage was obtained with method 2, with the digital dilatometer, according to Vogt et al. (2009). With this measuring method, the result from one hour up to 24 hours after casting is shown in Figure 3-7. The autogenous shrinkage after 24 hours was approximately 0.8 mm/m.

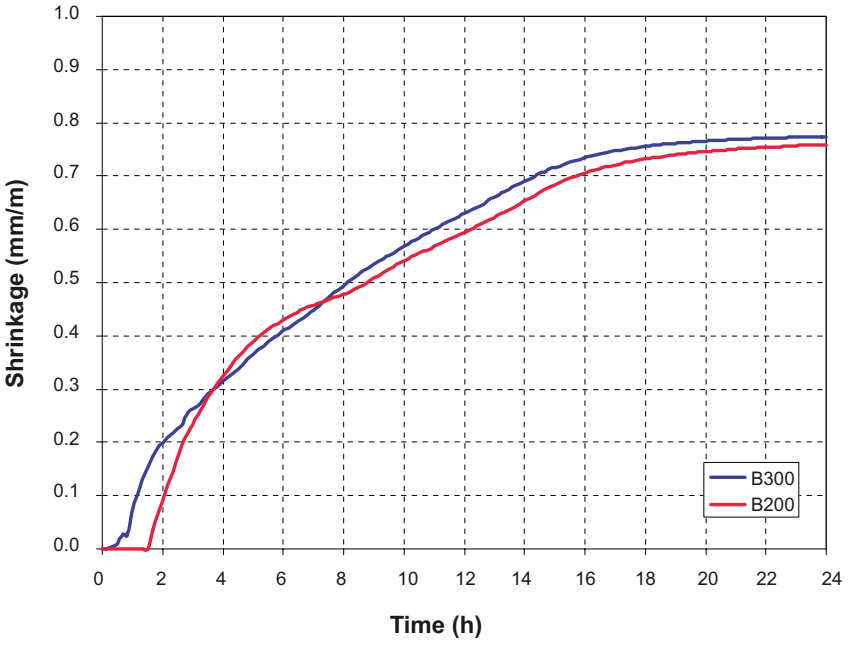

Figure 3-7. *Early age autogenous shrinkage, from Vogt et al. (2009).*

The shrinkage measured at 90 days with this method was suspected to overestimate the autogenous shrinkage since the permeable plastic tube surrounding the concrete specimen allows water to evaporate. Due to this, the measurements with this method unintentionally register drying shrinkage as well according to Vogt et al. (2009).

The sealed beams used in method 3 were proven watertight and therefore the sealed beams are suitable for measurement of shrinkage under sealed conditions after 24 hours. The measured shrinkage for sealed and unsealed samples is shown in Figure 3-8. The sealed samples measure, as long as the seal is watertight, only the autogenous shrinkage. The unsealed samples measure the sum of the autogenous shrinkage and the drying shrinkage at a relative humidity of 50%.

The most realistic description of the autogenous shrinkage for the plug is obtained by a combined shrinkage curve of dilatometer measurement (Figure 3-7) for the first 24 hours and sealed beams (Figure 3-8) for the following period of time, according to Vogt et al. (2009).

In Figure 3-8 it can be seen that the autogenous shrinkage, measured with the sealed specimen, is higher for the concrete recipe B300. The difference between the two unsealed specimens, measuring autogenous and drying shrinkage, is smaller than the difference between the two sealed specimens. This shows that the drying shrinkage is higher in the recipe B200.

One of the design requirements for the concrete plug is that it should be considered as stress free after 90 days. This means that the shrinkage during the first 90 days should be considered as free shrinkage, i.e. without restraint, and therefore the concrete plug has to release from the rock surface during this time. The early autogenous shrinkage after 24 hours was about 0.8 mm/m, as seen in Figure 3-7 and the additional autogenous shrinkage from 24 hours after casting to 90 days was about 0.1–0.2 mm/m, as seen in Figure 3-8, resulting in a total autogenous shrinkage after 90 days of about 0.9–1.0 mm/m. The autogenous shrinkage at 90 days would reduce the radius of the plug between 2.5 and 4.0 mm. The lower value corresponds to the reduction of the radius of the flat surface on the upstream side (r = 2.75 m) and the larger value corresponds to the radius from the centre to the 90-degree angle in the slot, that is the abutment of the concrete plug (r = 4.07 m). Unless the concrete plug is fixed for vertical displacements in the centre, the concrete plug will move downwards due to the gravity load. This gives that a zero slot will be obtained in the bottom and the slot increases around the perimeter up to the top of the plug, where twice the values mentioned earlier will appear.

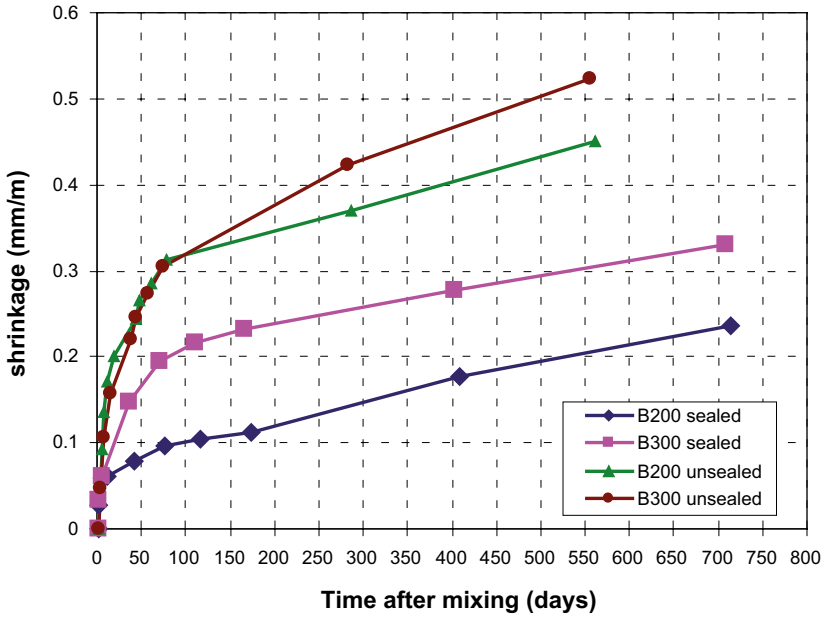

Figure 3-8. *Shrinkage of beam specimens (method 3), comparison of sealed and unsealed samples. The starting point of the measurement is 24 h (1 day) after casting.*

The slow casting of the concrete plug will reduce some of the initial shrinkage during the first 24 h. An attempt to estimate the amount of remaining shrinkage from casting to the point when the concrete plug is being grouted after approximately 90 days has been made as follows. If the rate of casting is 0.5 m/h, a total time of casting will be 16 hours for each plug. The bottom of the plug has an age of 16 hours and the top is zero hours directly when the casting is completed. The concrete in the bottom has been assumed to already been shrinking for this time and the reduction in volume during casting has been compensated by adding more concrete.

The vertical section of the concrete plug has been divided into 8 segments, each 1 m, as seen in Figure 3-9. The age difference between the top and bottom of each segment is 2 hours. At each division of segments, the difference between the total shrinkage after 24 hours and the corresponding shrinkage value at each age according to Figure 3-7 has been calculated and defined as $\Delta\varepsilon$. The average age of each segment is 1, 3, 5, 7, 9 11, 13 and 15 hours respectively. Based on the remaining shrinkage up to 24 h after casting in Figure 3-7 for each segment an average shrinkage for the whole plug can be calculated as 0.36 mm/m.

Based on the assumption that the concrete plug releases from the rock surface at the top and at the sides, the total gap at the top of the plug is 2.9 mm and 1.4 mm at each side 24 hours after casting. In addition to these values, the remaining shrinkage from 1 day to 90 days should be added according to Figure 3-8, giving a total shrinkage of 0.46 mm/m. The corresponding estimated slot between the rock surface and the concrete plug is illustrated in Figure 3-10. The plug will also shrink in the thickness direction and the shrinkage at midsection will be about 0.7 mm after 90 days based on the previous calculations.

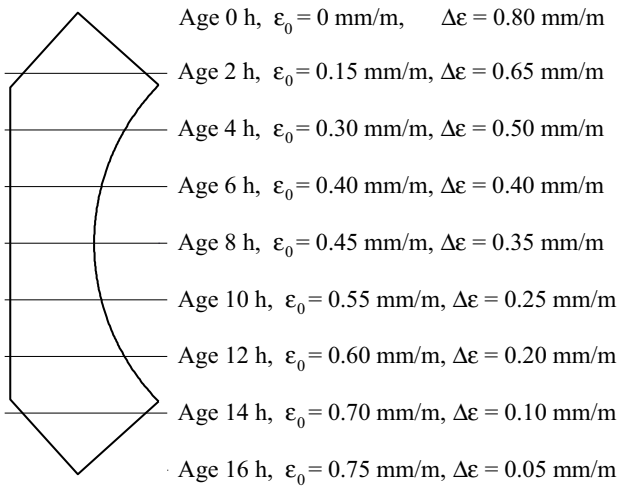

Figure 3-9. *Estimation of remaining shrinkage after casting.*

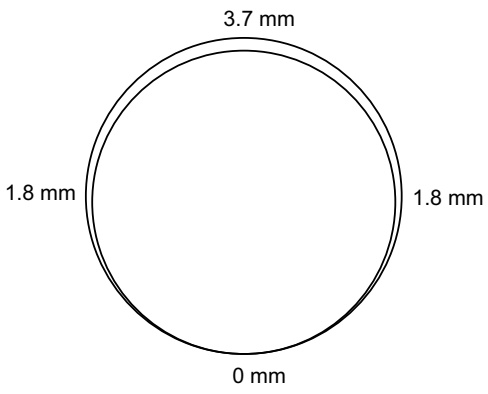

Figure 3-10. *Estimated slot between the concrete and the rock surface.*

Experiments were conducted on large specimens where the free shrinkage was measured in two cylinders with a diameter of 0.85 m and a height of 3 m. The cylinders are illustrated in Figure 3-11 and in Figure 3-12 it can be seen that the concrete has released from the steel cylinder and created a gap. The cylinders were measured with temperature gauges and linear variable differential transformers (LVDTs) to measure the heat generated by the hydration and the free shrinkage. More results from this experiment is found in Vogt et al. (2009).

According to the design criteria, the concrete plug should be considered as stress free after 90 days and the shrinkage that the concrete plug exhibits from the time of grouting up to 100 years can be obtained by reducing the curves shown in Figure 3-8 with their values at 90 days. Based on the resulting autogenous shrinkage, a logarithmic curve fitting has been performed and the extrapolated result for the period up to 100 years is shown in Figure 3-13. The autogenous shrinkage for the concrete recipe B300 is almost twice as high as for B200 after 100 years, 0.29 mm/m and 0.17 mm/m respectively.

Figure 3-11. *Two cylindrical steel moulds, diameter 0.85 m and height 3 m, instrumented with temperature gauges and one LVDT at the top to measure the settlement, were filled with low-pH SCC.*

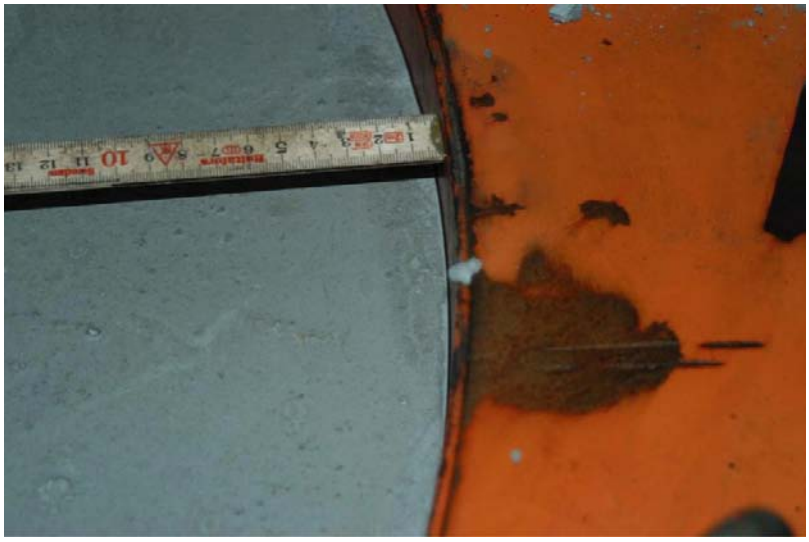

Figure 3-12. *Experimental gap between the concrete and the steel mould.*

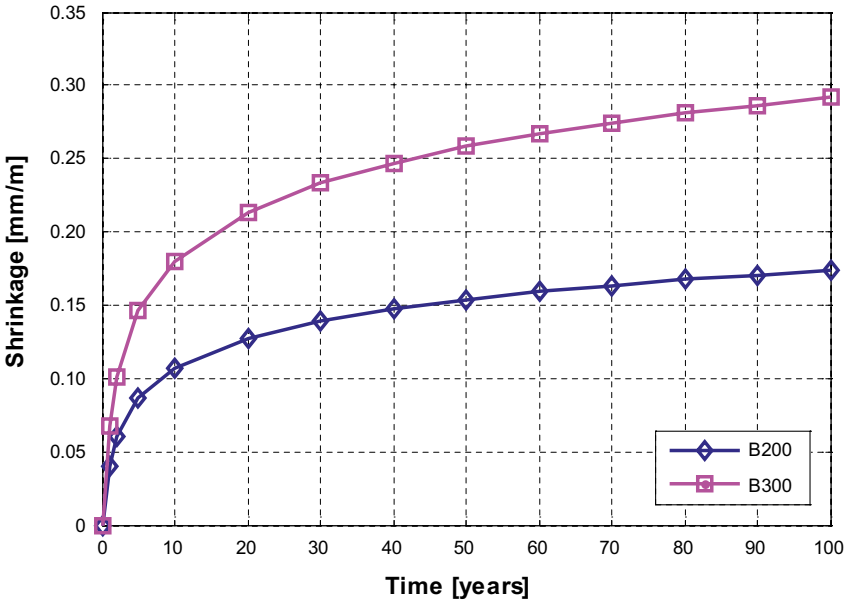

Figure 3-13. *Extrapolated autogenous shrinkage for concrete recipe B200 and B300. The starting point is 90 days after casting.*

The concrete plug will be cast in an environment with high relative humidity. It is likely that water will be present at the concrete surface on the upstream side, at least until the homogenization of the bentonite seal. It is planned that the surface is covered with a plastic sheet on the downstream side to accumulate all water that passes trough and around the concrete plug. This will be done to make it possible to measure the leakage of water. The concrete plug will thereby be subjected to a RH of almost 100% on the downstream side as well as the upstream side and due to this drying shrinkage will have a minor influence. The inclinations of B200 in the sealed and the unsealed specimens are almost identical after 90 days according to Figure 3-8. This implies either that the sealed specimen also measures drying shrinkage after this point or that the drying shrinkage has a minor effect after 90 days.

The concrete recipe B200 is preferred due to smaller autogenous shrinkage and material properties almost as good as for the recipe B300. According to Vogt et al. (2009) the autogenous shrinkage of recipe B300 should be used for design of the concrete plug due to uncertainties in the number of experimental data and can be seen as a conservative upper limit of possible shrinkage for concrete B200.

However, the difference in autogenous shrinkage for B200 and B300 is substantial and therefore new measurements of the shrinkage are being conducted. In these new experiments the shrinkage of 30 concrete beams, according to the third method, are being measured. Based on the new experimental shrinkage data, it should be possible to determine its distribution and thereby obtain a better representation of the autogenous shrinkage.

Creep

Creep was measured with two different test rigs, one hydraulic test rig used for early loading stages and one mechanical test rig for concrete specimens loaded after three months of curing. The applied load was taken as 20% of the corresponding compressive strength at the time of loading. All concrete specimens for the creep tests were sealed immediately after casting and remained sealed during the testing.

In Figure 3-14, the calculated creep ratio for concrete specimens with different time after the initial loading is shown. The assumption of a linear increase of creep deformation in the logarithmic time scale is, at present knowledge, the best estimation for the trend behavior of creep deformation according to Bažant (1975, 1988). This means that for practical applications a loading age has to be defined. The loading age corresponds to the age of the structure at time of initial loading, for the concrete plug, the loading age is 90 days which corresponds to the time when it is grouted. In addition, decisive load duration has to be defined, and in the case of the concrete plug, the load duration is equal to the life span i.e. 100 yrs. This situation can be described for practical engineers by a Young's modulus valid at the concrete age of three months together with the associated creep ratio describing the additional creep deformation after 100 yrs load duration.

In Figure 3-15 a comparison between the theoretical trend-line and the measured values for two test specimens of concrete B200 is shown. The experimental reading shows results that correspond to the theoretical curve and the small deviations were within the margin of accuracy of the measurement.

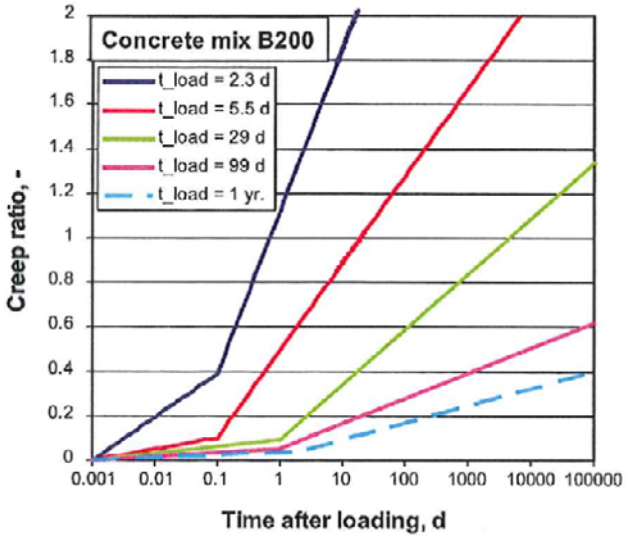

Loading at 90 d ≈ 99 d		
Time duration	Creep ratio φ'	$\chi \cdot \varphi'$
90 d	0.27	0.22
1 yr.	0.34	0.27
10 yrs.	0.46	0.36
100 yrs.	0.57	0.46

Figure 3-14. *Creep ratio at different times of initial loading.*

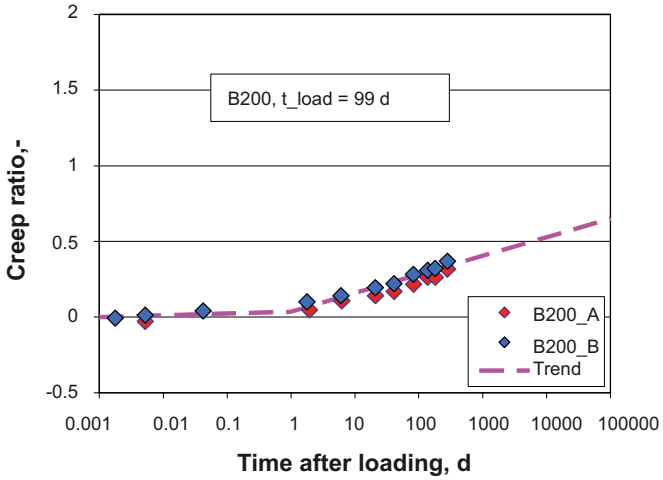

Figure 3-15. *Creep B200 loaded at 99 days after casting, comparison between theoretical and experimental results.*

In experimental series, today, only one experimental setup is still being monitored. Unfortunately the experimental setup still being observed is the case were the initial loading, i.e. the loading age, is one year.

The creep factor specified above is based on linear creep, which presumes that the concrete still acts linearly, i.e. that the stresses obtained in the concrete are low enough. The load level in-situ at the concrete plug will be higher than the load level at the creep test experiments, i.e. higher than 20% of the compressive strength, according to the numerical investigations presented in Section 4.3.3. The principle used in most of the design calculations has therefore been to limit the compressive stresses to the level where linear creep no longer can be assumed according to the design codes. According to Boverket (2004) the limit for elastic behavior of concrete in compression should be set to

$$\sigma_c \leq 0.6 f_{cc} \tag{3-1}$$

The tests on the low-pH concrete used in the plug showed a larger elastic portion than is the case for normal concrete. Based on this, the elastic limit of the compressive stresses was chosen by Dahlström et al. (2009) as

$$\sigma_c \leq 0.65 f_{cc} \tag{3-2}$$

In the analyses, this has been considered where the compressive strength has been reduced to correspond to the limit of linear creep for long-term loads, see Section 4.3.1.

A higher load than this is likely to cause non-linear deformations that are complicated to predict. The non-linear creep that occurs for high compressive loads could in some cases result in failure for a sustained load that is below the compressive strength. In, for instance, FHWA (2006), failure occurs due to non-linear creep in less than 30 minutes for a sustained load of 90% of the compressive strength.

Due to the uncertainties with non-linear creep, new test series have been suggested within the project. In these test series, it is planed to study long-term creep deformations at load levels between about 50% and 80% of the compressive strength.

3.3.4 Thermal loads

The deposit of copper canisters will cause a temperature increase in the surrounding rock, due to the heat generation from the spent nuclear fuel. Based on the thermal properties of the rock situated at Forsmark, an analytic solution was used to calculate the temperature increase during a time-period of 100 years, see Hökmark et al. (2009, 2010). The analytic solution is based on the assumption with homogenous thermal properties in all directions. This means that homogenous rock has been assumed and therefore the lower thermal conductivity in open tunnels is neglected as well as the effect from ventilation in these tunnels. The temperature increase shown in Figure 3-16 should therefore be seen as an upper limit on the temperature increase. The calculation is based on the thermal properties of Forsmark according to Stephens et al. (2007) and Sundberg et al. (2008) with a thermal conductivity of 3.57 W/(m·K) and a heat capacity of 2.06 MJ(m^3·K). The time dependent temperature increase is presented based on the following distances from the closest canister 3 m, 6 m, 10 m, 15 m and 20 m. In a final repository, the distance from the concrete plug to the closest deposited canister will be about 6 m. In the current design, which the full-scale test will be based on, the distance from the borehole of the closest canister to the upstream face of the concrete plug is approximately 5.4 m, as seen in Section 2.1.

In Figure 3-16 it is seen that the temperature at the position of the concrete plug has increased about +20°C after approximately 40 years and +25.5°C after 100 years for the curve 6 m from the canister.

In Ageskog and Jansson (1999) the temperature increase from the spent nuclear fuel was calculated with a finite element model for three different concepts of repository layout. Dahlström et al. (2009) interpreted the results from Ageskog and Jansson (1999) at the position of the concrete plug and concluded that the temperature increase at the mouth of the deposition tunnels was at maximum +25°C after 100 years, as seen in Table 3-2.

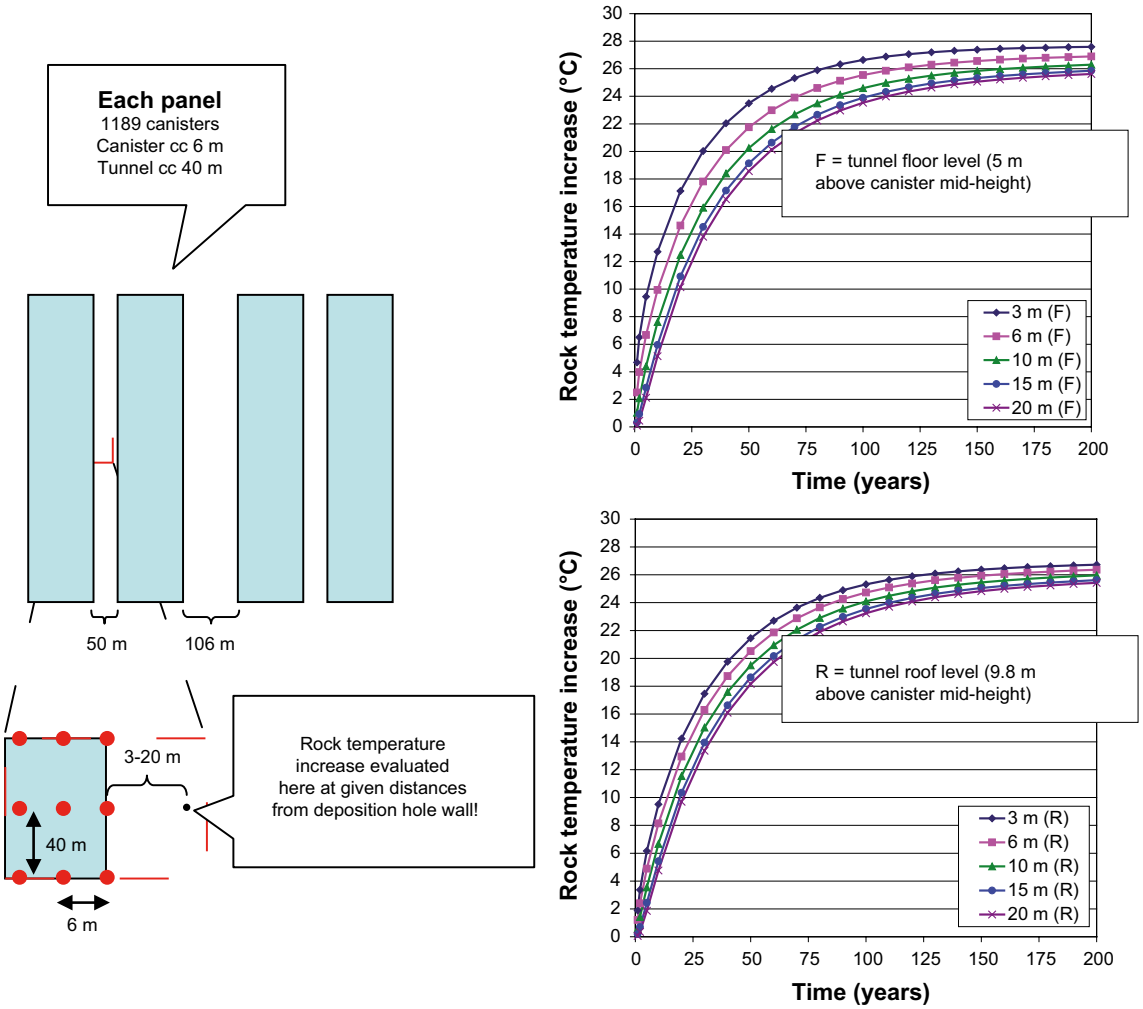

Figure 3-16. *Temperature increase due to spent nuclear fuel.*

Table 3-2. Maximum temperature increase from the spent nuclear fuel (Dahlström et al. 2009).

Time [years]	Temperature [°C]
0	+0
1	+1
10	+10
100	+25

The difference in temperature at floor of plug front (6 m) and at the roof of the plug end (10 m) is shown in Figure 3-17. It is shown in the figure that the maximum difference in temperature between these points is approximately 3.3°C after 10 years and 1.5°C after 100 years. These values do however underestimate the thermal gradient since the cooling of the plug end due to the ventilation of the transport tunnel is not considered.

The increase in temperature from the spent nuclear fuel have also been calculated by Fälth and Gatter (2009). Their study also showed that the temperature increase after 100 years is about +24°C, as seen in Figure 3-18. In their finite element model, the tunnels were included and the maximum temperature difference over a 4 m thick tapered concrete plug was 3.7°C and occurred after 5 years. The temperature difference over the thickness of the concrete plug reduced over time and after 100 years was only 1.7°C. Additional information regarding the results from the analyses of Fälth and Gatter (2009) is found in Section 4.1.

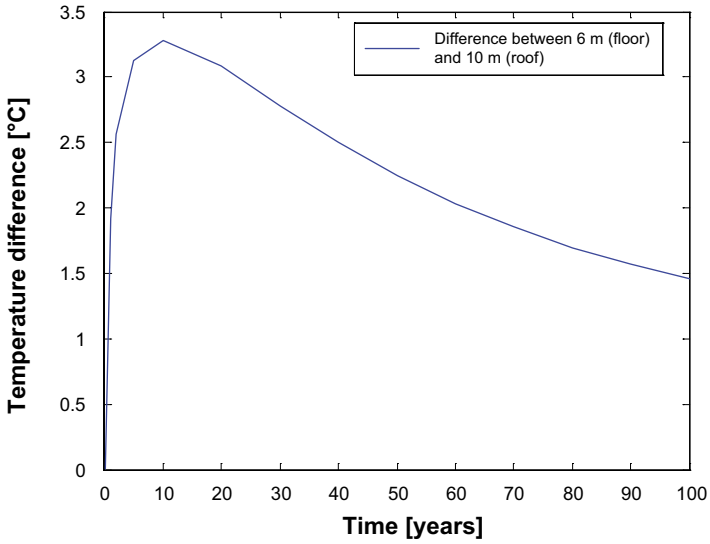

Figure 3-17. *Temperature difference between tunnel floor and roof.*

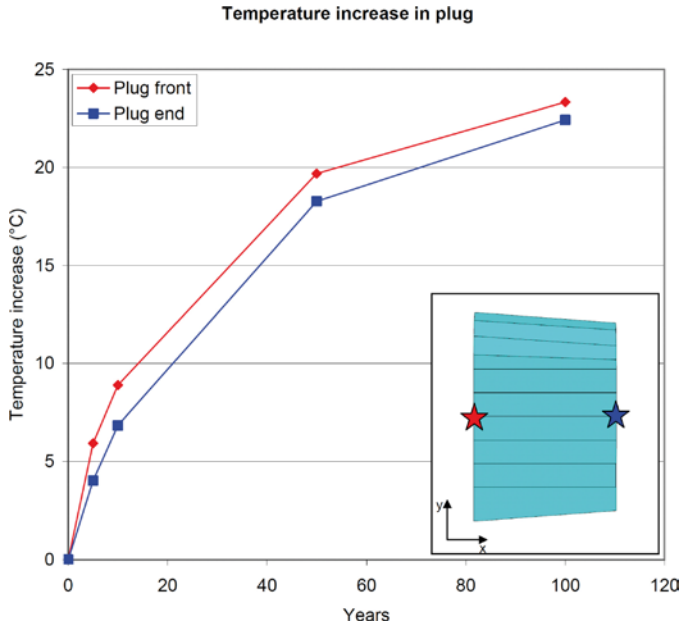

Figure 3-18. *Temperature increase due to spent nuclear fuel, from Fälth and Gatter (2009).*

A conservative upper limit of the thermal increase from the canisters with spent nuclear fuel can be taken as the values corresponding to a distance of 3 m from the closest canister according to Figure 3-16. These temperatures are higher than the expected in-situ due to the fact that open tunnels and their ventilation is neglected as well as the distance is less than at the final repository. In design load cases intended to estimate the effect of large compressive stresses in the concrete plug, the curve corresponding to a distance of 3 m and at the floor level of the plug is recommended. For these load cases, the temperature increase causes high compressive stresses in the concrete plug due to the restrained thermal expansion, but also due to the fact that the rock mass is heated and expands which introduce compressive stresses in the concrete plug.

The temperature increase from the spent nuclear fuel can for some load cases have a beneficial effect. In the design load cases, which cause large tensile stresses in the concrete plug and therefore could risk cracking, the temperature increase has an opposite effect to the shrinkage of the concrete. A conservative estimation of the temperature increase from the spent nuclear fuel should therefore be based on a low value if cracking is of interest. The most conservative approach is to neglect the increase in temperature completely. However, this approach could perhaps be too conservative and make it difficult to find any design that satisfies this criterion. Another possible approach for conservative estimation of the temperature increase is to estimate the thermal development based on the results from Ageskog and Jansson (1999) as shown by Dahlström et al. (2009) where minimum temperature increase from the spent nuclear fuel is presented in Table 3-3.

The temperature increase from the spent nuclear will be different for each concrete plug. The first concrete plug will be subjected to a high increase in temperature while the concrete plug in the last deposition tunnel will be subjected to a high initial temperature but at the same time a low increase with time.

Table 3-3. Minimum temperature increase from the spent nuclear fuel (Dahlström et al. 2009).

Time [years]	Temperature [°C]
0	+0
1	+0
10	+2
100	+7

3.3.5 Prestressing of the plug

The temperature measured at boreholes in Forsmark presented by SKB (2008a), shows that it is about +10.4°C and +11.6°C at the depth of 400 m and 500 m respectively. In previous studies, a higher temperature of approximately +15.0°C, based on the properties of Äspö, has been assumed.

The gap between the rock surface and the concrete plug is going to be grouted after approximately 90 days to compensate for the early age autogenous shrinkage of the concrete plug. The low-pH concrete has large early age autogenous shrinkage and the total shrinkage the first 90 days after casting is about 0.9–1.0 mm/m, as shown in Section 3.3.3. The early autogenous shrinkage would result in that the concrete plug shrink approximately 4 mm at the top and about half this value on each side of the plug. It is assumed that the concrete plug at an early age will debond from the rock surface and be subjected to free shrinkage. This implies that the concrete plug is stress free before grouting.

Cooling equipment will be provided in the concrete plug to reduce the temperature increase during hydration. After 90 days, the cooling equipment is intended to be used for reducing the temperature in the concrete even more, to improve the debonding between the concrete and the rock surface and to increase the slot between the rock and the concrete surfaces.

Before grouting the slot (between the rock surface and the concrete plug) it is planned to start cooling the concrete plug down to +4°C after approximately 90 days of curing. Based on the temperature measured at Forsmark, this results in a decrease in temperature of about 6.6°C – 7.6°C. This decrease in temperature will slightly increase the gap between the concrete and rock surfaces with about 0.5 mm at the top. After the concrete plug is grouted, the cooling stops and the temperature increases up to its initial value again. The cooling before grouting is thereby causing a prestress of the concrete plug.

According to Figure 3-16 the temperature at the position of the concrete plug has increased about +20°C after approximately 40 years and +25°C after 100 years for the curve 6 m from the canister. This means that the concrete plugs that are cast after approximately 40 years can only benefit from about +5°C increase in temperature from the spent nuclear fuel. On the other hand, these plugs will be able to have a higher prestress due to cooling at the time of grouting. The prestress after 40 years could be about 27°C, which would completely compensate for the shrinkage after 100 years. However, a too high prestress could cause the concrete plug to reach a compressive failure when subjected to the water and swelling pressure unless a load case verifying this has been studied in advance.

The prestress has just like the temperature increase from the spent nuclear fuel a beneficial effect for load cases concerning cracking of the concrete plug since it introduces compressive stresses in the concrete plug. Based on the characteristic value of the elastic modulus of 33.9 GPa according to Vogt et al. (2009), a thermal expansion coefficient of $\alpha = 10^{-5}$ 1/°C and a thermal prestress of 6.6°C corresponds to a compressive stress of $\sigma = E \cdot \Delta T \cdot \alpha = 2.2$ MPa in the radial direction of the concrete plug. The prestress is of course not beneficial in a load case intended to study large compressive stresses in the concrete plug.

3.3.6 Settlements in the rock foundation

At the location of the plug section, a very good quality of rock is required. The expected property of the rock at a final repository at Forsmark is presented in Section 3.2.2. Fallout of the rock, close to the v-shaped slot, is not allowed and should be avoided by carefully selecting a plug section without persistent rock fractures and critical orientations.

Settlements in the rock foundation should be included in the numerical analyses by means of choosing a low elastic modulus of the surrounding rock. In the numerical analyses presented in Section 4.3.1 an elastic modulus of the rock has been studied within the interval of 25–80 GPa. The expected elastic modulus of intact rock is within approximately 70–80 GPa according to Section 3.2.2. The low value of elastic modulus of 25 GPa has been considered to compensate for a rock with fractures in this study.

3.3.7 Earthquake

The concrete plug should be designed to resist earthquake loads according to a Swedish response spectrum. In seismic design, the earthquake loads are obtained by multiplying the masses with horizontal ground accelerations. The horizontal accelerations obtained are loads given in SKI (1992) and presented here in Figure 3-19. These are valid for accelerations at the ground surface.

The corresponding values at the level of the repository deposition, about 500 m below ground, are much smaller. According to Sharma and Judd (1991) there have been many reports of underground facilitates that performed satisfactorily during earthquakes although nearby surface structures suffered considerable damage. The main reason for the reduction in underground damage is the lower levels of shaking at depth in comparison with surface motions. According to Wang (1993) due to the fact that the underground structure is constrained by the surrounding rock it is unlikely to move to any significant extent independently of the medium or be subjected to vibration amplification.

Sharma and Judd (1991) show that for earthquakes below six on the Richter scale only a slight extent of damage is found for the studied earthquakes in underground tunnels. Another beneficial factor is the depth of the repository 500 m, which is far enough from the surface since a drastically difference in damage due to earthquakes is found for overburdened depths higher than 50 m. One other factor is that the cases were the overburden material consists of hard rock are those showing the smallest extent of damage during earthquakes. The effect of depth and overburden material is illustrated in Figure 3-20.

The load from a typical Swedish earthquake is in this aspect rather small, compared to the size of the swelling pressure of the bentonite clay and the water pressure. The earthquake load can therefore be neglected in the numerical analyses.

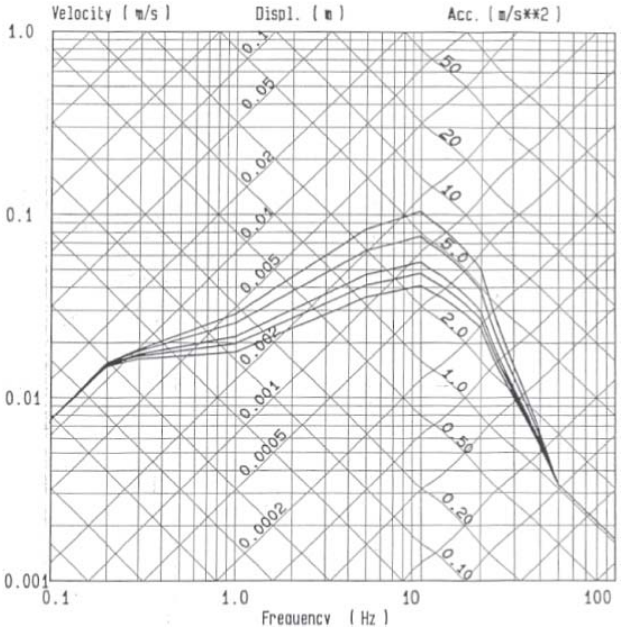

Figure 3-19. *Seismic ground spectra for horizontal ground accelerations. The curves represent different values for the damping in the construction 0.005, 0.02; 0.05; 0.07 and 0.10. From SKI (1992).*

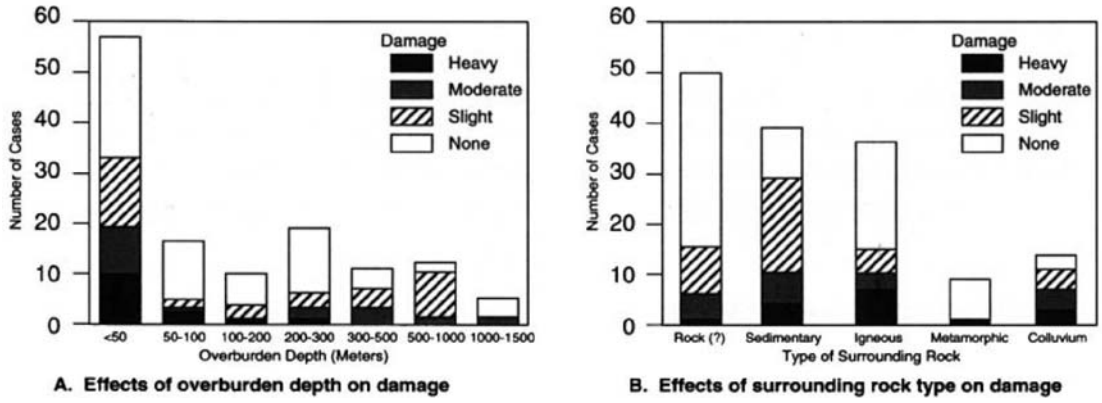

Figure 3-20. *Literature review of damages due to earthquakes depending on the depth and the surrounding rock type from Sharma and Judd (1991).*

4 Structural analyses of the concrete plug

Numerical studies have been performed on alternative designs of the concrete plug. The two main alternatives for the design of the concrete plug that have been studied are; a tapered plug (cone shaped) and a dome shaped plug. Numerical studies have been performed for different designs of these two alternatives, for instance different geometries have been studied and most of the designs that have been studied are unreinforced.

The analyses have been performed with different numerical software and by different persons. The finite element software's that have been used for evaluating the concrete plug, and that are presented in this report are 3DEC (Itasca, http://www.itascacg.com/3dec/), ABAQUS (Simulia, http://www.simulia.com/), ADINA (http://www.adina.com/index.shtml) and ANSYS (http://www.ansys.com/) . These results are compared and evaluated in this report to verify that the results all indicate the same behavior and give similar results. During the progress of this project, the preconditions have been changed. Therefore, the preconditions in all analyses have not been the same. Thus, the results from all numerical analyses are not identical. However, even though the preconditions have been interpreted differently in some cases, the results support each other and are not in contradiction. The principal strategy with the numerical analyses has been to perform them with a varying degree of conservatism. One example is the determination of the maximum swelling pressure from the bentonite clay. In the first analyses, a very conservative limit was used where the analyses were stopped when the stresses reached the design value and in the following, more detailed analyses the non-linear behavior was introduced where the crack opening process and the reduction in concrete strength due to cracking was included.

The purpose of this section is to summarize all calculations, compare the results from the different analyses and draw general conclusions regarding the structural safety.

4.1 Tapered plug

4.1.1 Linear analyses with elastic material properties

The first analyses of the tapered plug (cone shaped) were made by Fälth and Gatter (2009). In their report, the possibility to create an unreinforced concrete plug was presented. In the report, results from mechanical and thermo-mechanical models of the tapered concrete plug are presented. The models were analyzed with 3DEC and include the host rock around the intersection between a deposition tunnel and a main tunnel, as shown in Figure 4-1.

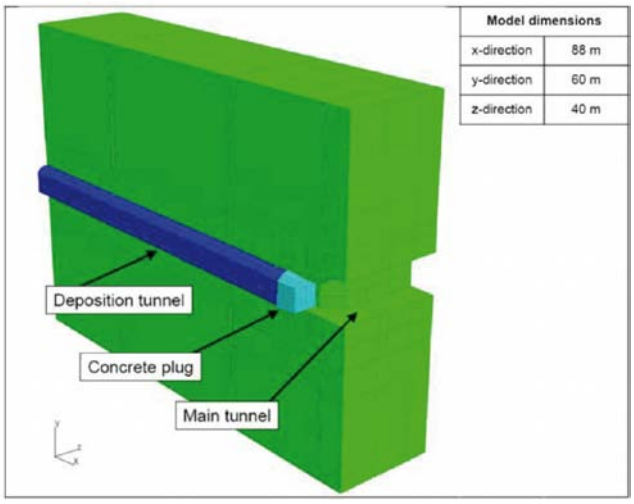

Figure 4-1. *3D model of the tapered concrete plug and the host rock.*

Below the most important characteristics of the analyses are summarized

+ Water pressure of 4 MPa and swelling pressure from the backfill of 2 MPa.
+ The thermo-mechanical effect due to heat generation from the spent fuel was also considered. The maximum temperature increase was calculated as +24°C and the largest temperature difference over the thickness of the concrete plug was calculated as +3.7°C.
– These calculations did not include; shrinkage, creep, prestressing due to cooling before grouting, the gravity load and settlements in the rock foundations.

In the analyses, only a high value of the temperature from the spent nuclear fuel has been used, see Section 3.3.4. The compressive stresses in the concrete plug are increased due to the high value of the surrounding temperature. The high value is conservative regarding the determination of the load capacity of the concrete plug. However, the high temperature will postpone the cracking in the concrete plug and it is therefore not conservative regarding the risk of cracking.

In the analyses, different approaches for describing the non-linear contact between the concrete plug and the rock were studied; the Mohr Coulomb law and the law in Model Code 90 (CEB 1993).

In the analysis, the excavation process and the installation of the backfill and casting of concrete were simulated. The calculation comprised the following steps

1. Application of in-situ stresses and establishment of initial equilibrium in an intact host rock.
2. Excavation of transport tunnel.
3. Excavation of deposition tunnel.
4. Installation of backfill material and of the plug. A 6 MPa stress was applied in the backfill material to simulate the total effect of swelling pressure and a pore water pressure inside the tunnel.
5. Thermo-mechanical calculation to examine effects of heat from the spent fuel.
6. The effect of pore water pressure in the plug-rock interface was applied (accidental case).

The maximum temperature increase in the plug is found after 100 years and is about 24°C. This temperature increase is in agreement with the estimation of the temperature development in the repository by Ageskog and Jansson (1999). The heating of the plug is non-even. There is a temperature gradient in the horizontal direction due to the open transport tunnel with no heat sources. There is also a temperature gradient in the vertical direction due to the location of the canisters below the tunnel floor. The gradients are largest at the beginning of the heating and become reduced after longer times. At the time when the model was set up, the details of the real repository layout were not known. Thus, the temperature calculations were based on a generic repository layout. Changes in the layout may also change the maximum temperature in the plug. One layout detail that is important for the temperature evolution is the distance between the nearest canister and the plug front. Here it was arbitrarily set to be equal to one canister distance, i.e. 6 m. An increase of this distance would result in a decrease of the temperatures in the plug.

The stresses along the wall-floor and wall-roof edges are in general higher than in the centre of the plug due to stress concentrations along the edges. The highest stresses are found at the end of the plug close to the walls and the floor. Without heating, the maximum compressive stress is locally about 50 MPa but about 20 MPa on average at these locations. The thermal load gives significant increase of the compressive stresses. The peak stress and the average stress along the edges at the plug-end increased by about 20 MPa and 10 MPa, after 100 years of heating respectively. The high impact of the heating is due to the high degree of confinement in the plug.

The sensitivity of the results to changes of constitutive models, to changes of the plug geometry and to pore water pressure in the rock-concrete interface was examined. The results indicate that the displacements in the plug will be within reasonable ranges but the stresses may locally exceed acceptable levels. However, they can be reduced by choice of an advantageous plug geometry and by having a good rock-concrete bond. The results also show that the stress additions in the rock due to the thermal load may yield stresses that locally exceed the spalling strength of the rock. It was concluded that, with choice of an appropriate design, the tapered plug seems to be an applicable concept for plugging of deposition tunnels. It was also concluded that further studies of the tapered plug concept should use material properties parameter values for low-pH concrete. Further, they should also include a closer examination of the rock-concrete interaction, a better model for the thermal load and a study of the effects of having rock fractures in the region around the plug.

4.1.2 Time history analyses with non-linear material properties

The same tapered concrete plug was studied with ANSYS version 10. In this analysis, only the concrete plug was modeled where rigid boundary conditions where applied to the perimeter of the plug. The reason for excluding the rock was that maximum tensile stresses occur in the concrete plug when the rock is assumed completely rigid. The concrete plug was modeled with non-linear material properties based on fracture mechanics. Cracks appear, when tensile stresses reach the tensile strength and these cracks will maintain their inclination regardless if the stress field rotates. If the stress field rotates a lot, new cracks can be formed perpendicular to the previous in the same element.

Below the most important characteristics of the analyses are summarized

+ Water pressure of 4–5 MPa and a swelling pressure of 2 MPa.
+ Gravity load.
+ Shrinkage (after grouting 90 days after casting) for recipe B200 and B300 according to Vogt et al. (2009), see Section 3.3.3.
+ Temperature increase due to the canisters with spent fuel according to Section 3.3.4.
+ Prestress from cooling the plug during grouting 0–11°C.
+ Shear key effects, some areas of the concrete plug are constrained for tangential displacements, to represent the constraint due to the irregular shape of the concrete rock interface.
– The calculations does not account for the creep.

A numerical analysis with the program is divided in steps, each corresponding to a load change from one magnitude to another. The state of the model in terms of stress, strain, displacements, etc is updated throughout all analysis steps. The effects of previous steps are always included in each new step. The calculations were performed in different steps to account for the time history changes in temperature from the spent nuclear fuel and the shrinkage, where the 100-year span was divided into 10 steps.

In the calculation the following material properties were used, corresponding to the characteristic properties of B200 according to Vogt et al. (2009):

- Tensile strength 2.9 MPa.
- Compressive strength 54 MPa.
- Elastic modulus (not including creep) 33.9 GPa.
- Poisons ratio 0.27.

The fracture energy was not measured in the experiment, instead it was chosen to 100 Nm/m^2. The concrete recipe specified above has material properties that exceed the concrete grade C50 according to Eurocode 2 (SIS 2005) and concrete grade C50/60 according to BBK 04 (Boverket 2004). Unfortunately, neither of these design codes specifies the size of the fracture energy. According to Model Code 90 (CEB 1993) the fracture energy is 105 Nm/m^2 for concrete C50 with a maximum gravel size of 16 mm.

All analyses were performed with the material properties corresponding to the strength for concrete recipe B200 as shown above. The experimental data regarding the autogenous shrinkage was somewhat limited and therefore analyses were performed with the shrinkage measured for both B200 and B300 to study the influence of the shrinkage. Assuming that the autogenous shrinkage is zero 90 days after casting, gives a final shrinkage of 0.29 mm/m after 100 years, based on the recipe B300 in Vogt et al. (2009). By a simple calculation it is possible to show that this shrinkage will lead to cracking. At free shrinkage, a slot of 1.0–1.5 mm, based on a tunnel diameter of 4–5 m, would appear in the top of the plug and half the thickness on both sides of the plug. This shrinkage will lead to cracking since the concrete plug is restrained to shrink due to the cohesion to the rock. According to the measurements in Vogt et al. (2009), a maximum tensile strain of about 0.05–0.12 mm/m can be reached before cracking. Based on the characteristic material properties, cracking will initiate at a tensile strain of 0.09 mm/m. The difference between the shrinkage strain and the maximum tensile strain before cracking, will appear as cracks unless some other effect can compensate for it. The effects that primarily will compensate for the shrinkage, are the prestressing due to cooling at the time of grouting and the increasing temperature due to the spent fuel canisters.

The results from the performed FE analyses confirm the statement above. One important conclusion from these calculations is that the prestress is vital to compensate for the cracking that occurs due to shrinkage from 90 days after casting to the end of the lifespan of 100 years. There is a large difference in the extent of cracking depending on, whether the shrinkage curve for B200 or B300 is used.

The variations with time for the shrinkage and the temperature increase from the canisters with spent nuclear fuel, result in a case where the total equivalent temperature is at a minimum about 10 years after the installation. After this point the temperature from the canisters increase faster than the shrinkage and the total equivalent temperature is thereby increasing from about 10 years to 100 years as seen in Figure 4-2. The temperature from the spent nuclear fuel is here taken as the maximum calculated temperature, 3 m from the closest canister, in Figure 3-16. It can be seen in Figure 4-2 that only for the case where both the prestress and the temperature from the nuclear fuel are included the temperature is above the equivalent temperature of –9°C which corresponds to the crack initiation strain mentioned above.

In Figure 4-3 the difference in equivalent temperature from shrinkage of B200 and B300, in combination with temperature increase from the nuclear fuel at a distance of 3 m or 20 m from the closest canister is shown. It can be seen that the risk for cracking increases if the lower values of the temperature, corresponding to the distance of 20 m, is used. The highest risk of cracking occurs after approximately 10 years with shrinkage according to B300 and about 5 years with shrinkage according to B200.

In the non-linear FE analyses, it was shown that, if both the favorable effects[1] are neglected, the tapered plug cracks along its perimeter (at the zone in contact with the rock) regardless if the shrinkage curve for B200 or B300 is used. These cracks will go through the entire thickness of the plug and would result in leakage.

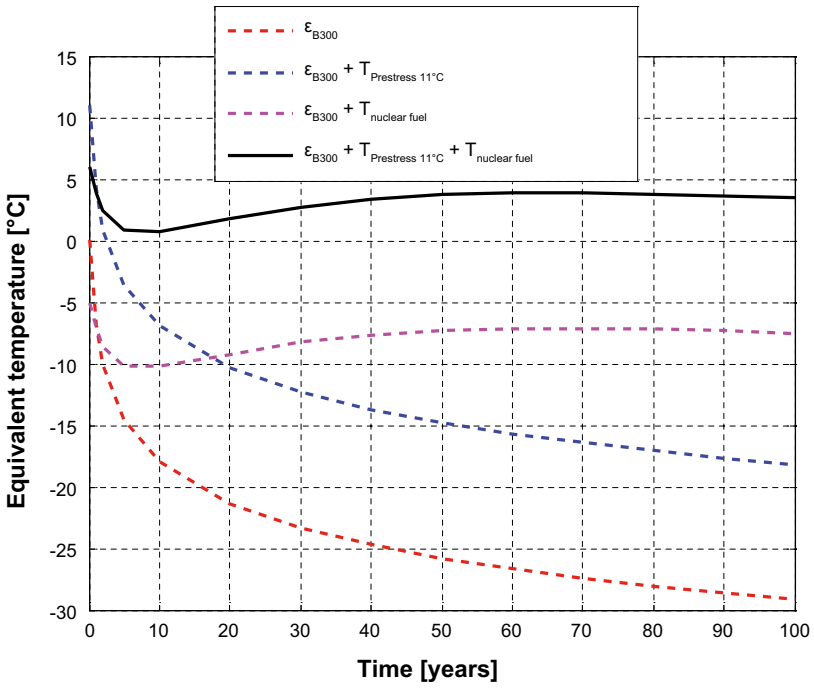

Figure 4-2. *Equivalent temperature loads from shrinkage, prestress due to cooling of the concrete plug before grouting and thermal effect from the nuclear fuel.*

[1] Temperature increase from the spent nuclear fuel contained in the copper canisters and the prestress effect caused by the cooling of the concrete plug before grouting.

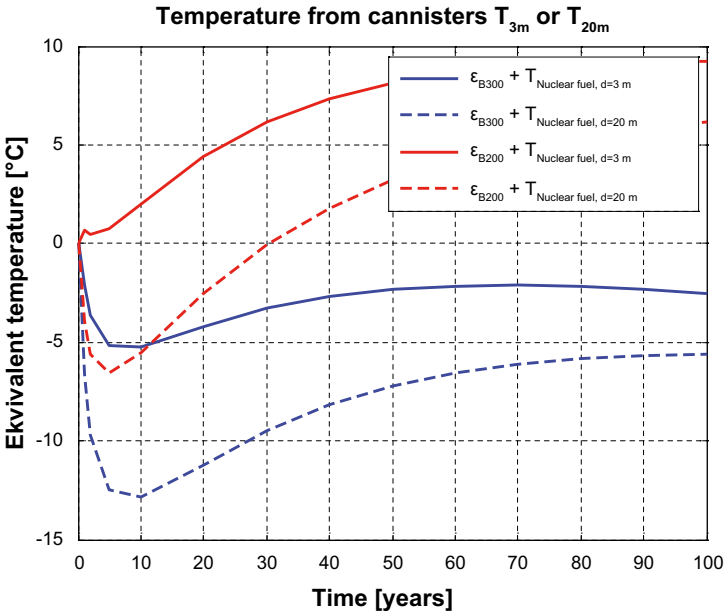

Figure 4-3. *Equivalent temperature loads from shrinkage (B300 and B200) and thermal effect from the nuclear fuel depending on the distance to the closest canister (3 m or 20 m).*

In a case where either the favorable effect of the prestress or the temperature increase is included, cracks along the perimeter and through the thickness of the plug appear in the calculations, if shrinkage according to recipe B300 is used. For the same calculations with shrinkage according to B200, on the other hand, only the first part of the concrete plug on the upstream side cracks. These cracks do not go through the entire thickness of the tapered plug and thereby should not result in leakage. In Figure 4-4 and Figure 4-5, the calculated extent of cracking is shown for a case where only one favorable effect is included to compensate for the autogenous shrinkage according to concrete recipe B200 and B300 respectively. In both figures, the favorable prestressing effect due to cooling the concrete plug to +4°C before grouting has been neglected. Similar results would be obtained if the increase in temperature due to the spent nuclear fuel had been neglected instead. In the figures, the elements that have cracked are illustrated with red circles in the centre. The inclination of each circle represents the average crack plane of the elements.

To prevent cracks going through the tapered plug, both heating from the spent fuel and the prestressing effect due to cooling before grouting must be taken into account if the autogenous shrinkage is based on the measured values for concrete recipe B300. If it is based on the measured autogenous shrinkage for recipe B200 on the other hand, only one of these favorable effects needs to be taken into account to compensate for the cracking caused by shrinkage.

It is likely to assume that due to the irregular shape of the rock surface, some areas will have a higher resistance to tangential movement between the rock and concrete surface. These arbitrary placed shear keys, will provide constraints for tangential translation while in between two shear keys a translation may be possible. To simulate this in a FE analysis, tangential displacements were constrained at nodes along the perimeter of the plug. In the thickness direction (z direction in Figure 4-4) varying degrees of the nodes, between 25 and 100%, were constrained. The result shows large cracks near the shear keys (constrained nodes) while the area between two shear keys is uncracked. This shows that if shear keys are considered in the analysis, much larger crack widths appear but these cracks are not necessarily forming a network of cracks through the thickness that could result in leakage.

The layer of bentonite clay behind the concrete plug will seal the plug construction from leakage. However, there is a risk that large cracks going through the concrete plug could cause erosion of the bentonite clay and hence the sealing effect may not occur especially if the crack occur before the seal have reached full saturation.

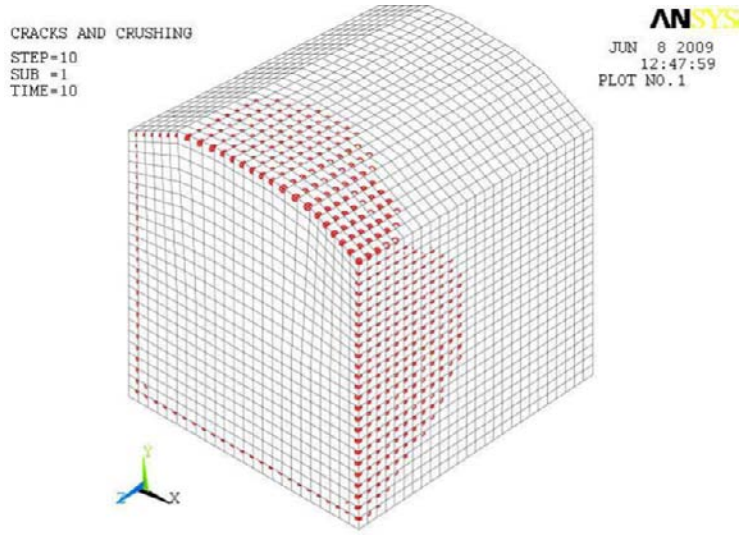

Figure 4-4. *Illustration of the extent of cracking due to the autogenous shrinkage for concrete B200 if the prestressing effect is neglected.*

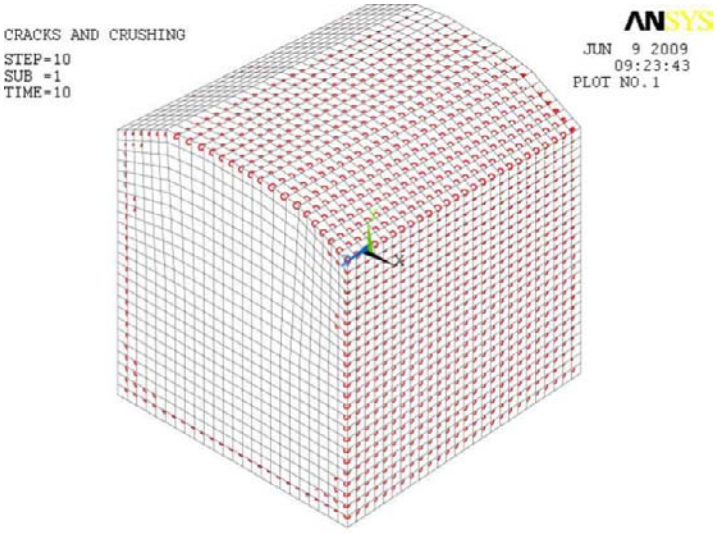

Figure 4-5. *Illustration of the extent of cracking due to the autogenous shrinkage for concrete B300 if the prestressing effect is neglected.*

4.2 Reinforced dome shaped plug

4.2.1 Linear analyses with elastic material properties

The first steps in the calculation of a dome shaped concrete plug was made for a reinforced plug presented in Dahlström (2009). The analysis was based on the concrete plug that was experimentally tested in the Prototype Repository called plug II, see Section 1.1.3. It consists of ordinary concrete and includes reinforcement. In this numerical study, different degrees of restraint between concrete and rock as well as the effect of the stiffness of the surrounding rock were evaluated.

The most important characteristics of the analyses are summarized below

+ Water pressure of 4.5 MPa (5.85 MPa including load factors) and a swelling pressure of the bentonite of 0.1 MPa (0.115 MPa including loading factors).
– Load effects from shrinkage, gravity load, prestress due to cooling before contact grouting and temperature increase due to the canisters with spent nuclear fuel are not included in these analyses.
– Effects from creep and settlements in the rock foundation are not included in the analyses.

The calculations show that the concrete plug primarily is subjected to compressive stresses if only water pressure and swelling pressure are considered. In some regions and for certain cases, tensile stresses occur in the concrete plug, but according to the performed calculations only the minimum amount of reinforcement according to Vägverket (1994) is required for the entire concrete plug. The contact pressure in the rock supports varies between 5 and 20 MPa when cohesion and friction of 0.75 between rock and concrete is assumed. The calculations show that increasing stiffness of the surrounding rock reduces the relative displacements between the rock and the concrete. The largest compressive stresses appear in the concrete plug when full interaction between the rock and concrete, i.e. no slip is allowed, is assumed. It is also in this case the largest tensile stresses occur in the concrete plug. The results from these analyses show that the most unfavourable boundary condition for the concrete plug is a rigid connection to the surrounding rock, i.e. no relative displacements between the rock and the concrete plug are allowed. This means that all imposed displacements will result in stresses in the concrete plug.

4.3 Unreinforced dome shaped plug

4.3.1 Linear analyses with elastic material properties

The purpose of this study was to determine whether it is possible to use low-pH concrete in a dome shaped plug and if it can be designed without reinforcement. The requirements on the concrete plug were that it should limit the leakage of water to an acceptable limit and that the stresses are below the specified strengths. The material parameters for low-pH concrete used in this project were based on the properties presented in Vogt et al. (2009). The project was initially based on the design in the previous study of Dahlström (2009). As a result from this project, suggestions on suitable modifications of the geometry of the plug were presented.

A summary of the loads considered in Dahlström (2009) is presented below

+ Water pressure of 4 MPa and swelling pressure of 2 MPa.
+ The temperature increase due to the canisters with spent nuclear fuel was assumed to result in a maximum increase of 25°C and a minimum increase of 7°C. The largest possible temperature difference over the dome shaped plug thickness was assumed as 25°C for the temperature increase of 25°C.
+ Prestressing due to cooling before contact grouting was assumed to correspond to 10°C.
+ The shrinkage was based on twice the measured autogenous shrinkage for recipe B200, starting from 90 days after casting. However, the shrinkage used in the analyses is almost the same as for B300.
+ Creep was accounted for by reducing the elastic modulus with a creep factor and limiting the allowable stresses according to BBK 04 (Boverket 2004).
+ Settlements in the rock foundation were considered by choosing low values on the elastic modulus of the surrounding rock.
– The influence of gravity was neglected.

A two-dimensional, axisymmetric finite element model was developed, as shown in Figure 4-6. In the analyses, an assumption of linear material properties for the rock and the concrete was made. The interaction between concrete and rock was simulated with contact friction to study the structural response of the dome plug. A total of 48 load combinations, including eight different loading scenarios and six combinations of material properties, have been studied. In four of these load combinations, the water was assumed to be present in the pressurized side of the slot due to cracking in the contact grouting. This will be verified later in this section as a valid assumption for a load case most severe to cracking of the dome shaped plug.

The load combination that was most critical regarding cracking in Dahlström (2009), included the following

- Prestressing of the plug after contact grouting, applied as an evenly distributed temperature of +10°C.
- Autogenous shrinkage in the concrete plug corresponding to −29°C.
- Temperature increase from the spent fuel, a low increase of +7°C is assumed for the rock and on the surface of the concrete plug facing the slot and the bentonite seal and a zero increase (0°C) in temperature on the downstream surface.

The temperatures applied on the surfaces of the concrete plug and in the rock are shown in Figure 4-8. It can be seen that the temperatures from the spent nuclear fuel are low compared to the calculated temperatures in Section 3.3.4.

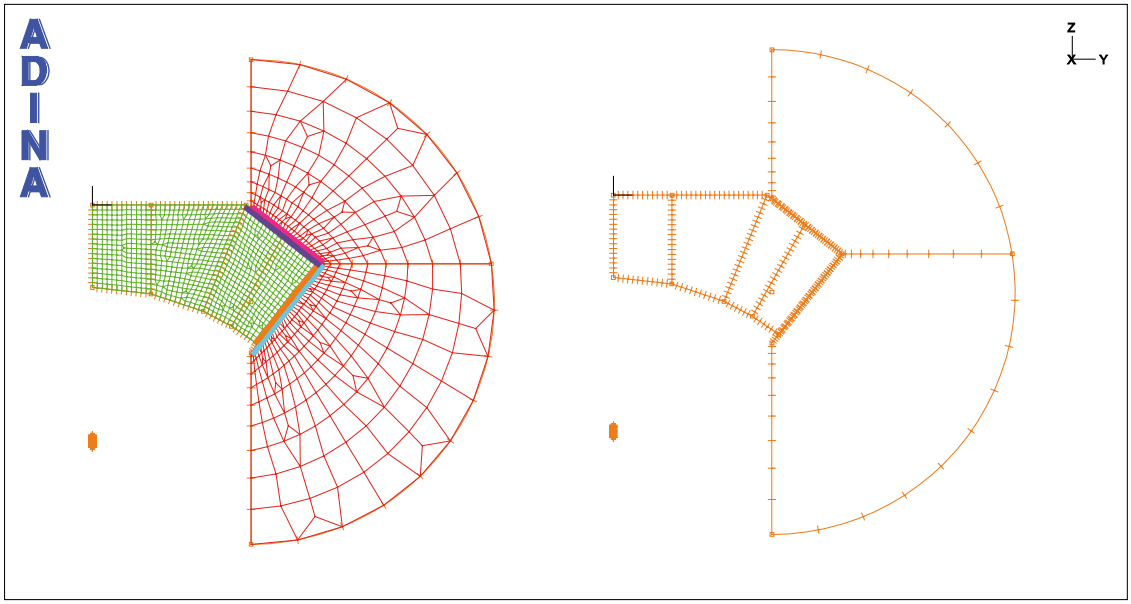

Figure 4-6. *Axisymmetric FE model of the plug, element mesh and geometry.*

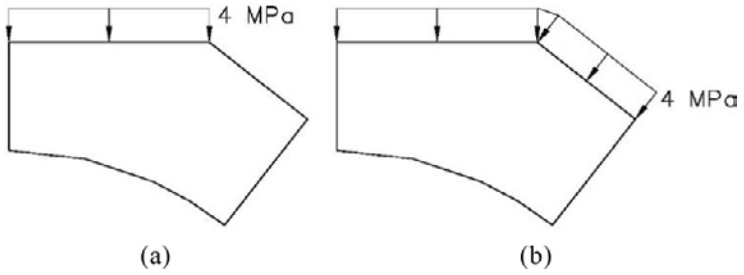

Figure 4-7. *Water pressure on concrete plug: (a) pressure on vertical part and (b) pressure on vertical and diagonal parts.*

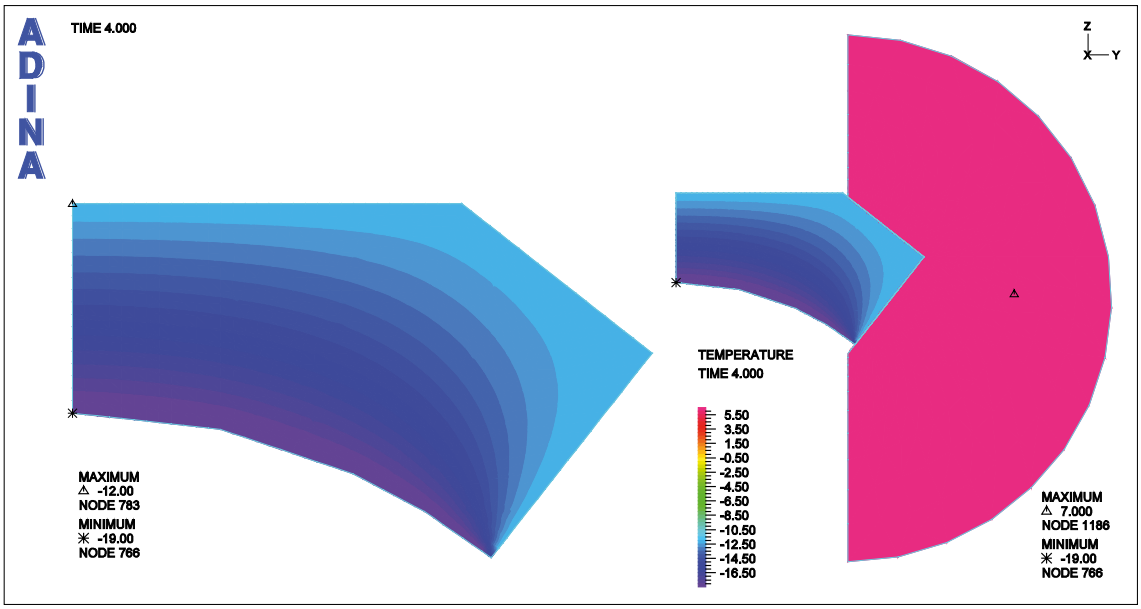

Figure 4-8. *Temperature distribution for the load combination regarding cracking.*

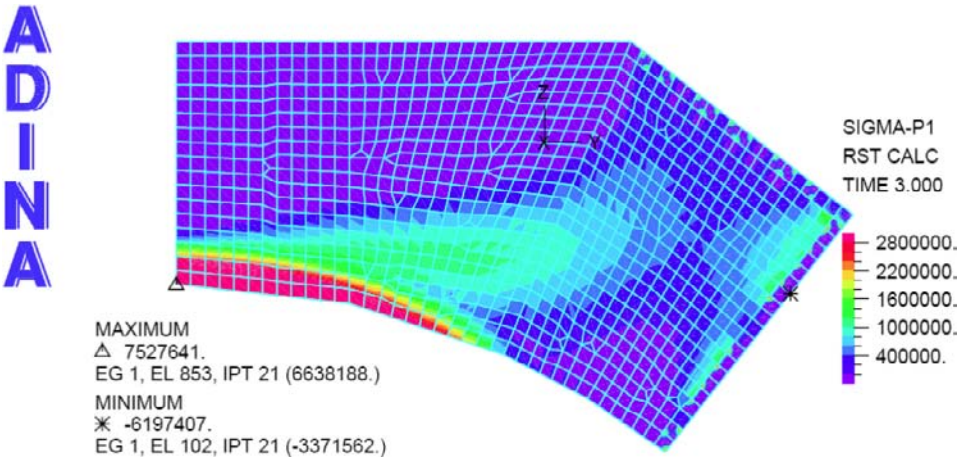

Figure 4-9. *Illustration of the extent of cracking, for the most severe load combination. The areas displayed in red color exceed the characteristic tensile strength and areas in green color exceed the design value of the tensile strength.*

It is shown in the report that the concrete plug will be cracked for some of the load combinations considered, but despite this, it is still probable that an unreinforced concrete dome shaped plug can satisfy the requirements. One of the requirements of the plug at the time was that a maximum of 0.01 l/min water should pass the concrete plug. This requirement corresponded to that a minimum thickness of 0.5 m concrete should remain uncracked in a section, based on the permeability of ordinary concrete of $5 \cdot 10^{-12}$ m/s. This requirement has changed during the progress of the feasibility study of the different solutions for plug design. Instead, the requirement today is that no pervasive cracks, that would result in leakage, may develop Today, it is said that the bentonite seal behind the plug should be designed to be watertight, while the concrete plug has to remain free from cracks going through the thickness of the plug. The concrete plug thereby should prevent erosion of bentonite clay during the homogenization process of the bentonite seal. The small areas subjected to cracking that were found in this study, are thereby not in contradiction to the requirements set on the concrete plug.

The maximum compressive stresses in the concrete plug are about 33 MPa and the maximal deformations in the dome shaped plug are about 3 mm in the centre of the plug. The maximum allowable compressive stresses were determined by the criteria of a linear creep behavior, which resulted in a limit of $0.65\,f_{cc} = 35$ MPa that was chosen for compressive stresses. A displacement of 3 mm was judged small enough to not affect the density of the backfill or the bentonite seal in any significant way.

In the report, it is concluded that some uncertainties regarding the requirements of the concrete plug as well as uncertainties of the material properties are still present. Below, the most important future work is summarized. The given proposals for future work are of different dignity, some are due to lack of knowledge and some due to shortage of time when the report was made. In the report suggestions for future studies and experiments of the low-pH concrete and more detailed analyses to be performed in order to cover the uncertainties and approximations of loads and load combinations made in their studies.

The following aspects require more work according to the authors

- Allowable displacements of the plug, especially the sliding along the rock interface, should be defined better.
- The concrete material parameters, including shrinkage, are based on Vogt et al. (2009) but since this is a new type of concrete and the tests carried out so far only cover a time period of less than two years there are still some uncertainties. Hence, the results in this report presume that there will be a continuous investigation of the material properties of the low-pH concrete. Of special interest is to confirm whether the increase in strength, due to ageing, develops as expected and whether the concrete shrinkage predicted and used in this report is correct or not.
- The value on the Poisson's ratio used is unusually high, a more normal value for concrete is about $\nu = 0.2$, and a sensitivity analysis of this should be carried out.
- The influence of lower Young's modulus for the concrete has not been fully investigated in the analyses and will have to be further studied.
- The load values used for the water pressure and swelling pressure of bentonite are not clearly defined and the effect of larger pressures may have to be further studied.
- The effect of uneven water pressure in the diagonal slit between plug and rock has not been taken into account in this study and will hence have to be further studied.
- In this report, it has been assumed that there will be high RH on either side of the concrete plug, thus justifying the concrete shrinkage used in the analyses. However, a case where no water on the inside of the plug is taken into account, and hence, a larger and uneven shrinkage, has to be taken into account.
- A load combination, considering the effect of shrinkage only without water or swelling pressure, taking into account a possible uneven shrinkage over the plug thickness, may be of interest. An analysis should be made whether this is a load combination of interest, and if so, a complementary analysis should be made.
- The rock temperatures used in the analyses are determined based on a rather early report in which the temperatures given include some rough uncertainties. Hence, it seems realistic to get a somewhat more precise prediction of the temperatures that will be valid for the chosen site at Forsmark.
- In the analyses, a temperature increase in the rock has been assumed. However, a load combination wherein this temperature increase is null should also be investigated.

4.3.2 Time history analyses with non-linear material properties

The same dome shaped concrete plug as described in Section 4.3.1 was studied with ANSYS version 10. In this study, only the concrete plug was modeled where a rigid boundary condition was applied to the perimeter of the plug. The dome shaped plug was studied in the same way as the tapered plug described in Section 4.1. The reason for excluding the rock was that maximum tensile stresses occur in the concrete plug when the rock is assumed completely rigid.

Below, the most important characteristics of the analyses are summarized

+ Water pressure of 4–5 MPa and a swelling pressure of 2 MPa.
+ Gravity load.
+ Shrinkage (after grouting 90 days after casting) for recipe B200 and B300 according to Vogt et al. (2009), see Section 3.3.3.
+ Temperature increase due to the canisters with spent fuel according to Section 3.3.4.
+ Prestress from cooling the plug during grouting 0–11°C.
+ Shear key effects, some areas of the concrete plug are constrained for tangential displacements, to represent the constraint due to the irregular shape of the concrete rock interface.
– The calculations do not account for the creep.

All analyses were performed with the material properties corresponding to the strength for concrete recipe B200 as shown in Section 4.3.1. The experimental data regarding the autogenous shrinkage was somewhat limited and therefore analyses were performed with the shrinkage measured for both B200 and B300 to study the influence of the shrinkage.

A numerical analysis with the program is divided in steps, each corresponding to a load change from one magnitude to another. The state of the model in terms of stress, strain, displacements, etc is updated throughout all analysis steps. The effects of previous steps are always included in each new step. The calculations were performed in different steps to account for the time history changes in temperature from the spent nuclear fuel and the shrinkage, where the 100-year span was divided into 10 steps. The external pressure was introduced in the analyses in the initial step, before applying shrinkage and the thermal effect.

The calculation of the dome shaped concrete plug shows that this design is sensitive to the shrinkage, although not to the same extent as the tapered concrete plug. The main difference between these two design alternatives is the extent and the location of the cracks. The tapered concrete plug cracks all around the plug due to shrinkage, as shown in Figure 4-5, resulting in an interface between concrete and rock that is fully cracked. The dome shaped plug is also subjected to cracking, and the cracks primarily of concern regarding leakage are found in the interface between concrete and rock. However, it is only on the pressurized side of the slot that cracks are formed. The abutment of the dome, i.e. the side of the slit closest to the transport tunnel, will remain uncracked. Water will most likely fill the voids between concrete and rock, but since there are no cracks on the side of the slot closest to the transport tunnel, the water will not be able to leak out via the concrete plug. This result verifies the assumption made in the previous analysis that the water pressure might be present on the side of the slit closest to the bentonite seal, i.e. the upstream side as shown in Figure 4-7.

In addition to these cracks, the dome shaped concrete plug cracks in both a radial and a tangential pattern on the curved surface on the downstream side of the plug. These cracks are a result from combination of the pressure loads and the shrinkage. In the numerical models, the green circles represent secondary cracks that have initiated perpendicular to the first crack (illustrated as red circles). In Figure 4-10 the extent of cracking for a load case where only the beneficial effect from the temperature increase from the spent fuel is included. In Figure 4-11 the cracking in the dome shaped plug is shown, based on autogenous shrinkage according to recipe B300 and the, in this aspect, beneficial effect of the heating due to the spent fuel canisters. This calculation is performed for an identical load combination as the results presented for the tapered plug in Figure 4-5. By comparing the result presented in these two figures, it is evident that the tapered plug has cracks that could transport water through the entire thickness of the plug, while this is not the case for the dome shaped plug where no continuous network of cracks is present. In a comparison between the tapered plug (Figure 4-4 and Figure 4-5) and the dome shaped plug (Figure 4-10 and Figure 4-11), it can also be seen that a much higher extent of cracking is obtained in the tapered plug compared to the dome shaped plug for a increase in shrinkage. Due to the fact that the experimental data regarding shrinkage is limited, it can be determined that the dome shaped plug is not as sensitive to increased values of the shrinkage.

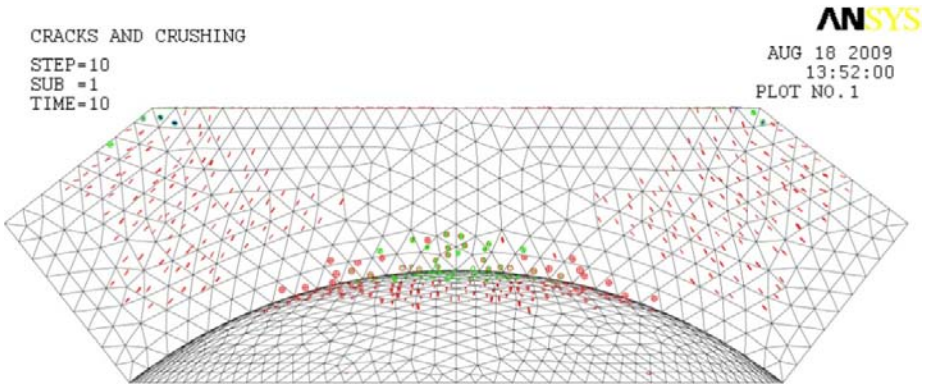

Figure 4-10. *A cross-section of the dome shaped concrete plug subjected to shrinkage according to B200 and without pre-stress. The calculation is performed for the same conditions as Figure 4-4.*

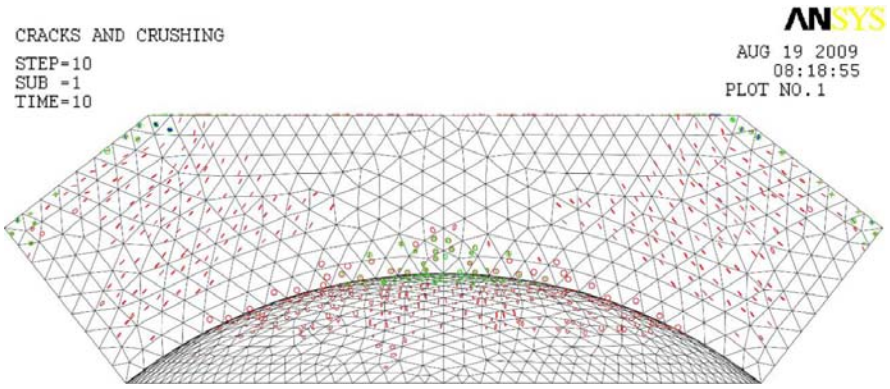

Figure 4-11. *A cross-section of the dome shaped concrete plug subjected to shrinkage according to B300 and without pre-stress. The calculation is performed for the same conditions as Figure 4-5.*

It is however not certain that the dome shaped concrete plug solely could limit the water transport out of the deposition tunnel. However, this is not the purpose of the concrete plug, since it only has to be watertight enough to allow the bentonite seal to saturate and then the bentonite seal will limit the water transport on its own. Altogether, the whole plug system should prevent water leakage from the deposition tunnel.

The influence of rock fallout has been studied in a simplified manner where the lower half circle of the slot was given a displacement of 1 mm while the upper half was maintained in its original position. This is a very unfavorable and improbable simulation and resulted in that the dome plug was divided in halves with a horizontal crack of nearly the size of the forced displacement.

4.3.3 Analyses of maximum load capacity

Several different analyses have been performed to determine the ultimate load capacity of the concrete dome shaped plug. The first step to determine the maximum swelling pressure that may be applied to the plug was made based on the linear model previously studied by Dahlström et al. (2009). In this analysis the concrete that was assumed to crack, i.e. areas where previous analyses had shown tensile stresses above the design value 1.0 MPa had been removed. The reduced geometry of the plug that was studied is presented in Figure 4-12.

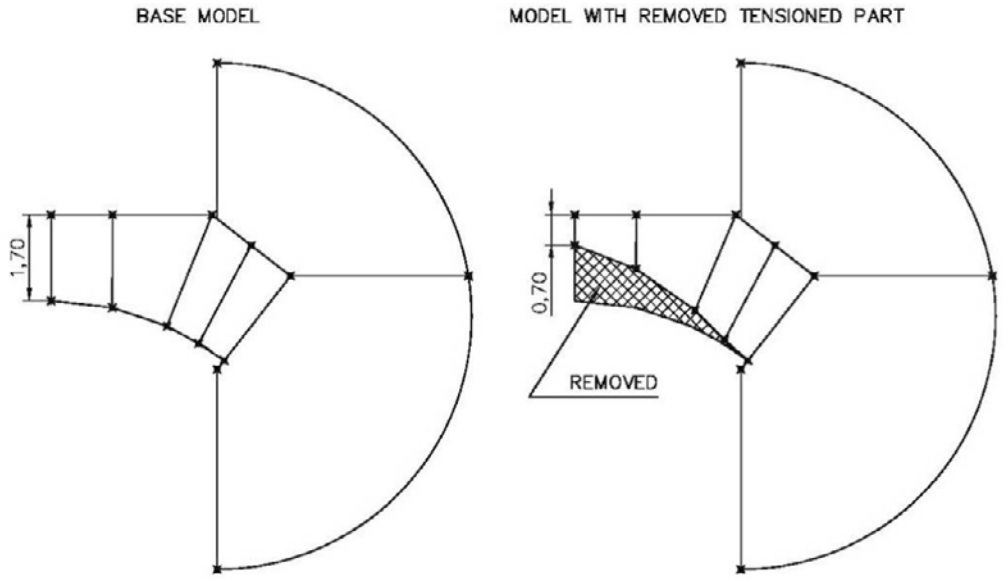

Figure 4-12. *Reduced area of the concrete plug to compensate for cracked concrete (Dahlström et al. 2009).*

In the first step of the analysis the same temperatures, as presented in Figure 4-8 were applied together with a water pressure of 4 MPa. In the next step, the swelling pressure was continuously increased. Both the swelling pressure and the strength of the concrete will develop with time. In the analysis, the development over time has not been considered instead a single analysis was performed for increasing pressure. The compressive stresses that occurred in the plug were compared to the maximum allowed compressive stresses according to the criterion of linear creep, i.e. 0.65 f_{cc} = 35 MPa, as seen in Figure 4-13. Based on the obtained compressive stresses, the result was that a swelling pressure of 2 MPa (6 MPa in total pressure) was the maximum pressure that could be allowed before the limit of compressive stresses was reached. With requirement of today where the water pressure is assumed to be 5 MPa instead of 4 MPa, see Section 3.3.1, this means that only 1 MPa in swelling pressure from the bentonite in the backfill and the seal could be allowed. If a 60% increase in strength in 100 years would be accounted for in the concrete, a maximum swelling pressure of approximately 6 MPa (10 MPa in total pressure) in could be allowed at 100 years after casting, as illustrated with the solid line in the figure.

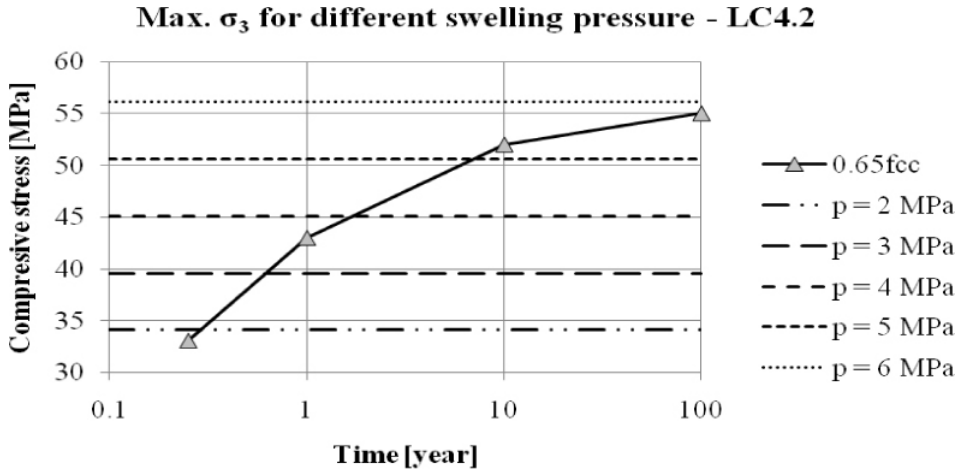

Figure 4-13. *Maximum compressive stresses in the center of the dome shaped plug for varying levels of swelling pressure (In addition 4 MPa water pressure is assumed). The solid line represents the maximum allowed stresses based on a 60% increase in strength with time.*

However, the results from these analyses are extremely conservative since even though the concrete is cracked it will still be able to carry tensile stresses in between the cracks, i.e. tension stiffening. In addition to this, the concrete will also carry compressive stresses in the principal direction perpendicular to the extension of the crack. Further, the compressive strength increases significantly if concrete exhibits compressive stresses in two or especially in three perpendicular directions. Concrete subjected to confinement has a substantial increase in compressive strength as shown for a typical 3D compressive state in Figure 4-14.

More refined analysis methods had to be used to get better estimations of the maximum allowed pressure on the concrete plug. These analyses was performed on the same model as presented in Section 4.3.1, with the exception that non-linear material properties were taken into consideration and the load was increased up to failure of the structure. Additional results from these analyses are presented in Appendix B. Therefore, an approach with non-linear material behavior was used. This analysis was based on fracture mechanics to simulate the non-linear behavior of concrete. The material model used in this study is almost the same as the model used for the time history analyses of the tapered and the dome shaped plug. The analysis was performed with the characteristic material parameters of the concrete, as shown below.

- Tensile strength 2.9 MPa.
- Elastic modulus (including creep) 26.7 GPa.
- Poisons ratio 0.27.

The fracture energy was not measured in the experiment, instead it was chosen to 100 Nm/m^2, as described in Section 4.1.2.

In the analysis the same temperatures, as presented in Figure 4-8 were applied together with a constantly increasing pressure that constitutes both water pressure and swelling pressure. The first initiation of a crack was obtained for a total pressure of 3 MPa, as seen in Figure 4-15.

It can be seen in Figure 4-15 that the first cracks initiate on the downstream surface in the centre of the dome. The red circles in the figure indicate crack initiation at integration points in the elements and the circle outline the crack plane. In Figure 4-15 it can be seen that the cracks initially propagate in a radial direction, i.e. from left to right in the figure.

During subsequent increase of the pressure, the radial cracks propagate on the downstream side of the dome shaped plug. In addition to these cracks, tangential cracks initiate in a direction perpendicular to the radial cracks near the centre of the downstream surface.

At the total pressure of 21 MPa (which implies a swelling pressure of 16 MPa) inclined cracks were formed as seen in Figure 4-16. The inclined crack is similar to a web shear crack that may occur in concrete beams with a low shear span to depth ratio, see Malm (2006). The inclined cracks in the dome shaped plug are approximately parallel to the downstream surface of the dome shaped plug.

In Table 4-1, a description of the initiation of cracks obtained in the calculation for increasing external pressure (water + swelling) is presented.

Table 4-1. Load level when cracks develop according to the analysis.

Description	Load level
First crack indication	3 MPa
First element fully cracked	4.5 MPa
First indication of an inclined shear crack	21 MPa
First fully developed inclined shear crack	21.5 MPa

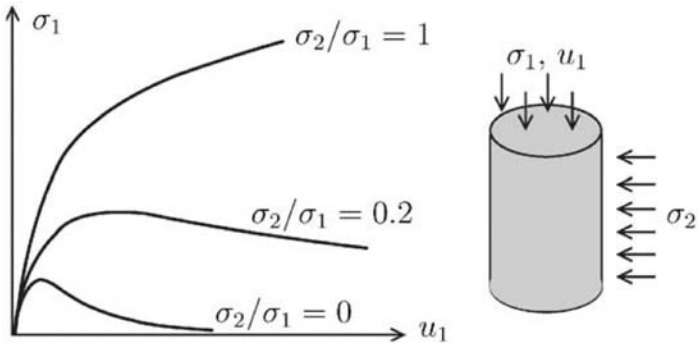

Figure 4-14. *Stress-displacement diagrams obtained from triaxial compression for three levels of confining pressure σ_2. From Mang et al. (2003).*

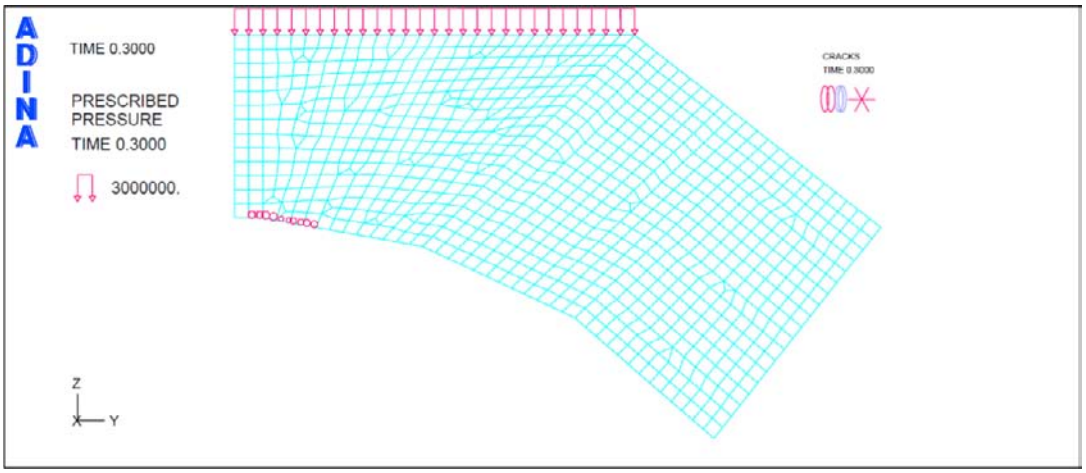

Figure 4-15. *Crack initiation at the total pressure level of 3 MPa.*

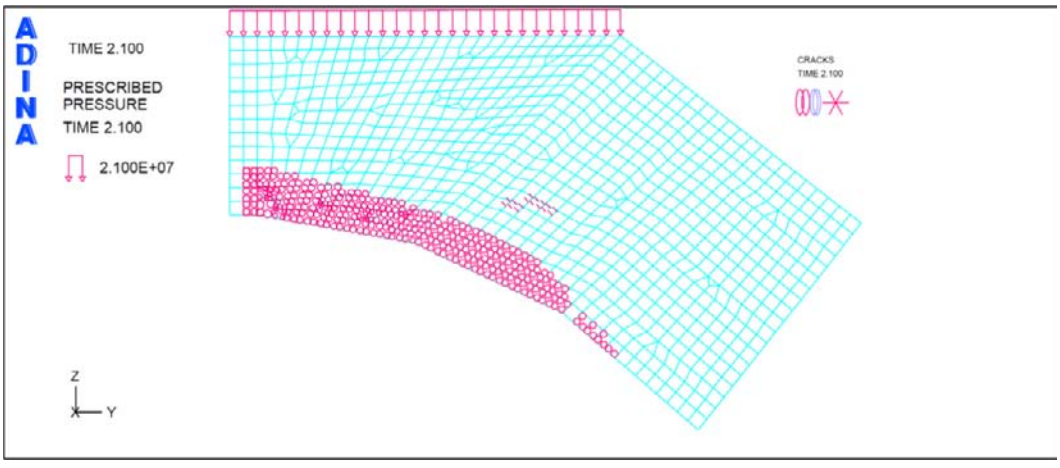

Figure 4-16. *Crack initiation at the total pressure level of 21 MPa.*

The failure load was not reached at 21.5 MPa, but the analyst responsible for the calculation determined this to be a conservative estimate of the ultimate level due to skepticism to the accuracy of the constitutive model in the FE program ADINA after inclined shear cracks had developed.

The failure of the analysis was reached at a total external pressure of 37.5 MPa. The extent of the induced cracks at this load level is illustrated in Figure 4-17. In the analysis, compressive failure was neglected and therefore this result cannot be considered as an accurate estimate of the total failure if crushing of the concrete is to be expected. It can be seen in Figure 4-18 that the compressive stresses in the centre of the surface of the concrete plug on the pressurized side are about twice as high as the uniaxial compressive strength. However, as shown in Figure 4-14, the compressive strength of concrete increases considerably when subjected to multiaxial compressive stresses. The stress in the z-direction is at the top surface equal to the applied external pressure and the stress in x- and y-direction are identical due to the symmetric geometry. Comparing the calculated stresses with Figure 4-14, the ratio between the calculated stresses is $\sigma_2 / \sigma_1 = 37.5 / 110 = 0.34$ and according to the figure it is possible that the compressive strength in a 3D compressive state may be at least twice as high as the uniaxial strength.

In the crack pattern at failure Figure 4-17 no pervasive cracks, that could result in leakage, are found. Based on this analysis, it seems as if the dome shaped concrete plug will be able to satisfy the criteria of preventing leakage until the bentonite seal have reached its full saturation and thereby prevents water leakage on its own.

The load and deformation response obtained from the analysis is shown in Figure 4-19. In the analysis all temperature effects, i.e. from the spent nuclear fuel, shrinkage etc., were applied between the load levels of 9 and 10 MPa. At the load level 9 MPa, corresponding to the design values of the water pressure and pressure from the bentonite clay, a displacement of approximately 5 mm was calculated. At the load level where the first inclined crack initiated, i.e. 21 MPa, the displacement at the centre of the plug is approximately 10 mm.

Based on the results above it can be said that the load capacity is at least 21 MPa of external pressure, but probably significantly higher than that and somewhere in the region of at least 30 MPa.

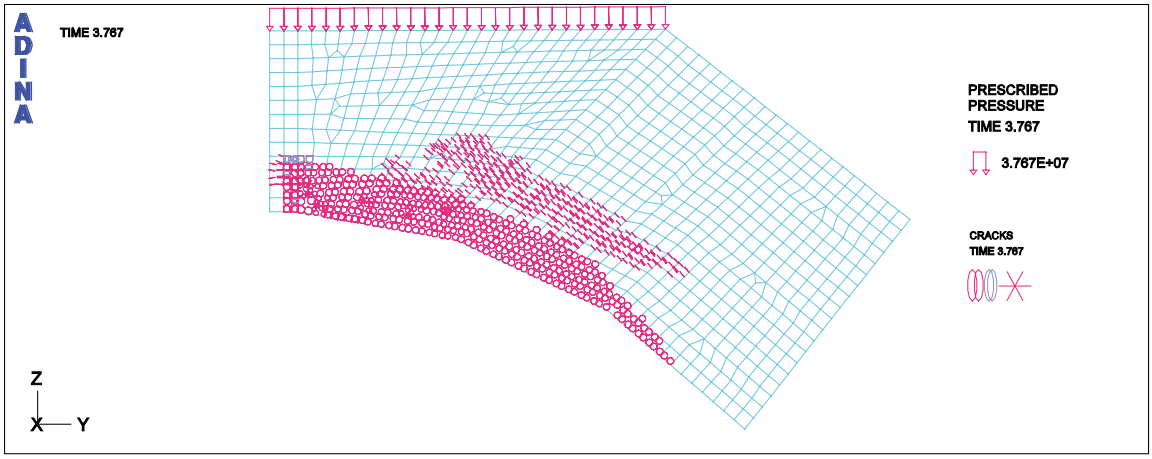

Figure 4-17. *Crack initiation at the maximum total pressure level of 37.5 MPa.*

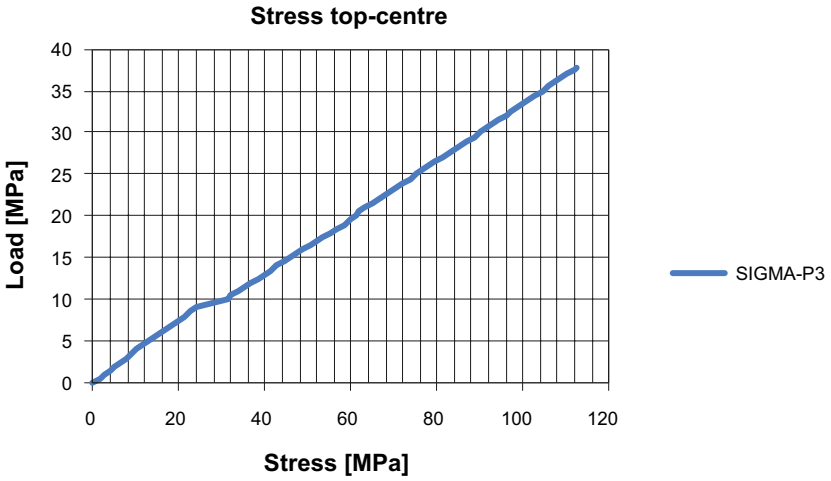

Figure 4-18. *Applied pressure on the concrete plug and the maximum compressive stresses.*

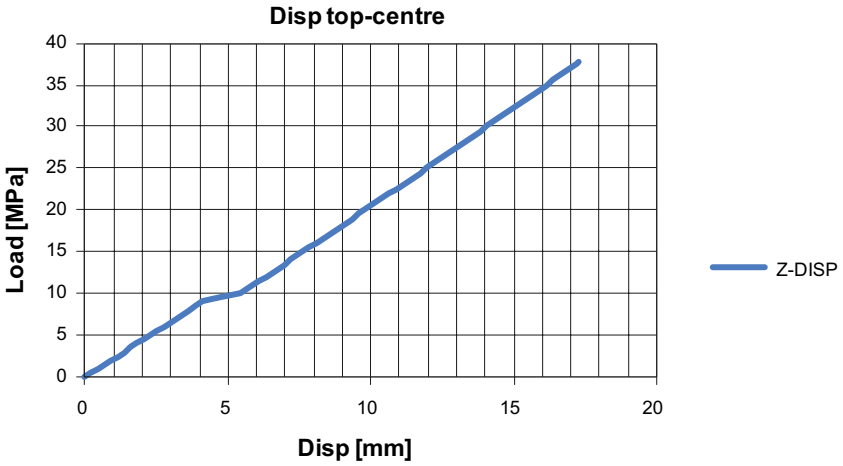

Figure 4-19. *Applied pressure and displacement of the centre of the concrete plug.*

4.3.4 Analyses with unevenly distributed loads

The external pressure in the previous analyses has always been applied as evenly distributed over the surface. However, the analyses of the bentonite clay showed that the swelling pressure might be unevenly distributed over the surface, as seen in Section 3.3.2. Due to this, the effect of unevenly distributed loads has to be studied regarding its effect on the safety of the unreinforced concrete dome shaped plug. The results from these studies are presented in Appendix B and summarized in this report below.

In these analyses the previously used axisymmetric models could not be used and therefore a 3D model of the concrete plug was created. The concrete and the rock were modeled as linear elastic while a non-linear contact formulation was used to describe the connection between concrete and rock.

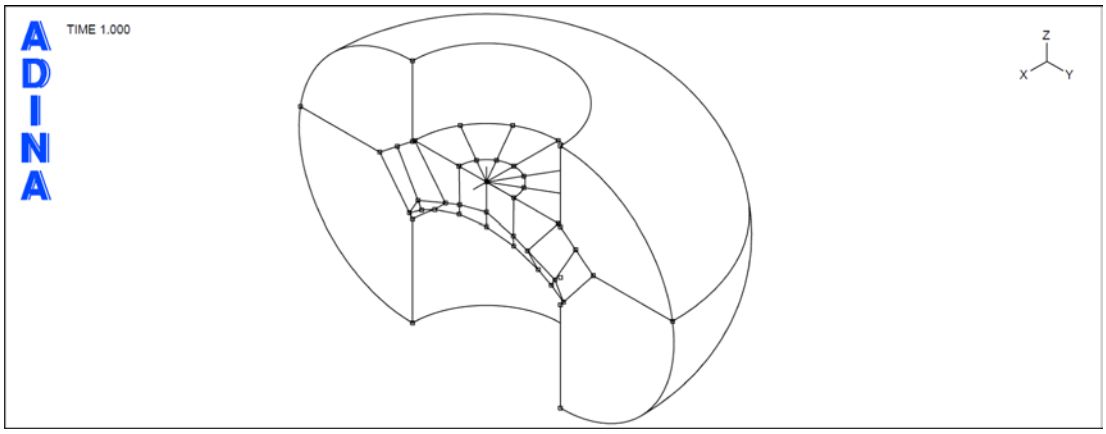

Figure 4-20. *3D model for the unevenly distributed load analyses.*

In the analyses the effect from unevenly distributed loads was simulated as half the pressurized surface applied at one load level and the other half of the surface applied at another load level. In Figure 4-21 the difference in result is shown for two cases; the black line represents an evenly distributed external pressure of 8 MPa on the whole surface and the red line represents the case where half the surface is subjected to a pressure of 4 MPa and the other half is subjected to 8 MPa. The average load is thereby 6 MPa for the case with unevenly distributed load. Based on these analyses, it can be concluded that the unevenly distributed load is not as severe as the evenly distributed load with an amplitude corresponding to the maximum value in the unevenly distributed load case.

The analyses also showed that it is possible to use superposition to a certain extent for different load cases to evaluate the stresses in the centre section. If only the external pressure was considered, superposition could be used with satisfactorily accuracy for the stresses in the cross-section. The numerical agreement was most accurate on the compressive side and the largest errors were found in the tensile stresses. A comparison between the case with 10 MPa in external pressure and the case where the stresses obtained for the load level five times 2 MPa, is seen in Figure 4-22.

The superposition principle did not give accurate results if restraint forces from shrinkage, temperatures from the spent nuclear fuel etc were considered. For these cases only the compressive stresses in the top of the centre section, i.e. the point with high compressive stresses, could be evaluated with accuracy.

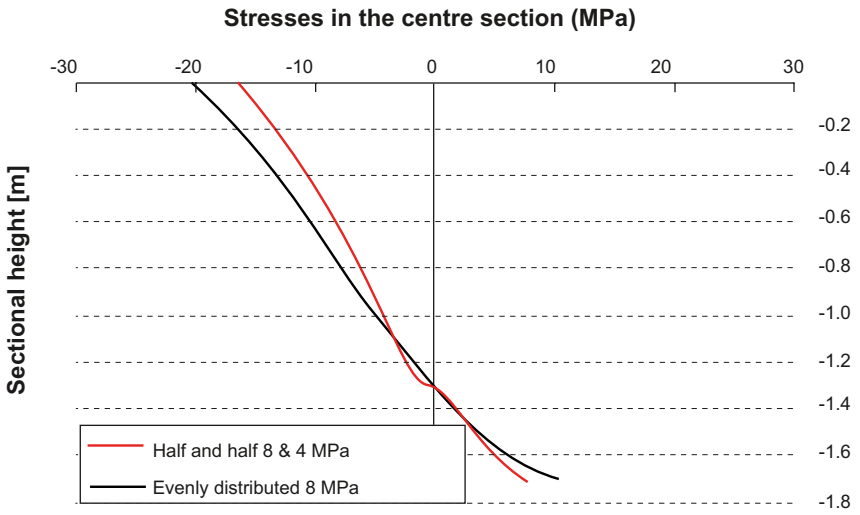

Figure 4-21. *Comparison of evenly distributed and unevenly distributed external pressure.*

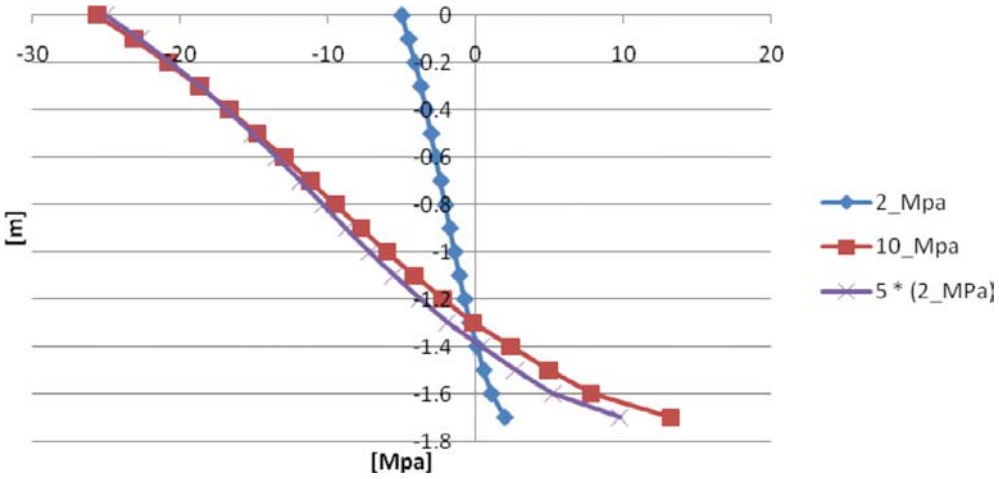

Figure 4-22. *Comparison between the results obtained for a external pressure of 10 MPa and the superposition of five times the stresses obtained at the external pressure 2 MPa.*

4.3.5 Analyses for optimization of the geometry

The concrete plug geometry studied in previous analyses is possible to optimize regarding the layout based on the loads acting on the structure. The optimization of the geometry was performed where changes are made to the previous geometry regarding the sectional height and the thickness of the concrete plug at the abutments. The main purpose of the optimization was to reduce the amount of concrete needed for each plug. The optimization study was conducted with two dimensions reduced as illustrated in Figure 4-23. The results from these studies are presented in Appendix B and summarized below.

The original sectional height was 1.7 m and the thickness at the abutments was 2.11 m. In the optimization study the sectional height was studied for the following values; 1.1 m, 1.3 m, 1.5 m and 1.7 m. The thickness at the abutments was studied for the following values 1.71 m, 1.91 m and 2.11 m.

The load cases presented in Section 4.3 were used for the optimization study. One difference was however that a water pressure of 5 MPa was used instead of the previous value of 4 MPa. The main criterion was that stresses in the top and the bottom at the centre of the plug should be within the interval -33 MPa $\leq \sigma_{c,\,top} \leq 0$ MPa in all the studied load cases. In Figure 4-24 below the calculated stresses in the top and the bottom of the section are shown for the different variations of geometries.

The most optimal geometry that was found is presented in Figure 4-25. In the new geometry, the sectional height has been reduced to 1.3 m and the thickness at the abutments has been reduced to 1.91 m.

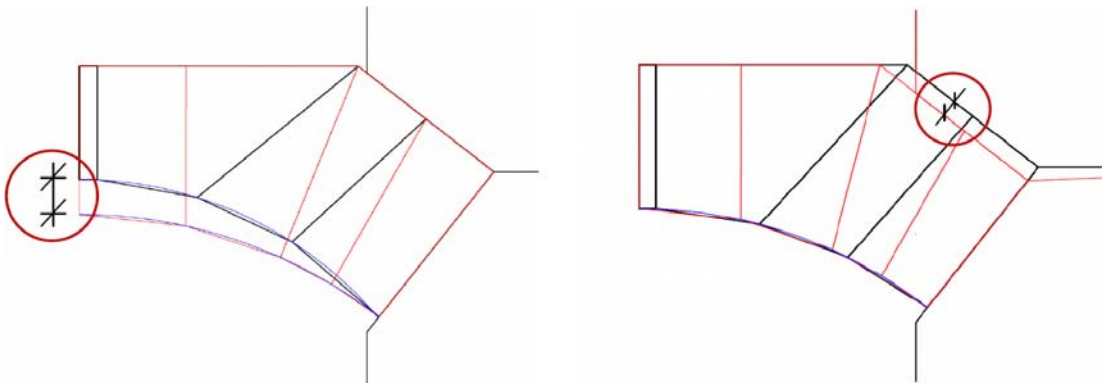

Figure 4-23. *Sketch of the two dimensions that are subject for optimization.*

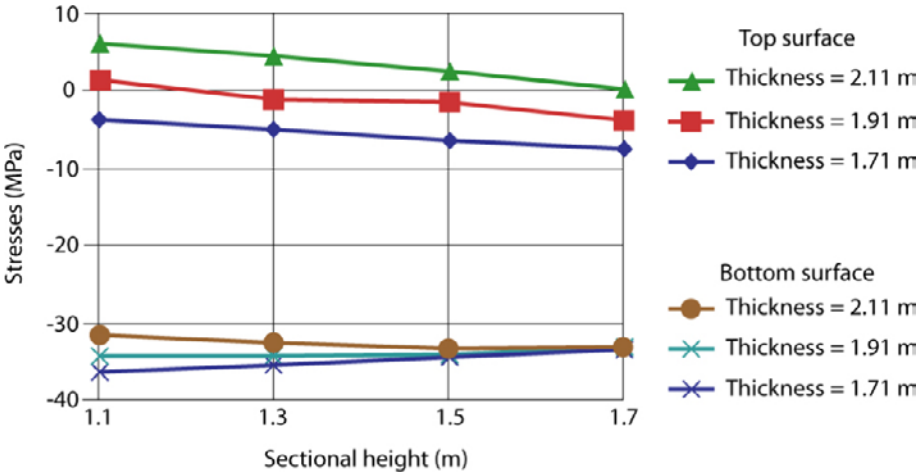

Figure 4-24. *Calculated stresses in the top and the bottom for different geometries.*

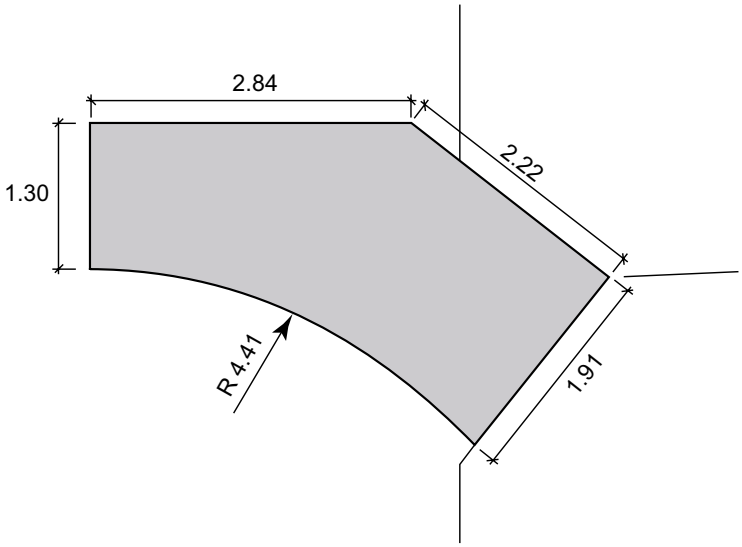

Figure 4-25. *The new geometry optimized to the loads acting on the concrete plug.*

4.3.6 Load capacity analyses of the final geometry

Based on the optimized geometry in Figure 4-25 a new design drawing was made. This design drawing was slightly modified compared to the figure shown above, since some changes had to be made to adjust the geometry of the concrete plug to fulfill other requirements on the tunnel geometry, for instance from the machines transporting the nuclear fuel canisters. The final geometry of the dome shaped plug is shown in Figure 4-26.

The changes made on the concrete plug, are all considered to have a small effect on the load capacity and the changes are all beneficial which should imply that a small increase in load capacity is to be expected.

Based on the new geometry new analyses were performed to estimate the maximum external pressure that can be applied to the dome shaped plug. An axisymmetric model was made in the FE program ABAQUS, where the external pressure was increased continuously until failure occurred. To simplify the model, it was assumed that the left abutment of the dome had a fixed boundary condition. In this calculation, unlike the analyses presented previously, only the external pressure was applied. The input file used for these analyses is included in Appendix A.

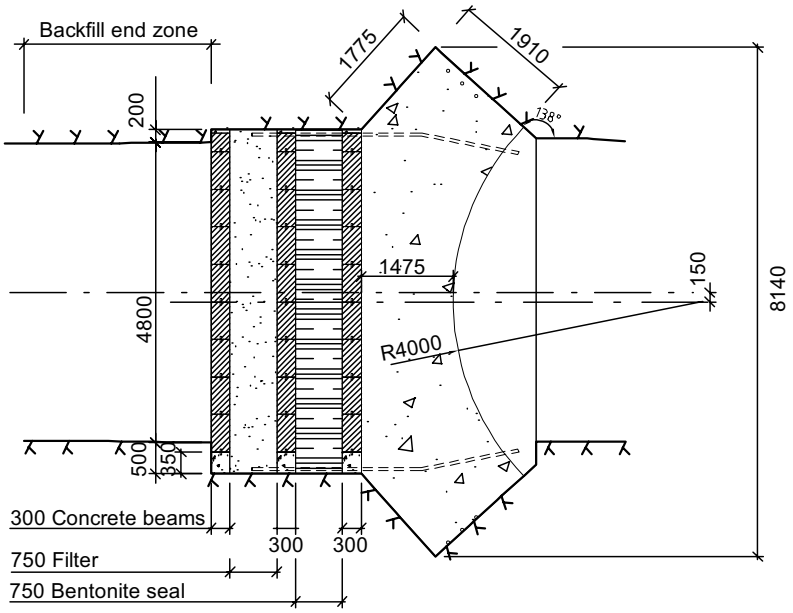

Figure 4-26. *The final, optimized geometry of the dome shaped concrete plug.*

The main purpose of this analysis is to constitute the base for the experimental tests that are planned. To design the test-setup the ultimate capacity of the dome shaped plug is needed. In addition to this, based on the analyses performed in this section it is later possible to calculate the global safety of the structure regarding the external pressure.

The material model used in the analyses is based on plasticity theory and is called *concrete damaged plasticity*. With this model, it is possible to define the material degradation of compression as well as tension, where the tensile softening behavior is based on a crack-opening law and fracture energy. Damage is associated with the failure mechanisms of concrete (cracking and crushing) and therefore results in a reduction of the elastic stiffness. More information regarding the material model can be found in ABAQUS and in Malm (2006).

Load controlled static analyses, where the load has to increase for each increment, have often problems reaching the ultimate load due to convergence difficulties. This is especially difficult if the failure is brittle and then it is not possible to know if the analysis has reached the ultimate load or stopped due to numerical instability. For instance, see Figure 4-19, where no plateau exists in the load and deformation curve and therefore it is impossible to determine if the maximum load has been reached.

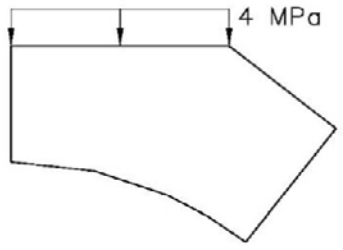

Figure 4-27. *Sketch of the axisymmetric model used for ultimate load capacity estimation.*

To be certain that this is not the issue, the analyses were also performed as quasi-static with an explicit integration scheme, intended for dynamic analyses, where controls were performed afterwards so that the structure was loaded slowly enough, i.e. low kinetic energy compared to the strain energy, to reduce the mass inertia effects.

All material parameters are based on the characteristic strengths of the low-pH concrete presented by Vogt et al. (2009) and are presented below:

- Tensile strength 2.9 MPa.
- Compressive strength 54 MPa.
- Elastic modulus 33.9 GPa.
- Poisons ratio 0.27.

In addition to this, analyses were also performed with mean values of the material properties. All material parameters are based on the mean value strengths of the low-pH concrete presented by Vogt et al. (2009) and are presented below:

- Tensile strength 3.3 MPa.
- Compressive strength 62 MPa.
- Elastic modulus 33.9 GPa.
- Poisons ratio 0.27.

For both the analyses with characteristic and mean values of the material properties, it was assumed that the tensile behavior of concrete was linear in both the ascending part up to the tensile strength and also in the descending part of the curve with the fracture energy of 100 Nm/m^2.

The uniaxial compressive curve used in the analyses is based on Model Code 90 (CEB 1993) and Cervenka et al. (2005). The ascending part of the uniaxial compressive curve has been assumed to correspond to a second-degree parabola, with the strain equal to $2 \cdot f_{cc} / E$ at the ultimate strength and the descending part of the curve has been assumed linear, as shown in Figure 4-28. In the calculation, it was assumed that the concrete curve was linear up to 60% of the compressive strength, in accordance with Vogt et al. (2009).

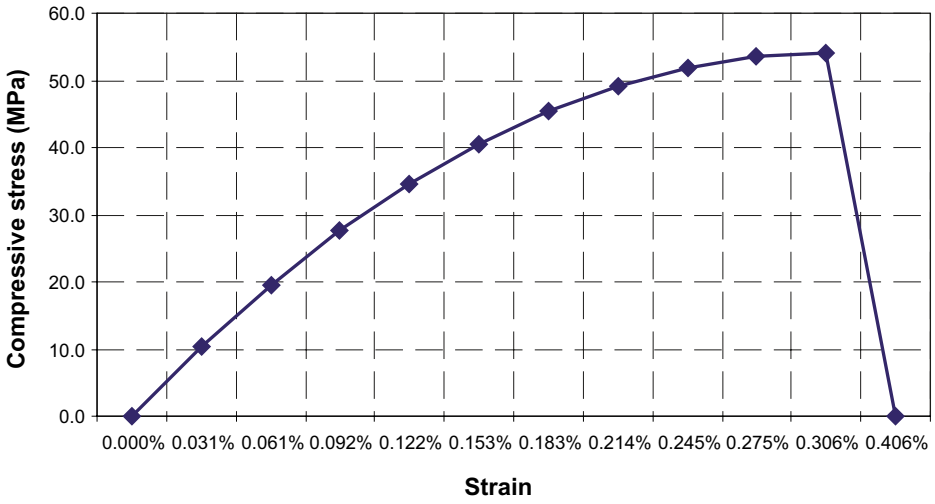

Figure 4-28. *Uniaxial compressive curve based on characteristic material properties used in the ultimate limit analyses.*

The failure mode obtained in all these analyses corresponds to the previous results obtained in the previous analyses. Initially bending cracks form on the downstream side in the centre of the dome. After some additional loading an inclined crack initiates and propagates throughout the rest of the analysis up to failure.

The load and deformation response of the static and the quasi-static analyses based on characteristic material properties are shown in Figure 4-29. In both the static and the quasi-static analyses, the inclined crack initiated at the load level of 20.0 MPa. The maximum load was reached at an external pressure of 38.1 MPa and 38.4 MPa for the static and quasi-static analysis respectively.

A comparison of the load and deformation response obtained from an analysis based on characteristic material properties and an analysis based on mean values of the material properties is shown in Figure 4-30. The ultimate limit load of the external pressure increases to 49.2 MPa when the analysis is based on mean values of the material properties.

In the material model *concrete damaged plasticity* the isotropic damage is associated with the failure mechanisms of concrete (cracking and crushing) and therefore results in a reduction of the elastic stiffness. The two damage parameters, d_t and d_c, account for the tensile and compressive damage respectively. For instance the remaining stiffness of a cracked element is calculated as $(1-d_t)\cdot E$.

In Figure 4-31 the induced tensile damage is shown. Elements with no tensile damage, i.e. uncracked concrete, are illustrated by white color and the red elements are completely cracked. Three figures are shown, in the upper figure cracks in a radial direction have initiated and in the middle figure the amount of cracking at the initiation of the inclined crack is shown. The bottom figure shows the extent of cracking just before the failure. The element length in the analysis was approximately 0.1 m and it can be seen that about 0.45 m of the height in the centre of the concrete plug are to be considered as cracked. The extent of cracking at failure does not give any cause for suspecting that the cracks could go through the thickness of the section and cause leakage. Based on this analysis, it seems as if the dome shaped concrete plug will be able to satisfy the criteria of preventing leakage until the bentonite seal have reached its full saturation. However, in this analysis the effect of shrinkage is not included, which would cause a higher degree of cracking. Based on the similarity in results in Figure 4-31 where shrinkage is not included and the results in Figure 4-17 where shrinkage is included, it is not likely that shrinkage will cause pervasive cracks, i.e. going through the thickness of the dome shaped concrete plug.

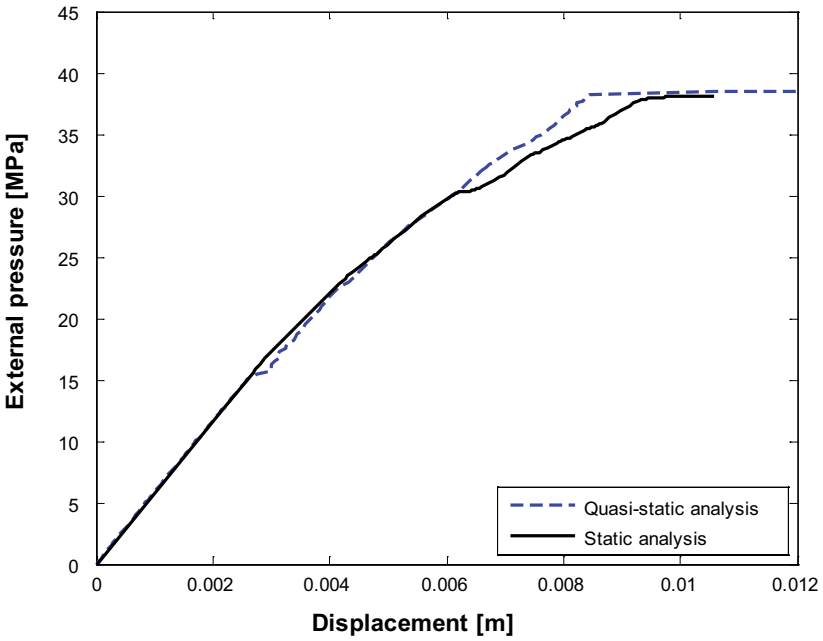

Figure 4-29. *Load and deformation curve for the ultimate load capacity analyses, with characteristic material properties.*

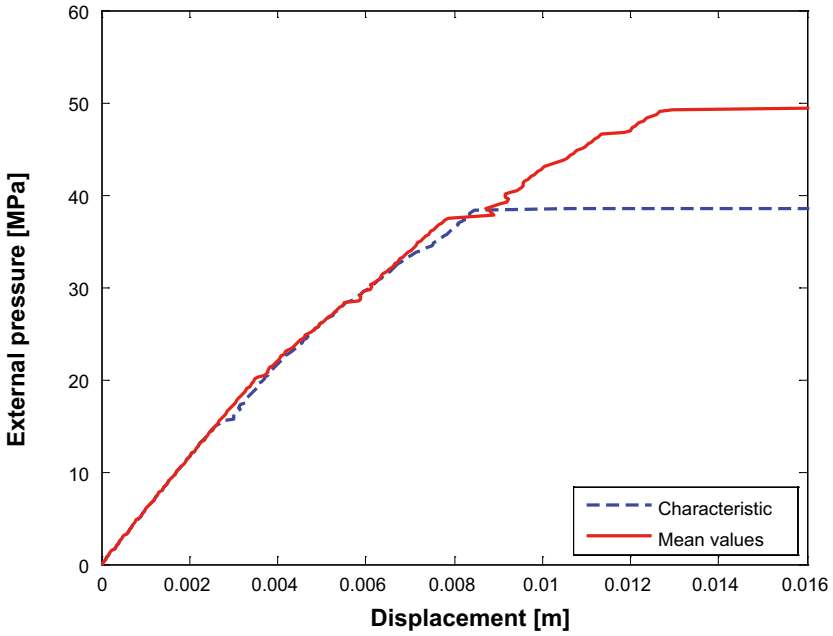

Figure 4-30. *Load and deformation curve for the ultimate load capacity analyses, with mean values of the material properties.*

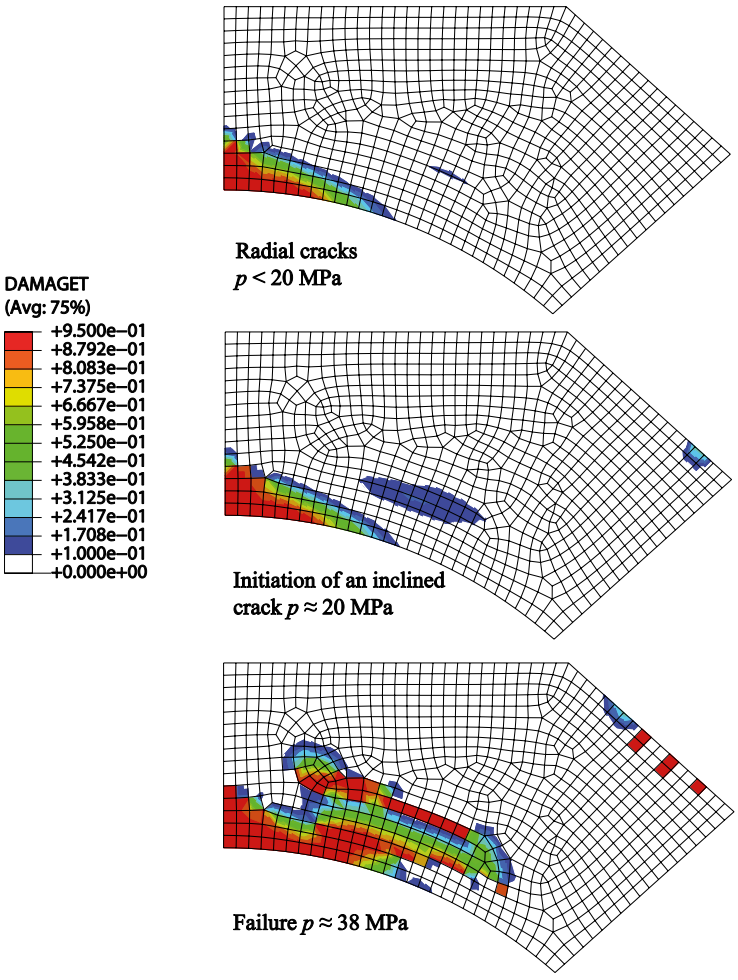

Figure 4-31. *Induced tensile damage (cracks) during monotonic loading.*

5 Evaluation of the design

5.1 Safety concept

The safety concept within this project is developed based on a factor of safety, *sf*, where the resistance R and the action S shall fulfill the following requirement:

$$S \le \frac{R}{sf} \tag{5-1}$$

The factor of safety is selected on the basis of experimental observations, past experience, economical and political considerations and should be large enough to provide sufficient safety towards unwanted events that is assumed to occur if

$$S > R \tag{5-2}$$

The partial factor method, which is used in many design codes, is a development of the factor of safety implying that the permissible actions (or required resistance) shall satisfy the following relation

$$\frac{R}{\gamma_{\mathrm{R}}} \ge \sum_{i=1}^{n} \gamma_{\mathrm{Di}} \cdot S_{\mathrm{Di}} + \sum_{i=1}^{m} \gamma_{\mathrm{Li}} \cdot S_{\mathrm{Li}} \tag{5-3}$$

where, S_{Di} is the dead loads, S_{Li} are the live loads and γ_{R}, γ_{Di}, γ_{Li} are partial factors. Actions with high variability can with this format be given greater partial factors than those with low variability, and thus better representation of the uncertainties associated with actions and resistance is obtained. (Westberg 2010)

5.1.1 Global safety factor for non-linear analyses

In a non-linear analysis, the response of the structure is best described if mean values are used for the material properties that are included in the analysis. All numerical material models and finite element programs are validated against experimental results based on average values. A global safety criteria adjusted to the partial factor method can be rewritten as

$$\frac{R_{\mathrm{m}}}{\gamma_{\mathrm{Rg}}} \ge \gamma_{\mathrm{S1}} \cdot S_{\mathrm{k1}} + \gamma_{\mathrm{S2}} \cdot S_{\mathrm{k2}} + \ldots + \gamma_{\mathrm{Sn}} \cdot S_{\mathrm{kn}} \tag{5-4}$$

where, R_{m} is the load capacity obtained from the non-linear analysis based on mean values of all material parameters and γ_{Rg} is a global safety factor of the load capacity. The global safety factor should consider the uncertainties for the variables that determine the load carrying capacity of the structure and the uncertainties of the numerical model. The safety is related to the average values of the load carrying capacity, and therefore γ_{Rg} represent a global central safety factor for the load capacity. The difficulty with this method is that the global safety factor incorporates a wide and unspecified number of uncertainties. (Carlson et al. 2008)

It is not rational to use a general value of γ_{Rg} for all concrete structures regardless of the failure mode in question. One general method described in Sustainable Bridges (2007) to determine the global safety of the structure is to perform two separate analyses of the load capacity of the structure. The first analysis should be based on the mean values of material properties and the second analysis should be based on characteristic material values. From these two analyses, the load capacity from the model based on mean values R_{m} and the load capacity R_{k} from the model based on characteristic material properties are obtained.

Based on the assumption that the distribution for the load capacity is lognormal, the coefficient of variation V_{Rf} can be determined as

$$V_{\mathrm{Rf}} = \frac{1}{1.65} \cdot \ln\left(\frac{R_{\mathrm{m}}}{R_{\mathrm{k}}}\right) \tag{5-5}$$

To estimate the coefficient of variation V_R the model uncertainties have to be taken into account. The model uncertainties are included with the factor, V_{Cf}, which is described in Section 5.1.2. The total uncertainties related to the load capacity R can thereby be calculated as

$$V_R = \sqrt{V_{Rf}^{\ 2} + V_{Cf}^{\ 2}} \tag{5-6}$$

The global safety factor γ_{Rg} can then be estimated based on the following equation

$$\gamma_{Rg} = 1 + \alpha_R \beta_T V_R \tag{5-7}$$

where, α_R is the sensitivity factor for R and can approximately be set equal to the conservative value $\alpha_R = 0.8$ according to Carlson et al. (2008), and β_T is the target value for the safety index according to design codes. According to Boverket (2010) the β_T values are defined for the different safety classes as shown in Table 5-1.

With the load capacity R_m directly calculated in the FE analysis and with the global safety factor calculated according to Eq. (5-4) the verification of the structural safety can be performed based on Eq. (5-4) directly. (Carlson et al. 2008)

Table 5-1. Safety index factors, annual failure probability and partial coefficient according to Boverket (2010).

Safety class	Safety index β	pf	Partial coefficient. γ_n
Low	3.7	10^{-4}	1.0
Normal	4.3	10^{-5}	1.1
High	4.8	10^{-6}	1.2

5.1.2 Model uncertainties

To determine the coefficient of variation V_R, the uncertainties in the numerical models also have to be accounted for. The uncertainties in the model regarding the load capacity can be determined according to NKB (1978) under the assumption that it is lognormal distributed with the mean value of 1.0. The coefficient of variation regarding the model uncertainties V_{Cf} can be estimated where three factors are taken into account, as seen in Table 5-2.

Table 5-2. Template for determination of model uncertainties.

Description				Comment
1. Detail and accuracy in the numerical model	Good	Normal	Poor	
2. Deviation between material strength in the structure and test specimens	Small	Medium	High	
3 a. Amount of control in the building process	Good	Normal	Poor	For new constructions
3 b. Knowledge regarding the material properties in the structure	Good	Normal	Poor	For evaluation of existing structures
V_{Cf} %	5	10	15	

Below, more detailed descriptions of the three factors are given, with the intention to provide a guide to how the different categories should be interpreted, according to von Schlotten et al. (2004) and Carlson et al. (2008).

1. Detail and accuracy in the numerical model

Normal detail and accuracy can be used in situations where the numerical model used is commonly accepted in relation to normal praxis. Good detail and accuracy can for instance be that the model is so simple that only small uncertainties can occur (for instance pure bending of a steel- or a reinforced concrete section), otherwise it can be where the model has been verified for the actual construction.

It is important to separate the systematic deviation and the uncertainties regarding the accuracy of the numerical model. Numerical models are often conservative and it should not be considered as poor due to this.

2. Deviation between strength in construction and test specimens

Here is the difference in the material properties in the actual structure compared to the material properties measured with the test specimens and used in the analyses. This is mainly a problem for concrete where the material properties measured with test specimens, such as concrete cylinders, can deviate from the material properties in-situ. The material properties can also vary within in the in-situ structure.

3a. Amount of control in the building process

Unfortunately, no information is given in the references (von Schlotten et al. 2004, Carlson et al. 2008) regarding how this category should be interpreted, since these only focus on existing structures.

3b. Knowledge regarding the material properties in the structure

The normal category can be used when the material properties are well documented and there is no reason to doubt that the construction has been performed according to the design drawings. The category "Good" can be used for instance when the material properties have been confirmed through in-situ investigations or if there are good documentation from the construction stage. The category "Poor" can be used when the documentation is incomplete or missing and when the material properties have to be estimated. (Carlson et al. 2008)

5.1.3 Material coefficients

According to section 2.3.1 in BBK 04 (Boverket 2004) the characteristic values for the tensile strength in the ultimate limit state should be reduced by a safety factor of 1.2 and a factor of 1.5 for uncertainties in material properties and in loads. The total safety factor included in ultimate limit state on the material parameters is thereby 1.8. If a crack free structure is accounted for when evaluating the strength in ultimate limit state a crack sensitivity factor of 2.0 should be included, according to 4.5.3 in BBK 04.

The total factor regarding the material is thereby equal to $1.2 \cdot 1.5 \cdot 2 = 3.6$ if the concrete plug should be crack free otherwise, the coefficient is $1.2 \cdot 1.5 = 1.8$. In the non-linear analyses, the characteristic strength has been used, which means that the calculated strength of the concrete plug afterwards has to be reduced regarding the material coefficient.

The design criterion does not require that the concrete plug is completely free from cracks. However, cracks passing through the full thickness of the plug are not allowed, due to the risk of opening a free flow path for the bentonite clay to erode away. Therefore, there is no requirement for a completely crack free structure, which makes the crack sensitivity factor not applicable in this case. As a practical approach, it is assumed that a crack is passing the structure whenever a crack has reached a distance closer than 100 mm from a free surface.

5.1.4 Load coefficients

The size of all loads in the calculations has been estimated to correspond to extreme values, i.e. the largest values that are likely to occur. If one load is judged beneficial for the structure, then a low value is chosen or the load is neglected. For different load combinations an external load can in some cases be beneficial while for other combinations have a negative effect on the structure. In those cases, two extreme values are included in Table 5-3 below.

Within the extreme design values, it is not possible to determine the probability of these loads to occur or especially the probability that all of them occur at the same time. Instead the safety concept is presented as, remaining safety factor when extreme values on all loads are used, see Section 5.1.5. In this section, an attempt to present the total safety factor is also made.

The design and probable values for all the loads are further described in Section 3.3. Note that all loads presented below are permanent loads, i.e. present during the entire service life.

The temperature increase from the canisters and the prestressing effect can have beneficial effects for some load cases, for instance if cracking is studied, and therefore one or both of these effects have been neglected in some analyses. For load cases where high compressive stresses are important both these effects are included in the analyses.

Ultimate limit state BKR 2010

For the design case in the ultimate limit state in BKR 2010 (Boverket 2010) (Design case 1 in Table 2:322a), all permanent loads should have a load coefficient of 1.0 and the dominating variable load should have a load coefficient of 1.3 while remaining variable loads have the coefficient of 1.0.

The water pressure, swelling pressure and the shrinkage can all be considered as permanent loads and should thereby have a load coefficient equal to 1.0 according to BKR 2010. Thereby, the loads used in the non-linear analysis include a higher safety margin than what is described according to BKR 2010.

Ultimate limit state Eurocode 2

For a design case where the permanent loads are the dominating loads acting upon the structure, the following load factors should be used

Unfavorable permanent loads	1.35
Favorable permanent loads	1.00
Variable loads	$1.5\ \psi_0$

where, ψ_0 ·is a factor that accounts for multiple variable loads acting on the structure. This factor can be found in Appendix A2 in SS-EN 1990. In the design of the concrete plug it is suitable to use ψ_0 ·= 1.0, that is to neglect the reduction for variable loads smaller than the designing variable load.

The water pressure, swelling pressure and the shrinkage can all be considered as unfavourable permanent loads and should thereby have a load coefficient equal to 1.35 according to Eurocode 2 (SIS 2005). Thereby, the loads used in the non-linear analysis include a higher safety margin than what is described according to Eurocode 2.

Table 5-3. Design load values and their probable values.

Type of load	Design value	Probable value	Factor
Water pressure	5 MPa	3 MPa	1.7
Swelling pressure	4 MPa	2 MPa	2.0
Maximum shrinkage	0.29 mm/m	0.17 mm/m	1.7
Temperature increase from the canisters	0 / +30°C	+ 25°C	0 / 1.2
Prestressing	0 / +10°C	+6°C	0 / 1.7
Creep factor	0.46	–	–

5.1.5 Global safety

In Section 4.3, it was shown that the engineer responsible for the calculations had defined the external pressure level corresponding to 21.5 MP as the conservative ultimate load level. In addition to this, the actual maximum load limit in the analysis was also presented as 37.5 MPa. However, this level of the external pressure is an overestimation of the ultimate load limit since crushing of the concrete was not included in the analysis and the compressive stresses in some areas were much higher than the compressive strength.

Based on the coefficients in BKR 2010

The total global safety of the dome shaped concrete plug can approximately be estimated as follows. The global safety factor is conservatively calculated based on the results in Section 4.3, where the external pressure was equal to 21.5 MPa when the first inclined crack initiated, and the maximum load in the same analysis where the maximum load obtained was 37.5 MPa. The calculated load capacity is then compared to the design pressure. According to Table 5-3, the probable values for the water pressure and for the swelling pressure are 3 MPa and 2 MPa respectively. The characteristic load value is not known for the water pressure and the swelling pressure and due to this, the probable load values have been treated as characteristic in this comparison. The characteristic values should probably be higher than the values specified as probable, and this leads to a slight overestimation of the safety factor. In the first approach to determine the global safety factor, the load coefficients according to BKR 2010 (Boverket 2010), equal to 1.0 for all permanent loads, are used. In addition, the material coefficients used in the analysis are compared to the load and material coefficients in the design code.

$$sf = \frac{21.5}{3 \cdot 1.0 + 2 \cdot 1.0} \cdot \frac{1}{1.8} = 2.4$$

In the same manner the global safety of the maximum load obtained in the analysis can be calculated.

$$sf = \frac{37.5}{3 \cdot 1.0 + 2 \cdot 1.0} \cdot \frac{1}{1.8} = 4.2$$

The actual global safety factor is within the two values mentioned above, i.e. $2.4 \leq sf \leq 4.2$. A global safety factor of 1.0 in this case would imply that the safety against failure is equal to the *high safety class* in BKR 2010, see Table 5-1, and the probability of failure is 10^{-6}/year. The calculations performed in this section show that the dome shaped concrete has a higher safety factor than prescribed in the design code.

In the design of the concrete plug, it has been determined that the design values for the water pressure and the swelling pressure should be 5 MPa and 4 MPa respectively, which implies load coefficients equal to 1.7 and 2.0. If the fact that higher load coefficients are used in the analyses than specified in the design code is accounted for and in addition to the material coefficient, the following global safety factor is obtained. In the second approach, the calculated load level is compared to the design values of the water and swelling pressure with the load coefficients in Table 5-3.

$$sf = \frac{21.5}{3 \cdot 1.7 + 2 \cdot 2.0} \cdot \frac{1}{1.8} = 1.3$$

In the same manner the global safety of the maximum load obtained in the analysis can be calculated.

$$sf = \frac{37.5}{3 \cdot 1.7 + 2 \cdot 2.0} \cdot \frac{1}{1.8} = 2.3$$

The safety factor is in this case within the interval between the two values above, i.e. $1.3 \leq sf \leq 2.3$ and is still above 1.0 and the dome shaped plug is thereby at least safer than what is prescribed in BKR 2010 for the *high safety class*.

Global safety factor for non-linear analyses

The total global safety of the dome shaped concrete plug can approximately be estimated as follows. The global safety factor is calculated based on the difference in external pressure for two analyses; one analysis with average values of the material properties and one analysis with characteristic material properties. In Section 4.3.6, the analysis with average values of the material properties reached an external pressure equal to R_m = 49.2 MPa. In the analysis with characteristic material properties the corresponding load level was R_k = 38.1 MPa.

The coefficient of variation V_{Rf} can be determined as

$$V_{Rf} = \frac{1}{1.65} \cdot \ln\left(\frac{R_m}{R_k}\right) = 0.155$$

To estimate the total coefficient of variation V_R the model uncertainties have been estimated as V_{Cf} = 0.10 according to Table 5-2. The total uncertainties related to the load capacity R is thereby

$$V_R = \sqrt{V_{Rf}^{\ 2} + V_{Cf}^{\ 2}} = 0.184$$

The global safety factor γ_{Rg} is then estimated based on the equation in Section 5.1.1 with the values α_R = 0.8, and β_T = 4.8.

$$\gamma_{Rg} = 1 + \alpha_R \beta_T V_R = 1.70$$

The water pressure can be assumed as rather well defined, while the swelling pressure on the other hand includes a large amount of uncertainty. The maximum allowed swelling pressure could therefore be calculated based on Eq. (5-1) as follows

$$\frac{R_m}{\gamma_{Rg}} \geq \gamma_{Water\_pressure} \cdot S_{Water\_pressure} + \gamma_{Swelling\_pressure} \cdot S_{Swelling\_pressure}$$

where, the values for $\gamma_{Water\_pressure}$, $S_{Water\_pressure}$ and $\gamma_{Swelling\_pressure}$ are taken from Table 5-3.

$$S_{Swelling\_pressure} \leq \frac{\frac{R_m}{\gamma_{Rg}} - \gamma_{Water\_pressure} \cdot S_{Water\_pressure}}{\gamma_{Swelling\_pressure}} = 11.97 \text{ MPa}$$

The maximum swelling pressure on the dome shaped concrete plug is approximately 12.0 MPa if all other loads except the water pressure are neglected, to satisfy the high safety class according to BKR 2010 (Boverket 2010).

5.2 Possibilities and limitations

5.2.1 Risk assessment

It was shown that creating a watertight plug design was the factor considered most critical. In order to create redundancy in the design, the concrete plug has to be as watertight as possible. In the plug design, the bentonite seal is intended for this, but ultimately all individual parts of the plug design should assist with the best of their capabilities to prevent leakage from the tunnel. This means that for instance, an increased leakage resistance of the concrete plug and reduced risk of cracking improves the whole plug design.

The function of the plug design will be verified in a future full-scale test. In the full-scale test, measurements will be performed where the amount of water passing through the plug will be continuously measured. The main idea of the full-scale test is that it should be as watertight as possible. The final criteria for acceptable leakage will be decided after the testing has been completed, when more information and experiences are available and the result has been evaluated.

Especially the high amount of shrinkage was a potential problem for the tapered concrete plug in combination with the difficulties to perform a contact grouting over its entire thickness. The shrinkage resulted in potential cracks along the perimeter of the plug in its the thickness direction, see Section 4.1.2.

A decision was made within the project to continue with the dome shaped plug for the reference design. The dome shaped concrete plug had advantages in most categories studied. One of the constraints with this alternative is that the maximum pressure is much lower than in the other alternative. However, since it is shown in Section 5.1 that the safety of the dome shaped plug is sufficient this is not an important issue.

It was determined that the tapered concrete plug could still be a valid and reasonable solution, but some measures have to be performed to reduce the risk of cracking in the interface between rock and concrete. Below a summary of the pros and cons for the two conceptual alternatives for the design of the concrete plug is presented.

Dome shaped plug

+ Low friction at the contact grouting.
+ Controllable casting of concrete.
+ Low risk of cracks going through the entire thickness.
+ Less influenced by shrinkage and leakage.
+ Standardized shape of the concrete plug.
+ Shorter concrete plug, larger amount of rock on the downstream side to carry the loads.
+ Shorter concrete plug, possibility to cast a new plug behind the first one if problems occur.
+ The concrete plug is compressed against the rock on the downstream side where the contact grouting tubes are installed, which leads to an increased water tightness.
+ No excavated damage zone at the plug location.
+ A similar construction has already been evaluated in the full-scale tests at Äspö.
– Sensitive to rock settlements.
– Complicated excavation of the rock.
– Lower swelling pressure can be allowed.
– Short leakage path.

Tapered plug

+ Capable to exhibit large pressures.
+ Easy rock excavation.
+ The circumferential shape of the concrete plug is unique for each tunnel, due to the irregularities of the rock.
+ Fast installation.
– Longer concrete plug, lower possibility to cast a new concrete plug behind if problems occur.
– Longer concrete plug, less amount of rock on the downstream side to carry the loads.
– Previously untested shape of the concrete plug (however somewhat similar to the shotcrete plug).
– Potential crack path along the perimeter of the plug in the thickness direction of the plug.
– Potentially high friction at the contact grouting.
– Initial problem with water leakage.
– May require alternative measures to reach an acceptable leakage.
– The casting of the concrete is more difficult to control.
– Sensitive to internal temperature variations during hydrations and thereby increased risk of cracking.

5.2.2 Back-up or alternative measures

For the technical development of plugs, as well as for development of other functional and technical designs, SKB applies a step-by-step development method. At certain points in time the present developed design is presented as the actual "reference design", with the objective to establish basic input for all other in parallel ongoing studies. The actual reference design is thoroughly reviewed within the SKB organization with respect to all technical and functional requirements influencing other systems, operation and maintenance viewpoints etc.

There are different possible measures that can be used if it shows that the plug design does not satisfy its requirements. However, all material components used in the plug design have to be clarified by the SKB Safety Analysis team. The SKB Safety Analysis team has to assure that the materials introduced in the plug design do not jeopardize the long-term safety of the KBS3-system.

One possible back-up solution is to do as in the TSX-plug (Martino et al. 2007), where grouting was performed several times to reduce the leakage to acceptable levels. Another possible back-up solution is to cast a new concrete plug behind the first one, if it shows that the leakage through the first concrete plug is unacceptable.

The design of the concrete plug is associated with uncertainties regarding material properties and loads. To achieve a robust plug design and limit the uncertainties, a possible measure could be including an additional watertight barrier just in front of the concrete plug. This could for instance be a steel plate on the upstream side of the concrete plug, inserted into a slot in the rock. The purpose of this would be to assure that the plug design is watertight before the bentonite seal have reached sufficient saturation. The concrete plug could thereby only be designed to maintain the load capacity and the crack free criteria could be removed.

5.3 Verification of the function

The function of the plug design will be verified in a future full-scale test. In the full-scale test, measurements will be performed where the amount of water passing through the plug will be continuously measured. The main idea of the full-scale test is that it should be as watertight as possible and based on the amount of leakage measured from this test it will be possible to define a reasonable limit of the acceptable leakage. The target value for the acceptable leakage is presently expressed "as low as possible". The final criteria for acceptable leakage will be decided after the testing has been completed, and more information and experiences from the performed full-scale test have been evaluated. In the upcoming full-scale test, the measuring system for the leakage is arranged for testing a maximum allowed leakage in the range of 0.0025 to 0.05 l/min, and obviously, the lower value will be the target value for the finally selected Design Criteria.

A substantial portion of the leakage out from the deposition tunnels is likely to pass through the rock. Therefore, it is also important to measure the amount of water that is transported via cracks in the rock. To measure some of this leakage, radial holes could be drilled in the rock on the downstream side of the plug and where the water is collected and measured.

The leakage measuring system is planned to be used on all future plugs to measure the amount of leakage out from each deposition tunnel. Thereby, good information can be gathered regarding the amount of leakage of each tunnel and measures can be taken if any of the plugs are not watertight enough, for instance perform additional contact grouting.

In the full-scale test, the load carrying capacity of the concrete plug will be tested by increasing the water pressure on the plug above the maximum water and swelling pressure expected on the plugs at the final repository. The load carrying capacity of the concrete plug will be so high that it is nearly impossible to artificially increase the pressure up to failure at the full-scale test. Therefore, instead downscaled concrete plugs could be cast in a dimension making it possible to load them to failure in a laboratory.

Several experiments will be performed regarding designing the bentonite seal, filter and backfill end zone. These will be performed in order to determine suitable design of these layers. Some examples of these experiments are for instance; a study of the bentonite seal and its possibility to seal cracks in the concrete plug. Several experiments are currently being planned regarding testing the concrete recipe, these are discussed in Section 7.1.

Before the experiments are conducted, numerical analyses are performed to simulate the leakage, development of swelling pressure, the ultimate load capacity of the concrete plug etc. Not all information of interest will be possible to determine through experimental tests and therefore the numerical simulations will be a complement to the results obtained in the experiments. The numerical simulations could for instance be used to as the structural analyses performed on the concrete plug presented in Chapter 4, or the development of swelling pressure described in Section 3.3.2.

6 Conclusions

The main purpose of this report was to summarize the evaluation process and the results of the suggested design for SKBs reference plug design. The purpose of the plug project is to develop a plug system that keeps the backfill in place and prevent an axial water flow. The plug system is preventing erosion of the buffer so that the buffer maintains its ability to prevent possible leakage of radioactive substances. The bentonite seal is intended for this, but ultimately all individual parts of the plug system should assist with the best of their capabilities to prevent leakage from the tunnel.

The backfilled deposition tunnels will be separated and sealed from the transport tunnels with a plug, consisting of different material layers and at the end, a cast-in-place concrete plug. The first layer in the reference design, closest to the backfill, is a filter and consist of typically sand or gravel. Its purpose is to buffer water and to be used for artificial controlled wetting of the bentonite seal. The filter should also be possible to drain water from the deposition tunnel until the concrete plug has reached adequate strength and if required the contact grouting has been performed. The filter should thereby also control the water pressure inside the plug system until the concrete has cured. Drainpipes will be arranged from the filter to the downstream side of the plug, as seen in Figure 2-1, with the purpose to drain the filter until the concrete plug is grouted. The drainpipes can also be to pump water into the filter again after the grouting, to control the time it takes to artificially saturate the bentonite seal and thereby ensuring a fast and homogenous wetting of the bentonite seal. The filter should also preserve a high water pressure in the case that the plug system is not sufficiently watertight. The controlled artificial wetting will ensure that the pressure build-up on the concrete plug is controlled regarding both its size and its time of arrival.

The layer closest to the concrete plug, the bentonite seal, consists of swelling clay which purpose is to prevent axial flow from the backfill and the buffer. The layer should intersect the EDZ, i.e. the excavated damaged zone. The main purpose of the bentonite seal is to prevent axial water flow out from the deposition tunnel. In addition, it should also heal cracks that may initiate on the upstream side of the concrete plug, and thereby prevent leakage out from the deposition tunnel.

The final layer is the concrete plug, which should be cast with low-pH concrete and without reinforcement. The preferable geometry of the concrete plug is a dome shape. The main purpose of the concrete plug is to resist the loads acting on the structure, and thereby act as a support to the rest of the plug system and the backfill. The two main external loads acting on the concrete plug are the hydrostatic water pressure from inside of the deposition tunnel and the swelling pressure from the backfill and the bentonite seal. In addition to this, the concrete plug must also be watertight until the bentonite seal has saturated and reached homogenization. After which, the bentonite seal will on its own act as the watertight barrier preventing leakage from the deposition tunnel into the transport tunnel.

Between each layer (filter, bentonite seal and the concrete plug) are delimiters assembled to separate the materials in the different layers from each other. The delimiters are in the present design arranged as prefabricated concrete beams, which was the solution used in the prototype test set-up. A principle sketch of the reference design is shown in Figure 2-1 and a drawing of the plug system with the suggested modifications is shown in Figure 6-1.

The result in this report is focusing on the concrete plug and its possibilities of assuring that the complete plug design can satisfy all requirements. The design of the plug system behind the concrete plug, will for instance affect the loads on the concrete plug. The requirements on the complete plug system influence the design of the individual parts of the system and ultimately determine which concrete plug design is most suitable. During the project, it has therefore been important to study the requirements, functions, preconditions, risks and possibilities of all individual parts as well as the whole plug design.

The results in this report have a focus on the concrete plug in the reference design and the evaluation of its design and safety concept.

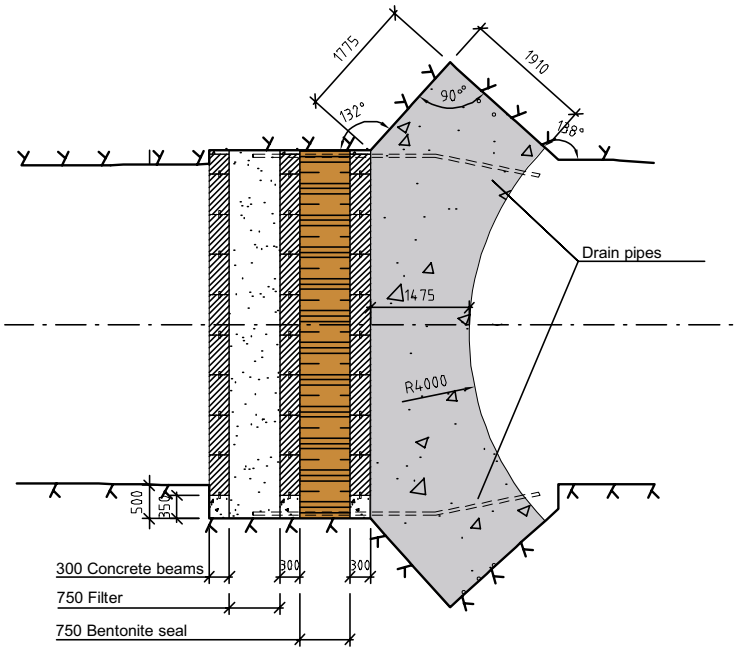

Figure 6-1. *Principle layout of the suggested design of the plug system.*

Within this project, a great deal of effort has been focused in defining the actions that act on the plug system. It has both been identifying the loads that may occur as well as estimating their effect and when the effect is likely to occur. The presented loads in this report are described with both their best estimate value and the conservatively chosen design value intended to be used in the numerical evaluation of the structural safety. In order to determine the overall safety towards failure simulations were made under design assumptions and the best estimate assumptions. The most significant load effects will not take in place until after several years, for instance the water pressure, swelling pressure, shrinkage, temperature increase from the spent nuclear fuel etc.

In accordance with conventional design principle, the analyses have been performed by assuming that the concrete plug has the strength equal to its early strength after hardening. For normal concrete this strength is chosen as the 28-day strength, while for the low-pH concrete this has been set equal to the 90-day strength. The reason for this, is that the low-pH concrete matures at a slower rate, has a high amount of early shrinkage and with the suggested design concept the concrete plug will not be subjected to any loads prior to the time of contact grouting of the plug. A significant increase in strength is expected in all concrete materials, this increase is typically between 40–70%. The size of the increase in strength with the low-pH concrete has not been measured for any longer time periods and therefore it is not possible to define the size of the expected increase in strength.

The dome shaped concrete plug has been shown to be able to carry the design loads from; water and swelling pressure, creep, shrinkage, temperature increase from the spent nuclear fuel and the prestressing due to cooling the plug before grouting. The numerical analyses show that a high margin of safety is obtained for the dome shaped concrete plug based on the design values of the external loads. The conclusion from the numerical finite element analyses is that the dome shaped plug has much better capabilities of remaining free from cracks that could cause leakage out from the deposition tunnel. The dome shaped plug has thereby a better capability to be watertight for the time period the bentonite seal needs to saturate than compared to the tapered concrete plug. One important conclusion from the calculations is that the prestress is vital to compensate for the cracking that occurs due to shrinkage from 90 days after casting to the end of the lifespan of 100 years. There is a large difference in the extent of cracking depending on, whether the shrinkage curve for B200 or B300 is used.

7 Future work

In the next phase of this project (called KBP 1004), several parts of the reference design will be studied further.

The aim of the next step is to design the backfill end zone, filter and bentonite seal. All of these are studied in the subproject called DP1. In the second subproject, DP2, all materials in the reference design are cleared with the SKB Safety Analysis team, and methods to determine the measuring system for leakage is developed. In the subproject three, DP3, different excavation methods are studied to determine the most suitable methods for excavating the different parts of the deposition tunnels. In subproject four, called DP4, development of the concrete material is performed in addition with complementary testing to determine the material properties of the low-pH concrete recipe. In subproject five, DP5, the design of the full-scale test is performed.

The following goals are determined for this project

- Determine the leakage through the plug system and in the contact between rock and concrete at a water pressure of 7 MPa.
- Apply a water pressure of 10 MPa to the plug system.
- Adjusting and complementary testing of the material properties for the low-pH concrete.
- Development of a reliable control method.
- Determine a functional requirement of the allowed leakage of the plug design.
- Clarify all materials used in the reference design with SKB Safety Analysis team.
- Determine and analyze the filter, bentonite seal and the drainage and make certain that they satisfy the requirements.

Below, a summary of the future work needed for further analyses of the concrete dome shaped plug are presented.

7.1 Experimental tests

In the following section, the need for tests regarding development of low-pH concrete properties, small-scale ultimate load capacity of the plug and a full-scale test are presented.

7.1.1 Low-pH concrete properties

The design of the concrete plug is based on the material properties presented in Vogt et al. (2009). Due to uncertainties and a limited amount of data, conservative recommendations were made where for instance the shrinkage corresponding to concrete B300 was used even though the material B200 is studied. There is a difference of about 100% between the measured autogenous shrinkage between these two concrete recipes.

The shrinkage is one of the most difficult loads for the concrete plug to remain free of cracks that could transport water and eroded bentonite clay out from the deposition tunnel. Due to this, new shrinkage tests are currently performed in the next phase of this project. A total of 30 concrete beams are being measured according to the most accurate method, see Section 3.3.3, according to the previous studies. The concrete beams are being studied under different conditions

1. Sealed specimens (only autogenous shrinkage).
2. Specimens stored in water.
3. Specimens subjected to RH 50% (autogenous and drying shrinkage).

Five specimens under each sealing condition are being studied in two different laboratories, giving the total of 30 specimens. Based on these experiments it will be possible to better determine an appropriate shrinkage curve to be used in the design of the concrete plug.

The numerical analyses are based on the strength corresponding to 90 days after casting and the increase in strength with time is not accounted for. It is however, interesting to determine the expected increase in strength to better determine the level of safety. Therefore, it is planned to perform compressive tests of cubes and cylinders that were saved from the original testing by Vogt et al. (2009). The concrete specimens are from 2007 and it is planned to test these at an age of five years. In addition to this, large volumes of concrete exist from the large shrinkage experiments shown in Figure 3-11. Cylinders may be taken out from these specimens and be used for measuring the strength development.

Standardized creep tests are performed at a load level equal to 30% of the compressive strength. The compressive stresses in the concrete plug are for the long-term load much higher than this in some areas. Creep test must therefore be performed with higher compressive stresses. Typically the test should be conducted with a compressive stress equal to approximately 50–70% of the compressive strength. The reason why these experiments should be performed is that it is possible that the structure will not exhibit linear creep for a load level this high.

The concrete compressive strength increases if normal concrete is subjected to compressive stresses in two or especially three directions, see Section 4.3.3. The concrete dome shaped plug will be subjected to large stresses in at least two directions. However, there is limited information regarding the biaxial and triaxial behavior of low-pH concrete. This effect is normally included in the non-linear finite element analyses. In order to account for this effect in the analyses more information is needed regarding the low-pH concrete. Therefore, it is suggested that specimens of the developed low-pH concrete recipe are experimentally tested for combinations of multiaxial stresses to determine its behavior.

7.1.2 Complementary experiments to the full-scale test

Based on the different techniques used for the excavation of the v-shaped slot used for abutment of the concrete plug, different roughness of the rock surface will be obtained. The bond between different types of rock surfaces, based on excavation method, and the concrete should be studied. The concrete plug is intended to release from the rock surface during its first 90 days, in order for the concrete plug to be considered as “stress free“ before grouting. The risk is that if the concrete plug does not release from the rock surface at this point it could either crack or develop large tensile stresses that could lead to cracks later on.

It will not be possible to test the load capacity of the concrete plug in a full-scale test. This is due to two reasons; first, the pressure needed to create a failure of the concrete plug is above 30 MPa, which is higher than what can be obtained. Secondly, if a failure of the concrete plug would occur a massive safety arrangement is needed since it is likely that the collapse of the concrete plug could cause severe damage to personnel, instruments and other test facilities in the Äspö HRL. Therefore, it is suggested that a smaller concrete plug that can be tested in a laboratory should be performed. Typically, testing a concrete plug of one tenth of the original size would produce a small-scale test that is small enough to be tested in a large load rig. This experiment would show the accuracy of the numerical analyses performed, and could be used to validate the results from the numerical analyses. Thereby, the small-scale experiment could be used to validate the safety of the final concrete plug.

7.1.3 Full-scale field test

The plug design consists of several different components with different purposes. A full-scale test is currently planned to start with the installation in the beginning of 2012 and thereafter a period of operation. At present, this period is estimated equal to two years but it could be prolonged on SKB's requests. During the full-scale test, the installation of the whole plug design will be tested. It will for instance be tested that the filter is capable to drain the tunnel during the time when the concrete plug is hardening and until the contact grouting has been conducted. After this point, the saturation of the bentonite seal will be tested. After sufficient saturation of the bentonite seal, the water pressure will be increased with a compression chamber and the filter can be filled with water to increase the water pressure even more. It is planned to artificially increase the water pressure up to 10 MPa to test at a level close to the design load of 9 MPa (5 MPa water pressure and 4 MPa of swelling pressure).

Changes made to the backfill material have resulted in that the expected swelling pressure has increased significantly. Therefore, the previous full-scale tests at Äspö HRL have not been subjected to a pressure of this magnitude before. The water tightness criteria of the plug will be important and have a large impact on the design of the plug system. From the full-scale test it will therefore be possible to see the amount of leakage that will pass through the plug system and the amount of leakage that will pass through networks of cracks in the rock. The intention of the full-scale test is to make it as watertight as possible. Based on the measured leakage it will be possible to define reasonable criterias for the maximum leakage from a deposition tunnel sealed with the current reference design. The purpose of the full-scale test is to verify that assumptions that have been made and that the conclusions drawn are correct.

The plans and the details for the full-scale test will be evaluated and developed further during the year of 2011 and the installation of the full-scale test is scheduled to start in the year of 2012.

8 References

SKB's (Svensk Kärnbränslehantering AB) publications can be found at www.skb.se/publications.

Ageskog L, Jansson P, 1999. Heat propagation in and around the deep repository. Thermal calculations applied to three hypothetical sites: Aberg, Beberg and Ceberg. SKB TR-99-02, Svensk Kärnbränslehantering AB.

Bažant Z P, 1975. Theory of creep and shrinkage in concrete structures: a précis of recent developments. Mechanics Today 2, 1–93.

Bažant Z P (ed), 1988. Mathematical modelling of creep and shrinkage of concrete: proceedings of the Fourth RILEM International Symposium, Northwestern University, Illinois, 26–29 August 1986. Chichester: Wiley.

Bergh-Christensen J, 1988. Design of High Pressure Concrete Plugs for Hydropower Projects. In: Proc Symposium on Rock Mechanics and Power Plants, September 12–16, Madrid, p 261–268.

Birgersson M, Börgesson L, Hedström M, Karnland O, Nilsson U, 2009. Bentonite erosion. Final report. SKB TR-09-34, Svensk Kärnbränslehantering AB.

Boverket, 2004. Boverkets handbok om betongkonstruktioner: BBK 04. 3rd ed. Karlskrona: Boverket. (In Swedish.)

Boverket, 2010. Regelsamling för konstruktion, BKR 2010. Karlskrona: Boverket. (In Swedish.)

Carlsson F, Plos M, Norlin B, Thelandersson S, 2008. Säkerhetsprinciper för bärighetsanalys av broar med icke-linjära metoder. Report TVBK-3056, Lunds University, Sweden. (In Swedish.)

CEB, 1993. CEB-FIP model code 1990. Lausanne: Comité Euro-International du Béton.

Cervenka V, Jendele L, Cervenka J, 2005. ATENA program documentation – Part 1: Theory. Prague.

Dahlström L-O, 2009. Experiences from the design and construction of plug II in the Prototype Repository. Prototype Repository. SKB R-09-49, Svensk Kärnbränslehantering AB.

Dahlström L-O, Magnusson J, Gueorguiev G, Johansson M, 2009. Feasibility study of a concrete plug made of low pH concrete. SKB R-09-34, Svensk Kärnbränslehantering AB.

Dixon D A, Börgesson L, Gunnarsson D, Hansen J, 2009. Plugs for deposition tunnels in a deep geologic repository in granitic rock. Concepts and experience. SKB R-09-50, Svensk Kärnbränslehantering AB.

Esping O, 2007. *Early age properties of self-compacting concrete: effects of fine aggregate and limestone filler*. PhD thesis. Chalmers University of Technology, Göteborg, Sweden.

FHWA, 2006. Material property characterization of ultra-high performance concrete. Publication FHWA-HRT-06-103, Federal Highway Administration, U.S. Department of Transportation.

Fälth B, Gatter P, 2009. Mechanical and thermo-mechanical analyses of the tapered plug for plugging of deposition tunnels. A feasibility study. SKB R-09-33, Svensk Kärnbränslehantering AB.

García-Siñeriz J L, Cruz Alonso M, Alonso J, 2008. Application of low pH concrete in the construction and the operation of underground repositories. In EURADWASTE 08: Seventh European Commission Conference on the Management and Disposal of Radioactive Waste, Luxembourg, 20–23 October 2008. Available at: ftp://ftp.cordis.europa.eu/pub/fp7/fission/docs/euradwaste08/papers/bure-module4f-esdred-application-of-low-ph-concrete-j-l-garcia-sineriz_en.pdf.

Hökmark H, Lönnqvist M, Kristensson O, Sundberg J, Hellström G, 2009. Strategy for thermal dimensioning of the final repository for spent nuclear fuel. SKB R-09-04, Svensk Kärnbränslehantering AB.

Hökmark H, Lönnqvist M, Fälth B, 2010. THM-issues in repository rock. Thermal, mechanical, thermo-mechanical and hydro-mechanical evolution of the rock at the Forsmark and Laxemar sites. SKB TR-10-23, Svensk Kärnbränslehantering AB.

Johannesson L-E, Nilsson U, 2006. Deep repository – engineered barrier systems. Geotechnical behaviour of candidate backfill materials. Laboratory tests and calculations for determining performance of the backfill. SKB R-06-73, Svensk Kärnbränslehantering AB.

Johannesson L-E, Börgesson L, Goudarzi R, Sandén T, Gunnarsson D, Svemar C, 2007. Prototype repository: a full scale experiment at Äspö HRL. Physics and Chemistry of the Earth, Parts A/B/C 32, 58–76.

Malm R, 2006. Shear cracks in concrete structures subjected to in-plane stresses. Department of Civil and Architectural Engineering, Royal Institute of Technology, Stockholm, Sweden. (Trita-BKN, Bulletin 88.)

Mang H, Lackner R, Meschke G, Mosler J, 2003. Computational modelling of concrete structures. In de Borst R, Mang A H (eds). Comprehensive structural integrity. Vol 3. Amsterdam: Elsevier Pergamon, 536–601.

Martino J B, Dixon D A, Vignal B, Fujita T, 2006. The tunnel sealing experiment: the construction and performance of full scale clay and concrete bulkheads at elevated pressure and temperature. In TopSeal 2006, Olkiluto, Finland, 17–20 September 2006. Available at: http://www.euronuclear.org/events/topseal/transactions/Paper-Poster-Martino.pdf.

Martino J B, Dixon D A, Kozak E T, Gascoyne M, Vignal B, Sugita Y, Fujita T, Masumoto K, 2007. The tunnel sealing experiment: An international study of full-scale seals. Physics and Chemistry of the Earth, Parts A/B/C 32, 93–107.

NKB, 1978. Recommendations for loading- and safety regulations for structural design. NKB-Report 36, Nordiska kommittén för byggbestämmelser, Copenhagen.

Pacovský J, 1999. Continuous measurements of stress and temperature during testing of a fibre shotcrete pressure plug. Geotechnical and Geological Engineering 17, 335–343.

Sharma S, Judd W R, 1991. Underground opening damage from earthquakes. Engineering Geology 30, 263–276.

SIS, 2000. SS 137215: *Concrete testing – Hardened concrete – Shrinkage*. Stockholm: Swedish Standards Institute.

SIS, 2005. SS-EN 1992-1-1:2005. Eurocode 2: Design of concrete structures – Part 1-1: General rules and rules for buildings. Stockholm: Swedish Standards Institute.

SKB, 2006. Äspö Hard Rock Laboratory. Annual report 2005. SKB TR-06-10, Svensk Kärnbränslehantering AB.

SKB, 2008a. Äspö Hard Rock Laboratory. Annual report 2007. SKB TR-08-10, Svensk Kärnbränslehantering AB.

SKB, 2008b. Site description of Forsmark at completion of the site investigation phase. SDM-Site Forsmark. SKB TR-08-05, Svensk Kärnbränslehantering AB.

SKB, 2009. Underground design Laxemar. Layout D2. SKB R-09-16, Svensk Kärnbränslehantering AB.

SKB, 2010a. Design, production and initial state of the backfill and plug in deposition tunnels. SKB TR-10-16, Svensk Kärnbränslehantering AB.

SKB, 2010b. Design, construction and initial state of the underground openings. SKB TR-10-18, Svensk Kärnbränslehantering AB.

SKI, 1992. Characterization of seismic ground motions for probabilistic safety analyses of nuclear facilities in Sweden. SKI Technical Report 92:3, Statens kärnkraftsinspektion (Swedish Nuclear Power Inspectorate).

SS EN 1990, 2010. Eurokod – Grundläggande dimensioneringsregler för bärverk. Swedish Standards Institute. 1st Edition.

Stephens M, Fox A, La Pointe P, Simeonov A, Isaksson H, Hermanson J, Öhman J. 2007. Geology Forsmark. Site descriptive modelling Forsmark stage 2.2. SKB R-07-45, Svensk Kärnbränslehantering AB.

Sundberg J, Wrafter J, Ländell M, Back P-E, Rosén L, 2008. Thermal properties Forsmark. Modelling stage 2.3. Complementary analysis and verification of the thermal bedrock model, stage 2.2. SKB R-08-65, Svensk Kärnbränslehantering AB.

Sundquist H, Örbom B M (eds), 1973. Konstruktionsanvisningar för skyddsbarriärer. Stockholm: Fortifikationsförvaltningen. (Publikation 35) (In Swedish.)

Sustainable Bridges, 2007. Guideline for load and resistance assessment of existing European railway bridges: advices on the use of advanced methods. Prepared by Sustainable Bridges – a project within EU FP6.

Svensson U, 2006. The Forsmark repository. Modelling changes in the flow, pressure and salinity fields, due to a repository for spent nuclear fuel. SKB R-05-57, Svensk Kärnbränslehantering AB.

Vogt C, Lagerblad B, Wallin K, Baldy F, Jonasson J-E, 2009. Low pH self compacting concrete for deposition tunnel plugs. SKB R-09-07, Svensk Kärnbränslehantering AB.

von Schloten C, Enevoldsen I, Arnbjerg-Nielsen T, Randrup-Thomsen S, Sloth M, Egelund S, Faber M, 2004. Reliability-based classification of the load carrying capacity of existing bridges: guideline document. Report 291, Danish Road Directorate, Copenhagen.

Vägverket, 2004. Bro 94: allmän teknisk beskrivning för broar. 4. Betongkonstruktioner. Borlänge: Vägverket. (In Swedish.)

Wang J-N, 1993. Seismic design of tunnels: a simple state-of-the-art design approach. New York: Parsons Brinckerhoff.

Westberg M, 2010. Reliability-based assessment of concrete dam stability. PhD thesis. Division of Structural Engineering, Lund University. (Report TVBK-1039.)

Wimelius H, Pusch R, 2008. Backfilling of KBS-3V deposition tunnels – possibilities and limitations. SKB R-08-59, Svensk Kärnbränslehantering AB.

Åkesson M, Börgesson L, Kristensson O, 2010a. SR-Site Data report. THM modeling of buffer, backfill and other system components. SKB TR-10-44, Svensk Kärnbränslehantering AB.

Åkesson M, Kristensson O, Börgesson L, Dueck A, Hernelind J, 2010b. THM modelling of buffer, backfill and other system components Critical processes and scenarios. SKB TR-10-11, Svensk Kärnbränslehantering AB.

Appendix A

ABAQUS input file

The following input data is used in Section 4.3.6. The node and element generation as well as all node and element sets have been suppressed since every node and element is shown in the input-file.

```
*Heading
** Job name: Valvplugg_expl_mean_slow Model name: Expl_mean
** Generated by: Abaqus/CAE Version 6.8-1
*Preprint, echo=NO, model=NO, history=NO, contact=NO
**
**********************************************************************
****************** Definition of the geometry ******************
**********************************************************************
** PARTS
**
*Part, name=Part-1
*Node
** Node 1 to 834 are defined here
*Element, type=CAX3
** Element number 1 to 11 are defined here
*Element, type=CAX4R
** Element number 12 to 784 are defined here
** Section: Section-1
*Solid Section, elset=_PickedSet2, material=Concrete_mean
1.,
*End Part
**
**
** ASSEMBLY
**
*Assembly, name=Assembly
**
*Instance, name=Part-1-1, part=Part-1
*End Instance
*Surface, type=ELEMENT, name=Surf-1
_Surf-1_S4, S4
_Surf-1_S1, S1
_Surf-1_S2, S2
**
** INTEGRATED OUTPUT SECTIONS
**
*Integrated Output Section, name=Top, surface=_PickedSurf8, project
orientation=NO
*End Assembly
*Amplitude, name=Amp-1
          0.,           0.,           4.,           2.
**
**********************************************************************
****************** Definition of the material ******************
**********************************************************************
** MATERIALS
** Characteristic material properties
*Material, name=Concrete
*Density
2400.,
*Elastic
```

```
 3.39e+10, 0.27
*Concrete Damaged Plasticity
35.,   0.1,  1.16, 0.667,    0.
*Concrete Compression Hardening
  3.24e+07,       0.
 3.456e+07, 0.000267
  4.05e+07, 0.000573
 4.536e+07, 0.000879
 4.914e+07, 0.001185
 5.184e+07, 0.001491
 5.346e+07, 0.001796
   5.4e+07, 0.002101
   540000., 0.003102
*Concrete Tension Stiffening, type=GFI
 2.9e+06,100.
*Concrete Compression Damage
   0.,       0.
 0.04, 0.000267
 0.15, 0.000573
 0.24, 0.000879
 0.31, 0.001185
 0.36, 0.001491
 0.39, 0.001796
  0.4, 0.002101
  0.9, 0.003102
*Concrete Tension Damage, type=DISPLACEMENT
   0.,      0.
 0.95, 6.8e-05
** Material properties based on mean values
*Material, name=Concrete_mean
*Density
2400.,
*Elastic
 3.39e+10, 0.27
*Concrete Damaged Plasticity
35.,   0.1,  1.16, 0.667,    0.
*Concrete Compression Hardening
  3.72e+07,       0.
 3.968e+07, 0.000329
  4.65e+07, 0.000658
 5.208e+07, 0.000987
 5.642e+07, 0.001316
 5.952e+07, 0.001645
 6.138e+07, 0.001973
   6.2e+07, 0.002302
   620000., 0.003302
*Concrete Tension Stiffening, type=GFI
 3.3e+06,100.
*Concrete Compression Damage
   0.,       0.
 0.04, 0.000329
 0.15, 0.000658
 0.24, 0.000987
 0.31, 0.001316
 0.36, 0.001645
 0.39, 0.001973
  0.4, 0.002302
  0.9, 0.003302
*Concrete Tension Damage, type=DISPLACEMENT
   0.,       0.
 0.95, 6.06e-05
```

```
** BOUNDARY CONDITIONS
**
** Name: BC-1 Type: Displacement/Rotation
*Boundary
_PickedSet4, 1, 1
_PickedSet4, 2, 2
**************************************************************
******************** Definition of the step ********************
**************************************************************
**
** STEP: Step-1
**
*Step, name=Quasi-static load
*Dynamic, Explicit
, 2.081
*Bulk Viscosity
0.06, 1.2
**
** LOADS
**
** Name: Pressure_load   Type: Pressure
*Dsload, amplitude=Amp-1
_PickedSurf5, P, 5e+07
**
** OUTPUT REQUESTS
**
*Restart, write, number interval=1, time marks=NO
**
** FIELD OUTPUT: F-Output-1
*Output, field
*Node Output
CF, RF, U
*Element Output, directions=YES
DAMAGEC, DAMAGET, LE, P, PE, PEEQ, PEMAG, S
*Contact Output
CSTRESS,
**
** HISTORY OUTPUT: H-Output-1
*Output, history, variable=PRESELECT, frequency=1
**
** HISTORY OUTPUT: H-Output-3
**
*Output, history, time interval=0.01
*Node Output, nset=Load_surf
U2,
** HISTORY OUTPUT: H-Output-2
**
*Node Output, nset=centrum
U2,
*End Step
```

Appendix B

ADINA results

The results in this Appendix have been calculated by Reinertsen under the supervision of Morgan Johansson. The following input data and results in this appendix are discussed in report, in the following sections; Section 4.3.3, Section 4.3.4 and Section 4.3.5.

Content

B1 Summary

B1.1 Orientation

The following document is written in Swedish. An English summary, though, is given below based on the summary given in Chapter B2. Further, in Appendix B1 translations of the figure and table texts provided in this document are given.

Below a brief description is made of the changes that have been made in the simulations, the main results that are provided in this document and a summary of what conclusions that Reinertsen has made in their FE analyses of the concrete plug for deposit of spent nuclear fuel. The analyses have mainly been carried out during autumn 2009. This document has been put together by Jonas Ekström and Morgan Johansson.

The work carried out includes the following areas:

- Reduced plug geometry.
- Nonlinear analyses of plug.
- Asymmetric loading of plug.

B1.2 Revised input for material and loads

Analyses

The analyses carried out are based on the input data that were used in report R-09-34 (Dahlström et al. 2009). Some changes, though, have been made, among all in accordance with the guideline of this project, as shown below (previous values in parenthesis).

Material

Rock
- $E_{rock,min}$ = 40 GPa (25 GPa).
- $E_{rock,max}$ = 80 GPa (75 GPa).
- ν = 0.235 (0.2).

Concrete
- Nonlinear analysis (linear analysis)
  - f_{ct} = 0.8–2.9 MPa.
  - G_F = 27.8–100 N/m.

Geometry

- Centric height = 1.1–1.7 m (1.7 m).
- Abutment = 1.71–2.11 m (2.11 m).

Boundary conditions

- No changes.

Loads

- Water pressure = 5 MPa (4 MPa).
- Swell pressure = 4 MPa (2 MPa).
- Asymmetric load: 2/4 MPa swell pressure (0 MPa).

Two extreme cases from R-09-34 have been studied:

- Load case 4.2 – Maximal tensile stresses.
- Load case 5.5 – Maximal compressive stresses.

Further, different combinations of load case 5.5 have been investigated where the outer pressure due to swelling and water have been reduced to zero.

B1.3 Reduced geometry of plug

Controls have been made for load case 5, which gives maximal compressive stresses. Further, a variant of this load case has been investigated where the outer pressure due to swelling and water have been reduced to zero.

The plug geometry is reduced by modified thickness in the plug centre and reduced thickness at its abutment. Based on these analyses it is proposed that a reduced plug geometry according to Figure B1-1; the centric height is reduced from 1.7 m to 1.3 m and the abutment thickness is reduced from 2.11 m to 1.91 m. This results in a reduced volume from 125 m^3/plug to 107 m^3/plug; i.e. a reduction of about 15%.

B1.4 Nonlinear analyses of plug

Different materials have been used in the nonlinear analyses:

- Material 1: Characteristic material values for 90 days strength.
- Material 3: Design material values with a crack safety factor of 2.0.

The use of material 1 is recommended since it best corresponds to the real response of the plug. When evaluating the plug reliability all safety margins are preferably applied afterwards when comparing the expected load with the expected capacity.

Control has been made for load case 4, which results in maximal tensile stresses.

Table B1-1 summarises the outer pressure load (swell pressure + water pressure) that can be applied before a certain "damage" (crack) is initiated in the plug. For material 1 it is possible to reach convergence in the analysis for an outer pressure of at least 30 MPa. However, it is somewhat unclear to what degree it is possible to rely on this result since one, based on previous experience, should be careful to fully trust the response of nonlinear FE analyses with the type of shear cracks that appear here.

Table B1-1. Summary of crack development for material 1 and 3. Stress values specify the pressure load due to water and swelling that is applied at the given moment.

Description	Material 1	Material 3
First crack initiation	R + (T) ½ element 3 MPa	R + (T) ½ element 1 MPa
First fully open crack	4.5 MPa	1.5 MPa
First initiation of shear crack	21 MPa	7.5 MPa
Fully open shear crack	21.5 MPa	10 MPa and half the temperature load (2 nearby cracks)

Presented results indicate that it is possible to apply a considerable outer pressure load before any problems with cracking appear. A conservative evaluation of a permitted load of 21 MPa, assuming material 1, would result in a safety of 21 / 9 = 2.3.

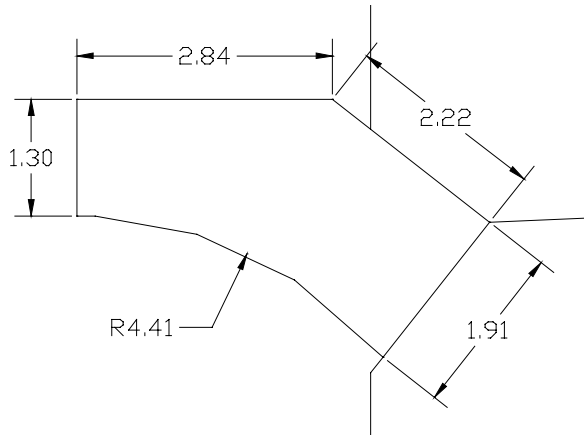

Figure B1-1. *Proposal for reduced plug geometry.*

B1.5 Asymmetric load on plug

Control of asymmetric swell pressure and water pressure (in the slot) has been carried out. These controls show that the asymmetry has little consequence of the total stress distribution. Further, super positioning of asymmetric load provides good agreement with combined load.

B2 Sammanfattning

B2.1 Orientering

Nedan ges en kort beskrivning av vilka ändringar i modellering samt huvudsakliga resultat som tagits fram i detta PM samt en övergripande sammanfattning av vad Reinertsen kommit fram till i sina FE-analyser av betongplugg för kärnbränsleförvaring. Analysarbetet har huvudsakligen utförts under hösten 2009. Detta tekniska PM har sammanställts av Jonas Ekström och Morgan Johansson.

Utfört arbete behandlar följande områden:

- Reducerad geometri hos plugg.
- Olinjära analyser av plugg.
- Osymmetrisk belastning av plugg.

B2.2 Ändrade material- och lastdata

Analyser

Utförda analyser är baserade på de indata som användes i rapport R-09-34 (Dahlström et al. 2009). Vissa ändringar har dock gjorts, bland annat utgående från riktlinjer givna i detta projekt, enligt nedan (tidigare värden inom parantes).

Material

Berg
- $E_{berg,min}$ = 40 GPa (25 GPa).
- $E_{berg,max}$ = 80 GPa (75 GPa).
- ν = 0,235 (0,2).

Betong
- Olinjär analys (linjär analys).
  – f_{ct} = 0,8–2,9 MPa.
  – G_F = 27,8–100 N/m.

Geometri

- Centrumhöjd = 1,1–1,7 m (1,7 m).
- Infästning = 1,71–2,11 m (2,11 m).

Randvillkor

- Inga ändringar.

Laster

- Vattentryck = 5 MPa (4 MPa).
- Svälltryck = 4 MPa (2 MPa).
- Osymmetrisk last: 2/4 MPa svälltryck (0 MPa).

Två extremfall från R-09-34 har främst studerats:

- Lastfall 4.2 – Maximala dragspänningar.
- Lastfall 5.5 – Maximala tryckspänningar.

Vidare har även kombinationer av lastfall 5.5 undersökts där det yttre trycket av svällning och vatten satts till noll.

B2.3 Reducerad geometri hos plugg

Kontroll har gjorts för lastfall 5, vilket resulterar i maximala tryckspänningar. Vidare har en variant av denna lastkombination undersökts där yttre trycket av svällning och vatten satts till noll.

Pluggens geometri minskas genom ändrad tjocklek i pluggens mitt samt minskad höjd i anfang (höger). Utgående från utförda beräkningar föreslås en reducerad pluggeometri enligt figur B2-1 – centrumhöjd minskas från 1,7 m till 1,3 m och anfangshöjd minskas från 2,11 m till 1,91 m. Detta medför en volymminskning från 125 m^3/plugg till 107 m^3/plugg, dvs. en minskning med ca 15 %.

B2.4 Olinjära analyser hos plugg

I de olinjära analyserna har olika materialsamband använts:

- Materialsamband 1: Karakteristiska materialvärden för 90-dygnshållfasthet.
- Materialsamband 3: Dimensionerande materialvärden med en spricksäkerhetsfaktor på 2,0.

Användandet av materialsamband 1 förespråkas eftersom det bäst motsvarar den verkliga responsen hos pluggen. Vid utvärdering av pluggens tillförlitlighet läggs säkerhetsmarginaler lämpligen på i efterhand – jämförelse av förväntad och tillåten last.

Kontroll har gjorts för lastfall 4, vilket resulterar i maximala dragspänningar.

Tabell B2-1 sammanfattar vilken yttre trycklast (svälltryck +vattentryck) som kan appliceras innan en viss ”skada” (spricka) uppstår i pluggen. För materialsamband 1 går det att driva analysen till en belastning med ett yttre tryck på minst 30 MPa. Det är dock något oklart i vilken grad det går att lita på dessa analysvärden eftersom man erfarenhetsmässigt bör man vara försiktig med att förlita sig på responsen från olinjära FE-analyser hos den typ av skjuvsprickor som uppstår här.

Tabell B2-1. Sammanställning av sprickförlopp för materialsamband 1 och 3. Spänningsvärden anger aktuell trycklast av vatten och svällning som applicerats på pluggen vid givet tillfälle.

Beskrivning	Materialsamband 1	Materialsamband 3
Första sprickan	R + (T) ½ element 3 MPa	R + (T) ½ element 1 MPa
Element fullt sprucket	4,5 MPa	1,5 MPa
Första indikation på skjuvspricka	21 MPa	7,5 MPa
Fullt öppen skjuvspricka	21,5 MPa	10 MPa och halva temperaturlasten (2 intilliggande sprickor)

Framtagna resultat indikerar att det finns möjlighet att lägga på en betydande yttre trycklast innan problem med upp-sprickning uppstår. En konservativ bedömning av tillåten last på 21 MPa, vid antagande av materialsamband 1, innebär en säkerhet på 21 / 9 = 2,3.

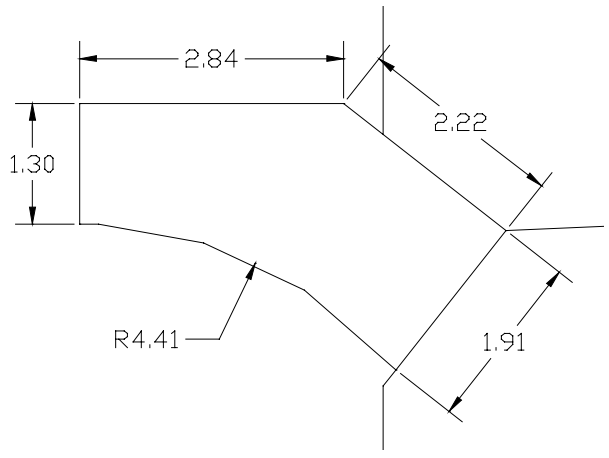

Figur B2-1. *Förslag till reducerad pluggeometri.*

B2.5 Osymmetrisk belastning av plugg

Kontroll av osymmetriskt svälltryck samt vattentryck (i slitsen) har utförts. Dessa kontroller visar att osymmetrin har liten inverkan på den totala spänningsbilden. Superponering av symmetrisk och osymmetrisk last ger god överensstämmelse med kombinerad last.

B3 Introduktion

B3.1 Bakgrund

Utförda analyser är baserade på de indata som användes i rapport R-09-34 (Dahlström et al. 2009). Vissa ändringar av material och laster har dock gjorts, bland annat utgående från riktlinjer givna i detta projekt. Studerad geometrisk utformning utgår dock från vad som anges i R-09-34 , se figur B3-1.

För mer utförlig information om använd modellering, materialdata, randvillkor och laster hänvisas till rapport R-09-34 (Dahlström et al. 2009).

B3.2 Undersökta lastkombinationer

Känslighetsanalyser utförda i R-09-34 har visat att för lastfall 4.2 kommer pluggens underkant att spricka upp relativt mycket, se figur B3-2, figur B3-3 tabell B3-1 och tabell B3-2 för beskrivning av lastfall 4.2. Linjärelastiska analyser där sprucken betong tagits bort helt från konstruktionen har visat att en så låg centrumhöjd hos pluggen som 0,5 meter skulle kunna bära en trycklast på totalt 10 MPa. En mer optimerad geometri hos pluggen har därför efterfrågats. Resultaten i detta dokument visar effekter som uppstår då pluggens geometri i olika avseende ändras.

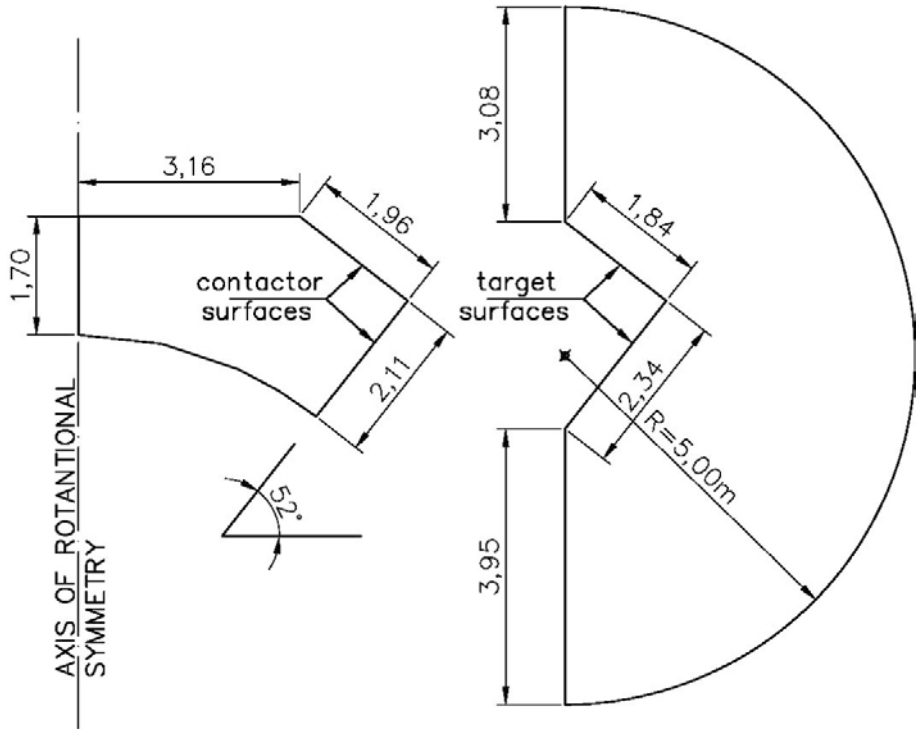

Figur B3-1. *Geometrisk utformning hos plugg och omgivande berg enligt R-09-34.*

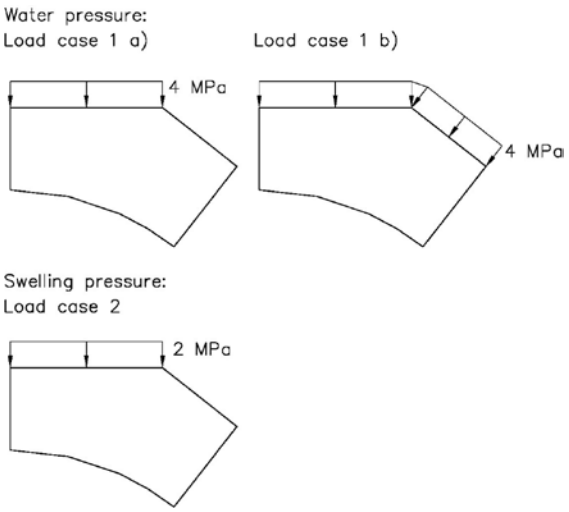

Figur B3-2. *Trycklaster, lastfall 1a, 1b and 2. Från R-09-34.*

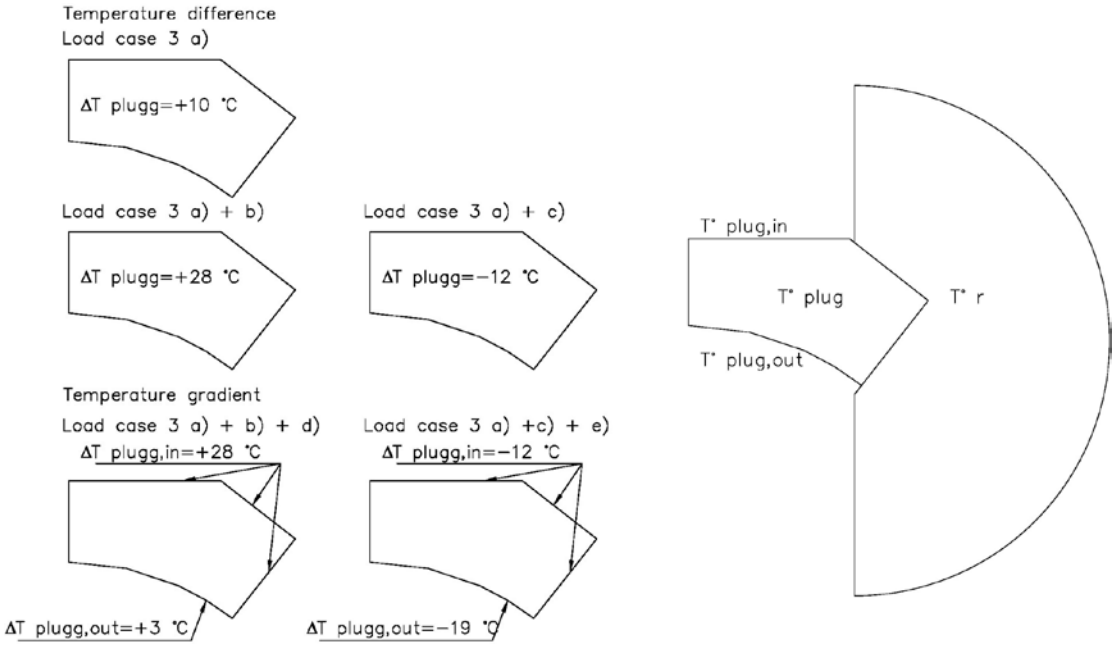

Figur B3-3. *Temperaturlaster, lastfall 3a – 3e.*

Tabell B3-1. Lastfall och lastkombinationer studerade i tidigare analyser. Från R-09-34 .

		Lastfall							
		1a	1b	2	3a	3b	3c	3d	3e
Lastkombinationer	1	x		x	x	x			
	2	x		x	x	x		x	
	3	x		x	x		x		
	4	x		x	x		x		x
	5		x	x	x	x			
	6		x	x	x	x		x	
	7		x	x	x		x		
	8		x	x	x		x		x

Tabell B3-2. Lastfall erhållna vid sammanställning av de 8 lastkombinationerna i tabell B3-1 och de 6 möjliga materialvariationerna för det omgivande berget. Från Från R-09-34.

Lastkombination X, X = 1–8		
Lastfall	**E_r**	**μ**
	[GPa]	
X.1	25	0,3
X.2	25	2,0
X.3	50	0,3
X.4	50	2,0
X.5	75	0,3
X.6	75	2,0

Lastkombination 4.2 i R-09-34 är en lastkombination som genererar så stora dragspänningar som möjligt i pluggens centrumsnitt, vilket via tabell B3-2 innebär att bergets elasticitetsmodul är låg (25 GPa) samt friktionen hög (μ = 2,0).

Lastkombination 5.5 i R-09-34 är en lastkombination som genererar så stora tryckspänningar som möjligt i pluggens centrumsnitt, vilket via tabell B3-2 innebär att bergets elasticitetsmodul är hög (75 GPa) samt friktionen låg (μ = 0,3).

B4 Reduktion hos pluggens geometri

B4.1 Konceptuell geometrisk förändring

Pluggens geometri har reducerats med två olika parametrar – pluggens centrumhöjd samt pluggens tjocklek vid anfanget, se figur B4-1 respektive figur B4-2. För reduktion av pluggens centrumhöjd har radien hos pluggens undersida minskats tillsammans med minskad centrumhöjd. Detta är gjort för att pluggens totala spännvidd skall bli densamma. Pluggens tjocklek vid anfanget har minskats genom att bergets kant flyttats nedåt på ett sådant sätt att tunnelväggarnas innerdiameter bibehålls.

B4.2 Ändrade förutsättningar jämfört med tidigare analyser

Inom detta projekt har bergets lägsta E-modul ändrats till 40 GPa från 25 GPa och bergets högsta E-modul till 80 GPa från 75 MPa, för att bättre representera materialegenskaperna hos berget i Forsmark. Tidigare analyser har visat att det är dessa övre och undre gränser som kommer vara kritiska för de två lastfallen där maximala spänningar i pluggen erhålls. Vidare har betongens tvärkontraktion ändrats 0,200 till 0,235. En ökning av vattentrycket är gjord från 4 MPa till 5 MPa.

En känslighetsanalys av svälltryckets inverkan har tidigare gjorts. I denna undersökning fastställdes att ett svälltryck upp till 6 MPa kan appliceras över pluggen utan att betongens gräns för linjärelastiska respons överskrids, förutsatt att hållfasthet vid 100 år används. I denna analys har ett väldigt konservativt sprucket tvärsnitt använts. Fortsättningsvis ansätts ett svälltryck på 4 MPa. Detta svälltryck har då en osäkerhetsfaktor gånger 2 multiplicerat till sig.

Designkrav för pluggen är att inga genomgående sprickor skall uppkomma i pluggen.

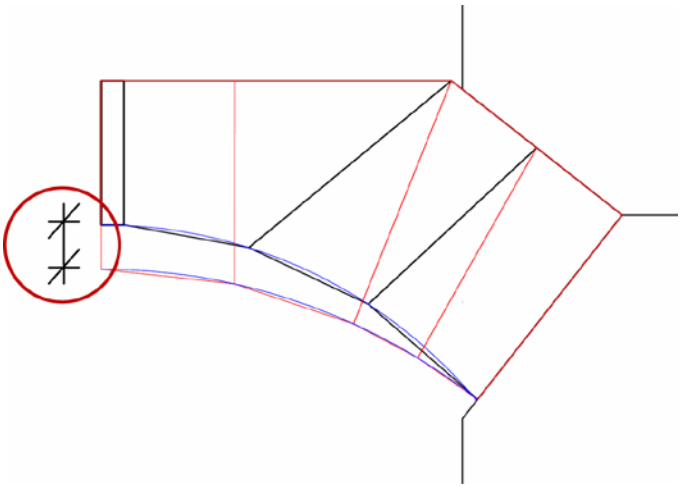

Figur B4-1. *Reduktion av pluggens centrumhöjd.*

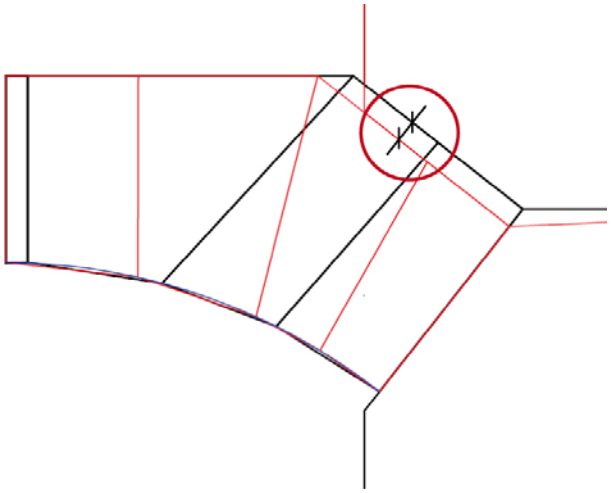

Figur B4-2. *Reduktion av pluggens tjocklek vid anfanget.*

B4.3 Begränsningar

Underlaget för slutsatserna i detta dokument är i första hand framtagna med linjärelastiska FE-modeller. När den slutliga geometrin är framtagen har olinjära analyser utförts för att mer detaljerat uppskatta pluggens uppsprickning. Pluggens respons är bara undersökt för lastfall 4.2 och lastfall 5.5, se figur B3-2, figur B3-3 tabell B3-1 och tabell B3-2 i avsnitt B3.2. Dessa lastfall har för tidigare kontrollerad geometri fastställts vara de mest kritiska. Effekten av osymmetrisk last har inte undersökts för den nya geometrin.

B4.4 Utvärderade lastfall

Tidigare lastfall med avseende på temperaturlaster har använts. När det kommer till trycklaster på pluggen har både vattentryck och svälltryck ökats till 5 MPa respektive 4 MPa. Lastfall avseende trycklaster blir därför enligt figur B4-3 och figur B4-4.

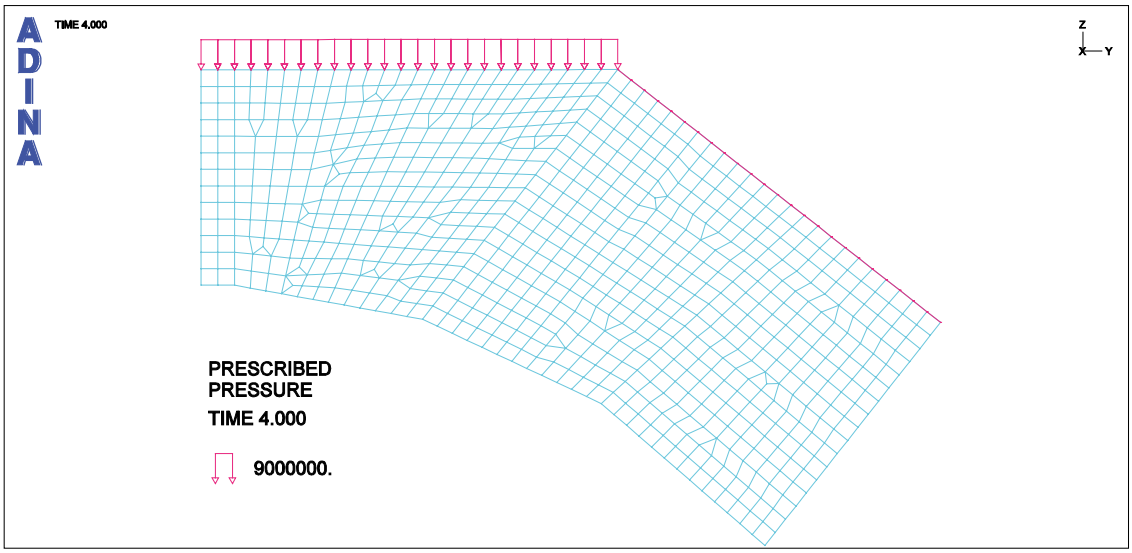

Figur B4-3. *Svälltryck och vattentryck för lastfall 4.*

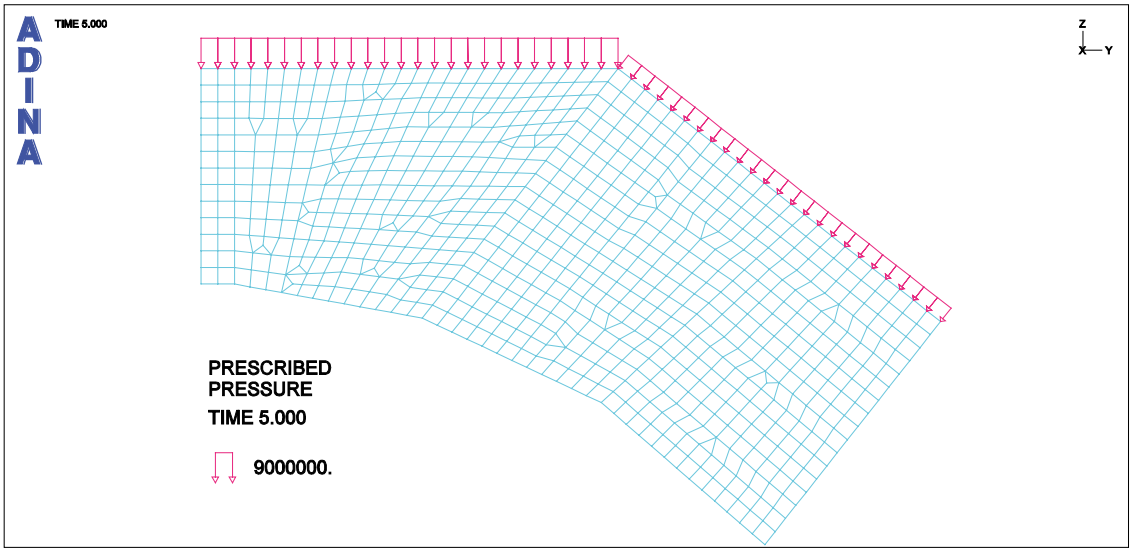

Figur B4-4. *Svälltryck och vattentryck för lastfall 5.*

B4.5 Reduktion av tvärsnittet

För att hitta en geometri som uppfyller tidigare ställda krav har pluggens spänningsfördelning i centrumsnittet undersökt. Ställda krav på maximalt tillåtna spänningar i pluggens centrumsnitt är -33 MPa $\leq \sigma_{c,top} \leq 0$ MPa. Detta krav gör att dragspänningar inte ska uppstår och maximala tryckspänningen i pluggen inte överskrider gränsen för linjärelastisk respons hos betongen.

Som framgår i avsnitt B3.2 har olika höjder på pluggens centrumsnitt och olika tjocklekar på pluggens infästning undersökts. De valda värdena för dess parametrar framgår av tabell B4-1.

Tabell B4-1. Undersökta geometrier vid tvärsnittsreduktion.

Centrumhöjd [m]	Infästningstjocklek [m]	Reduktion [m]
(0,9)		
1,1	2,11	0,0
1,3	1,91	0,2
1,5	1,71	0,4
1,7		

En första reglering av geometrin har gjorts där undersidan av pluggens mitt har slätats ut så att den i de två första elementraderna från symmetriaxeln är horisontell, se figur B4-5. Detta gjordes eftersom det noterades att en vinkel i pluggens undersida ger upphov till olämpliga spänningskoncentrationer i detta område. Eftersom spänningsfördelningen i just centrumsnittet har använts i jämförelsen mellan olika geometrier är det av extra vikt att spänningsfördelningen inte innehåller några koncentrationer som gör det svårt att uppskatta effekten av ändrad geometri.

Resultaten för analyserna med maximalt pålagd trycklast, 4 MPa svälltryck och 5 MPa vattentryck, tillsammans med lastfall 5 visas i figur B4-6 till figur B4-9. Spänningarna i centrumsnittets ovansida respektive undersida är sammanställda i figur B4-10.

Enligt resultaten presenterade i figur B4-10 kommer alla undersökta geometrier uppfylla ställda krav för lastfall 5 med maximal pålagd trycklast. Alla spänningar i pluggens centrumsnitt ligger inom intervallet $-33\ \text{MPa} \leq \sigma_c \leq 0\ \text{MPa}$.

Belastning av trycklaster (svällning och vatten) resulterar i en dragen undersida i pluggens centrumsnitt. Övriga laster (krympning och temperatur) ger dock en tryckt undersida i samma snitt. Trycklaster av vatten och svällning har således en gynnsam inverkan på spänningsfördelningen i centrumsnittet, vilket gör att det farligaste lastfallet utgörs av lastfall 5, men utan inverkan av yttre trycklast. Resultat för detta lastfall presenteras i figur B4-11 till figur B4-14. Normalspänningar i centrumsnittets ovankant och underkant är sammanställt i figur B4-15.

Av sammanställningen i figur B4-15 framgår att de tryckspänningar som uppstår i pluggens undersida är hanterbara, maximal tryckspänning understiger 37 MPa. På pluggens översida finns, beroende på vilken kombination som studeras, dock risk att dragspänningar uppstår i pluggens centrumlinje. För att säkerställa att genomgående sprickor inte riskerar uppstå är det önskvärt att undvika en lastkombination där dragspänningar uppstår i pluggens översida. Detta, kombinerat med låg betongvolym som ett önskat kriterium, medför att en tvärsnittshöjd på 1,3 meter i pluggens centrum och en yttre tjocklek på 1,91 meter, (0,2 meters reduktion), är den mest optimala reduceringen av tvärsnittet. Denna reducerade geometri illustreras i figur B4-16 och används i här fortsatta analyser.

Den totala volymen hos den ursprungliga pluggeometrin var ca 125 m^3. Reduktionen av pluggens centrumhöjd ger en ny pluggvolym på 117 m^3 och när även pluggens yttertjocklek reduceras fås en totalvolym på ca 107 m^3. Detta ger en total volymreduktion på ca 15 %.

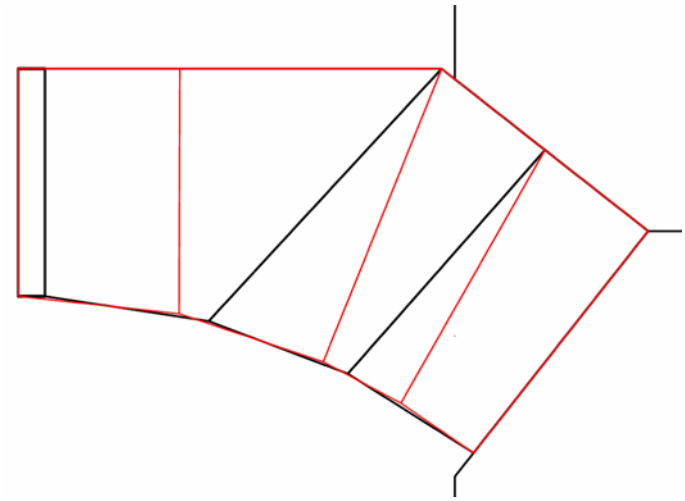

Figur B4-5. Reglering av pluggens geometri för att minska spänningskoncentrationer i centrumsnitt.

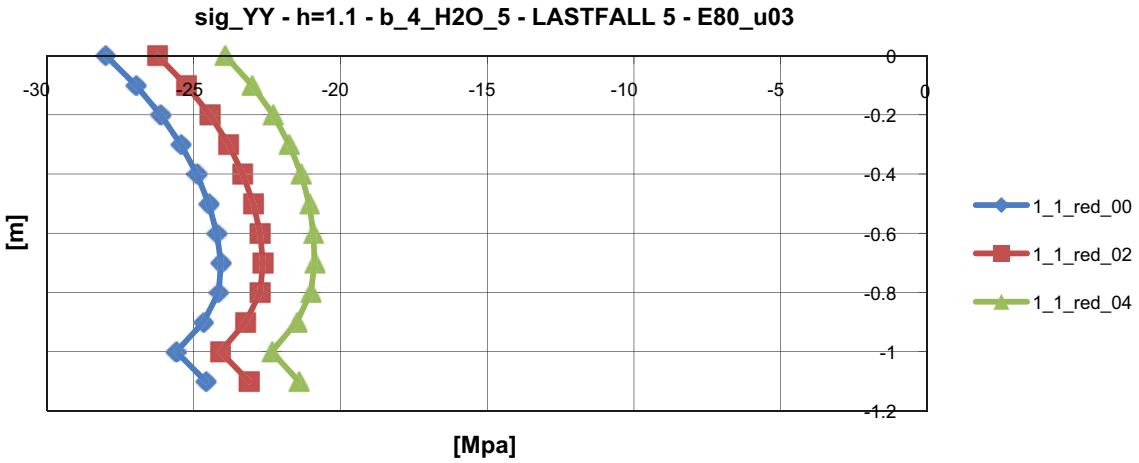

Figur B4-6. Normalspänningsfördelning i centrumsnitt för olika värden på pluggens yttertjocklek, maximal trycklast, centrumhöjd 1,1 m, nivå 0 motsvarar pluggens ovankant.

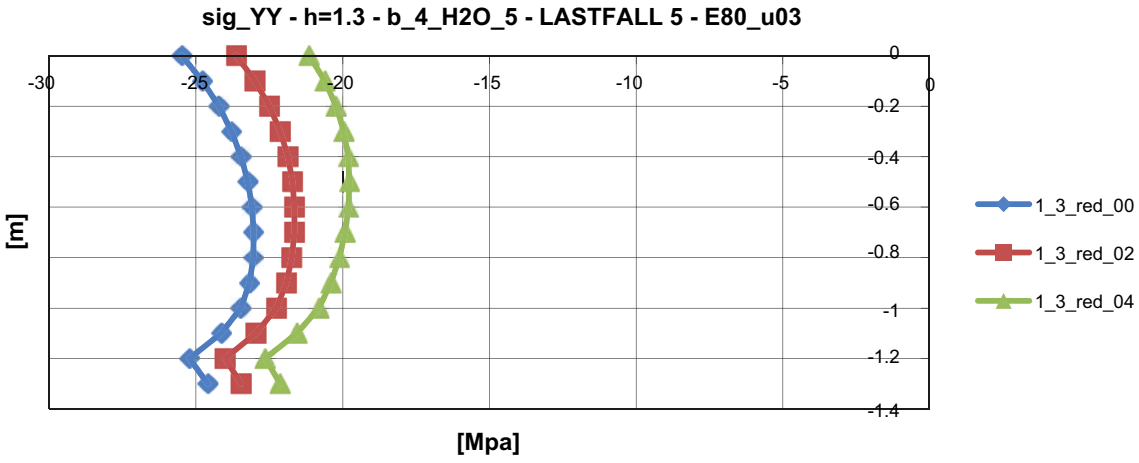

Figur B4-7. Normalspänningsfördelning i centrumsnitt för olika värden på pluggens yttertjocklek, maximal trycklast, centrumhöjd 1,3 m, nivå 0 motsvarar pluggens ovankant.

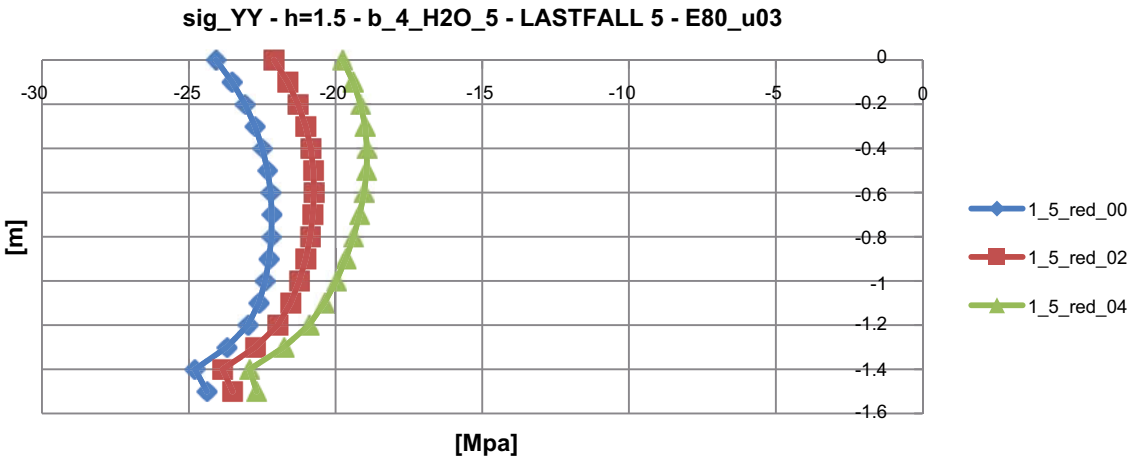

Figur B4-8. *Normalspänningsfördelning i centrumsnitt för olika värden på pluggens yttertjocklek, maximal trycklast, centrumhöjd 1,5 m, nivå 0 motsvarar pluggens ovankant.*

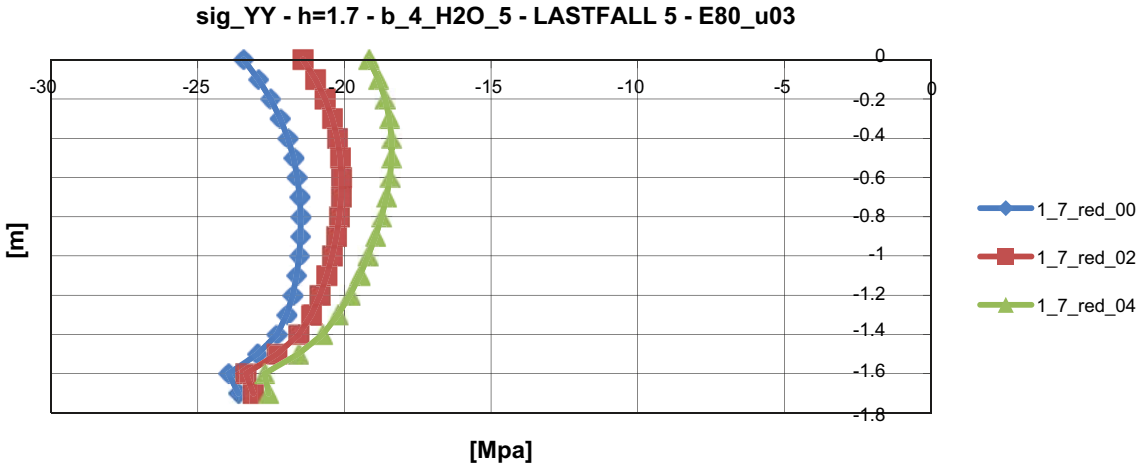

Figur B4-9. *Normalspänningsfördelning i centrumsnitt för olika värden på pluggens yttertjocklek, maximal trycklast, centrumhöjd 1,7 m, nivå 0 motsvarar pluggens ovankant.*

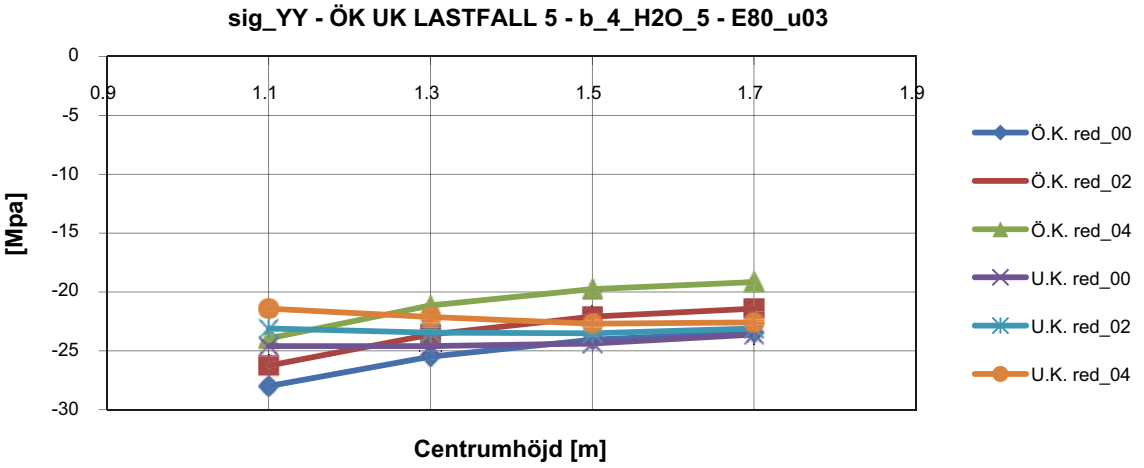

Figur B4-10. *Normalspänningar i överkant och underkant som funktion av centrumsnittets höjd för de undersökta yttertjocklek, maximal trycklast.*

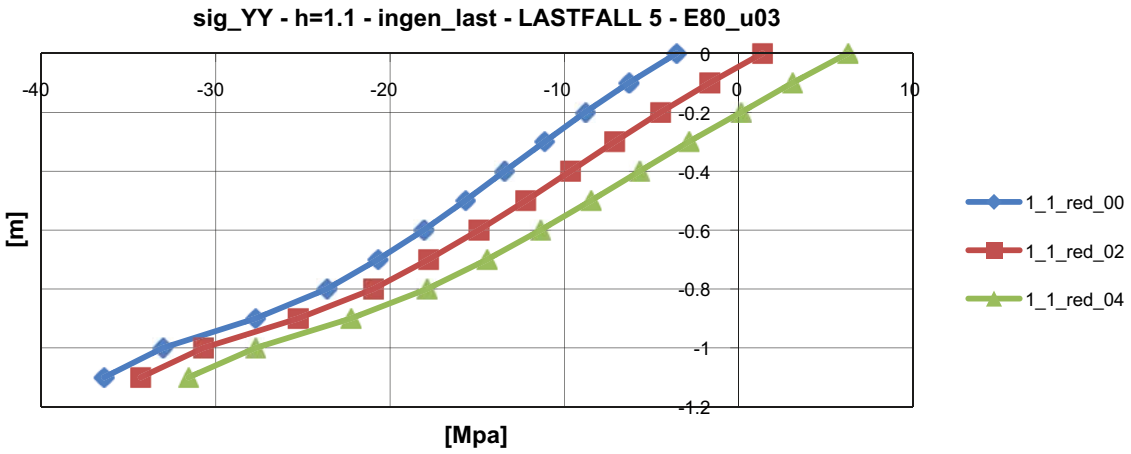

Figur B4-11. Normalspänningsfördelning i centrumsnitt för olika värden på pluggens yttertjocklek, ingen trycklast, centrumhöjd 1,1 m, nivå 0 motsvarar pluggens ovankant.

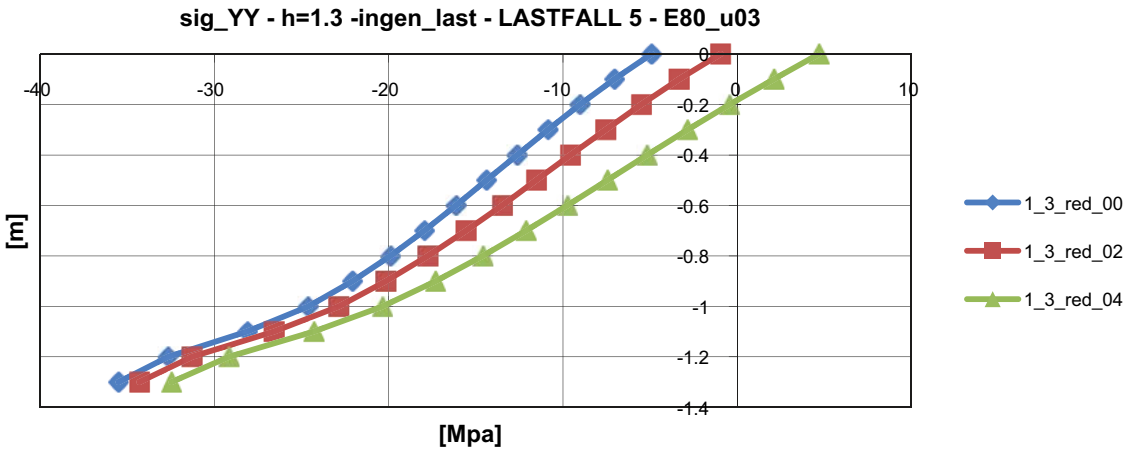

Figur B4-12. Normalspänningsfördelning i centrumsnitt för olika värden på pluggens yttertjocklek, ingen trycklast, centrumhöjd 1,3 m, nivå 0 motsvarar pluggens ovankant.

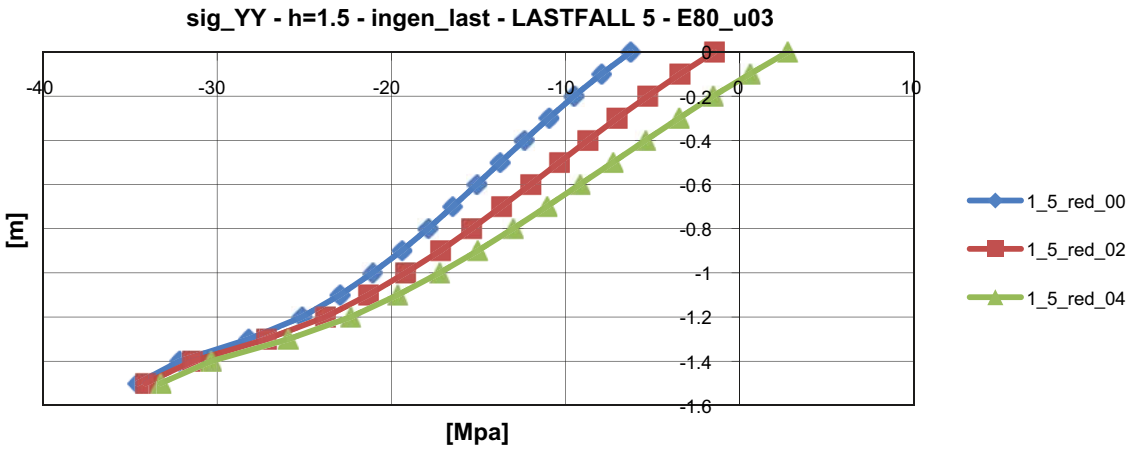

Figur B4-13. Normalspänningsfördelning i centrumsnitt för olika värden på pluggens yttertjocklek, ingen trycklast, centrumhöjd 1,5 m, nivå 0 motsvarar pluggens ovankant.

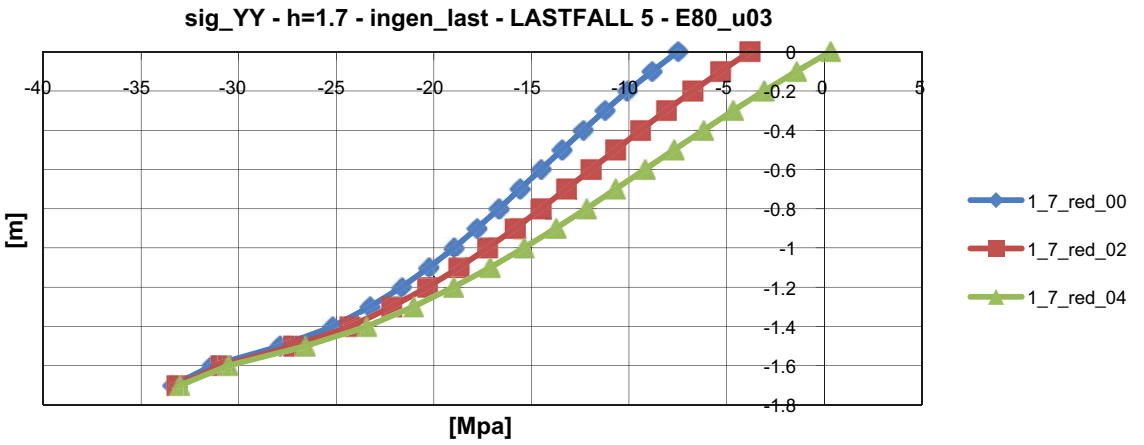

Figur B4-14. *Normalspänningsfördelning i centrumsnitt för olika värden på pluggens yttertjocklek, ingen trycklast, centrumhöjd 1,7 m, nivå 0 motsvarar pluggens ovankant.*

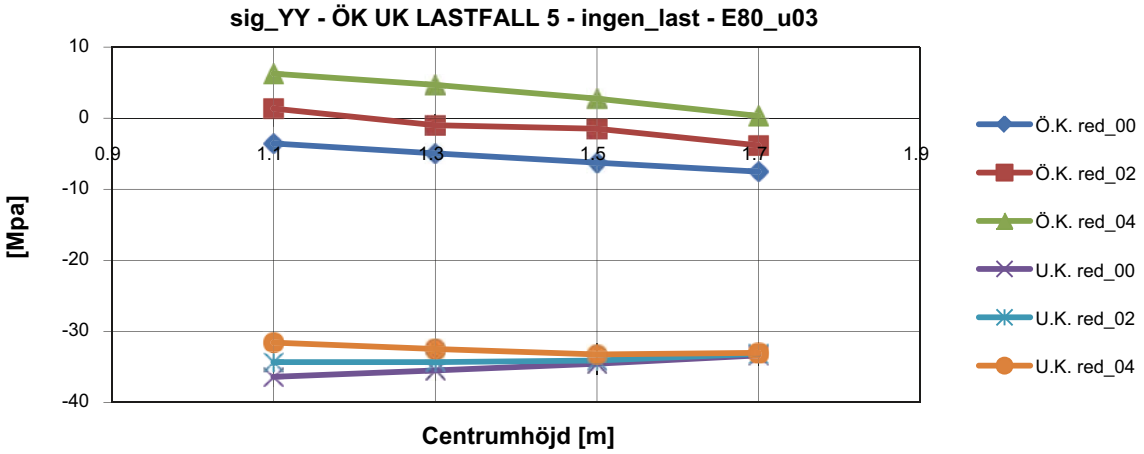

Figur B4-15. *Normalspänningar i överkant och underkant som funktion av centrumsnittets höjd för de undersökta yttertjocklek, ingen trycklast.*

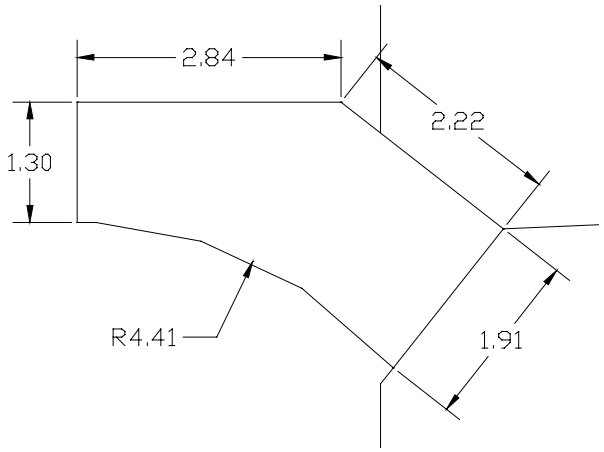

Figur B4-16. *Reducerad geometri för fortsatta analyser.*

B5 Olinjära analyser av ny pluggeometri

B5.1 Studerad geometri

I detta kapitel redovisade analyser baseras på geometri enligt figur B4-16 samt material- och lastdata enligt avsnitt B3.2.

B5.2 Benämning och riktningar för sprickor och spänningar

När det diskuteras sprickor och deras uppkomst i betongpluggen är följande sprickor aktuella:

- **Tangentiella sprickor:** Uppkommer till följd av radiella spänningar (spänningar parallella med pluggens radie).
- **Radiella sprickor:** Uppkommer till följd av tangentiella spänningar eller ringspänningar, (spänningar vinkelräta pluggens radie).

Sprickornas utbredning illustreras i figur B5-1. I praktiken är det framförallt radiella sprickor som uppkommer av tangentiella spänningar som är avgörande för pluggens respons eftersom dessa spänningar ökar snabbast. När radiella sprickor uppkommer avlastas även spänningarna i radiella riktningen så att uppkomsten av tangentiella sprickor begränsas.

B5.3 Materialsamband

Tre materialsamband har diskuterats för betongpluggen. Karakteristiska draghållfasthetsvärden, dimensionerande draghållfasthetsvärden samt dimensionerande draghållfasthetsvärden med en spricksäkerhetsfaktor lika med 2,0. Brottenergin är vald till 100 N/m för karakteristiska materialvärden. Brottenergin för de andra materialsambanden är anpassade på ett sådant sätt att den totala töjningen när sprickan är fullt öppen är densamma för alla materialsamband, se tabell B5-1 och figur B5-2.

Tabell B5-1. Indata för materialsamband med avseende på dragspänningar.

	Draghållfasthet [MPa]	Brottenergi [N/m]	ξ
Modell 1	2,9	100	12,7
Modell 2	1,6	55,6	22,9
Modell 3	0,8	27,8	45,7

Parametern ξ beräknas enligt ekvation (B5-1) med elasticitetsmodul E_c = 26,7 GPa och elementlängden som integrationspunkternas arbetslängd, $l_{el}/2$ då element med 4 integrationspunkter används.

$$\xi = \frac{2 \cdot G_F \cdot E_c}{f_{ct}^2 \cdot l_{el}} \qquad \text{(B5-1)}$$

Indata för betongens spruckna respons är således elementnätsberoende, dvs. endast aktuellt för en specifik elementlängd. I modellen används $l_{el} \approx 0{,}1$ m. Elementnätet hos nyttjad modell har dock en sådan utformning att inget element har en större längd än 0,1 m. Därav följer att det exakta värdet av parametern ξ används, alternativt ett konservativt värde, när $l_{el} < 0{,}1$ m.

Den sprickmodell som används i FE-programmet ADINA är en utsmetad sprickmodell med fixerade sprickor som kan uppstå ortogonalt mot redan förekommande sprickor. För att undvika numeriska problem har i analyserna angivits en hög tryckhållfasthet, innebärande att betongens respons i tryck varit linjärelastisk. Denna approximation utgör en avvikelse mot verklig arbetskurva hos betongen men bedöms i sammanhangen vara en tillräckligt god approximation.

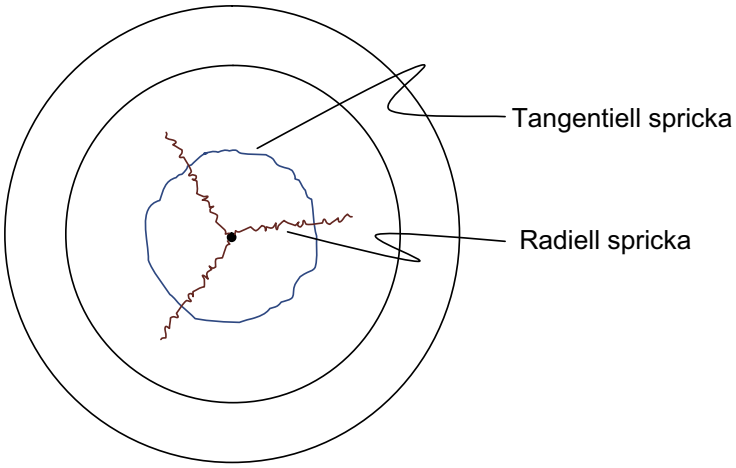

Figur B5-1. *Illustration av tangentiella och radiella sprickor.*

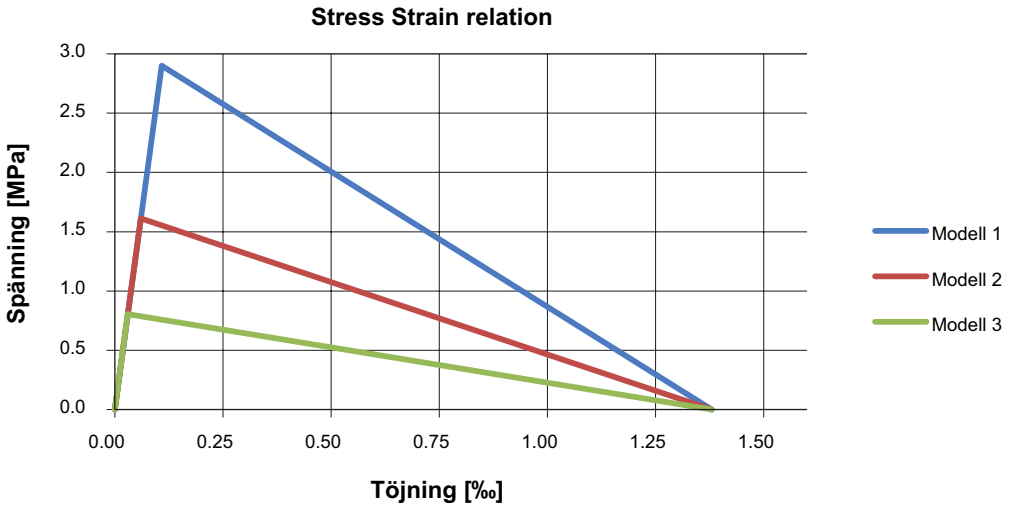

Figur B5-2. *Spänning-töjningsdiagram för dragen betong i studerade materialsamband. I här utförda analyser har modell 1 eller modell 3 använts.*

B5.4 Lastfall 4.2

Lastfall 4.2, avsnitt B3.2, är det mest kritiska lastfallet med hänsyn till böjning och uppsprickning av pluggens undersida. Lasten appliceras endast på pluggens ovansida eftersom last längs med pluggens sidokant har positiv inverkan på responsen. Pluggens respons undersöks för materialsamband 1 och materialsamband 3 enligt kapitel B5.3. Sammanställning av pluggens respons med hänsyn till sprickförloppet för de två materialsambanden visas i tabell B5-2. Efterföljande figurer visar sprickbilder för respektive fall beskrivet i tabell B5-2 samt sprickbilder vid 10 MPa trycklast och full temperaturlast pålagd. Temperaturlasten appliceras mellan tiden 10 och 11. Under denna period är trycklasten på pluggen oförändrad för att sedan ökas efter att full temperaturlast är applicerad.

En känslighetsanalys har utförts för olika kombinationer av när trycklast respektive temperaturlast appliceras på pluggen. Analyserna visar att den slutliga maximala tryckspänningen blir relativt lika oavsett när temperaturen läggs på, 27,3 MPa respektive 28,4 MPa, se figur B5-3.

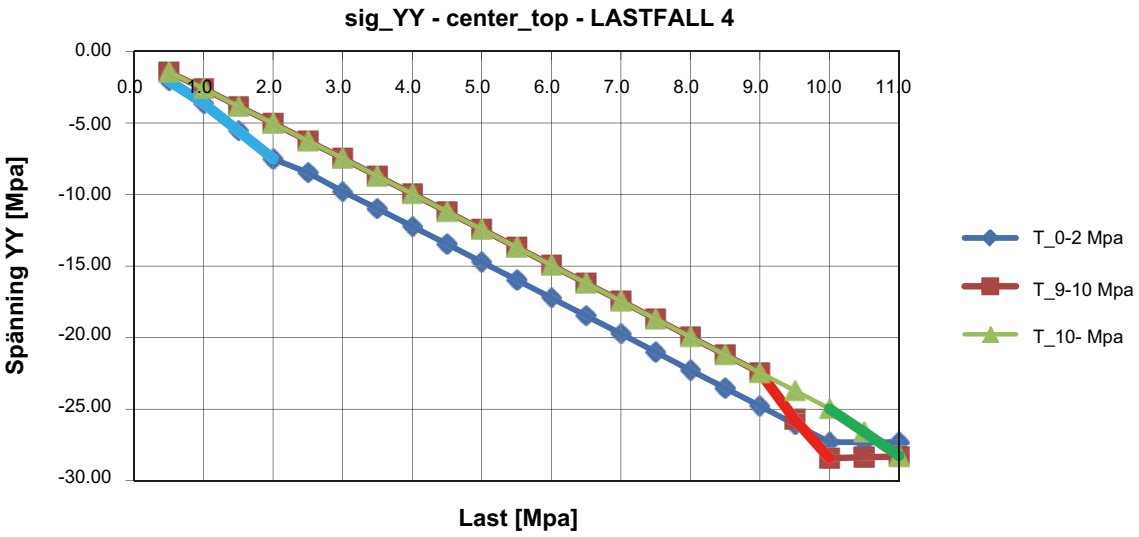

Figur B5-3. *Känslighetsanalys av effekt på maximal tryckspänning på översida pluggens centrumlinje när trycklast av vatten och svällning appliceras under tiden 0–10 men med varierande tidpunkt på temperaturens applicering.*

Tabell B5-2. Sammanställning av sprickförlopp för materialsamband 1 och 3. Spänningsvärden anger aktuell trycklast av vatten och svällning som applicerats på pluggen vid givet tillfälle.

Beskrivning	Materialsamband 1	Hänvisning	Materialsamband 3	Hänvisning
Första sprickan	R + (T) ½ element 3 MPa	Figur B5-4	R + (T) ½ element 1 MPa	Figur B5-5
Helt element sprucket	4,5 MPa	Figur B5-6	1,5 MPa	Figur B5-7
Första indikation på skjuvspricka	21 MPa	Figur B5-8	7,5 MPa	Figur B5-9
Fullt öppen skjuvspricka	21,5 MPa	Figur B5-10	10 MPa och halva temperatur-lasten (2 intilliggande sprickor)	Figur B5-11

Vid en trycklast på över 12 MPa överstiger tryckspänningarna i centrumsnittets översida de 33 MPa som ställts upp som kriterium för linjärelastisk respons hos betongen. I FE-analyserna beaktas dock inte detta eftersom trycksidan modellerats linjerelastiskt, se avsnitt B5.3. För en trycklast på 21 MPa fås, för materialsamband 1, en maximal tryckspänning i centrumsnittet på 58 MPa. Denna spänningsnivå är visserligen högre än uppställt kriterium på tillåten spänning men bedöms, med hänsyn till tredimensionella inneslutningseffekter samt möjlig hållfasthetsökning på grund av betongens åldring, ändå inte vara kritiskt i sammanhanget.

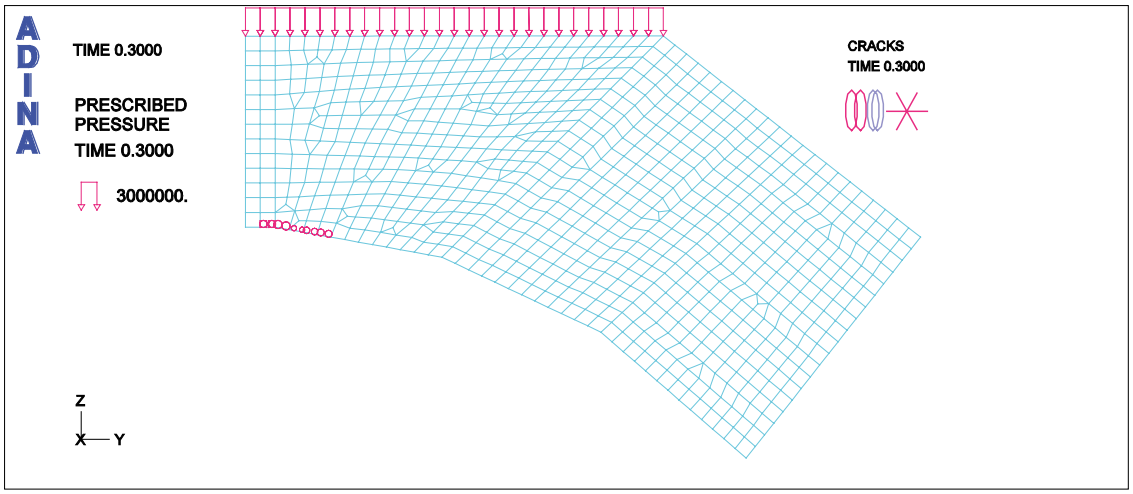

Figur B5-4. *3 MPa tryck på pluggens ovansida. Första sprickindikationerna för materialsamband 1, radiella sprickor samt någon enstaka tangentiell spricka.*

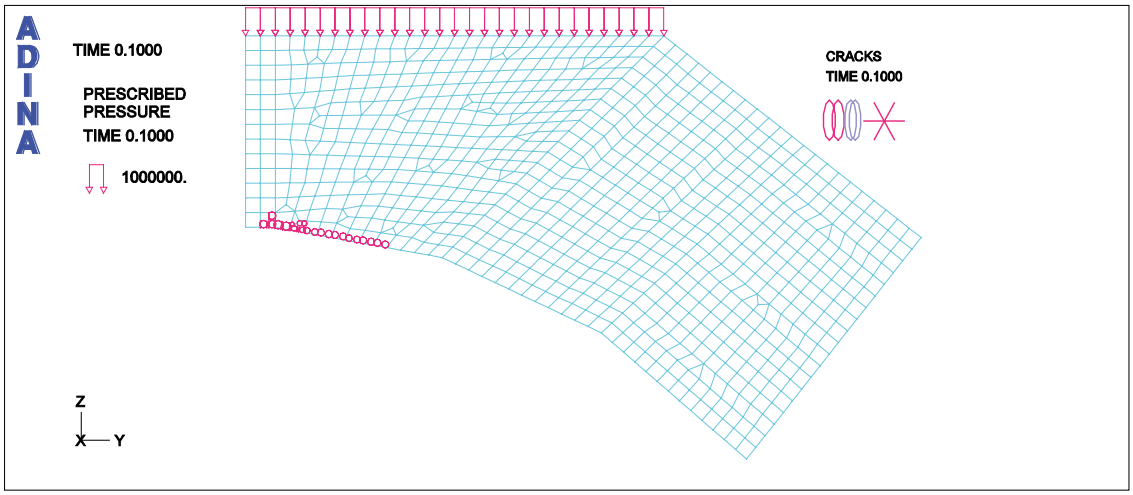

Figur B5-5. *1 MPa tryck på pluggens ovansida. Första sprickindikationerna för materialsamband 3, radiella sprickor samt någon enstaka tangentiell spricka.*

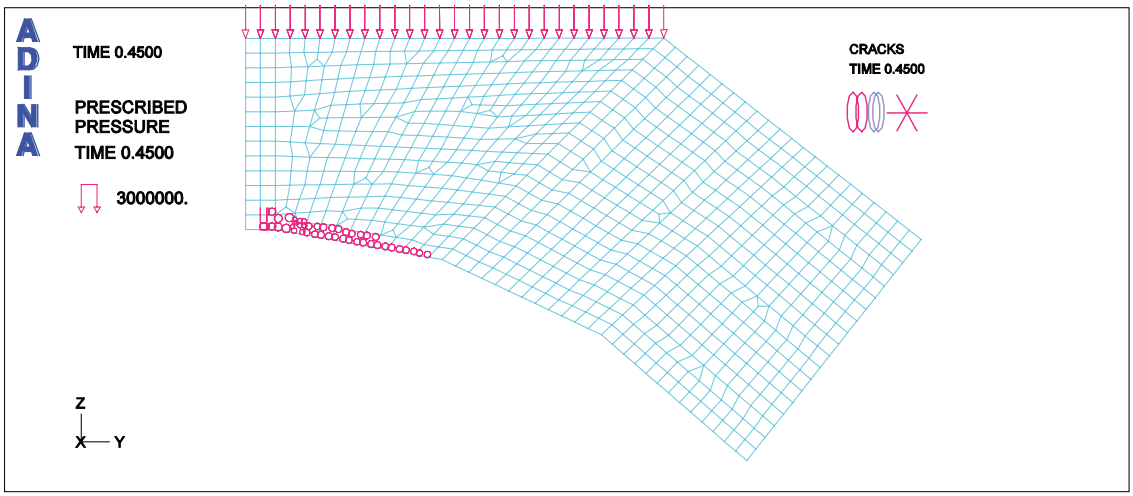

Figur B5-6. *4,5 MPa tryck på pluggens ovansida. Första hela elementet med sprickor materialsamband 1.*

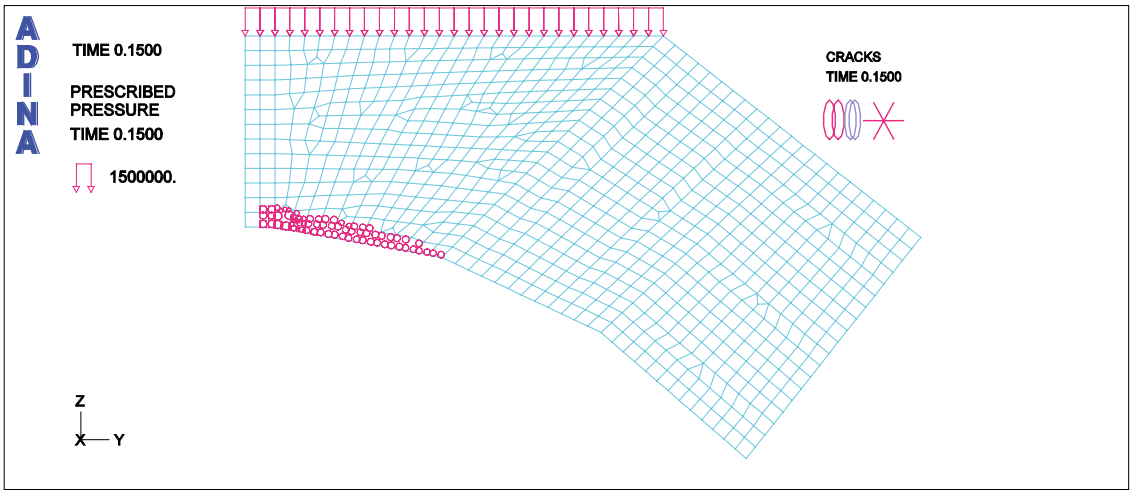

Figur B5-7. *1,5 MPa tryck på pluggens ovansida. Första hela elementet med sprickor materialsamband 3.*

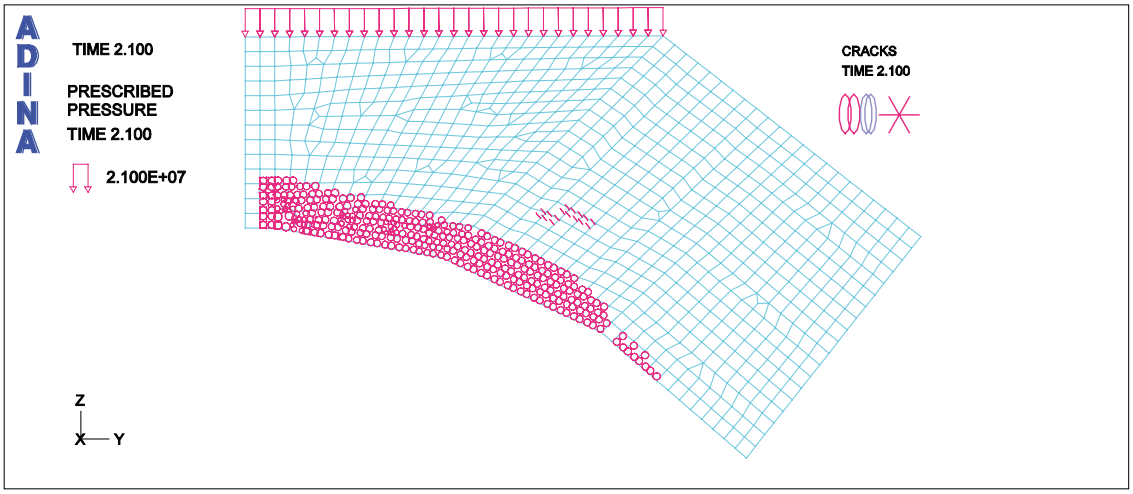

Figur B5-8. *21 MPa tryck på pluggens ovansida, hela temperaturlasten applicerad. Första indikationen på skjuvspricka materialsamband 1.*

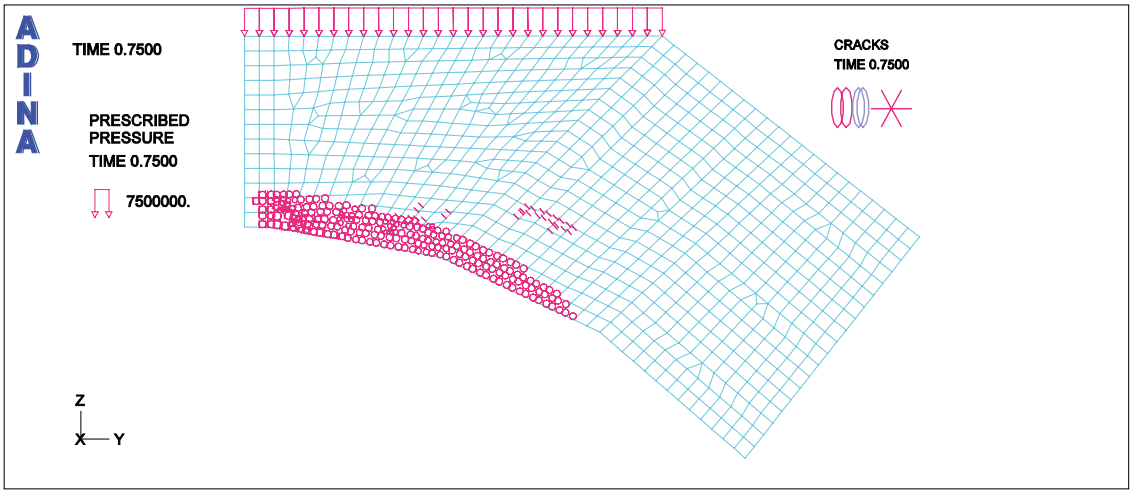

Figur B5-9. *7,5 MPa tryck på pluggens ovansida. Första indikationen på skjuvspricka materialsamband 3.*

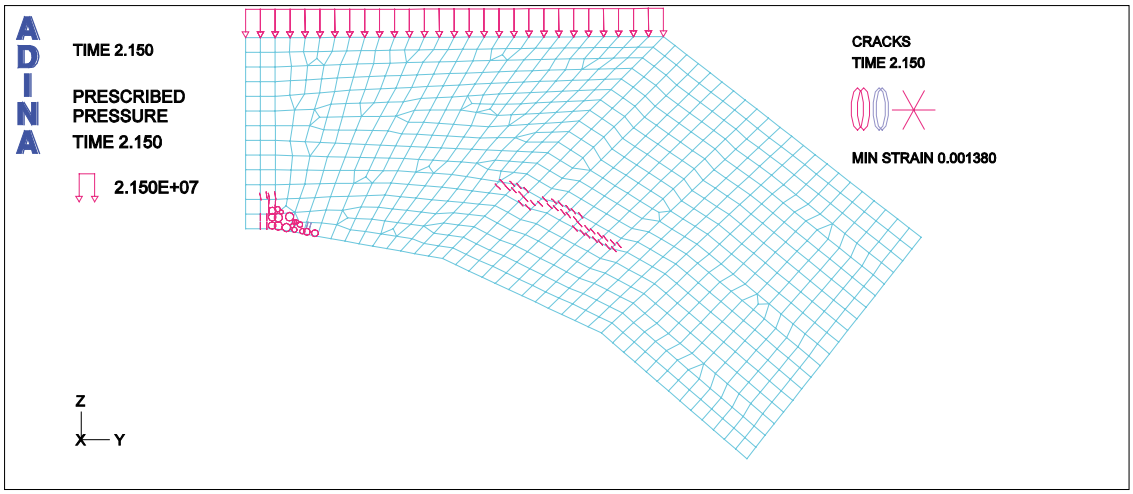

Figur B5-10. *21,5 MPa tryck på pluggens ovansida, hela temperaturlasten applicerad. Fullt öppen skjuvspricka för materialsamband 1.*

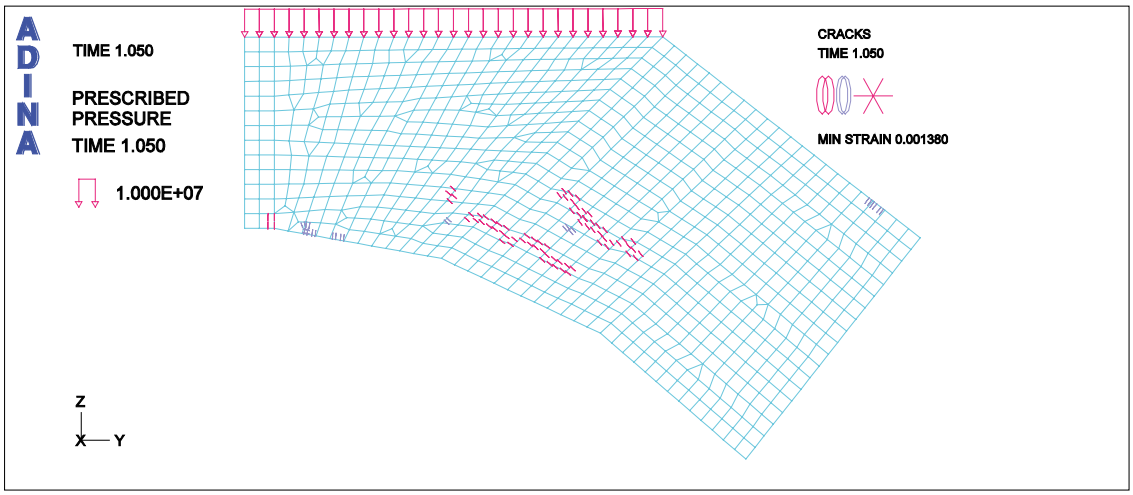

Figur B5-11. *10 MPa tryck på pluggens ovansida, halva temperaturlasten pålagd. Fullt öppen skjuvspricka för materialsamband 3.*

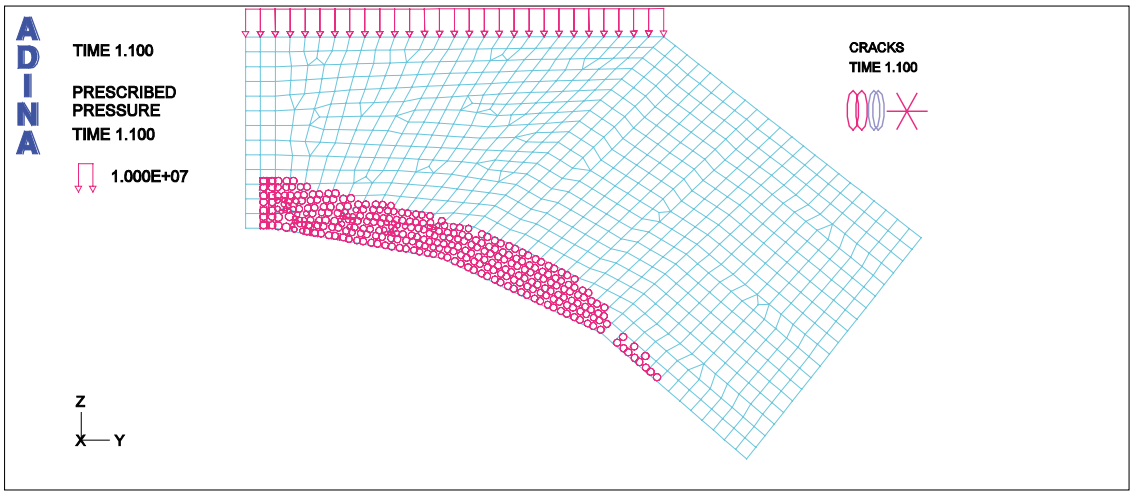

Figur B5-12. *10 MPa tryck på pluggens ovansida, hela temperaturlasten pålagd. Sprickbild för initierade sprickor för materialsamband 1.*

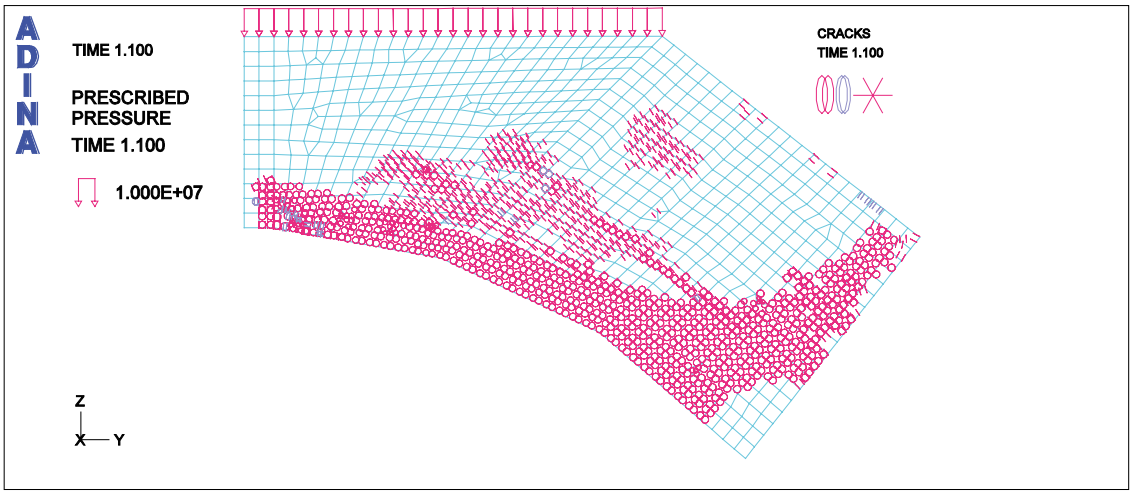

Figur B5-13. *10 MPa tryck på pluggens ovansida, hela temperaturlasten pålagd. Sprickbild för initierade sprickor för materialsamband 3.*

B5.5 Lastfall 5.5

Lastfall 5.5 är det fall när pluggen utsätts för störst tvångskrafter till följd av liten krympning i pluggen samt stor temperaturutveckling i berget, se avsnitt B4.2. För materialsamband 1 uppstår endast sprickor i betongen vid kontakten mellan plugg och berg på ovansidan av pluggen, se figur B5-14. Dessa sprickor uppstår pga. den lokala spänningskoncentration som uppkommer i denna punkt. Denna spricka utvidgas inte vidare efter uppkomst. I övrigt finns inga sprickindikationer för detta materialsamband för det aktuella lastfallet.

För materialsamband 3 når denna sprickindikering dock djupare ner i pluggen, se figur B5-15. Den avgörande sprickan som uppkommer är dock en skjuvspricka som får hela pluggens ovansida att skjuvas av, se figur B5-16 till figur B5-18. Denna skjuvspricka uppkommer när 62 % av temperaturlasten applicerats och utvecklas till fullt öppen spricka omedelbart efter uppkomst, se figur B5-16. Sprickbilden för pluggen vid 100 % applicerad temperaturlast visas i figur B5-17 och figur B5-18 för initierade respektive fullt öppna sprickor.

Uppkomsten av denna skjuvspricka beror på hålrummet mellan pluggens ovankant och utskärningen i berget, se figur B5-19. Genom att modifiera bergets geometri så detta hålrum avlägsnas fås gynnsammare randvillkor för pluggen, varvid skjuvsprickan i figur B5-18 inte längre uppstår vid användande av materialsamband 3, se figur B5-20. Denna ändring av pluggens kontakt med berget påverkar även spänningsbilden i pluggens centrumsnitt, se figur B5-21.

Av figur B5-21 framgår att den resulterande dragspänningen i pluggens översida i centrumsnittet påverkas starkt av hur anliggningen mellan berg och plugg ser ut. I kapitel B4 används lastfall 5 för att bestämma hur mycket av pluggens centrumhöjd som kan reduceras. Utifrån jämförelse i figur B5-21 kan det därför konkluderas att utformningen av kopplingen mellan berg och plugg är viktigt för hur mycket höjd i centrumsnittet som kan reduceras. Det finns således en eventuell möjlighet att reducera centrumhöjden ytterligare om koppling mellan berg och plugg utförs mer optimalt.

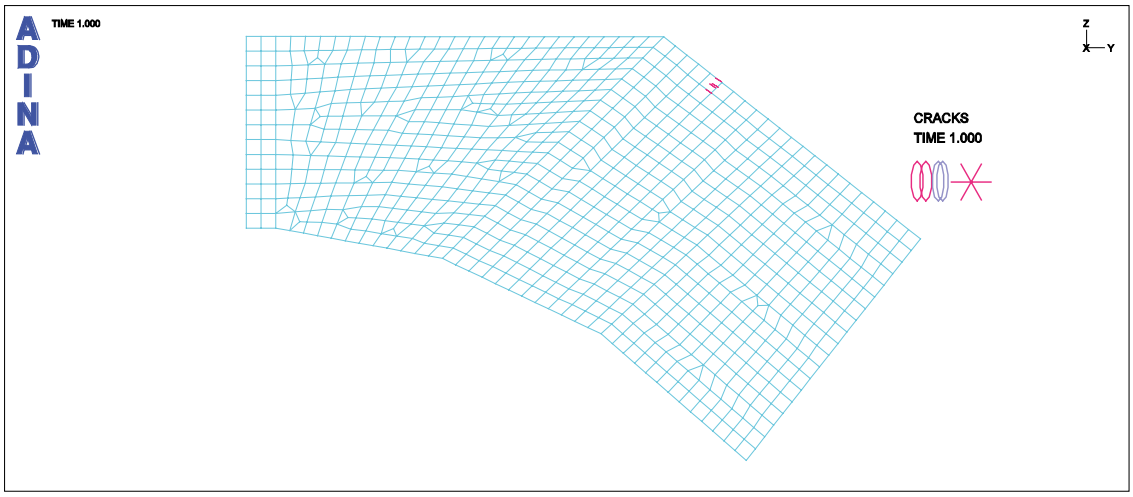

Figur B5-14. *100 % av temperaturlasten pålagd, materialsamband 1.*

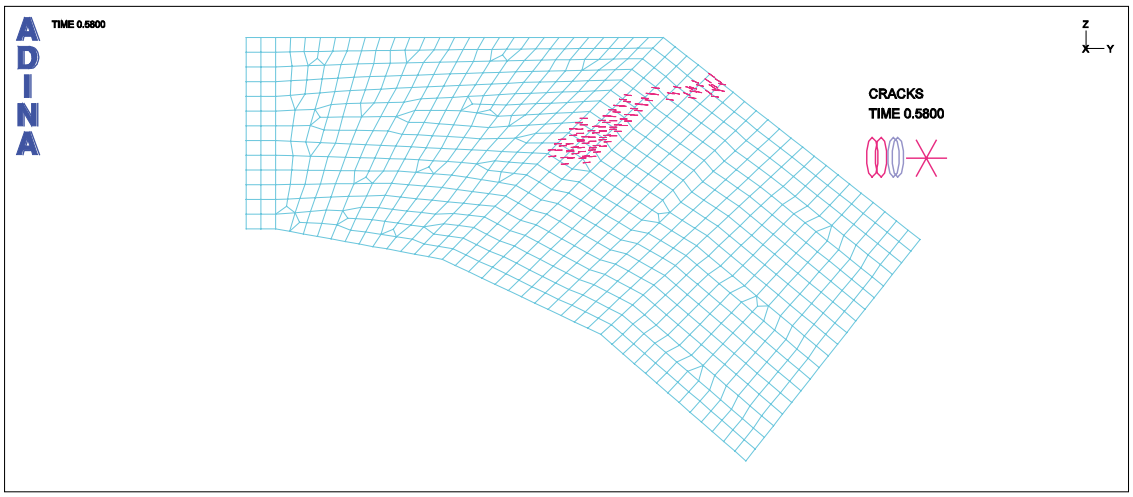

Figur B5-15. *58 % av temperaturlasten pålagd, initierade sprickor. Första indikationen av denna spricka fås vid 50 % applicerad temperaturlast, materialsamband 3.*

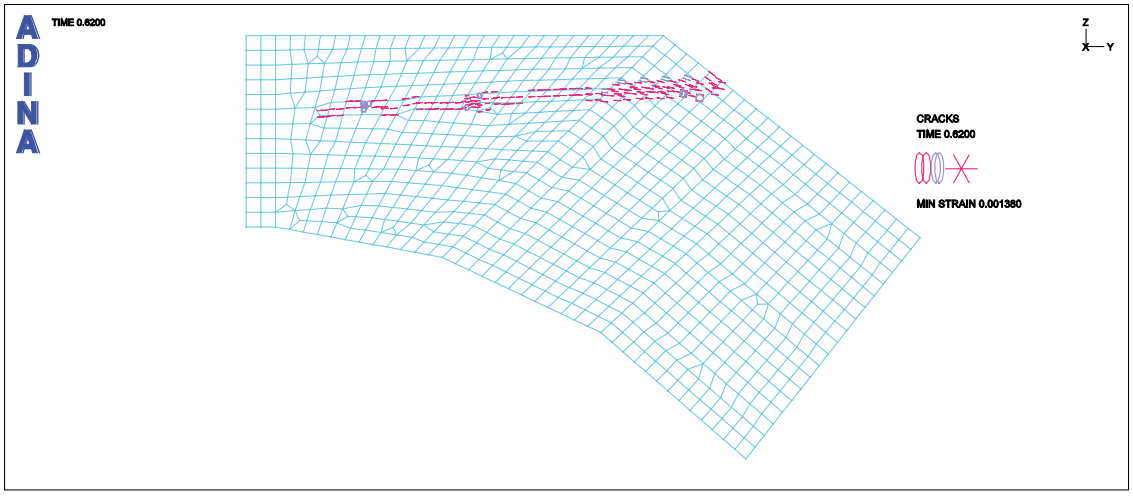

Figur B5-16. *Uppkomst av skjuvspricka vid 62 % applicerad temperaturlast. Sprickan utvecklas till fullt öppen spricka omedelbart efter uppkomst, materialsamband 3.*

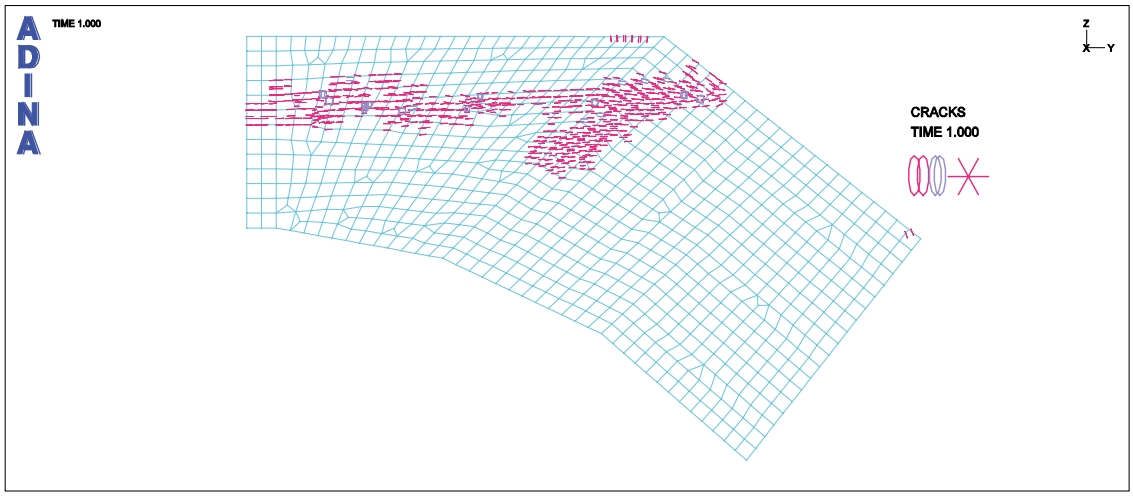

Figur B5-17. *Initierade sprickor vid 100 % applicerad temperaturlast, materialsamband 3.*

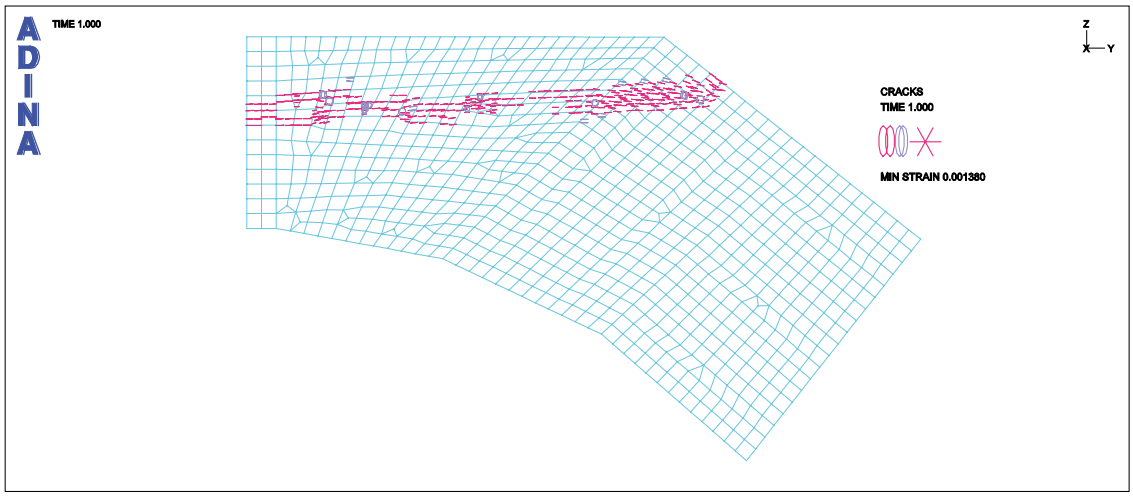

Figur B5-18. *Fullt öppna sprickor vid 100 % applicerad temperaturlast, materialsamband 3.*

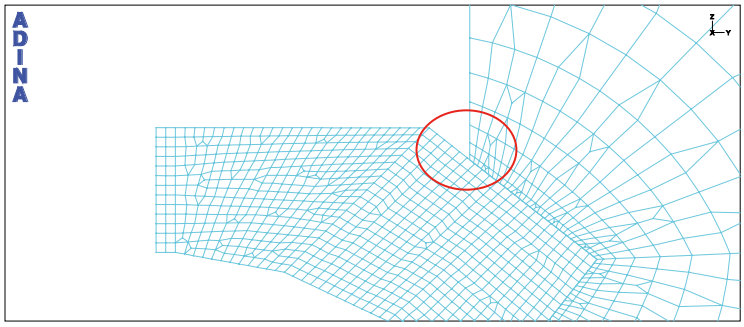

Figur B5-19. *Kritisk kant för pluggen med hänsyn till skjuvspricka.*

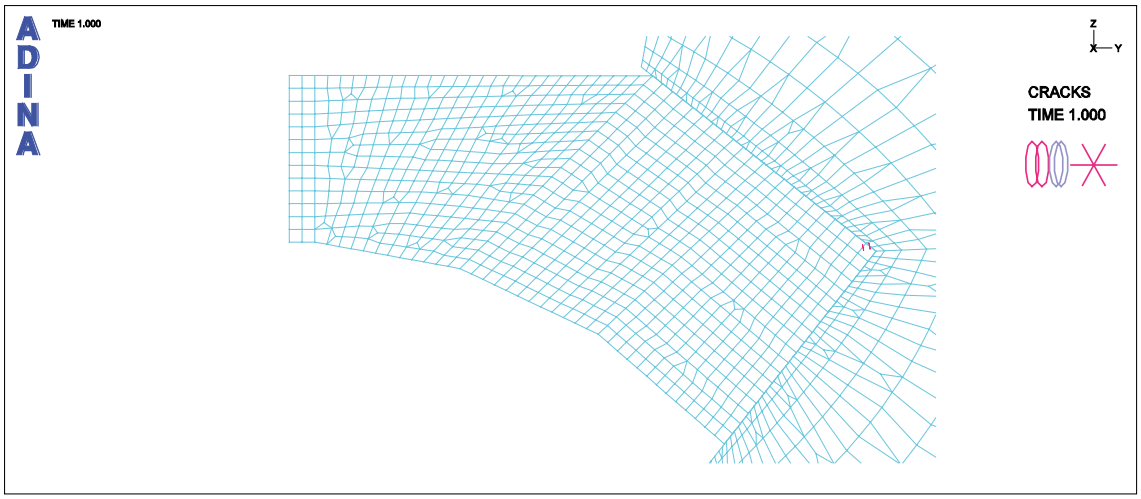

Figur B5-20. *Sprickor vid 100 % temperaturlasten applicerad då pluggen sidor har kontakt med berget.*

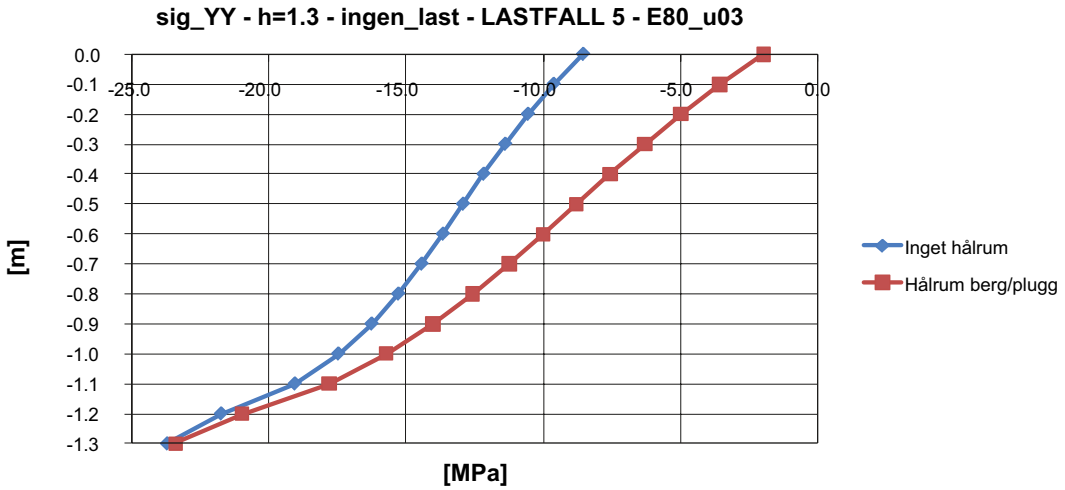

Figur B5-21. *Normalspänningsfördelning i centrumsnitt för de två inspänningsförhållandena mot berget, ingen trycklast, centrumhöjd 1,3 m, nivå 0 motsvarar pluggens ovankant.*

B6 Superponering av laster och 3-dimensionell modell för analys av osymmetriska laster

B6.1 Geometri och material

I detta kapitel redovisade analyser baseras på geometri enligt figur B3-1 samt material- och lastdata enligt avsnitt B3.2. Studerad pluggeometri är således inte identisk med den som används i kapitel B4 och B5 men skillnaden bedöms vara sådan att här dragna slutsatser bedöms vara giltiga även för reducerad geometri enligt figur B4-16.

Analyserna är utförda med linjärelastiska materialegenskaper för betong och berg och olinjära kontaktytor mellan betong och berg.

B6.2 Osymmetrisk belastning

Tidigare modeller i detta PM samt i R-09-34 har byggt på lastfall som verkat symmetriskt över pluggens yta. Diskussioner har dock förts huruvida osymmetrisk påläggning av svälltryck och vattentryck skulle kunna vara speciellt kritiskt för en i detta fall oarmerad konstruktion.

För att utvärdera osymmetriska laster kan dock inte tidigare använda axialsymmetriska modeller användas. För osymmetriska laster har därför en 3-dimensionell modell används där halva pluggens geometri modelleras, se figur B6-1.

De laster som har utvärderats i denna modell är svälltryck där halva ovansidan av pluggen är utsatt för ett svälltryck medan den andra halvan av pluggen är obelastad, se figur B6-2. Ett annat möjligt lastfall är osymmetriskt verkande vattentryck, se figur B6-3. Detta lastfall innebär att vattentrycket är osymmetriskt genom att det i vissa delar av pluggen verkar i slitsen och andra inte, jämför lastfall 1a och 1b i figur B3-2.

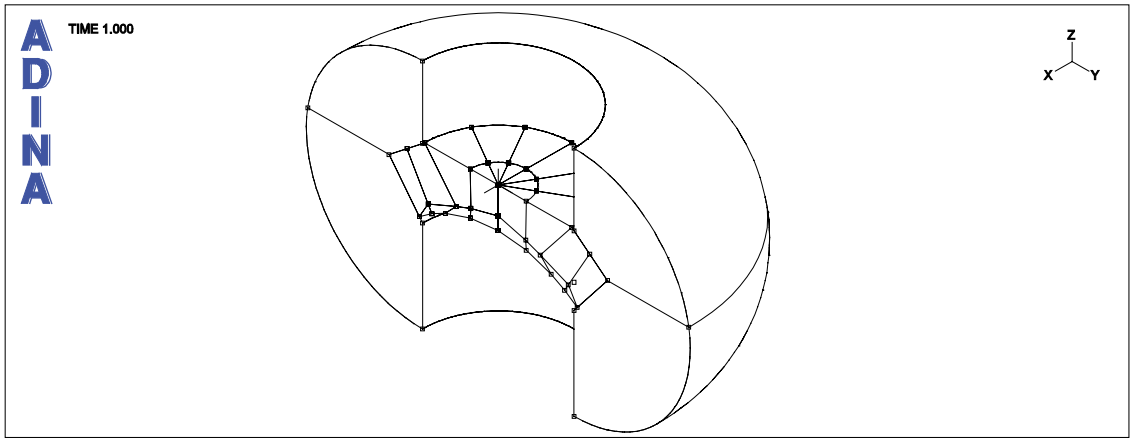

Figur B6-1. *3-dimensionell modell för utvärdering av osymmetriska laster.*

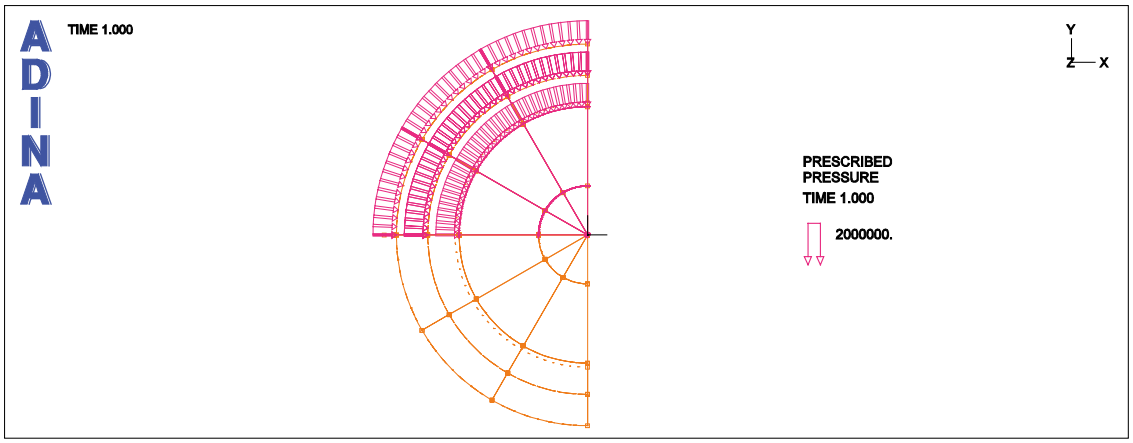

Figur B6-2. *Osymmetrisk last för svälltryck, 2 MPa.*

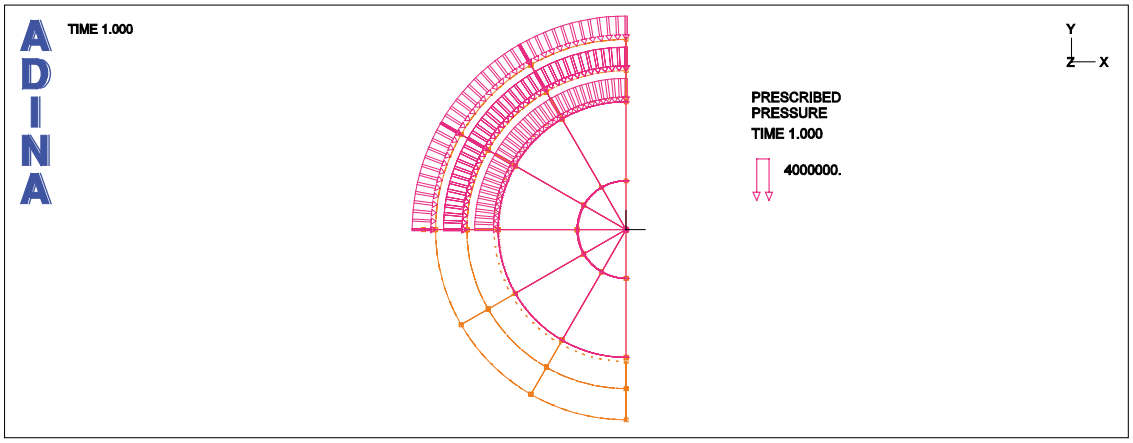

Figur B6-3. *Osymmetrisk last för vattentryck, 4 MPa.*

B6.3 Superpositionering av laster

B6.3.1 Superponering av 2D-modell

Tidigare resonemang om superponering av laster har varit att en direkt summering av laster och resultat inte är möjlig pga. den olinjära responsen hos kontaktytorna. Utförda analyser visar dock att det framförallt är temperaturens inverkan på spänningar i konstruktionen som inte går att uppskatta om endast temperaturlasten på pluggen utvärderas utan pålagd trycklast. I ett sådant fall kan pluggen röra sig fritt vid påläggning av temperaturen eftersom det inte uppstår några reaktionskrafter i kontaktytorna när någon trycklast inte är närvarande. Någon typ av superponeringsunderlag är ändå av intresse för att grovt bedöma effekter av olika laster. Nyttjade modellers känslighet vid superponering har därför utvärderats.

Första superponeringsjämförelsen har gjorts för den 2-dimesionella modellen, där effekten av superponering av trycklaster jämförs. Pluggen har här belastats med en trycklast på 2 MPa. Resulterande spänningar i pluggens centrumlinje har multiplicerats med en faktor 5 och jämförts med analysresultat för 10 MPa trycklast, se figur B6-4.

Från dessa jämförelser går det att dra slutsatsen att superponering av normalspänningar i centrumlinjen, orsakade av trycklaster, fungerar relativt bra. I undre delen av pluggen avviker de superponerade spänningarna från de verkliga spänningarna men eftersom det i regel kommer att vara tryckspänningarnas värde i ovankant av pluggen som är av störst intresse är det möjligt att använda superponering av trycklast som en approximation för konceptuell diskussion av pluggens strukturella respons.

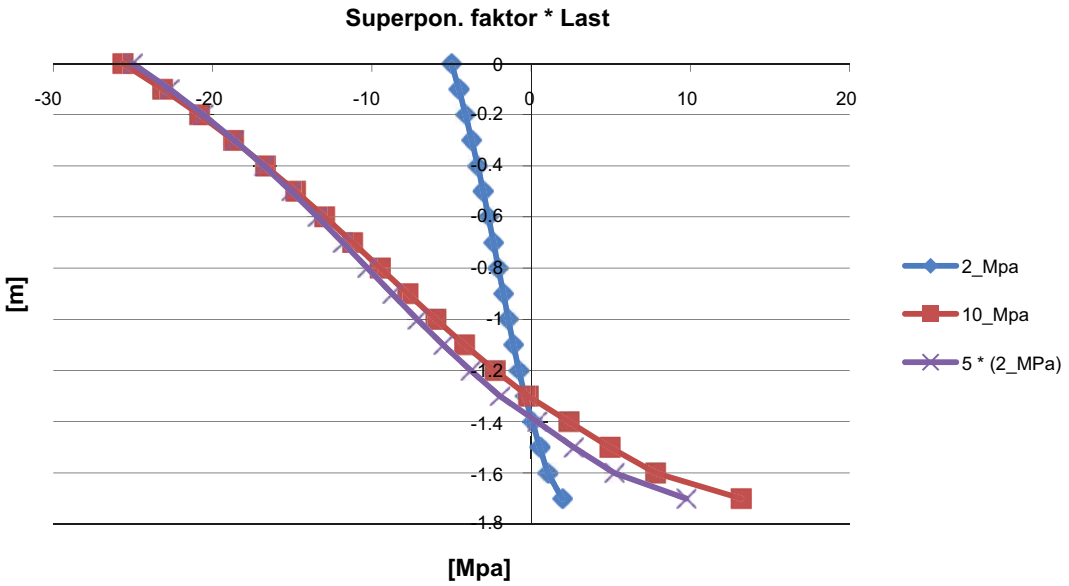

Figur B6-4. *Superponering av trycklast för 2D-modell, 2 MPa, 10 MPa och 5*2MPa.*

För att få en korrekt påverkan av temperaturen krävs att någon typ av tryckkraft skapar tillräcklig friktion så att pluggens rörelse, pga. temperaturlasten, förhindras. Ett fall där 2 MPa trycklast på pluggens ovansida verkar tillsammans med temperaturlast har undersökts för att se om en sådan last är tillräcklig för att fånga temperaturens effekt på pluggen.

Normalspänningar i pluggens centrumsnitt har undersökts för temperaturlast tillsammans med 10 MPa trycklast. Normalspänningarna har jämförts för ett superponerat lastfall bestående av 2 MPa trycklast tillsammans med temperaturlast och ett fall med 8 MPa trycklast utan temperaturlast, se figur B6-5.

Superponeringen i figur B6-5 visar att temperaturens effekt på normalspänningarna fångas relativt bra om temperaturen kombineras med en trycklast på 2 MPa – på samma sätt som i figur B6-4 är det framförallt eventuella tryckspänningar i pluggens översida som är av intresse. Av detta kan konstateras att 2 MPa trycklast tycks därför vara tillräkligt för att bygga upp den friktion i kontaktytorna som krävs för att fånga temperaturens effekt på centrumsnittet.

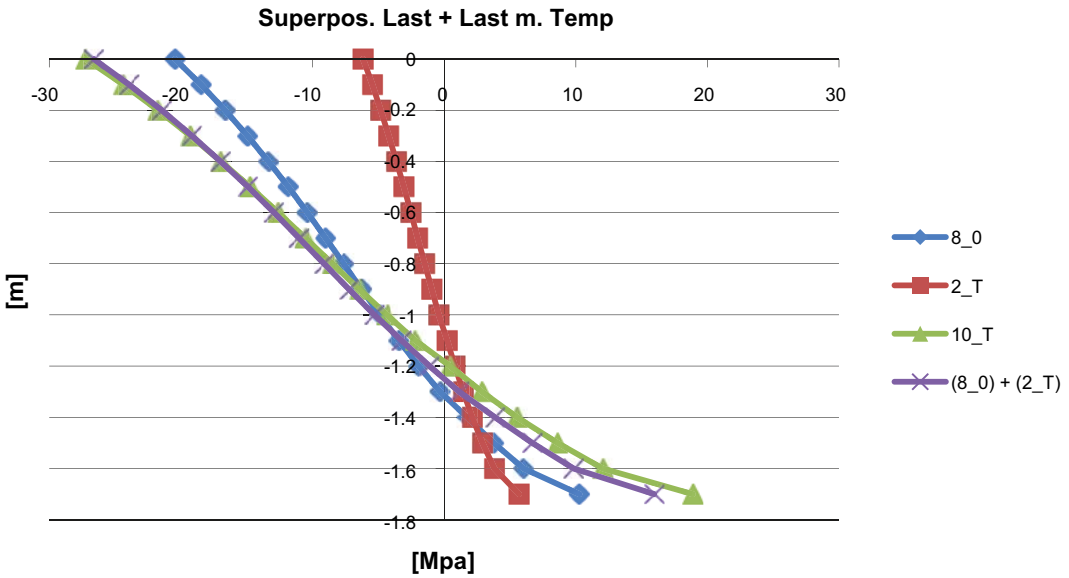

Figur B6-5. *Superponering av trycklast och temperaturlast kombinerat med trycklast.*

I figur B6-6 och figur B6-7 har superponering av lastfall 4 respektive lastfall 5 genomförts. I dessa figurer framgår tydligt problematiken med superponering av temperaturlasten – överensstämmelsen mellan verkligt och superponerat fall är betydande. I lastfall 4, figur B6-6, där temperaturlasten består av negativa temperaturer över hela pluggen, försvinner eventuell lastpåverkan eftersom pluggen i stort sett kan röra sig fritt över kontaktytorna om alla trycklaster utesluts.

För lastfall 5, som visas i figur B6-7, fås istället en för stor effekt av temperaturen när tryck och temperatur superponeras. Detta kan förklaras om man tittar på hur de olika lasterna deformerar pluggen. Enbart temperaturlast kommer att leda till en expansion av pluggen, vilket resulterar i en viss spänningsbild. När lasterna istället appliceras tillsammans kommer kombinationen av tryck- och temperaturlast medföra att pluggens deformation blir annorlunda, något som därför också påverkar resulterande spänningsbild. För det verkliga fallet, tryck och temperatur tillsammans, kommer pluggens övre kontaktyta inte vara i kontakt med berget, se figur B6-8, vilket innebär att resulterande spänningsbild i pluggens centrumsnitt uppvisar en betydande skillnad för verkligt och superponerat fall, se figur B6-7.

En hypotes här är att om modellen där temperaturlasten är enda lasten modelleras med fast inspänning längs den ena ytan, så som visas i figur B6-9, skulle en mer riktig spänningsbild från temperaturlasten erhållas. En sådan modell skulle även kunna tänkas ge bättre resultat av ensam temperaturlast för lastfall 4.

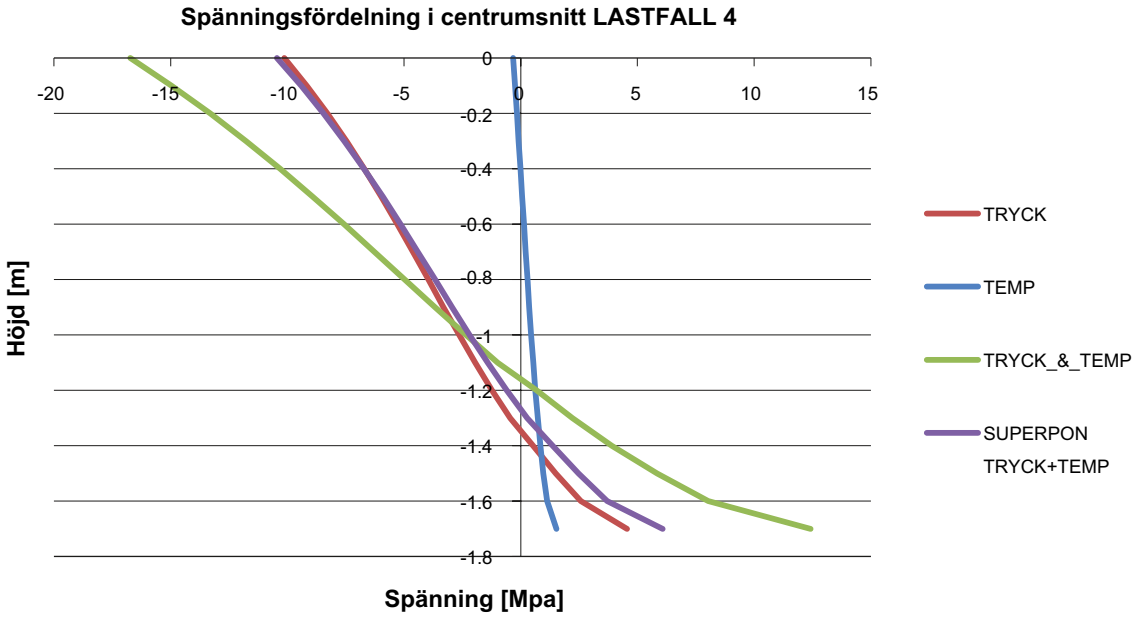

Figur B6-6. *Superponering av lastfall 4.*

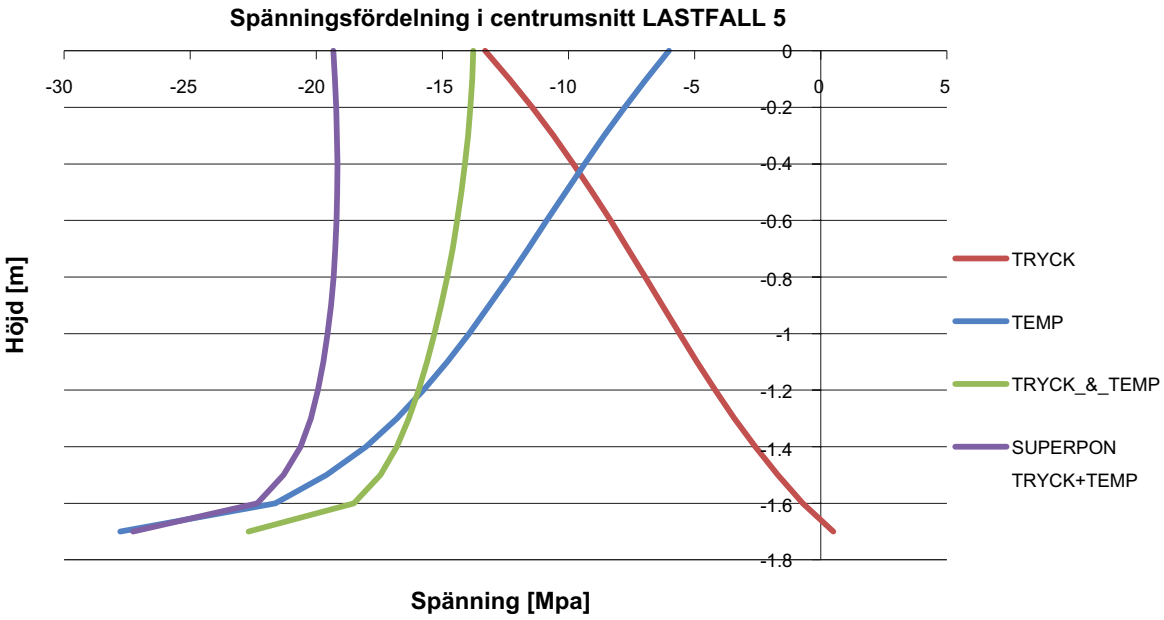

Figur B6-7. *Superponering av lastfall 5.*

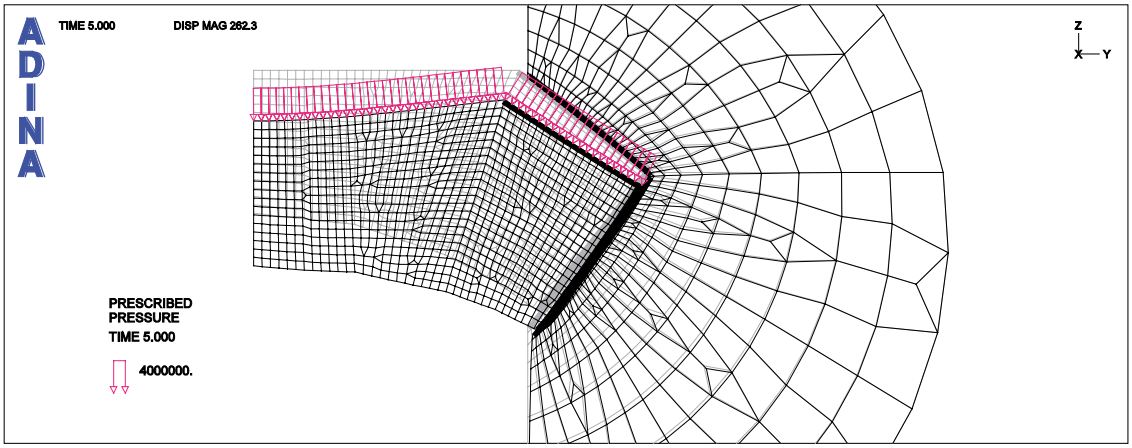

Figur B6-8. *Principiellt deformationsbeteende för lastfall 5.*

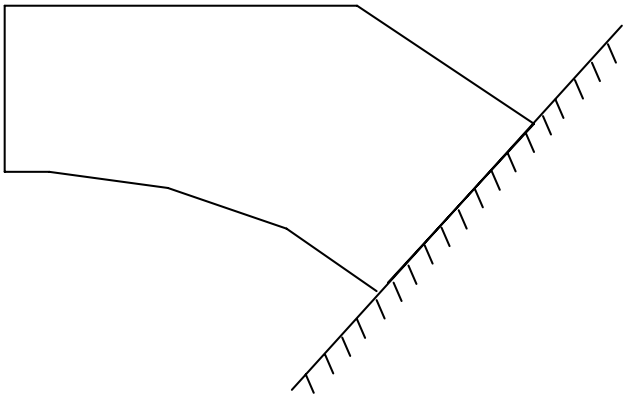

Figur B6-9. *Alternativ modellering för temperaturlast.*

B6.3.2 Superponering av 3D-modell

Den 3-dimensionella modellen som används för att modellera de osymmetriska lasterna är, pga. sin storlek, väldigt kapacitetskrävande. En möjlighet att till viss del kunna använda sig av superponerade resultat skulle därför underlätta vid grövre uppskattning av påfrestningar i pluggen när den belastas med osymmetriska laster.

Det första superponeringsfallet är när svälltrycket över halva pluggens ovansida är dubbelt så högt jämfört med intilliggande halva. Det tryck som har valts i denna undersökning är 4 MPa på ena sidan och 2 MPa på den andra sidan, se figur B6-10.

Dessa svälltryck är därefter modellerade med dubbel storlek, 8 MPa respektive 4 MPa. Kontroll av superponeringen görs genom att normalspänningar längs centrumsnittet i det första fallet, figur B6-10, multipliceras med 2 och jämförs med spänningar för belastningsfallet med dubbla laster, se figur B6-11. Jämförelse av resulterande spänningar ger att överensstämmelsen är god. Den avvikelse som uppstår är störst i pluggens dragna undersida, medan spänningarna i den tryckta översidan i princip blir desamma för verkligt och superponerat fall.

Osymmetriskt vattentryck har diskuterats och lastpåläggning enligt figur B6-12 har då antagits som ett möjligt lastfall. Detta lastfall är sedan uppdelat i två lastbidrag, figur B6-13, som vid kombination ger samma lastpåläggning som lastfall i figur B6-12.

Resulterande normalspänningar i centrumsnittet för det korrekta lastfallet och superponering av de två bidragen beskrivna i figur B6-13 jämförs i figur B6-14. Spänningsbilderna stämmer inte helt överens men bedöms ändå vara såpass lika att superponering kan användas för att ge en grov uppfattning om hur vattentryck på de olika delarna av pluggen påverkar normalspänningarna i centrumsnittet av pluggen.

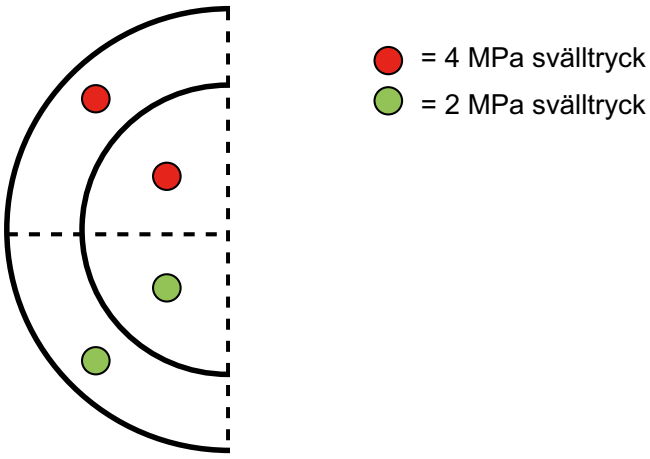

Figur B6-10. *Halva pluggen sedd uppifrån med osymmetriskt svälltryck.*

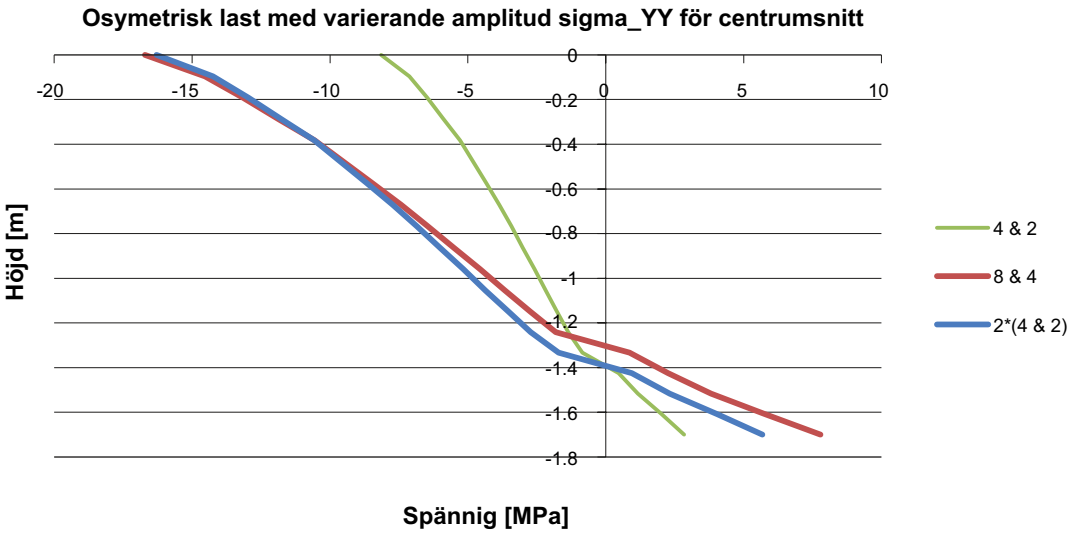

Figur B6-11. Superponering av osymmetriskt sälltryck, 4 resp. 2 MPa och 8 resp. 4 MPa.

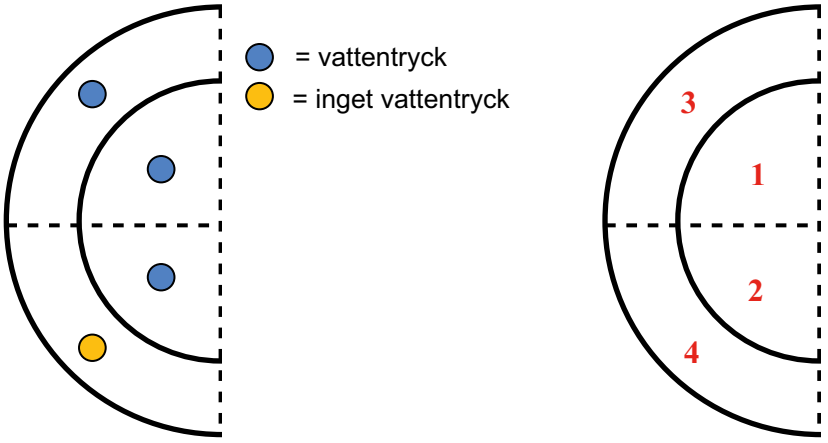

Figur B6-12. Osymmetriskt lastfall för vattentryck (vänster) samt ytnumrering för pluggen (höger).

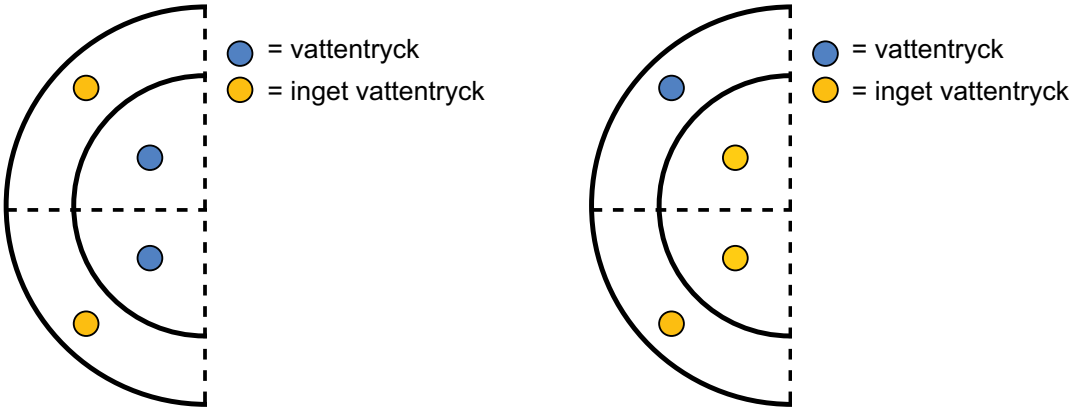

Figur B6-13. Osymmetriskt lastfall för vattentryck, bidrag 1 (vänster) samt bidrag 2 (höger).

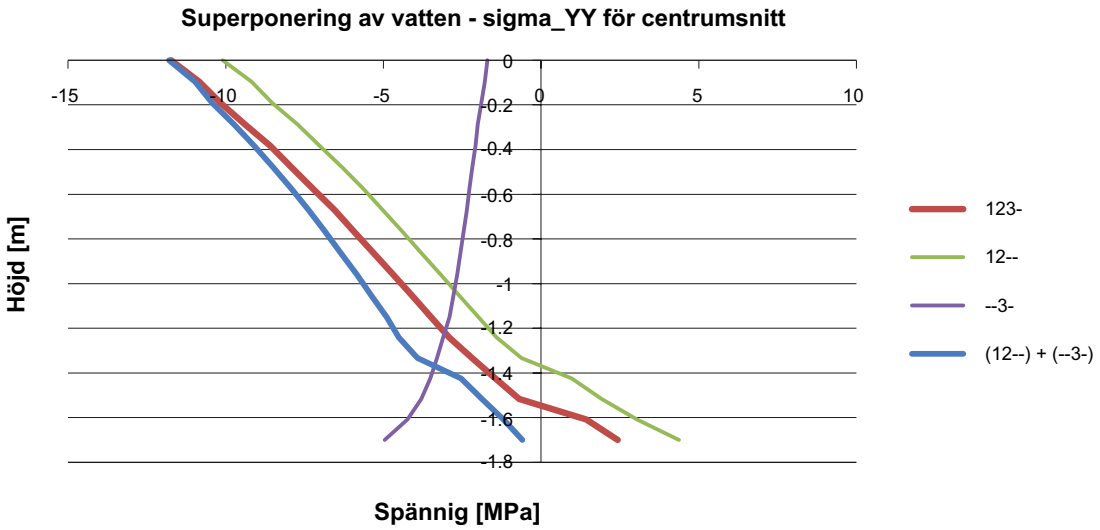

Figur B6-14. *Superponering av osymmetriskt vattentryck som verkar på olika delar av pluggen, numrering 1234 enligt figur B6-12.*

B6.3.3 Kommentarer

De viktigaste slutsatserna som kan dras utifrån analyserna för osymmetrisk last är dels att det approximativt går att uppskatta spänningsfördelningar genom superponering av olika lastfall. Vidare kan konstateras att det inte uppkommer några oroväckande höga spänningar i pluggens centrumsnitt för varken drag- eller tryckspänningar.

För dragspänningar som överskrider betongens draghållfasthet är det därför rimligt att anta att en begränsad uppsprickning av pluggens undersida i form av radiella sprickor kommer att uppkomma men eftersom tidigare analyser har visat att denna uppsprickning avstannar är det rimligt att även denna uppsprickning kommer att bli relativt begränsad. Tryckspänningarna är även såpas låga vid de linjärelastiska analyserna att inte heller tryckspänningar i pluggens topp behöver förväntas bli kritiska när undersidan börjar spricka upp. En viss spänningsökning kan förväntas av osymmetrisk trycklast men inte i den utsträckningen att den maximalt tillåtna spänningsgränsen kommer att uppnås.

B7 Referenser

Dahlström L-O, Magnusson J, Gueorguiev G, Johansson M, 2009. Feasibility study of a concrete plug made of low pH concrete. SKB R-09-34, Svensk Kärnbränslehantering AB.

B8 Appendix B1 – Translation of figure and table texts

B8.1 Translation of figure texts

Figure	Figure text
Figur B2-1	Proposal for reduced plug geometry.
Figur B3-1	Geometric layout of plug and surrounding rock.
Figur B3-2	Pressure loads, load case 1a, 1b and 2. From R-09-34.
Figur B3-3	Temperature loads, load case 3a – 3e.
Figur B4-1	Reduction of plug centric height.
Figur B4-2	Reduction of plug thickness at abutment.
Figur B4-3	Swelling pressure and water pressure for load case 4.
Figur B4-4	Swelling pressure and water pressure for load case 5.
Figur B4-5	Regulation of plug geometry to decrease stress concentration at centric section.
Figur B4-6	Distribution of normal stresses in centric section for different values of plug thickness, maximum pressure load, centric height 1.1 m, level 0 corresponds to the plug topside.
Figur B4-7	Distribution of normal stresses in centric section for different values of plug thickness, maximum pressure load, centric height 1.3 m, level 0 corresponds to the plug topside.
Figur B4-8	Distribution of normal stresses in centric section for different values of plug thickness, maximum pressure load, centric height 1.5 m, level 0 corresponds to the plug topside.
Figur B4-9	Distribution of normal stresses in centric section for different values of plug thickness, maximum pressure load, centric height 1.7 m, level 0 corresponds to the plug topside.
Figur B4-10	Normal stresses at top and bottom edge as a function of the centric height for investigated plug thickness, maximum pressure load.
Figur B4-11	Distribution of normal stresses in centric section for different values of plug thickness, no pressure load, centric height 1.1 m, level 0 corresponds to the plug topside.
Figur B4-12	Distribution of normal stresses in centric section for different values of plug thickness, no pressure load, centric height 1.3 m, level 0 corresponds to the plug topside.
Figur B4-13	Distribution of normal stresses in centric section for different values of plug thickness, no pressure load, centric height 1.5 m, level 0 corresponds to the plug topside.
Figur B4-14	Distribution of normal stresses in centric section for different values of plug thickness, no pressure load, centric height 1.7 m, level 0 corresponds to the plug topside.
Figur B4-15	Normal stresses at top and bottom edge as a function of the centric height for investigated plug thickness, no pressure load.
Figur B4-16	Reduced geometry for continued analyses.
Figur B5-1	Illustration of tangential and radial cracks.
Figur B5-2	Stress-strain diagram for concrete in tension for studied material relations. Analyses carried out here have used model 1 or model 3.
Figur B5-3	Sensitivity analysis of maximum compressive stress on the plug topside in the centric section when water and swelling pressure are applied during time 0–10, but with varied time application of the temperature load.
Figur B5-4	3 MPa pressure on the plug topside. First cracks are initiated for material 1, radial cracks and an occasional tangential crack.
Figur B5-5	1 MPa pressure on the plug topside. First cracks are initiated for material 3, radial cracks and an occasional tangential crack.
Figur B5-6	4.5 MPa pressure on the plug topside. Fully cracked element, material 1.
Figur B5-7	1.5 MPa pressure on the plug topside. Fully cracked element, material 3.
Figur B5-8	21 MPa pressure on the plug topside, full temperature load applied. First indication of shear crack, material 1.
Figur B5-9	7.5 MPa pressure on the plug topside. First indication of shear crack, material 3.
Figur B5-10	21.5 MPa pressure on the plug topside, full temperature load applied. Fully open shear crack, material 1.
Figur B5-11	10 MPa pressure on the plug topside. Fully open shear crack, material 3.
Figur B5-12	10 MPa pressure on the plug topside, full temperature load applied. Crack pattern for all initiated cracks, material 1.
Figur B5-13	10 MPa pressure on the plug topside, full temperature load applied. Crack pattern for all initiated cracks, material 3.
Figur B5-14	100% of temperature load applied, material 1.
Figur B5-15	58% of temperature load applied, initiated cracks. First indication of this crack appears at 50% temperature load, material 3.
Figur B5-16	Appearance of shear crack at 62% of temperature load. The crack develops to a fully open crack directly after initiation, material 3.
Figur B5-17	Initiated cracks at 100% applied temperature load, material 3.
Figur B5-18	Fully open cracks at 100% applied temperature load, material 3.
Figur B5-19	Critical edge for the plug with regard to the shear crack.
Figur B5-20	Cracks at 100% temperature load applied when the plug edges are in contact with the rock.

Figure	Figure text
Figur B5-21	Distribution of normal stresses for the two boundary conditions with the rock, no pressure load, centric height 1.3 m, level 0 corresponds to the plug topside.
Figur B6-1	Three dimensional model for evaluation of asymmetric loads.
Figur B6-2	Asymmetric load for swelling pressure, 2 MPa.
Figur B6-3	Asymmetric load for swelling pressure, 4 MPa.
Figur B6-4	Super positioning of pressure load for 2D model, 2 MPa, 10 MPa and 5*2 MPa.
Figur B6-5	Super positioning of pressure load and temperature load combined with pressure load.
Figur B6-6	Super positioning of load case 4.
Figur B6-7	Super positioning of load case 5.
Figur B6-8	Principal deformations for load case 5.
Figur B6-9	Alternativ modelling for temperature load.
Figur B6-10	Half the plug seen from above with asymmetric swelling pressure.
Figur B6-11	Super positioning of asymmetric swelling pressure, 4 and 2 MPa, respectively; and 8 and 4 MPa, respectively.
Figur B6-12	Asymmetric load case for water pressure (left) and surface numbering for the plug (right).
Figur B6-13	Asymmetric load case for water pressure, contribution 1 (left) and contribution 2 (right).
Figur B6-14	Super positioning of asymmetric water pressure acting on different parts of the plug, numbering 1234 as shown in Figur 5.12.

B8.2 Translation of table texts

Table	Figure text
Tabell B2-1	Summary of crack development for material 1 and 3. Stress values specify the pressure load due to water and swelling that is applied at the given moment.
Tabell B3-1	Load cases and load combinations that have been studied in previous analyses. From R-09-34.
Tabell B3-2	Load cases from the summary of the 8 load combinations in Tabell 2.1 and the 6 possible material variations for the surrounding rock. From R-09-34.
Tabell B4-1	Studied geometries when reducing the plug section.
Tabell B5-1	Input data for materials regarding tensile stresses.
Tabell B5-2	Summary of crack development for material 1 and 3. Stress values specify the pressure load due to water and swelling that is applied at the plug at a given moment.

B9 Appendix B2 – Input data for FE analyses

```
********** Input file for 2D structural models **********************
************************************************************
***************** Definition of the geometry ******************
************************************************************
COORDINATE POINTS SYSTEM=0
1000     -5          0          -5

LINE EXTRUDED NAME=1000 POINT=1000 DX=0.25 SYSTEM=0 PCOINCID=YES
PTOLERAN=1.0E-05

SURFACE EXTRUDED NAME=1000 LINE=1000 DZ=0.25 SYSTEM=0 PCOINCID=YES
PTOLERAN=1.0E-05 NDIV=1 OPTION=VECTOR

*** Read 2D geometry drawing
LOADDXF '2D_geometry_drawing.dxf' GCT=0.001
** Geometry lines and points are imported from AutoCad dfx-drawing. Geometries are presented in main
report

*** Complement to the geometry input
LINE ARC NAME=1022 MODE=1 P1=1018 P2=1015 CENTER=1019 PCOINCID=YES,
    PTOLERAN=1.00000000000000E-05 MODIFY-L=YES DELETE-P=YES

LINE ARC NAME=1023 MODE=1 P1=1015 P2=1017 CENTER=1019 PCOINCID=YES,
    PTOLERAN=1.00000000000000E-05 MODIFY-L=YES DELETE-P=YES

SURFACE PATCH NAME=1005 EDGE1=1017 EDGE2=1020 EDGE3=1022 EDGE4=1018
SURFACE PATCH NAME=1006 EDGE1=1018 EDGE2=1023 EDGE3=1019 EDGE4=1021

*** Model subdivision
SUBDIVIDE MODEL MODE=LENGTH SIZE=0.1 NDIV=1 PROGRESS=GEOMETRIC MINCUR=1

SUBDIVIDE LINE NAME=1000 MODE=LENGTH SIZE=1.0
** Subdivision of rock geometry is made here

SUBDIVIDE LINE NAME=1000 MODE=DIVISIONS NDIV=10 RATIO=10
PROGRESS=ARITHMETIC
** Subdivision of rock geometry is made here

SUBDIVIDE LINE NAME=1000 MODE=LENGTH SIZE=0.05
** Subdivision of rock contact surfaces are made here
```

```
*****************************************************************
****************** Definition of Materials ******************
*****************************************************************
*** Linear elastic concrete
MATERIAL ELASTIC NAME=1 E=26.7E+9 NU=0.27 DENSITY=2400 ALPHA=1e-5

*** Non linear concrete
MATERIAL CONCRETE NAME=1 OPTION=KUPFER E0=26.7E+9,
    NU=0.27,
SIGMAT=2.9E+6,                  % Material model 1
SIGMAT=0.8E+6,                  % Material model 3
    SIGMATP=0.00,
    SIGMAC=-1000.0E+06,
    EPSC=-60e-3,
    SIGMAU=-800.0E+06,
    EPSU=-100e-3,
    BETA=0.75,
    C1=0.58333 C2=-0.40
XSI=12.699,                     % Material model 1
XSI=45.753,                     % Material model 3
    STIFAC=0.0001 SHEFAC=0.5,
    ALPHA=1e-5          TREF=0 INDNU=CONSTANT,
    GF=0       DENSITY=2400.0 TEMPERAT=NO,
    MDESCRIP='NONE'

*** Rock material
MATERIAL ELASTIC NAME=2
E=40E+9                         % Rock model 1
E=80E+9                         % Rock model 2
NU=0.235 DENSITY=2400 ALPHA=7e-6

*****************************************************************
****************** Definition of Contact properties ******************
*****************************************************************

CONTACT-CONT NSUPPRES=10

CGROUP CONTACT2 NAME=1 SUBTYPE=DEFAULT FRICTION=0.0 EPSN=1.0E-12,

CONTACTSURFA NAME=1
** Contact surface "1" is defined here
CONTACTSURFA NAME=2
** Contact surface "2" is defined here
CONTACTSURFA NAME=11
** Contact surface "11" is defined here
CONTACTSURFA NAME=12
** Contact surface "12" is defined here
CONTACTPAIR NAME=1 TARGET=1 CONTACTO=2
FRICTION=0.3                    % Friction model 1
FRICTION=2.0                    % Friction model 2
CONTACTPAIR NAME=2 TARGET=11 CONTACTO=12
FRICTION=0.3                    % Friction model 1
FRICTION=2.0                    % Friction model 2
```

```
************************************************************
****************** Definition of Elements and boundary conditions ******
************************************************************

EGROUP TWODSOLID NAME=1 SUBTYPE=AXISYMMETRIC MATERIAL=1
GSURFACE NODES=4 NCOINCID=BOUNDARIES NCTOLERA=1.00000000000000E-05 GROUP=1
** Elements of the concrete plug are defined here
EGROUP TWODSOLID NAME=2 SUBTYPE=AXISYMMETRIC MATERIAL=2
GSURFACE NODES=4 NCOINCID=GROUP NCTOLERA=1.00000000000000E-05 GROUP=2
** Elements of the modeled rock are defined here

FIXBOUNDARY LINES FIXITY=ALL
** The outer limit of the rock is defined with fixed boundary conditions here

************************************************************
****************** Definition of Loads and Time functions ******
************************************************************
LOAD PRESSURE NAME=1 MAGNITUD=-10e6

APPLY-LOAD BODY=0
** Pressures are applied at the plug here

TIMEFUNCTION NAME=1
** Time function for pressure applying is defined here

TIMESTEP NAME=DEFAULT
** Time step for the model is defined here

** Applying thermal map
THERMAL-MAPP FILENAME='thermal_map.map' EXTERNAL=ALL


************************************************************
****************** Definition of Analysis properties ******
************************************************************

KINEMATICS DISPLACE=LARGE STRAINS=SMALL UL-FORMU=DEFAULT PRESSURE=NO,
    INCOMPAT=AUTOMATIC RIGIDLIN=NO

ITERATION METHOD=FULL-NEWTON LINE-SEA=YES MAX-ITER=100 PRINTOUT=ALL,
    PLASTIC-=1

TOLERANCES ITERATION CONVERGENCE=ENERGY ETOL=1e-3 STOL=.5

MASTER ANALYSIS=STATIC MODEX=EXECUTE IDOF=100111 AUTOMATI=ATS
LOAD-CAS=NO                 % for incremental analyses
LOAD-CAS=YES                % for load case analyses
```

```
************ Input file for 2D thermal models ************************
*****************************************************************
***************** Definition of the geometry *****************
*****************************************************************

*** Same geometry input as for structural 2D model is used here
SUBDIVIDE MODEL MODE=LENGTH SIZE=0.1 NDIV=1 PROGRESS=GEOMETRIC MINCUR=1

*****************************************************************
***************** Definition of Loads and Time functions ******
*****************************************************************
LOAD TEMPERATURE NAME=1 MAGNITUD=1.0

TIMEFUNCTION NAME=2
** Time function for applying of temperatures are defined here

TIMEFUNCTION NAME=3
** Time function for applying of temperatures are defined here

TIMEFUNCTION NAME=4
** Time function for applying of temperatures are defined here

TIMESTEP NAME=DEFAULT
** Time step for the model is defined here

APPLY-LOAD BODY=0
** Temperatures are applied at the plug and rock geometry here

*****************************************************************
***************** Definition of Material and Element properties******
*****************************************************************
MATERIAL ISOTROPIC NAME=1 K=1.28 C=1.98e, JOULE-HE=NO ELECTRIC=0.0
MDESCRIP='NONE'

EGROUP TWODCONDUCTION NAME=1 SUBTYPE=AXISYMMETRIC MATERIAL=1

GSURFACE NODES=4 NCTOLERA=1.0E-05 GROUP=1
** Elements of the concrete plug are defined here

EGROUP TWODCONDUCTION NAME=2 SUBTYPE=AXISYMMETRIC MATERIAL=1

GSURFACE NODES=4 NCTOLERA=1.0E-05 GROUP=2
** Elements of the modeled rock are defined here

*****************************************************************
***************** Definition of Analysis properties ******
*****************************************************************
MASTER ANALYSIS=STEADY-STATE MODEX=EXECUTE AUTOMATI=OFF

ADINA-T OPTIMIZE=SOLVER FILE='thermal_map.dat' FIXBOUND=YES MID=NO
OVERWRIT=YES
```

```
************* Input file for 3D structural models ***********************
*****************************************************************
****************** Definition of the geometry ******************
*****************************************************************
COORDINATE POINTS SYSTEM=0
1000      -5          0          -5

LINE EXTRUDED NAME=1000 POINT=1000 DX=0.25 SYSTEM=0 PCOINCID=NO
PTOLERAN=1.0E-05

SURFACE EXTRUDED NAME=1000 LINE=1000 DZ=0.25 SYSTEM=0 PCOINCID=NO
PTOLERAN=1.0E-05 NDIV=1 OPTION=VECTOR

*** Read 2D geometry drawing
LOADDXF '2D_geometry_drawing.dxf' GCT=0.001
** Geometry lines and points are imported from AutoCad dfx-drawing. Geometries are presented in main
report

LINE ARC NAME=1031 MODE=1 P1=1015 P2=1018 CENTER=1019 PCOINCID=NO,
    PTOLERAN=1.00000000000000E-05 MODIFY-L=YES DELETE-P=YES

LINE ARC NAME=1032 MODE=1 P1=1017 P2=1015 CENTER=1019 PCOINCID=NO,
    PTOLERAN=1.00000000000000E-05 MODIFY-L=YES DELETE-P=YES

SURFACE PATCH NAME=1009 EDGE1=1017 EDGE2=1020 EDGE3=1031 EDGE4=1018
SURFACE PATCH NAME=1010 EDGE1=1018 EDGE2=1032 EDGE3=1019 EDGE4=1021
SURFACE PATCH NAME=1005 EDGE1=1022 EDGE2=1023 EDGE3=1005 EDGE4=0

TRANSFORMATI ROTATION NAME=2 MODE=AXIS SYSTEM=0 AXIS=ZL ANGLE=30.
TRANSFORMATI ROTATION NAME=3 MODE=AXIS SYSTEM=0 AXIS=ZL ANGLE=60.
TRANSFORMATI ROTATION NAME=4 MODE=AXIS SYSTEM=0 AXIS=ZL ANGLE=90.
TRANSFORMATI ROTATION NAME=5 MODE=AXIS SYSTEM=0 AXIS=ZL ANGLE=120.
TRANSFORMATI ROTATION NAME=6 MODE=AXIS SYSTEM=0 AXIS=ZL ANGLE=150.
TRANSFORMATI ROTATION NAME=7 MODE=AXIS SYSTEM=0 AXIS=ZL ANGLE=180.

*** Plug geometry
VOLUME REVOLVED NAME=1001 MODE=AXIS SURFACE=0 ANGLE=30,
    SYSTEM=0 AXIS=ZL PCOINCID=NO PTOLERAN=1.0E-05 NDIV=1
** Revolving of 2D geometry into 3D geometry for the first part of the plug is defined here

VOLUME TRANSFORMED NAME=2001 PARENT=1001 TRANSFORMATION=2 PCOINCID=NO
PTOLERAN=1.0E-05
** 3D geometry is for the second part is defined here
…
…
…
VOLUME TRANSFORMED NAME=6001 PARENT=1001 TRANSFORMATION=6 PCOINCID=NO
PTOLERAN=1.0E-05
** 3D geometry is for the sixth part is defined here

*** Rock geometry
VOLUME REVOLVED NAME=101 MODE=AXIS SURFACE=1009 ANGLE=180,
    SYSTEM=0 AXIS=ZL PCOINCID=YES PTOLERAN=1.0E-05 NDIV=1

VOLUME REVOLVED NAME=102 MODE=AXIS SURFACE=1010 ANGLE=180,
    SYSTEM=0 AXIS=ZL PCOINCID=YES PTOLERAN=1.0E-05 NDIV=1


SUBDIVIDE MODEL MODE=LENGTH SIZE=0.1 NDIV=1 PROGRESS=GEOMETRIC MINCUR=1
** Different subdivision schemes are used for lines 1017-1536
```

```
*** Rotate coordinate system
SKEWSYSTEM CYLINDRICAL
1 0. 0. 0. 0. 0. 1. A

DOF-SYSTEM VOLUMES
** Rotation of coordinate system for all volumes are defined here

************************************************************
****************** Definition of Materials ******************
************************************************************

*** Linear elastic concrete
MATERIAL ELASTIC NAME=1 E=26.7E+9 NU=0.27 DENSITY=2400 ALPHA=1e-5

MATERIAL ELASTIC NAME=2 E=50E+9 NU=0.2 DENSITY=2400 ALPHA=1e-15

*** Rock material
MATERIAL ELASTIC NAME=2
E=40E+9                         % Rock model 1
E=80E+9                         % Rock model 2
NU=0.235 DENSITY=2400 ALPHA=7e-6

************************************************************
****************** Definition of Contact properties ******************
************************************************************

CONTACT-CONT NSUPPRES=10

CGROUP CONTACT3 NAME=1 FRICTION=0.0 EPSN=1.0E-12,

CONTACTSURFA NAME=1
** Contact surface "1" is defined here
CONTACTSURFA NAME=2
** Contact surface "2" is defined here
CONTACTSURFA NAME=11
** Contact surface "11" is defined here
CONTACTSURFA NAME=12
** Contact surface "12" is defined here
CONTACTPAIR NAME=1 TARGET=1 CONTACTO=2
FRICTION=0.3                    % Friction model 1
FRICTION=2.0                    % Friction model 2
CONTACTPAIR NAME=2 TARGET=11 CONTACTO=12
FRICTION=0.3                    % Friction model 1
FRICTION=2.0                    % Friction model 2
```

```
************************************************************
****************** Definition of Elements and boundary conditions ******
************************************************************

EGROUP THREEDSOLID NAME=11 MATERIAL=1
EGROUP THREEDSOLID NAME=21 MATERIAL=1
EGROUP THREEDSOLID NAME=31 MATERIAL=1
EGROUP THREEDSOLID NAME=41 MATERIAL=1
EGROUP THREEDSOLID NAME=51 MATERIAL=1
EGROUP THREEDSOLID NAME=61 MATERIAL=1

GVOLUME NODES=4 NCTOLERA=1.0E-05 GROUP=11
** Elements of the concrete plug, slice 1 are defined here

GVOLUME NODES=4 NCTOLERA=1.0E-05 GROUP=21
** Elements of the concrete plug, slice 2 are defined here

GVOLUME NODES=4 NCTOLERA=1.0E-05 GROUP=31
** Elements of the concrete plug, slice 3 are defined here

GVOLUME NODES=4 NCTOLERA=1.0E-05 GROUP=41
** Elements of the concrete plug, slice 4 are defined here

GVOLUME NODES=4 NCTOLERA=1.0E-05 GROUP=51
** Elements of the concrete plug, slice 5 are defined here

GVOLUME NODES=4 NCTOLERA=1.0E-05 GROUP=61
** Elements of the concrete plug, slice 6 are defined here

EGROUP THREEDSOLID NAME=111 MATERIAL=2 SAVE=NO

GVOLUME NODES=4 NCOINCID=GROUP NCTOLERA=1.0E-05 GROUP=111 MESHING=FREE-
FORM
** Elements of the modeled rock are defined here

*** Boundary conditions for surfaces with symmetry properties
FIXITY NAME=SYMM
@CLEAR
 'Y-TRANSLATION'
@

** Boundary conditions for center axis
FIXITY NAME=CENTRE
@CLEAR
 'X-TRANSLATION'
@

FIXBOUNDARY SURFACES FIXITY=ALL
** The outer limit of the rock is defined with fixed boundary conditions and the symmetry surfaces with
symmetry boundary conditions here

FIXBOUNDARY LINES FIXITY=ALL
** The center line of the plug is defined with symmetry boundary conditions here
```

```
*****************************************************************
****************** Definition of Loads **********
*****************************************************************

*** Defining pressure load
LOAD PRESSURE NAME=1 MAGNITUD=2e6
** Pressures for unsymmetrical load cases are defined here

*** Load case analysis is performed
LOAD-CASE NAME=1

APPLY-LOAD BODY=0 LCASE=1
** Pressures are applied at the plug here

*** Applying thermal map
THERMAL-MAPP FILENAME='thermal_map_BIG.map' EXTERNAL=ALL TIME=0.0

*****************************************************************
****************** Definition of Analysis properties ******
*****************************************************************

KINEMATICS DISPLACE=LARGE STRAINS=SMALL UL-FORMU=DEFAULT PRESSURE=NO,
    INCOMPAT=AUTOMATIC RIGIDLIN=NO

ITERATION METHOD=FULL-NEWTON LINE-SEA=YES MAX-ITER=100 PRINTOUT=ALL
PLASTIC-=1

MASTER ANALYSIS=STATIC MODEX=EXECUTE IDOF=000111 LOAD-CAS=YES
```

```
************* Input file for 3D thermal models ************************
*********************************************************************
****************** Definition of the geometry ******************
*********************************************************************

*** Same geometry input as for structural 3D model is used here

*********************************************************************
****************** Definition of Material and Element properties******
*********************************************************************

MATERIAL ISOTROPIC NAME=1 K=1.28 C=1.98e6 JOULE-HE=NO ELECTRIC=0.0
MDESCRIP='NONE'

EGROUP THREEDCONDUCTION NAME=1 MATERIAL=1
GVOLUME NODES=4 PATTERN=0 GROUP=1 MESHING=FREE-FORM
** Elements of the concrete plug are defined here

EGROUP THREEDCONDUCTION NAME=2 MATERIAL=1
GVOLUME NODES=4 PATTERN=0 GROUP=1 MESHING=FREE-FORM
** Elements of the modeled rock are defined here


*********************************************************************
****************** Definition of Loads and Time functions ******
*********************************************************************

LOAD TEMPERATURE NAME=1 MAGNITUD=1.0

TIMEFUNCTION NAME=2
** Time function for applying of temperatures are defined here

TIMEFUNCTION NAME=3
** Time function for applying of temperatures are defined here

TIMEFUNCTION NAME=4
** Time function for applying of temperatures are defined here

TIMESTEP NAME=DEFAULT
** Time step for the model is defined here

APPLY-LOAD BODY=0
** Temperatures are applied at the plug and rock here

*********************************************************************
****************** Definition of Analysis properties ******
*********************************************************************
MASTER ANALYSIS=STEADY-STATE MODEX=EXECUTE

ADINA-T OPTIMIZE=SOLVER FILE='thermal_map_BIG.dat' FIXBOUND=YES MID=NO
OVERWRIT=YES
```